MOLECULAR MODELLING AND SYNTHESIS OF NOVEL LIGANDS RELATED TO CELLULAR DIFFERENTIATION

A thesis submitted to the Cardiff University for the Degree of

Doctor of Philosophy

By

Ahmed Safwat Mohamed Mohamed

June 2009

Medicinal Chemistry Division, Welsh School of Pharmacy,

Cardiff University

ProQuest LLC
789 East Eisenhower Parkway
P.O. Box 1346
Ann Arbor, MI 48106-1346

CARDIFF UNIVERSITY
PRIFYSGOL CAERDYDD

DECLARATION

This work has not previously been accepted in substance for any degree and is not concurrently submitted in candidature for any degree.

Signed ..Ahmed Safwat Mohamed.. (candidate) Date 23/07/2009

STATEMENT 1

This thesis is being submitted in partial fulfillment of the requirements for the degree of PhD.

Signed ..Ahmed Safwat Mohamed.. (candidate) Date 23/07/2009

STATEMENT 2

This thesis is the result of my own independent work/investigation, except where otherwise stated.
Other sources are acknowledged by explicit references.

Signed ..Ahmed Safwat Mohamed.. (candidate) Date 23/07/2009

STATEMENT 3

I hereby give consent for my thesis, if accepted, to be available for photocopying and for inter-library loan, and for the title and summary to be made available to outside organisations.

Signed ..Ahmed Safwat Mohamed.. (candidate) Date 23/07/2009..

Acknowledgments

To the almighty God, ALLAH, who has granted me all these graces to fulfill this work, supported me and blessed me by His mercy in all my life. To Him I extended my heartfelt thanks.

Indeed, my appreciation and profound indebtedness are due to **Dr. Claire Simons**, Senior lecturer of Medicinal Chemistry, Welsh School of Pharmacy, Cardiff University, for suggesting the subject of this work, kind supervision, continuous encouragement, direct guidance and valuable support.

I would like to thank **Egyptian Ministry of Higher Education**, especially the **Mission Department**, for financial support and funding of this work. I am also grateful to the **Egyptian Embassy** and **Culture Bureau** in London for their continuous support and supervision.

My extreme thanks to all staff members, at the **Welsh School of** Pharmacy, my colleagues and department technicians for their encouragement and help.

Abstract

Cancer is a leading cause of death all over the world. Retinoic acid and vitamin D3 play an important role in cellular proliferation and differentiation and as such have potential therapeutic value as differentiating agents in the treatment of cancer and hyperkeratinising diseases.

The use of differentiating agents to suppress prostate and breast cancer proliferation is now one of the new therapeutic strategies. However, the use of all *trans* retinoic acid (ATRA) and vitamin D3 as differentiating agents is limited by their rapid metabolism through the self induction of the cytochrome P450 enzymes that are involved in their catabolism. The P450 enzymes responsible for the metabolism of ATRA and 1α,25-$(OH)_2$-D_3 (calcitriol) are cytochrome P450 26 (CYP26A1) and cytochrome P450 24 (CYP24A1) respectively. Therefore the use of potent and selective inhibitors of CYP26A1 and CYP24A1 with ATRA and 1α,25-$(OH)_2$-D_3 respectively may represent a new strategy for the treatment of cancer.

The pharmacophore model of CYP26A1 inhibitors was constructed using MOE software. A database of 71 inhibitors with different conformations have been built and arranged according to activity. The resulting pharmacophore model has 8 features of which 5 features are essential to get the CYP26A1 inhibitory activity. The designed model was used to build new inhibitors, which have reasonable activity.

Two series were synthesised for CYP26A1 inhibition. The first series was designed to investigate the effect of changing the structure of the lead compound on the inhibitory activity against CYP26A1 and was depending mainly on presence of imidazole moiety, and the second series was a result of the pharmacophore search and was mainly oxadiazole derivatives. These two series were biologically evaluated using a MCF-7 breast cancer cell assay previously described by our group and also some of the compounds were tested in the biochemical assay. Changing of the structure could be tolerated to a certain limit as long as the imidazole ring is included which is the main part responsible for the binding with the haem in CYP26A1 enzyme. Some of the resulting compounds has good activity, specially methyl *anti*-3-(1*H*-1-imidazolyl)-3-[4-(phenylamino)phenyl]-2-methylpropanoate which should IC_{50} of 26 nM in the biochemical CYP26A1 assay. The oxadiazole derivatives did not show very good activity against CYP26A1 cell based assay, may be owing to the decrease in the

flexibility of the molecules. Further investigation in the first series, i.e. the imidazole containing compounds, is being continued in our group.

As for CYP24A1 inhibition, two series; the azoles and the tetralones, were synthesised and biologically evaluated. The tetralones do not seem to have a very good activity against CYP24A1, as the most active compound, which is 2-[1-(2-ethylphenyl)methylidene]-6-methoxy-1,2,3,4-tetrahydro-1-naphthalenone showed IC_{50} of 1.92 μM which about 4 folds less potent than ketoconazole (IC_{50} = 0.52 μM). As for the azoles, it seems that the azoles would be much more active than the tetralone derivatives as *N*-[2-(1*H*-1-imidazolyl)-2-phenylethyl]-4-[(*E*)-2-phenyl-1-ethenyl] benzamide displayed greater inhibitory activity (IC_{50} = 0.3 μM) than the standard ketoconazole (IC_{50} = 0.52 μM). As a result of this work, it seems that the azole type of these compounds could be of interest for future development.

Contents

1. Introduction

1.1. Cytochrome P450:

Each day we are barraged by a bestiary of exotic chemicals. Our food is filled with unpleasant compounds: the plants we eat contain complex poisons and cooking forms a variety of reactive scorched molecules. Living in an industrial society, we are subject to all manner of pollutants. Our vices dose us with depressants and stimulants. Fortunately, we effectively recognise, transform, and eliminate these dangerous molecules, rendering them harmless. The human body is designed to absorb carbon-rich molecules, so that we can use the fats and vitamins in our diet. Unfortunately, many unwanted molecules, such as poisons and drugs, are also swept along with these nutrients into the body. To make matters worse, we are not designed for excreting these foreign carbon-rich molecules. The urinary system and digestive system are best at removing soluble compounds, such as urea. So, to ensure that carbon-rich toxins do not accumulate and poison us, we have a special system to take these molecules and make them more soluble, and thus more suitable for elimination. Cytochrome P450 **(Figure 1.1)** is at the heart of this transformation system [1].

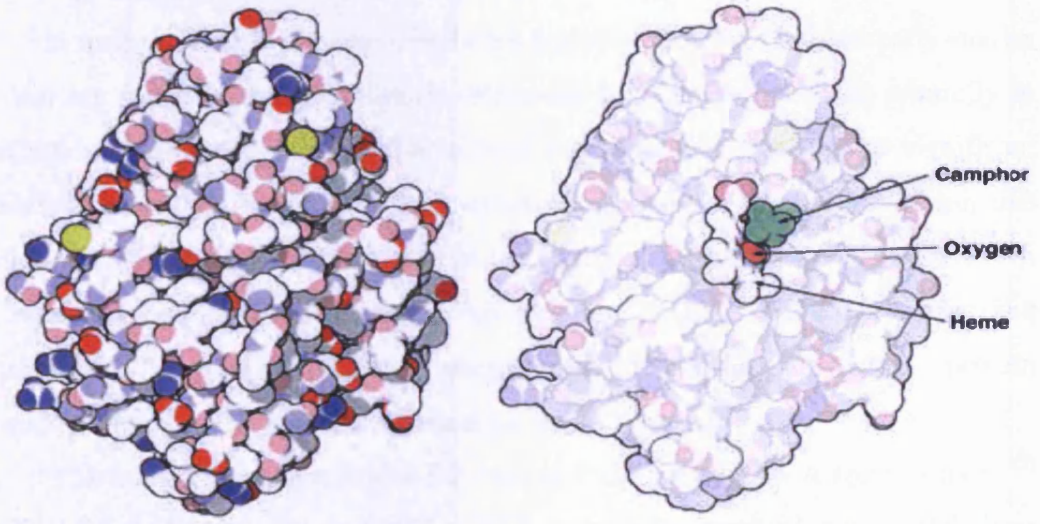

Figure 1.1. Cytochrome P450. The molecule shown here is from a bacterial cell that can grow using camphor as its sole source of carbon. This bacterial cytochrome P450 is free-floating in the cell, whereas our own enzymes are typically tethered to the surface of the endoplasmic reticulum. Coordinates were taken from entry 1dz8 at the Protein Data Bank (www.pdb.org).

1.1.1. Historical introduction:

Perhaps the beginning of the cytochrome P450 monooxygenase story [2] should acknowledge the early compilation of knowledge of the metabolism of xenobiotics (compounds foreign to the body) by R.T. Williams in 1947 and the subsequent, much larger volume [3]. From such studies, as well as work from the laboratories of Brodie [4] and Miller [5], it became clear that liver microsomes were the source of NADPH-dependent, oxidative enzymes capable of metabolising a number of xenobiotics. While an extremely large number of compounds are known substrates of the liver microsomal enzymes, the types of the reactions that are catalysed are finite and the manner of oxygen activation appears to be common for all of the mechanisms. It is clear that the active catalyst in the process is the haemoprotein cytochrome P450.

The name cytochrome P450 is derived from the spectral properties of this haemoprotein. In its reduced (ferrous form), it binds carbon monoxide to give a complex that absorbs light maximally at 450 nm.

1.1.2. Distribution and types of cytochrome P450:

In mammals, all P450s are membrane bound, a fact that hindered early studies [6]. Most are found in the endoplasmic reticulum, but five are localised primarily in mitochondria. However, work by Avadhani's group has revealed that significant fractions of several of the P450s that are usually considered to be microsomal can also localise to mitochondria [7]. The P450s in the endoplasmic reticulum all interact with and receive electrons from a single flavoprotein, NADPH–P450 reductase. The mitochondrial P450s use an electron transport chain with the iron–sulphur protein adrenodoxin and the flavoprotein adrenodoxin reductase.

The human genome encodes fifty-seven P450 proteins [8]. A recent survey [9] classified fifteen P450s, such as CYP1, CYP2, and CYP3, involved in the metabolism of xenobiotic chemicals (i.e., chemicals, such as drugs, not normally found in the body); fourteen primarily involved in the metabolism of sterols (including bile acids); four that oxidise fat-soluble vitamins, such as CYP26A1; and nine involved in the metabolism of fatty acids and eicosanoids, such as CYP11, CYP17 and CYP19. Substrates (either xenobiotic or endobiotic) are essentially unknown for the remaining fifteen of the fifty-seven.

1.1.3. P450s as therapeutic targets:

Some P450s are well-established targets for rational drug design [6]. Chief among these is CYP19A1, the aromatase enzyme. This P450 catalyses the three-step oxidation of androgens to oestrogens; decreased expression of CYP19 is desirable in oestrogen-dependent tumours [10]. Another long-standing target is CYP5A1, usually known as thromboxane synthase [11].

Other P450s are less well developed as targets. One possibility for further study is CYP3A4, the main human P450 in liver and small intestine. Research has been undertaken to find safe and effective inhibitors of CYP3A4 in order to enhance the bioavailability of expensive drugs such as HIV protease inhibitors. However, most of these studies are still in their infancy [6].

1.1.4. P450s and their endogenous substrates:

The majority of the P450s with known functions are those that oxidise steroids and vitamins [6]. Historically, less attention has been given to these P450s by pharmacologists working in drug metabolism, probably because of the relatively narrow range of substrate selectivity among these P450s. Most of the available information at the molecular level has developed in the last five to ten years. Associated with defects in at least thirteen different human P450s are several diseases, including glaucoma (CYP1B1), adrenal hyperplasia (CYP11A1, CYP21A2), mineralocorticoid excess (CYP17A1), and rickets (CYP27B1) [12]. The endogenous P450 substrates may be divided into several major classes (**Table 1.1**): cholesterol and bile acids; steroids; prostaglandins; vitamins A and D; and other eicosanoids. P450s in these five categories generally do not contribute to the metabolism of drugs.

Substrates	P450
Cholesterol and bile acids	CYP7A1, CYP7B1, CYP8B1, CYP27A1, CYP39A1, CYP46A1, CYP51
Steroids	CYP11A1, CYP11B1, CYP11B2, CYP17A1, CYP19A1, CYP21A2
Prostaglandins	CYP5A1, CYP8A1
Vitamins A and D	CYP24A1, CYP26A1, CYP26B1, CYP27A1, CYP27B1, CYP2R1
Other eicosanoids	CYP2C8, CYP2C9, CYP2J2, CYP4A11, CYP4B1, CYP4F2, CYP4F3, and CYP4F8

Table 1.1. Endogenous substrates of P450s.

1.2. Retinoids:

The retinoids are a class of chemical compounds that are related chemically to vitamin A. They are either natural analogues such as: retinoic acid and retinol, or synthetic analogues such as: etretinate and acitretin.

Retinoids, either natural or synthetic derivatives, are known to play a crucial role in cellular and tissue differentiation [13] and that is why retinoids are used in medicine.

1.2.1. Types:

According to the basic structure, retinoids can be classified into four main generations:

1) First generation retinoids:

These retinoids contain a β-ionine ring and include retinol, retinal, tretinoin (Retin-A), isotretinoin and alitretinoin **(Figure 1.2)**.

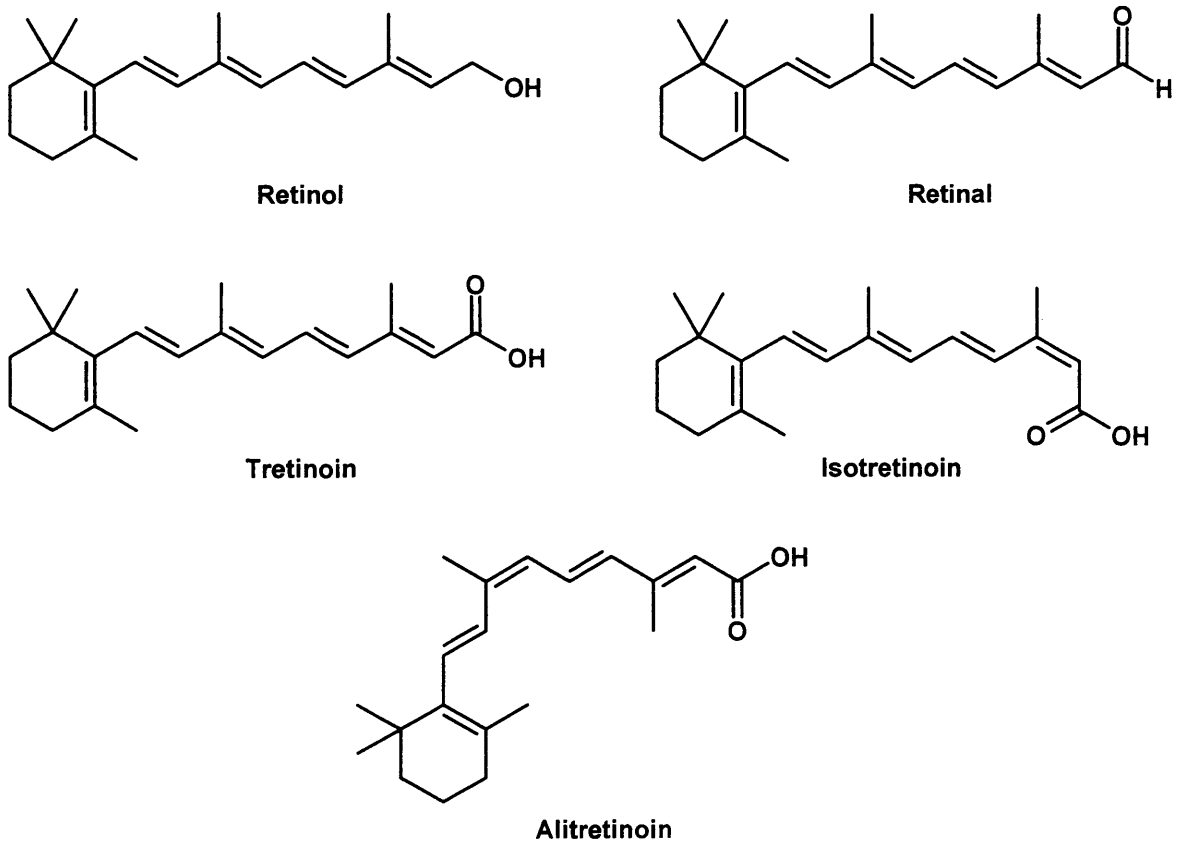

Figure 1.2. First generation retinoids.

2) Second generation retinoids:

The second generation retinoids **(Figure 1.3)** have an aromatic ring in place of the β-ionine ring and include etretinate and its metabolite acitretin .

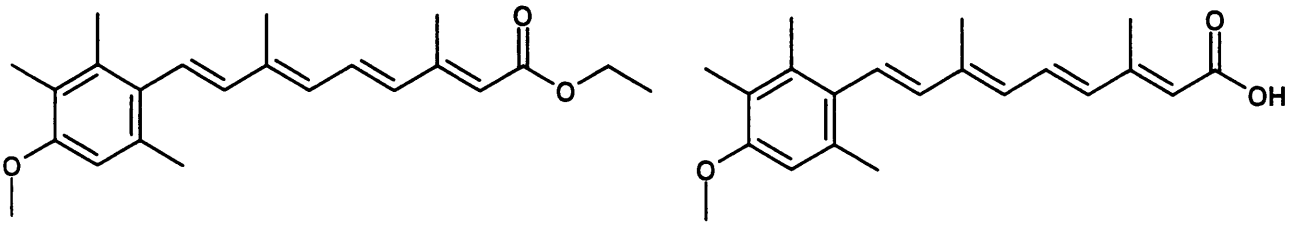

Etretinate **Acitretin**

Figure 1.3. Second generation retinoids.

3) Third generation retinoids:

They have two aromatic rings and so they are less flexible. They include tazarotene and bexarotene **(Figure 1.4)**.

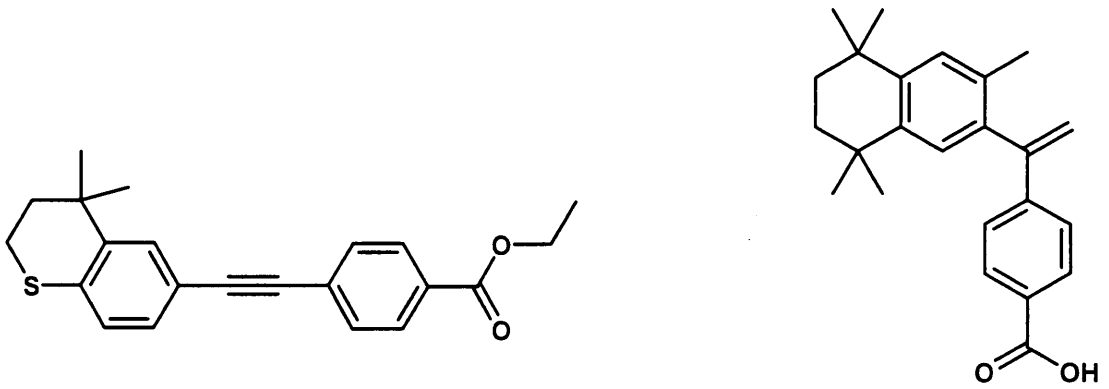

Tazarotene **bexarotene**

Figure 1.4. Third generation retinoids.

4) Acyclic retinoid [14]:

This is a novel synthetic retinoid, with a 20 carbon acyclic structure **(Figure 1.5)** that binds to the cellular retinoic acid–binding protein (CRABP) and has relatively low toxicity.

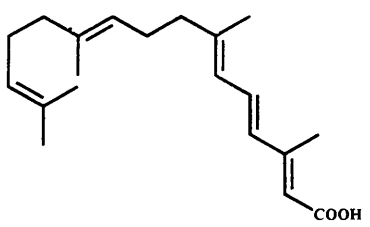

Figure 1.5. Chemical structure of acyclic retinoid (polyprenoic Acid).

1.2.2. Mechanism of action of retinoids:

The actions of retinoids are mediated through the nuclear retinoid receptors, which are members of the steroid/thyroid/retinoid hormone receptor family [13,15]. Retinoid receptors act as ligand-inducible transcription factors that enhance the transcription of target genes by binding to retinoic acid response elements (RAREs) in the promoter region of retinoid-responsive genes. The retinoid receptors can be divided into six regions, designated A through E [16,17] **(Figure 1.6)**. The C domain is a cysteine-rich DNA-binding domain which contains two zinc finger structures. The E domain contains the ligand (retinoid)-binding site and also has a region required for dimerisation with other receptors. The amino acid sequences of the C and E domains are highly conserved across the classes of retinoid receptors, whereas the A, B, and F domains are less conserved across receptors but remain highly conserved for the same receptors across different species.

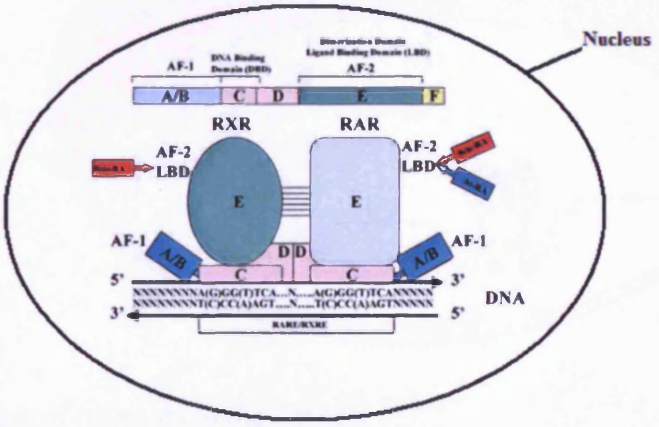

Figure 1.6. Retinoid receptors (modular structure) [17].

Two families of retinoid nuclear receptors have been described, the retinoic acid receptors (RARs) [19,20] and the retinoid X receptors (RXRs) [21,22]. The RARs (α, β, and γ) bind the naturally occurring retinoid all trans retinoic acid (ATRA) with high affinity, whereas the RXRs (α, β, and γ) do not bind ATRA [23]. 9-*cis*-retinoic acid (9*c*RA) is a naturally occurring, biologically active isomer of ATRA [24] that is capable of binding and transactivating both the RXRs as well as the RARs. This multiplicity of receptors and gene pathways may in part explain the diverse effects of retinoids on a wide range of cellular processes.

Under normal physiologic conditions, the concentration of ATRA and other naturally occurring retinoids is under tight metabolic control. The physiological

plasma concentration of ATRA is approximately 5 nM [25]. Although circulating ATRA enters cells via passive diffusion, its contribution to intracellular ATRA levels is likely to be inconsequential under normal conditions because cells derive retinoic acid from intracellular oxidation of retinaldehyde, a metabolite of retinol [26]. Intracellular ATRA is bound to specific binding proteins, the cellular retinoic acid binding proteins (CRABPs) [27] **(Figure 1.7)**. CRABP I and CRABP II are highly conserved throughout evolution and appear to regulate the amount of retinoic acid capable of binding to their nuclear receptors [28]. Binding of ATRA to CRABP appears to facilitate intracellular oxidative catabolism of ATRA to the inactive metabolite, 4-hydroxy-retinoic acid [29].

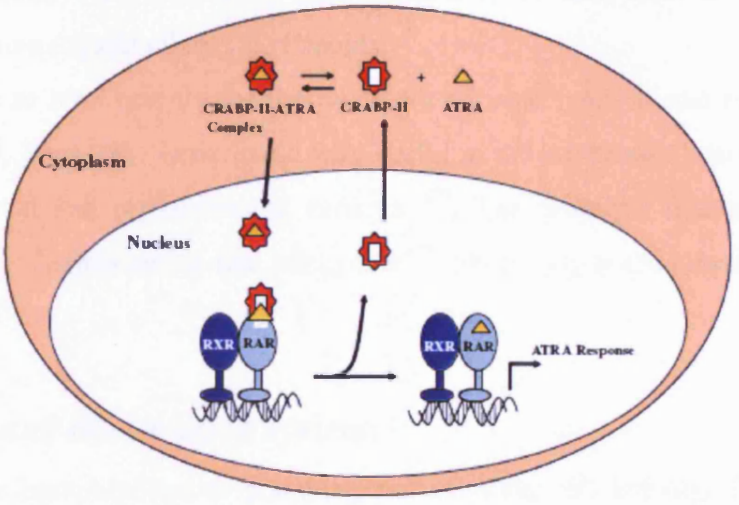

Figure 1.7. Binding of retinoids to the CRABP [30].

1.2.3. Clinical uses and trials of retinoids:

1.2.3.1. Retinoids and cancer:

The relationship between retinoids and cancer has been known for many years [31] and has been reviewed by several investigators [32,33]. Retinoids have been demonstrated to inhibit development of a number of different types of tumours such as: epithelial tumours associated with the skin [34,35], respiratory tract [36], colon [37], mammary glands [38] and prostate cancer [39]. They also have been found to be effective in treatment of cancers occurring secondary to immune deficiency such Kaposi sarcoma [40,41] and to inhibit the growth of a variety of neoplastically transformed cells, such as HL-60 promyelocytic leukaemia cells [42] by differentiating these cells [43], suggesting their potential role as a cancer chemotherapeutic agent.

Also retinoids have been evaluated as chemopreventive agents, and found to be effective in suppressing tumour development in several carcinogenesis models, including those of the skin, breast, oral cavity, lung, prostate, bladder, liver and pancreas [44, 45]. Administered either topically or systemically, in the diet or intragastrically, and before, concurrently or after a carcinogen or a tumour-promoting agent, certain retinoids were found to possess differentiating activity.

1.2.3.2. Retinoids and dermatology:

The use of natural retinoids preceded the use of synthetic retinoids in dermatological condition. However the development of synthetic retinoids, such as isotretinoin and etretinate, with less toxicity than the natural retinoids resulted in the study of different dermatological effects of retinoids.

The retinoids are used mainly for the treatment of acne vulgaris and related acne form diseases [46]. They have been found very useful in the treatment of psoriasis vulgaris and its pustular and erythrodermic variants [47]. The profound first use of retinoids in disorders of keratinisation like ichthyosis [48] often ends at the mention of potential side effects [49].

1.2.3.3. Retinoids and the immune system:

Retinoids have been reported to potentiate natural killer cell activity, T-cell-mediated cytotoxicity, antibody responses, and macrophage functions [50]. Mononuclear phagocytes (monocytes/macrophages) play a key role in host immune responses and may also be involved in mediating the immunopotentiating effects of retinoids [50]. Retinoids have been shown to modulate several mononuclear phagocyte functions, such as IL-1 production, tumoricidal activity, phagocytosis, Fc receptor expression, and synthesis of macrophage tissue transglutaminase [51]. Both retinoic acid and retinyl palmitate have been reported to stimulate production of IL-1 from murine peritoneal macrophages, human peripheral blood mononuclear cells, and a murine macrophage cell line [52]. Retinoids may be causing an increased production of IL-1 through inducing increased gene expression. It has been assumed that retinoids regulate cellular functions through alteration of gene expression [53]. Thus, retinoids may be altering macrophage functions at the transcriptional level.

1.2.3.4. Miscellaneous Uses:

The retinoids also show promising results in many other fields, which include suppressing growth of vascular smooth muscle cells (SMCs) from the systemic and pulmonary circulation in asthmatic patients [54], decreasing the hypertrophic process after myocardial infarction [55] and accelerating wound healing through reversing the inhibitory effects of glucocorticoids and enhancing the formation of healthy granulation tissue [56].

1.2.4. Resistance to Retinoids:

Resistance almost invariably develops when ATRA is administered as a maintenance agent on a daily basis [13]. The precise mechanisms of resistance have not been determined, but there are several potential mechanisms, based on the assumptions that a threshold concentration of free retinoic acid must be achieved at the site of nuclear receptors and that receptor-bound ligands are required to activate target genes. Thus drug resistance could develop as a result of:

A) alteration to the retinoic acid receptor, RARα;

B) alterations in the mechanisms regulating intracellular retinoic-acid binding and metabolism; or

C) insufficient concentrations of ATRA, which result from rapid upregulation of its catabolism through a specific type of cytochrome endogenous P450 which is CYP26A1.

The following section will focus on the specific endogenous P450, CYP26A1.

1.3. CYP26A1:

1.3.1. Definition and History:

CYP26A1 (P450RAI) is a cytochrome P450 enzyme that specifically metabolises retinoic acid (RA) **(Figure 1.8)**. It was first cloned and characterised from zebrafish [57].

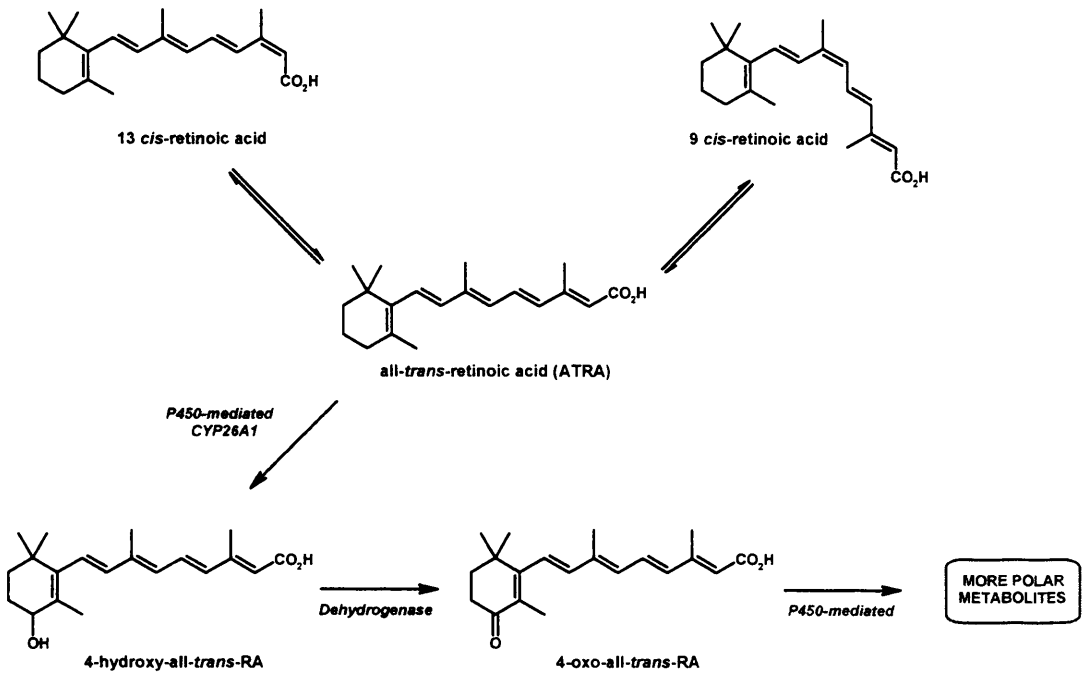

Figure 1.8. Metabolism of RA. [58]

CYP26A1 metabolises RA to more polar derivatives including 4-hydroxy retinoic acid (4-OH RA), 18-hydroxy retinoic acid (18-OH RA) and 4-oxo retinoic acid (4-oxo RA) [59].

1.3.2. Distribution and role of CYP26A1:

CYP26A1 is expressed in the liver, heart, pituitary gland, adrenal gland, testis, duodenum, colon, and in specific regions of the brain and the placenta [60-62]. Based on recent studies [61], it is suggested that the major role of CYP26A1 is a protective one, that is, the regulation of intracellular ATRA steady-state levels, exhibiting a similar negative feedback as has been demonstrated for CYP24, which is involved in cholecalciferol catabolism [30,63].

Although the major retinoid products (4-hydroxy- and 4-oxo-ATRA) of CYP26A1 were originally considered to be inactive retinoids, there is compelling evidence to suggest that they are highly active modulators of positional specification in amphibian embryonic development and they bind and activate RAR subtypes as efficiently as ATRA [64, 65]. Thus, in development CYP26A1 may fulfil functions distinct from metabolic inactivation of ATRA.

CYP26A1 is readily induced by ATRA in a variety of normal and some cancer cells (MCF7, T47D, NB4, HepG2, HPK1A, and LNCaP) and the enzyme efficiently

converts ATRA into its oxygenated derivatives. Although the therapeutic potential of ATRA has been demonstrated, a major drawback to its clinical application is the prompt emergence of resistance, attributed to the induction of oxidative catabolism through CYPs [66-69], and CYP26A1 could be a major contributor. Because ATRA deficiency is associated with the progression of some cancers [70-72], it is possible that ATRA-induced CYP26A1 is involved in rapid metabolism of ATRA in cancer patients. In addition, it is firmly established that inappropriate metabolism of ATRA by CYPs can generate a condition of retinoid deficiency, which is characterised by hyperkeratinisation and desquamation as seen in dermatological diseases such as acne, psoriasis, and ichthyosis [73].

The cloning and characterisation of CYP26A1 represents an important development in ATRA (retinoid) biochemistry and molecular biology. The enzyme's inducibility by ATRA and its ATRA metabolic/catabolic activity define a feedback loop, which may be critical in regulating both normal and therapeutic levels of ATRA. This emphasises the importance of maintaining stable physiological levels of ATRA. Thus, compounds designed to inhibit CYP26A1 activity may be useful in elevating normal tissue ATRA levels or maintaining high therapeutic levels of ATRA. As stated earlier, since ATRA has proven useful in the treatment and/or chemoprevention of some cancers and skin disorders, it is now possible to investigate the contributions of the expression/activity of CYP26A1 (or lack thereof) in various diseases [30].

CYP26A1 has recently been mapped to human chromosome 10q23–q24 [74], a region where several suppressor gene loci have been described [75] as well as the split-hand-split foot syndrome (SHSF-3) [76]. Thus, it is possible that mutations in CYP26A1 may play a role in these diseases. On the other hand, CYP26B1 is localised on chromosome 2P12 with 6 exons and codes 512 amino acid proteins [77]. CYP26C1 is not widely expressed in the adult but is inducible by ATRA in HPK1a, transformed keratinocyte cell lines, and it is suggested that it may play a specific role in catabolising both ATRA and 9-*cis*-retinoic acid (9*c*RA) [78].

1.3.3. CYP26A1 Inhibitors:

A number of ATRA-metabolism inhibitors have been developed over the past 20 years. Early studies focused on the antimycotics **(Figure 1.9)**, ketoconazole, miconazole and clotrimazole [79,80], which showed moderate inhibition of RA

metabolism, but in the following years, many compounds have been investigated.

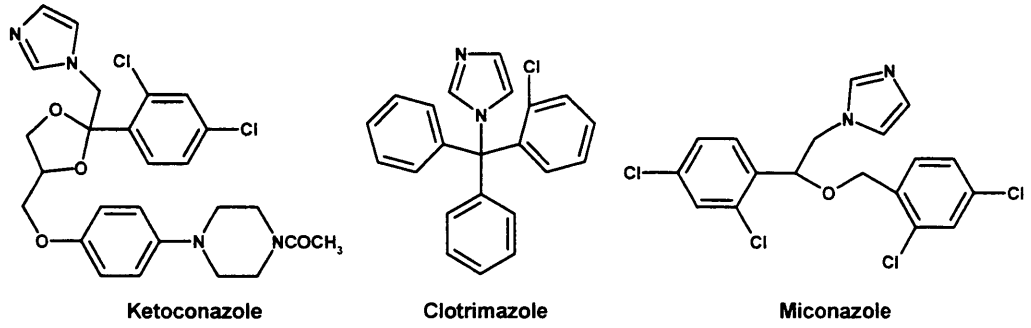

Figure 1.9. Chemical structures of antimycotics.

1) Liarozole and related compounds:

Liarozole **(Figure 1.10)** is the only retinoic acid metabolism blocking agent (RAMBA) that has been evaluated clinically in patients with cancer. Liarozole is an imidazole-containing compound that inhibits the cytochrome P450-dependent metabolism of ATRA. *In vitro,* Liarozole (IC_{50}, 2.2 μM) suppressed the P450-mediated conversion of RA to more polar metabolites by hamster liver microsomes. *In vivo,* it enhanced the plasma level of RA from mostly undetectable values (less than 0.5 ng/mL) in control rats to 1.4 ± 0.1 and 2.9 ± 0.1 ng/mL in animals treated orally with 5 and 20 mg/kg of liarozole, respectively [81]. Although Liarozole displays good activity, its use is limited due to the adverse side effects and lack of specificity toward CYP enzymes [82].

Two other Liarozole analogues have been investigated; R115866 (talarozole [83]) and R116010 **(Figure 1.10)** that showed potent activity. With regard to potency, R115866 is a nanomolar (IC_{50} = 4 nM) inhibitor of the CYP26A1-dependent RA conversion and about three orders of magnitude more powerful than liarozole (IC_{50} = 2.2 μM). As for its selectivity, R115866 shows trivial inhibitory effects on the CYP-dependent formation of testosterone and oestradiol, whereas liarozole suppressed the biosynthesis of these gonadal hormones more potently (IC_{50} = 0.2–0.3 μM) than the RA conversion by CYP26A1 [84].

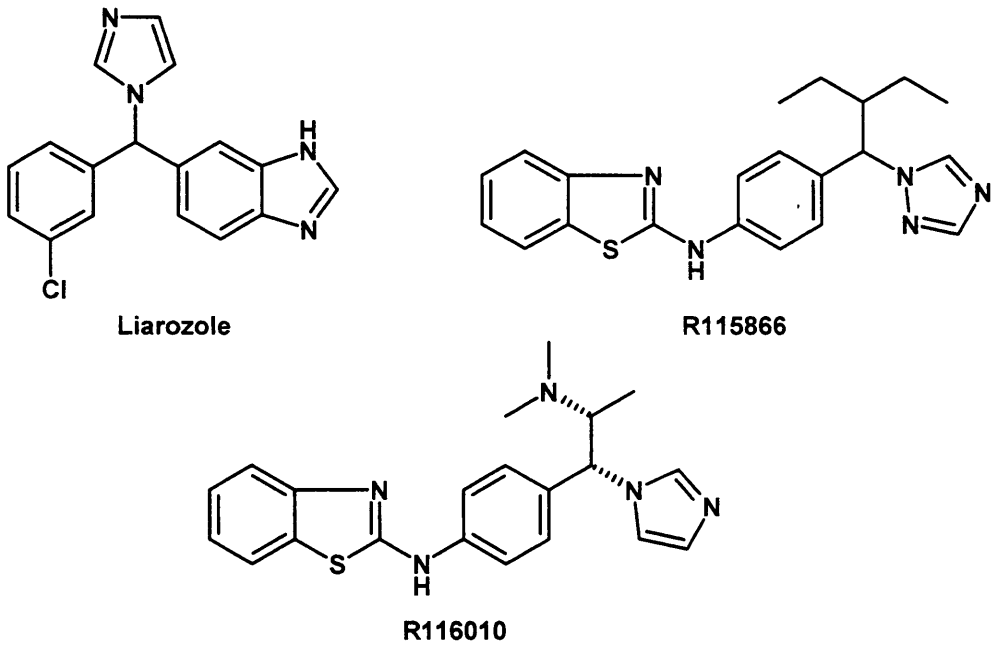

Figure 1.10. Structures of liarozole, R115866 and R116010.

In intact T47D cells, R116010 potently inhibits RA metabolism with an IC_{50} value of 8.7 nM. As such, R116010 is more than 100-fold more potent than liarozole-fumarate, R116010 is also more selective compared with liarozole-fumarate [85].

Another series of benzofuran triazoles (a) **(Figure 1.11)** was synthesised in an effort to enhance the activity of liarozole, but these compounds showed only comparable activity with liarozole [58].

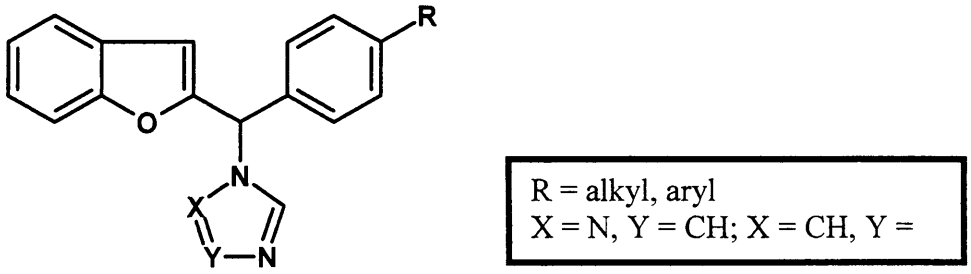

Figure 1.11. Benzofuran triazoles derivatives (a).

2) Azolyl retinoids and related compounds:

These compounds **(Figure 1.12)** have been developed through introduction of an azole group at C-4 of ATRA to yield potent inhibitors of RA metabolism [86-88].

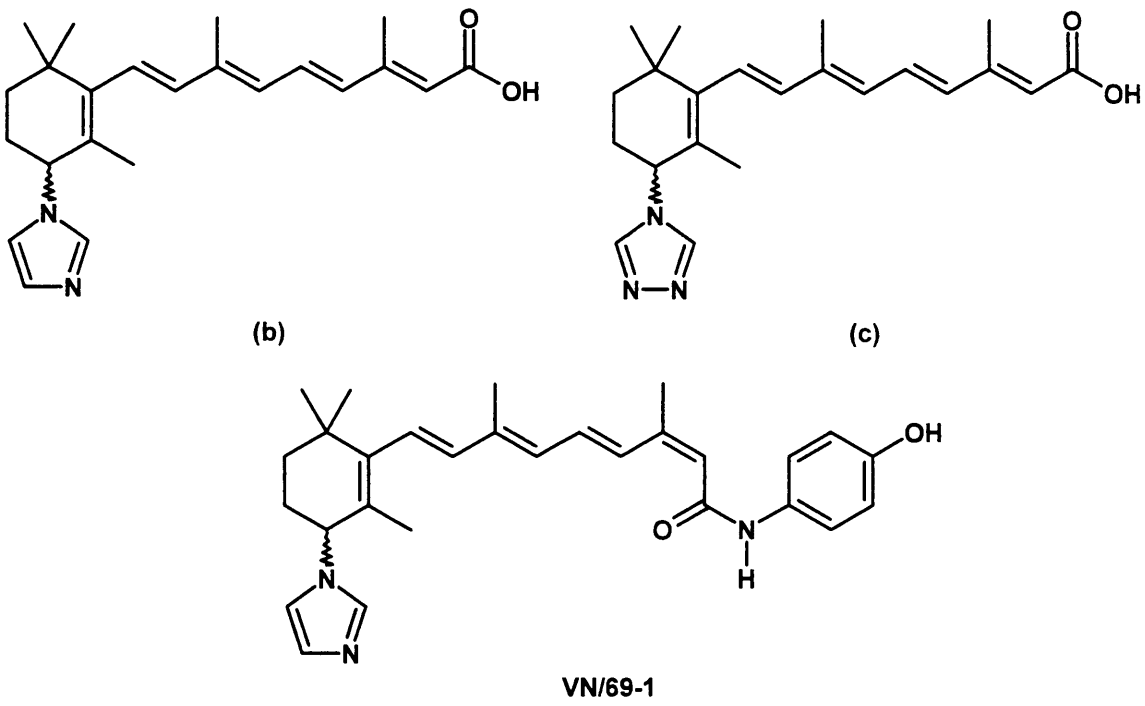

Figure 1.12. Examples of Azolyl retinoids.

In these compounds, the nature of the C-4 substituent is important in determining affinity for the enzyme and also the corresponding methyl esters and imidazole amide are significantly (24- to 48-fold) more potent than the corresponding free acids [86]. Compounds with 4-imidazole substitutions were the most potent inhibitors. Thus, it would appear that the imidazolyl nitrogen lone pair makes the strongest coordination to the iron atom of the haem in the active site of the enzyme.

3) **2,6-Disubstituted naphthyl derivatives:**

The design of these compounds (**Figure 1.13**) depends on fusing the haem-binding imidazolylpropylamino moiety of R116010 with a naphthalene core carrying a CYP26A1 selectivity handle at the 6-position [89-91]. The 2,6-disubstituted naphthalene core, from a 2-D perspective, overlays in a complementary fashion with the conjugated olefinic moiety of the tetraenoic acid side chain of ATRA. Additionally, a suitable tether at the 6-position of the naphthyl core was proposed to mimic that of the ATRA side chain. The presence of a terminal carboxylate increases the selectivity in these compounds.

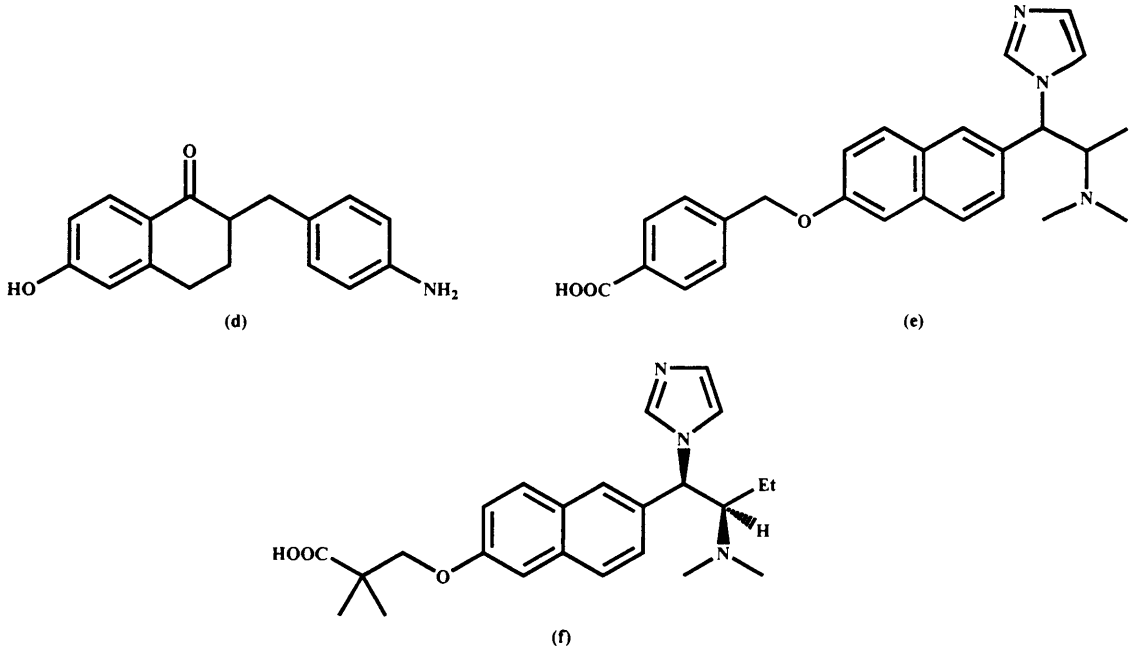

Figure 1.13. Examples of 2,6-disubstituted naphthyl derivatives.

4) Benzeneacetic acid derivatives:

The design of these compounds is not clear, but they show potent activity against CYP26A1. The most potent inhibitor of these compounds with an IC_{50} of 14 nM [92] is shown in (**Figure 1.14**).

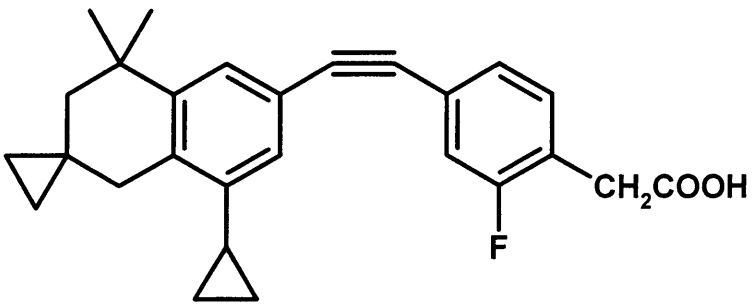

Figure1.14. Most potent derivative of benzeneacetic acid series.

5) Miscellaneous Compounds:

These compounds are of diverse structures (**Figure 1.15**), which include: pyrrolidine derivatives [93], indole derivatives [94], diphenylethane derivatives [95] or tetralone derivatives [96]. These compounds showed moderate activities.

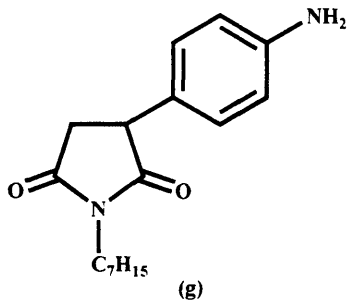

(g)

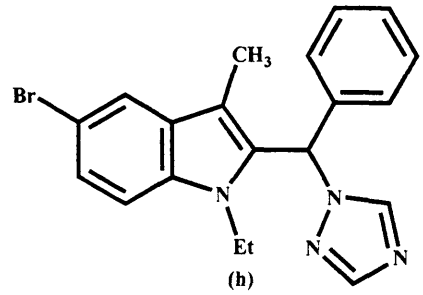

(h)

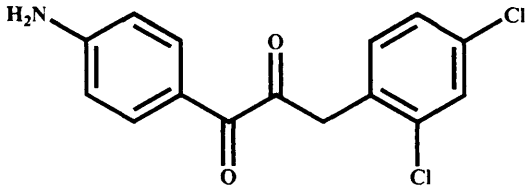

(i)

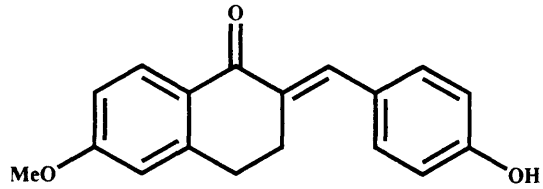

(j)

Figure 1.15. Miscellaneous compounds.

1.4. Vitamin D:

Vitamin D is a group of fat-soluble prohormones. Several forms of vitamin D have been discovered which chemically are secosteroids, i.e. broken-open steroids. They are classified into five forms [97] (**Figure 1.16**):

- D_2: ergosterol.
- D_3: cholecalciferol.
- D_4: 22,23-dihydroergocalciferol.
- D_5: sitosterol (24-ethylcholecalciferol).
- D_6: stigmasterol.

The two major forms of vitamin D, are vitamin D_2 or ergocalciferol, and vitamin D_3 or cholecalciferol.

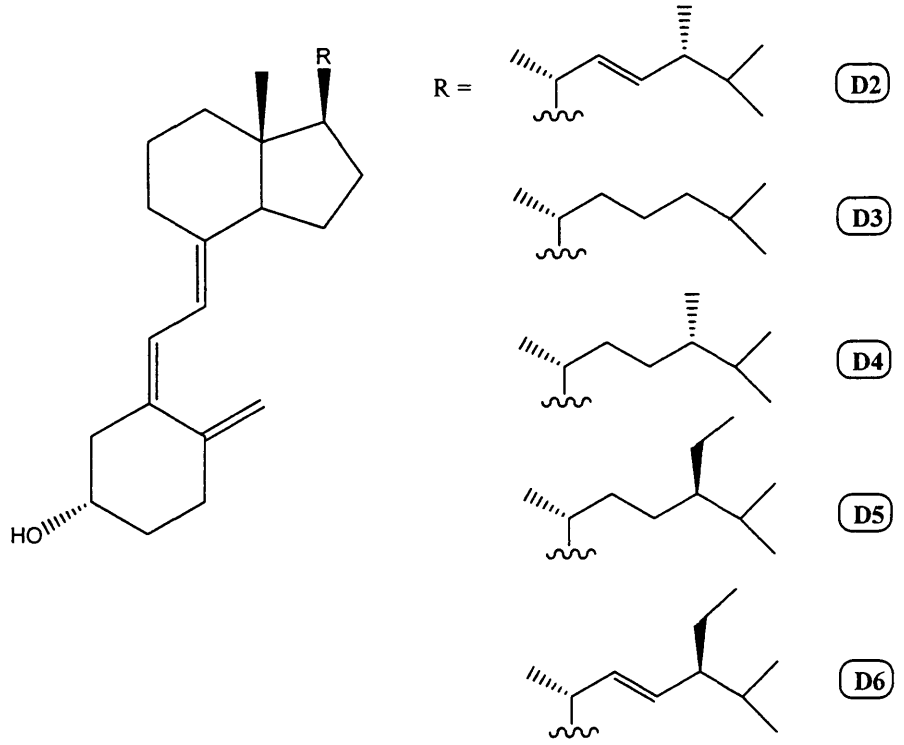

Figure 1.16. Structural differences of vitamin D.

Vitamin D_2 is derived from fungal and plant sources but not produced in the human body. Vitamin D_3 is in the skin when 7-dehydrocholesterol reacts with ultraviolet light with peak synthesis occurring at wavelengths between 295-297 nm [97].

In the next section the focus will be on the most important form of vitamin D, vitamin D_3.

1.4.1. Biosynthesis and Metabolism of Vitamin D_3:

Upon UV irradiation, 7-dehydrocholesterol is converted to previtamin D_3 in the human skin. This precursor is transformed by a rearrangement of double bonds to form vitamin D_3 **(Figure 1.17)**.

The next step that occurs in the liver, involves hydroxylation of vitamin D_3 at carbon 25 to give 25-hydroxyvitamin D_3 (25-(OH)-D_3) by vitamin D_3-25-hydroxylase (CYP27A1). Further processing occurs in the kidney which involves the enzyme 25-hydroxyvitamin D_3-1α-hydroxylase (CYP1α) that introduces a hydroxyl group at the α-position of carbon 1 of the A ring to produce 1α,25-dihydroxyvitamin D_3 (1α,25-$(OH)_2$-D_3) also known as calcitriol which is the hormonally active metabolite. The enzyme 25-hydroxyvitamin D_3-24-hydroxylase (CYP24A1) in the kidney, is involved in the catabolism of 25-(OH)-D_3 and calcitirol to 24,25-dihydroxyvitamin D_3 (24,25-$(OH)_2$-D_3) and 1α,24,25-trihydroxyvitamin D_3 (1α,24,25-$(OH)_2$-D_3) respectively **(Figure 1.17)**.

The degradation of calcitriol to form calcitrioic acid, involves several steps catalysed by the CYP24A1 enzyme via the C-24 oxidation pathway **(Figure 1.17)**.

The three vitamin D_3 hydroxylases mentioned above have been isolated and cloned. Based on their sequence-alignment [98-100], they were found to contain haem-binding and functional domains typical of cytochrome P450 haem protein enzyme [101].

1.4.2. Biological actions of Vitamin D_3:

Vitamin D_3 and its active metabolites play an important role in the maintenance of organ systems:

- Regulation of Ca^{2+} homeostasis: Vitamin D_3 regulates the calcium and phosphorus levels in the blood by promoting their absorption from food in the intestines, and by promoting re-absorption of calcium in the kidneys [102].
- Mobilisation of bone mineral: it promotes bone formation and mineralisation and is essential in the development of an intact and strong skeleton. However, at very high levels it will promote the resorption of bone [102].
- Vitamin D_3 affects the immune system through its influences on cytokine production [103].

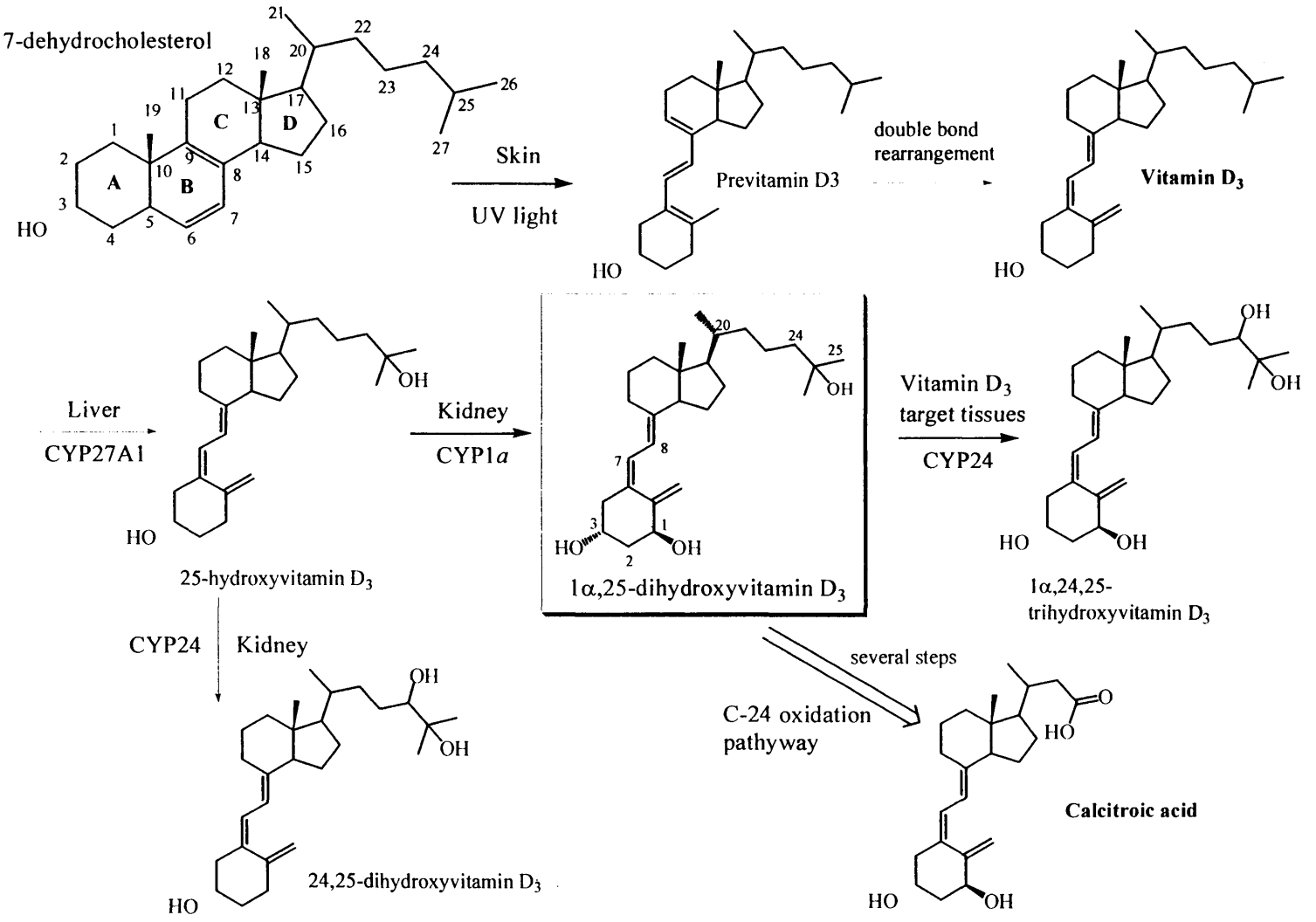

Figure 1.17. Biosynthesis and metabolism of vitamin D_3 [102, 104].

1.4.3. Mechanism of action:

As with vitamin A, most of the effects of vitamin D involve a nuclear receptor. The vitamin D receptor (VDR) is a member of the steroid/thyroid hormone superfamily of receptors. When 1α,25-OH D_3 binds to its receptor, the complex forms a heterodimer with an unoccupied RXR. This heterodimer subsequently binds to the regulatory regions on specific genes in target tissue [105]. These regions are called vitamin D response elements (VDREs). The binding to VDREs can increase or decrease expression of genes. The proteins thus made carry out the functions of vitamin D.

1.4.4. Therapeutic uses of vitamin D:

1) Nutritional Rickets:

Nutritional rickets results from inadequate exposure to sunlight or deficiency of dietary vitamin D [102]. The usual practice is to administer vitamin A in combination with vitamin D. A number of balanced vitamin A and D preparations are available for this purpose. Vitamin D_2 or Vitamin D_3 is used in this condition.

2) Hypoparathyroidism:

Vitamin D_3 and its analogues are a basic therapy of hypoparathyroidism. Dihydrotachysterol (DHT) (**Figure 1.18**) has a faster onset, shorter duration of action, and a greater effect on bone mobilisation than does vitamin D_3 and traditionally has been a preferred agent [102]. Calcitriol (**Figure 1.18**) is also effective in the management of hypoparathyroidism and certain forms of pseudohypoparathyroidism in which endogenous levels of calcitriol are abnormally low [102].

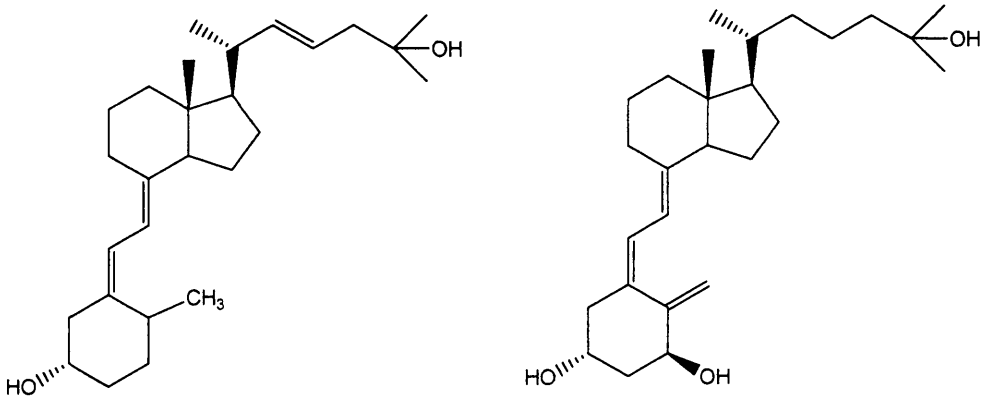

Dihydrotachysterol **Calcitriol**

Figure 1.18. Structures of Dihydrotachysterol and Calcitriol analogues of Vitamin D.

3) Hyperparathyroidism secondary to chronic renal failure:

Hyperparathyroidism is a frequent complication of chronic renal failure and requires close monitoring and treatment to prevent the complications of renal osteodystrophy [102]. Therapy includes prevention of hyperphosphatemia by the administration of phosphate binders (calcium carbonate or acetate) and the use of vitamin D_3 compounds such as calcitriol. For patients on haemodialysis intravenous calcitriol achieves effective suppression of elevated parathyroid hormone (PTH) levels. However, hypercalcemia and/or hyperphosphatemia are frequent complications that limit the calcitriol therapy [102]. Synthetic vitamin D_3 analogues [102], such as: paricalcitol, Calcifediol, Doxercalciferol and Oxacalcitriol (**Figure 1.19**) appear to represent more effective agents to control secondary hyperparathyroidism associated with end stage renal disease since it suppresses intact PTH (IPTH) levels with less impact on calcium and phosphorus metabolism.

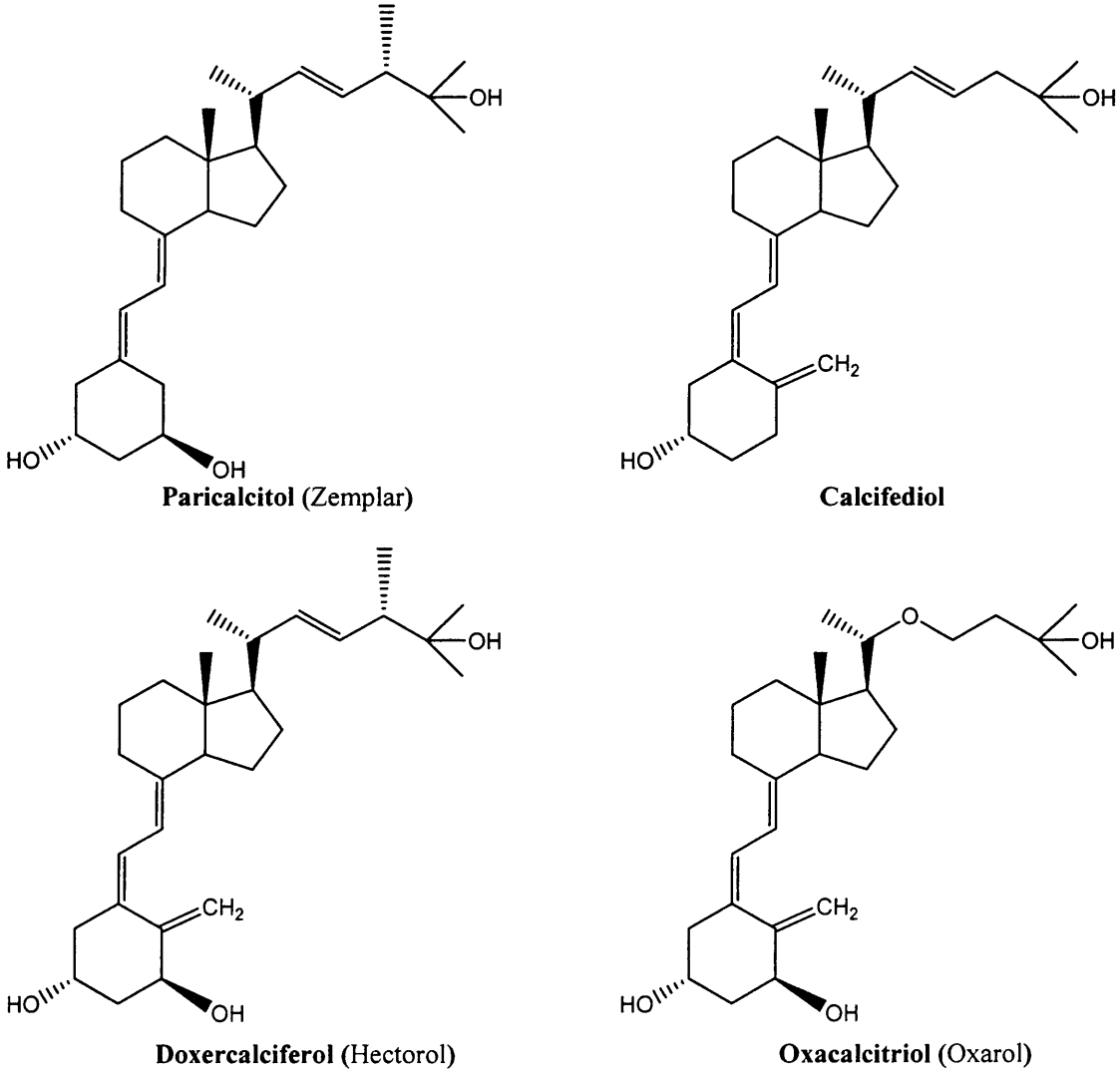

Paricalcitol (Zemplar)

Calcifediol

Doxercalciferol (Hectorol)

Oxacalcitriol (Oxarol)

Figure 1.19. Structures of analogues of Vitamin D used in hyperparathyroidism.

4) Psoriasis:

Calcipotriene (**Figure 1.20**) is a synthetic vitamin D_3 analogue indicated for topical application in the treatment of moderate plaque psoriasis [103]. It has the same affinity for the vitamin D receptor as calcitriol, but its effect on calcium metabolism is 100 to 200 times less [103]. Calcipotriene inhibits epidermal cell proliferation and enhances cell differentiation. It reduces cell numbers and total DNA content [102].

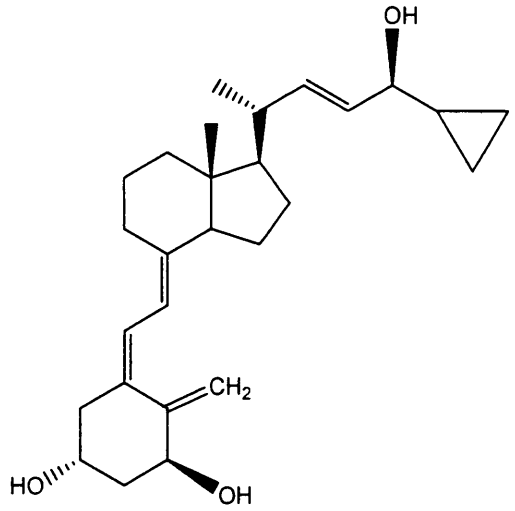

Calcipotriene

Figure 1.20. Structure of Calcipotriene.

1.4.5. Vitamin D and cancer:

There are many studies, which are mostly based on observational or case controlled studies [106], that correlate vitamin D and cancer prevention. The findings by Abe et al. [107] in 1981 that 1α,25-$(OH)_2D_3$ inhibited the proliferation of variety of human leukemic cell lines, led to a considerable interest in the design and synthesis of 1α,25-$(OH)_2D_3$ mimics by the pharmaceutical industry [108].

The major drawback of 1α,25-$(OH)_2D_3$, however, is its effect on calcium metabolism, which results in hypocalcaemia and hypercalciuria [108]. Newly developed vitamin D analogues with lower calcemic activity have been shown to retain many therapeutic properties of 1α,25-$(OH)_2D_3$ [109]. More than 2000 synthetic analogues of the biologic form of vitamin D (1α,25-$(OH)_2D_3$) are presently known [109]. Studies using the human osteosarcoma cell line MG-63 demonstrated that 3 of these analogues (KH1060, EB1089, and CB1093 (**Figure 1. 21**)), have a greater antiproliferative effect than 1α,25-$(OH)_2D_3$ [109]. Several other analogues are currently

being tested in preclinical and clinical trials for the treatment of various types of cancer [109].

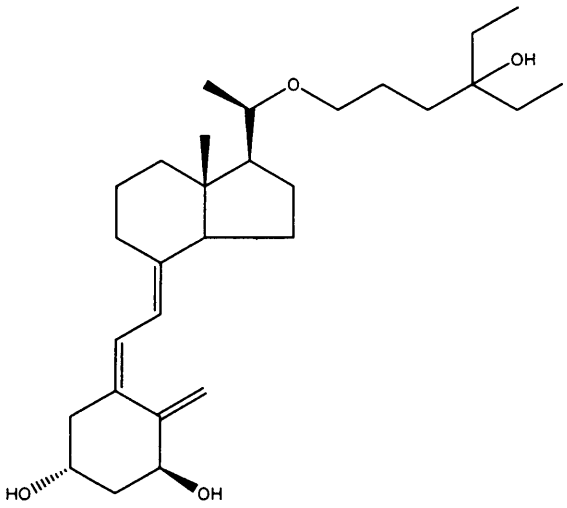

KH1060

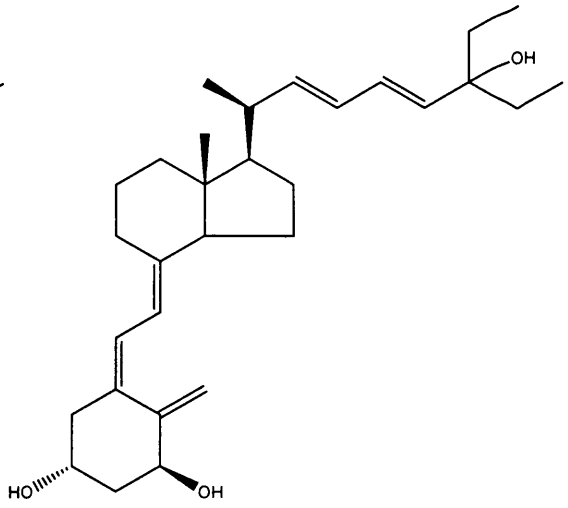

EB1089

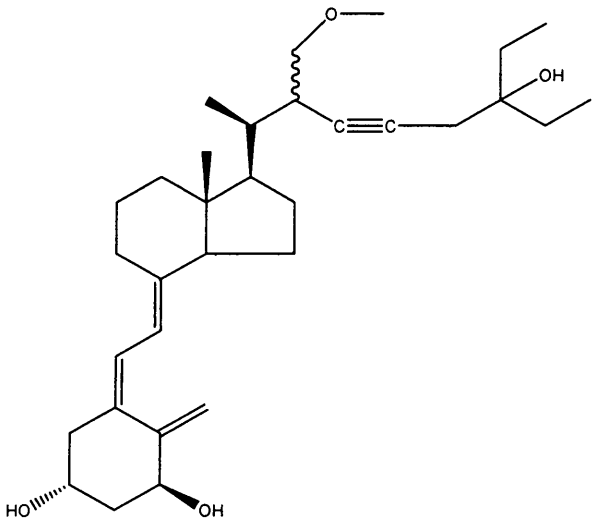

CB1093

Figure 1.21. Vitamin D (1α,25-$(OH)_2D_3$) analogues.

Although the exact mechanism underlying the growth inhibitory actions of vitamin D and its analogues in cancer cells is not fully understood, the volume of data supports a multipronged effect involving [109]:

1) **Cell cycle regulators:**

   The 1α,25-$(OH)_2D_3$-VDR system arrests the cancerous cell cycle at the G_0-G_1 transition through multiple mechanisms [109].

2) **Growth factors and growth factor receptors:**

   The growth inhibition of cancer cells by 1α,25-$(OH)_2D_3$ is also associated with growth factor signalling. Transforming growth factor-h (TGF-h) is a potent

inhibitor of the proliferation of many cell types and is involved in cell cycle control and apoptosis. Vitamin D analogues induce autocrine TGF-h activity through increasing expression of TGF-h isoforms and/or TGF-h receptors in nonmalignant and malignant breast cells [109].

3) **Apoptosis:**

$1\alpha,25\text{-}(OH)_2D_3$-induced apoptosis is an important contributor to the growth-suppressing properties of the sterol in cancer. In cancer cells, $1\alpha,25\text{-}(OH)_2D_3$ analogues induce apoptosis through reciprocal modulation in the antiapoptotic protein Bcl-2 and the proapoptotic protein Bax content [109].

4) **Differentiation:**

$1\alpha,25\text{-}(OH)_2D_3$ regulates proliferation and differentiation of different kinds of cells, including keratinocytes, osteoblasts, and hematopoietic cells [109].

5) **Invasion and metastasis:**

For tumour suppressive activity, besides growth inhibition, vitamin D and its analogues decrease the invasiveness of several cell types *in vitro*, and they inhibit angiogenesis and metastasis in xenograft and transgenic mouse models *in vivo* [109].

1.5. Vitamin D hydroxylase (CYP24A1):

The hydroxylase enzymes that are involved in the metabolism of 25-hydroxyvitamin D_3 (CYP1α and CYP24A1) are members of the cytochrome P450 superfamily [110].

The important role of vitamin D in many physiological and pathological processes [104, 111-112] has attracted many researchers in developing new drugs for targeting the key enzymes in the synthesis or metabolism of the active vitamin D_3 hormone, $1\alpha,25(OH)_2\text{-}D_3$:-

- 25-Hydroxyvitamin D-1α-hydroxylase (CYP27B1 or CYP1α): the key enzymes in the synthesis of the biological active metabolite, calcitriol.
- 1α,25-Dihydroxyvitamin D 24-hydroxylase (CYP24A1): a multicatalytic enzyme, that causes side-chain oxidative cleavage of $25(OH)_2\text{-}D_3$ resulting in calcitroic acid formation [113]. This multicatalytic sequence is also known as the C-24 oxidation pathway **(Figure 1.17)**.

  Although there have been successes in cloning the rat 24-hydroxylase enzyme

and in determining the enzyme's derived sequence [114], structural information from X-ray crystallography or NMR analysis is still missing.

1.5.1 CYP24A1 inhibitors:

Various azole compounds have been shown to inhibit CYP24A1. The azole compounds bind directly to the prosthetic haem iron via a lone pair of electrons from the heterocyclic nitrogen and through interaction with other sites in the binding pockets [115]. A few standard azole compounds from other companies have been shown to inhibit CYP24A1, *e.g.* ketoconazole and liarozole (**Figure 1.9** and **1.10**). The use of CYP24A1 inhibitors could potentially slow down the metabolism and depletion of the active vitamin D hormone, calcitriol.

However, selectivity is a crucial demand in designing CYP24A1 inhibitors in order to avoid impairment of $1\alpha,25(OH)_2$ -D_3 synthesis by 1α-hydroxylase, a distinct, but related mitochondrial CYP.

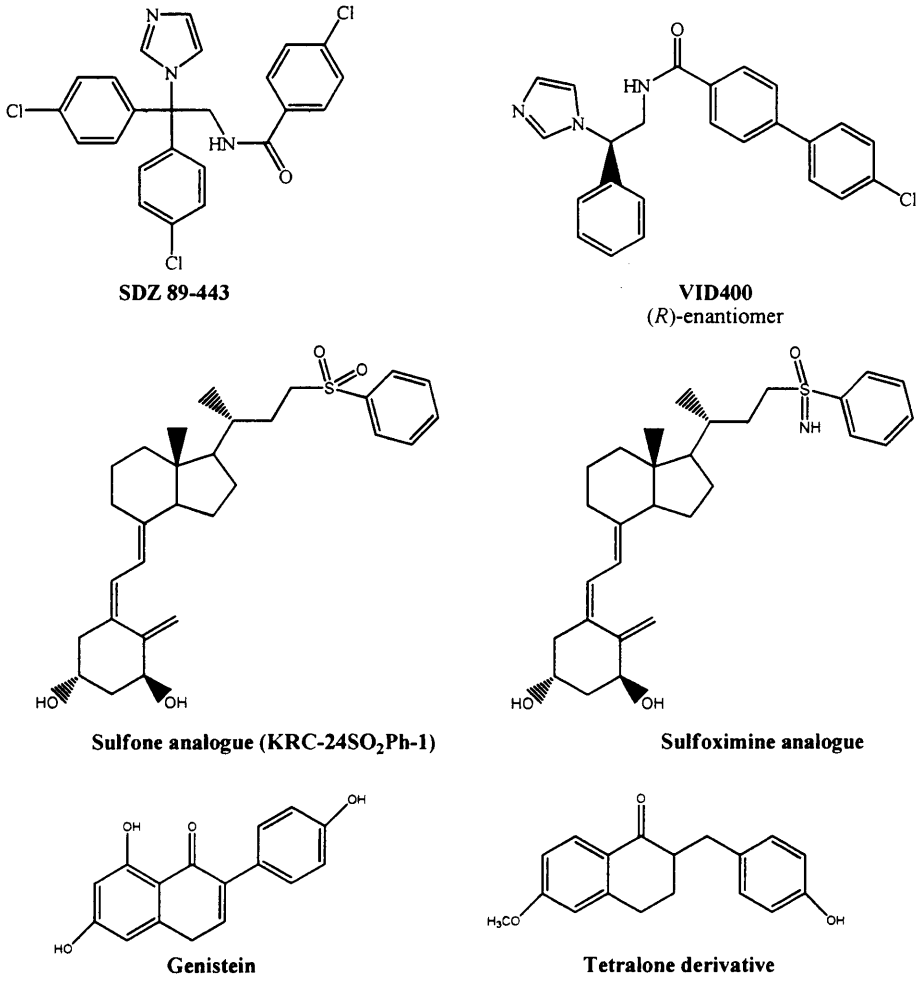

Figure 1.22. Azole and calcitriol analogues which show inhibition of CYP24A1.

SDZ 89-443 and VID400 (**Figure 1.22**) have been identified as potent CYP24A1 inhibitors and also very selective for CYP24A1 compared with CYP27B [116]. These selective inhibitors of CYP24A1 were used by the Schuster group to study vitamin D metabolism in human keratinocytes.

Other compounds that have been described as potent, selective and low-calcemic inhibitors of CYP24A1 include some 24-sulfone [117] and 24-sulfoximine [118] analogues (**Figure 1.22**) of the hormone $1\alpha,25(OH)_2$ -D_3.

It has been postulated from *in vivo* studies, that CYP24A1 inhibitors can be useful agents for the treatment of androgen-independent prostate cancer [119].

Ly and co-workers [120] have added liarozole to calcitriol in an androgen-independent DU145 cell line; this resulted in an increase in the half-life of calcitriol and enhanced up-regulation of the vitamin D receptor. Liarozole, a CYP24A1 inhibitor was also used in Phase II trials for hormone-refractory prostate cancer [121]. There are also promising results from preclinical studies carried out in prostate cancer cells to study the combination of ketoconazole (CYP24A1 inhibitor) with calcitriol [122-123]. It was shown in rat osteosarcoma cells that ketoconazole can inhibit the self-induced metabolism of calcitriol [124].

An enhancement of antiproliferative activity of calcitriol analogues by P450 enzyme inhibitors has been demonstrated in different cell lines. For example, Zhao and co-workers showed that ketoconazole and liarozole (P450 enzyme inhibitors, including CYP24A1 inhibitor) enhanced the antiproliferation of MCF-7 and T47-D breast cancer cell lines, this combination therapy might synergise the anticancer properties [125].

More recently, tetralone derivatives (**Figure 1.22**) synthesised by the Welsh School of Pharmacy group greatly enhanced the apoptotic and the differentiation effect of endogenous calcitriol on prostate cancer cell lines DU-145 and PC-3 by reducing the metabolism of calcitriol resulting in greater inhibition of proliferation of the cancer cells [126]. In vitro studies with genistein (**Figure 1.22.**), a soy isoflavone that is able to inhibit calcitriol metabolising enzyme (CYP24A1), have shown induction of apoptosis and inhibition of cell growth in androgen-sensitive (LNCaP) and androgen-independent (PC3 and VeCaP) prostate cancer cell lines [127].

CYP24A1 inhibitors could be a promising combination therapy together with calcitriol, as indirect differentiation therapy for hormone-refractory (androgen-independent) prostate cancer by sustaining the level of calcitriol and allowing the dose

of calcitriol to be reduced thus reducing the side-effects of calcitriol. This combination has been shown to slow the growth of the prostate cancer cells and restore normal responses to hormonal signalling [126, 128].

2. Aims & Objectives

Aims and Objectives

The aim of this project was to develop new, potent and selective inhibitors of CYP26A1 and CYP24A1 that could be used in the differentiation therapy of different types of cancer, such as prostate and breast cancer.

1) CYP26A1 Inhibitors:

From previous work that has been done within our group, a lead compound (**Figure 2.1**) had been developed [129] which showed very high activity against CYP26A1 with IC_{50} of 2.8 nM in a biochemical based assay.

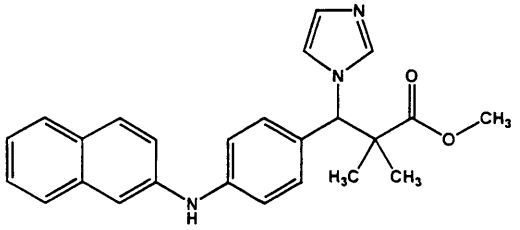

Figure 2.1. The structure of the lead compound.

The aim of this project was to:

1) Build a pharmacophore model for CYP26A1 inhibitors. Molecular Operating Environment (MOE) was used for this purpose.

2) Investigate the effect of changes of the lead structure on the inhibitory activity **Figure 2.2**.

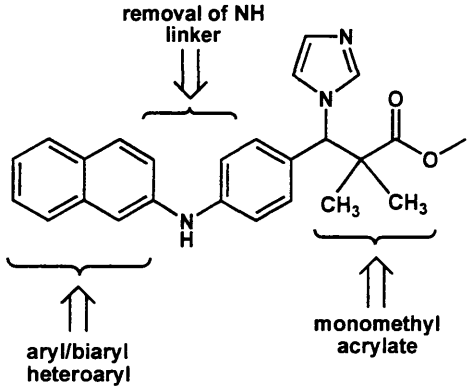

Figure 2.2. Developments in the lead structure.

3) Beside this, we intended to use the produced pharmacophore to build new compounds which could show comparable activity but involved easier synthetic pathways.

2) CYP24A1 Inhibitors:

As there are no available compounds which inhibit CYP24A1 on the market, we hoped to find an inhibitor which is potent and at the same time selective in the inhibition of CYP24A1.

Two series were designed to try to manage this approach. The first series of CYP24A1 inhibitors was chosen to resemble **VID 400**, combined with calcitriol as the lead compound for this series (**Figure 2.3**).

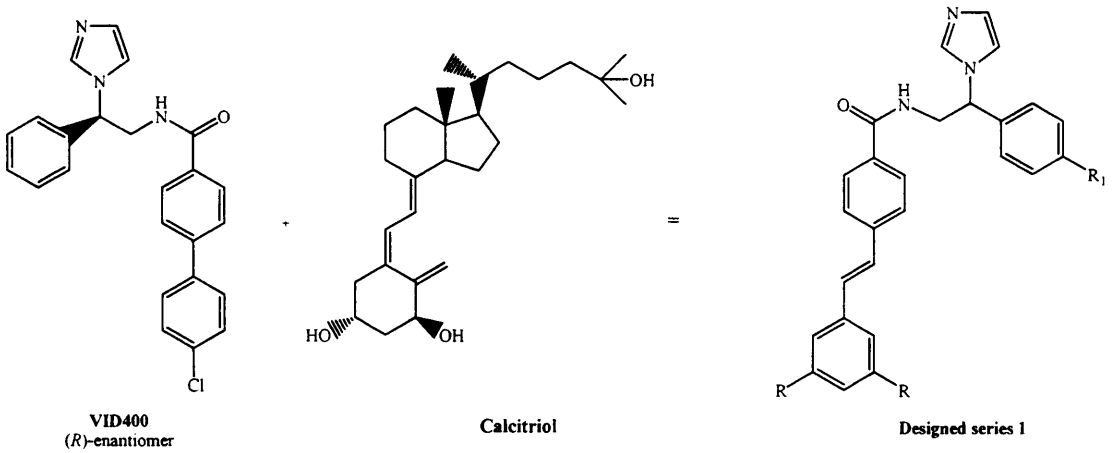

Figure 2.3. Designing of the CYP24A1 first series.

The second series took the tetralone [124] compounds synthesised in our group as the lead compound with modification to increase the activity and the selectivity (**Figure 2.4**).

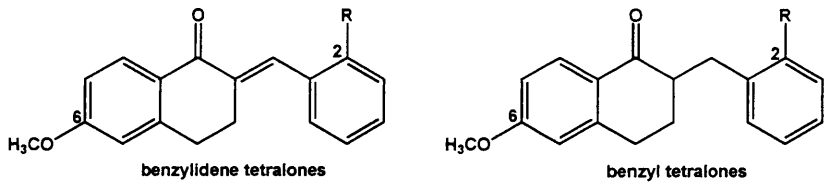

Fig. 2.4. The designed tetralone compounds.

3. Results & Discussion

3.1. CYP26A1 inhibitors pharmacophore modelling

3.1.1. Introduction:

The official definition of pharmacophore elaborated by the IUPAC and published in 1998 [130] is the ensemble of steric and electronic features that is necessary to ensure the optimal supramolecular interactions with a specific biological target structure and to trigger (or to block) its biological response.

A pharmacophore could be considered as the most common features of a group of molecules exhibiting a similar biological activity, which are recognised by the same active site of the target protein.

The concept of pharmacophores as a simple representation of molecules and chemical groups in certain order was introduced about a century ago, there has been increasing interest and focus on pharmacophores in recent years following the advances in computational chemistry research [131].

There are many ways of constructing pharmacophores and several computer-based applications with the ability to build pharmacophores have been introduced since the 1980s [132] such as: APOLLO [133], ALADDIN [134], DANTE [135-138], RAPID [139], SCREEN and its PMapper from ChemAxon [140] and ChemX fingerprints [141] from Chemical Design (now Accelrys). Not all of these programmes are intensively used today.

The representation of pharmacophores varies from one package to another and includes the nature of the pharmacophore points (fragments, chemical features) and the geometric constraints connecting these points (distances, torsions, three-dimensional coordinate location constraints).

There are two main techniques for building pharmacophores [142], which depends mainly on the availability of the three-dimensional structure of the binding site of the target:

1) If the 3D structure of the target is known, the structure-based pharmacophore could be built. Several programmes are available for this task, such as: Cerius^2 software package, available from Accelrys Inc [143], the unity programme available from Tripos Inc [144] and the molecular operating environment MOE software package [145].
2) If the 3D structure of the target is unknown and only the active ligands structures are available, the ligand-based pharmacophore can be used. There are several programmes available for this technique, including Catalyst [146],

available from Accelrys Inc, DiscoTech [147], and Gasp [148], both from Tripos Inc.

3.1.2. Pharmacophores in MOE:

MOE (Molecular Operating Environment) is the modeling platform developed by the Chemical Computing Group. All the applications in MOE have been integrated using the Scientific Vector Language (SVL) [149] and this was the chosen programme for building a CYP26A1 inhibitor pharmacophore.

3.1.3. Building a Pharmacophore model for CYP26A1 Inhibitors:

In this study, a ligand-based three-dimensional model for CYP26A1 inhibitors was developed in an attempt to find a new class of compounds with affinity to CYP26A1.

The Pharmacophore building was performed according to the following steps:

1) As there is no available database for CYP26A1 inhibitors, the first step was the building of the training set database of the CYP26A1 inhibitors.
2) The structures of the CYP26A1 inhibitors are very diverse, therefore the second step was the alignment of the most active CYP26A1 inhibitors instead of alignment of the whole set.
3) Running the Pharmacophore consensus which provides us with the suggested features of the aligned molecules.
4) Using Pharmacophore search together with the Pharmacophores query editor to focus the query.
5) Finally, refining the query using the output results from the Pharmacophore search.

(1) Building the training set:

A set of 71 compounds with biological activity ranging from 0.009 nM to 15.17 μM published in different papers [150-162]. Structures of these compounds are listed below in **Table 3.1.1.** with their activities. The compounds were built using the MOE builder in MOE software package and were minimised to the closest local minimum using the MMFF94s force field implemented in the programme, with 0.00001 gradient. The compounds in the database have been sorted according to their activities, from the highest to the lowest activity.

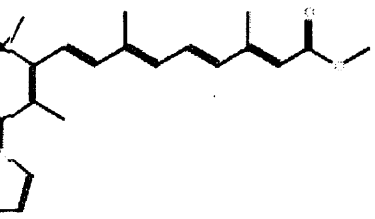

(**a**) 0.009 nM[159]

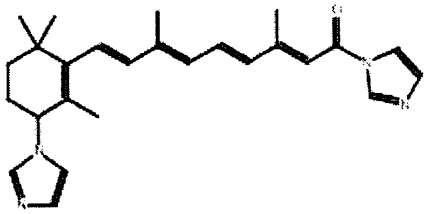

(**b**) 0.05 nM[159]

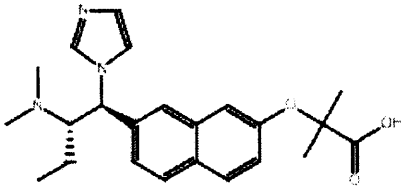

1.3 nM[161]

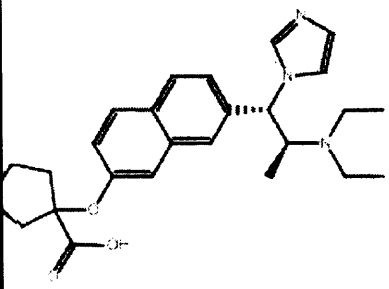

1.4 nM[161]

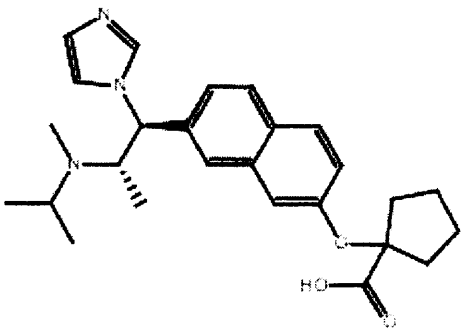

1.6 nM[161]

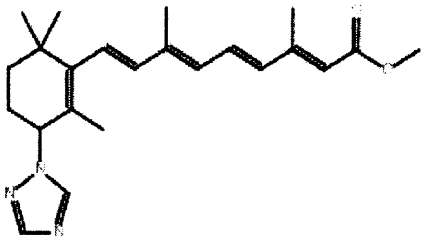

2 nM[159]

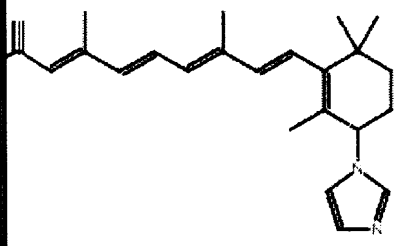

2.33 nM[159]

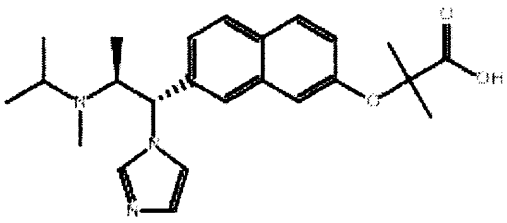

3 nM[161]

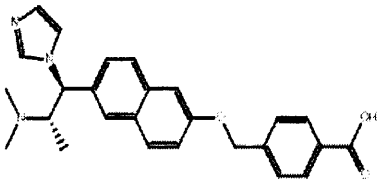

3.3 nM[161]

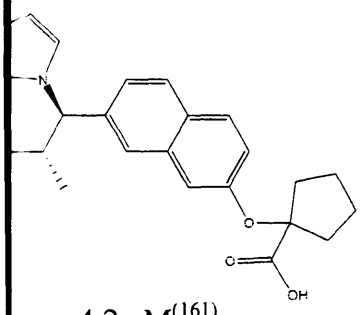

4.2 nM[161]

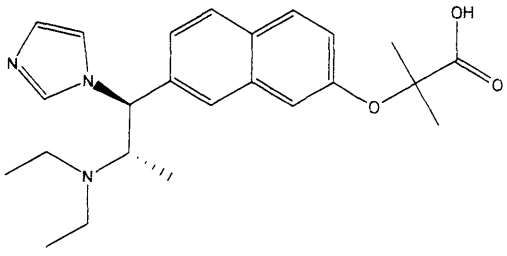

5 nM[161]

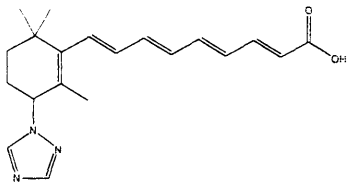

5.84 nM[159]

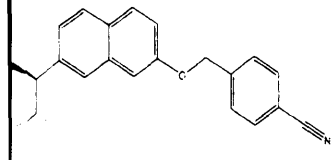

6 nM[161]

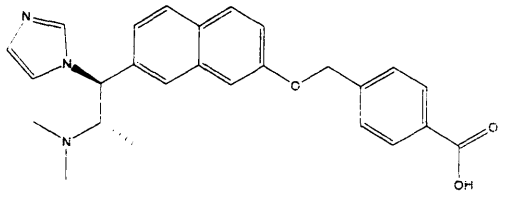

6.3 nM[161]

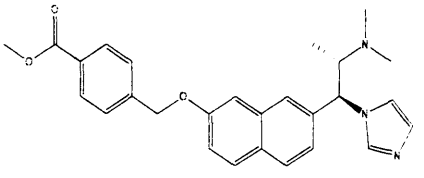

7.0 nM[161]

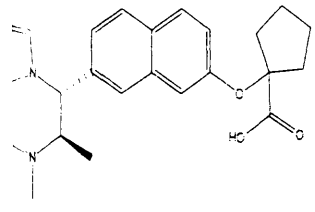

7.4 nM[161]

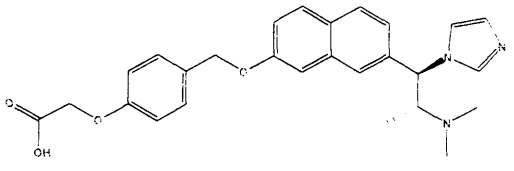

8 nM[161]

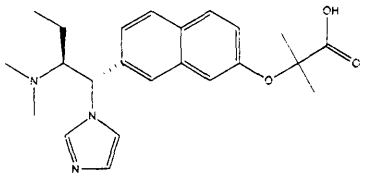

9 nM[161]

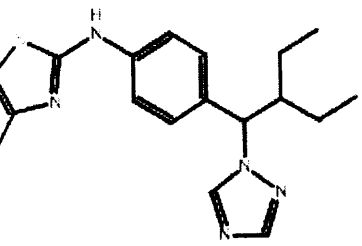

11 nM (R115866)[155]

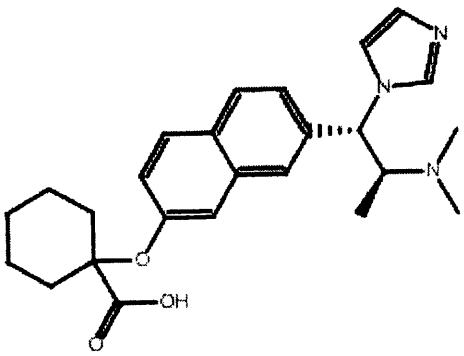

11.2 nM[161]

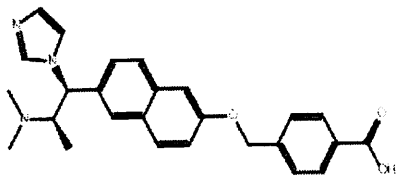

12 nM[161]

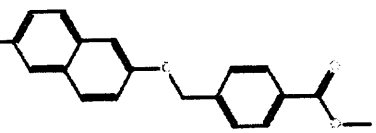

14.4 nM[161]

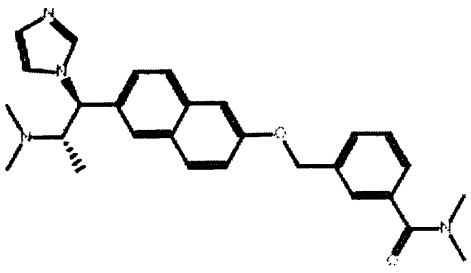

16 nM[161]

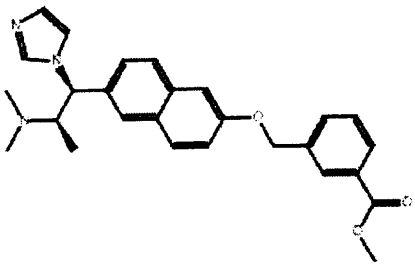

18 nM[161]

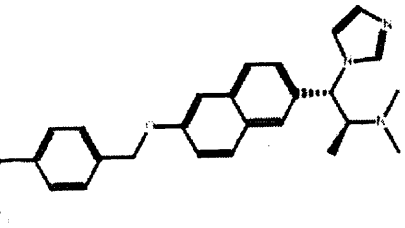

19 nM[161]

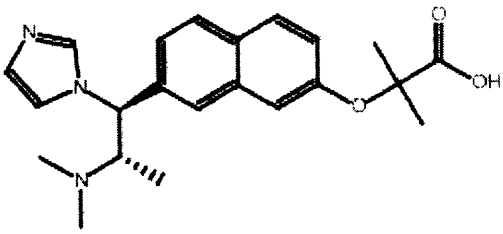

20 nM[161]

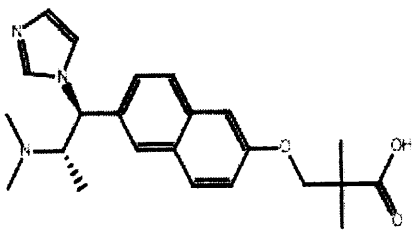

20 nM[162]

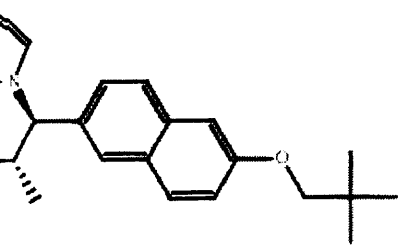

21.4 nM[161]

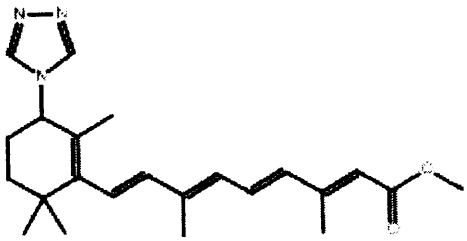

21.67 nM[159]

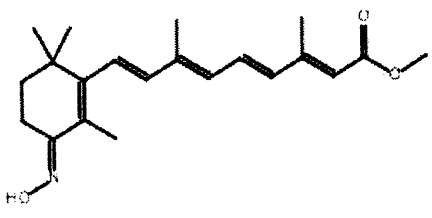

23 nM[159]

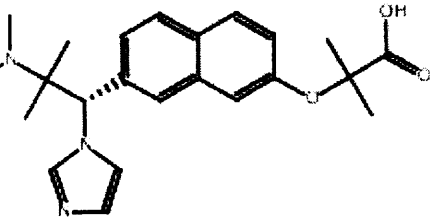

25 nM[161]

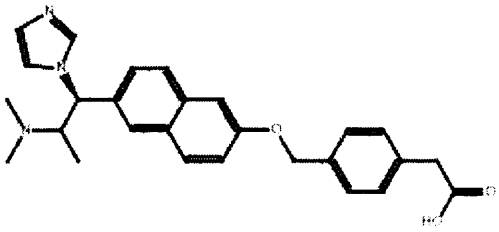

26 nM[161]

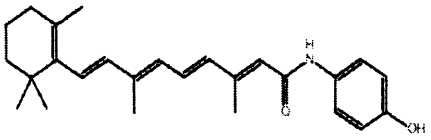

31.85 nM (4HPR)[30]

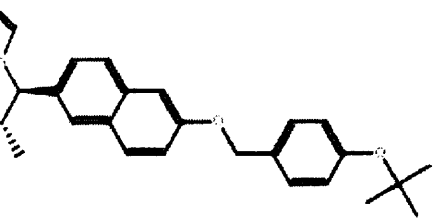

34 nM[161]

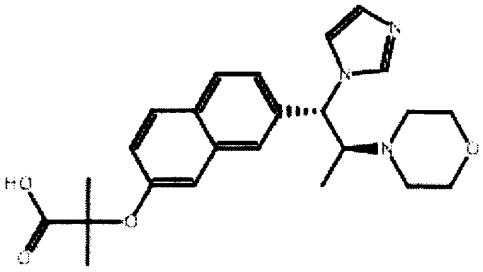

34 nM[161]

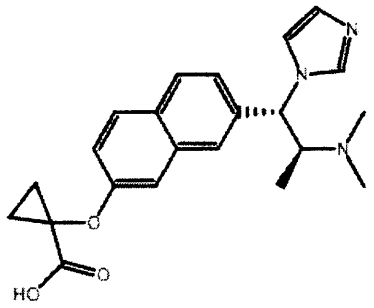

34.7 nM[161]

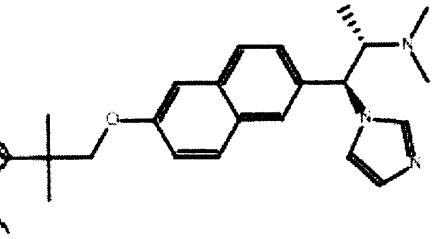

35 nM[161]

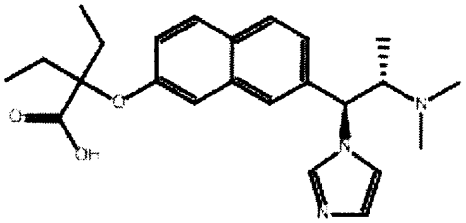

37 nM[161]

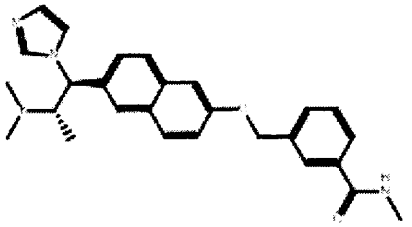

37 nM[161]

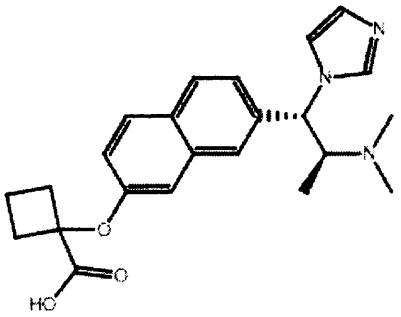

40 nM[161]

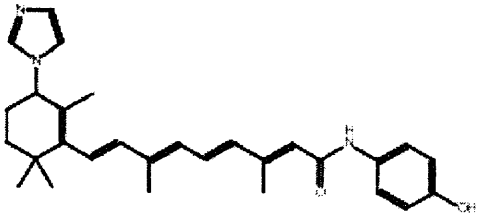

43.73 nM[159]

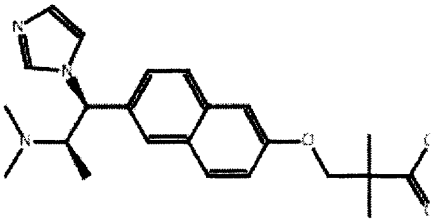

46 nM[162]

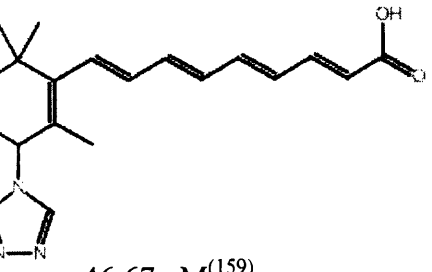

46.67 nM[159]

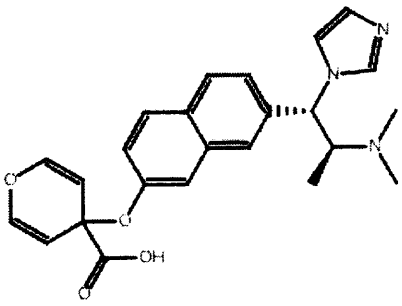

46.7 nM[161]

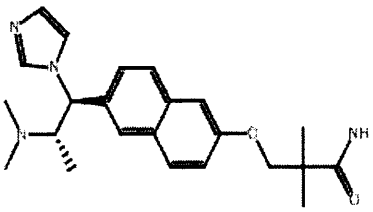

47 nM[161]

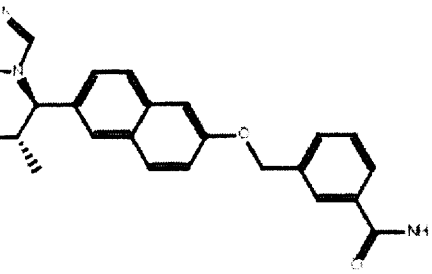

48 nM[161]

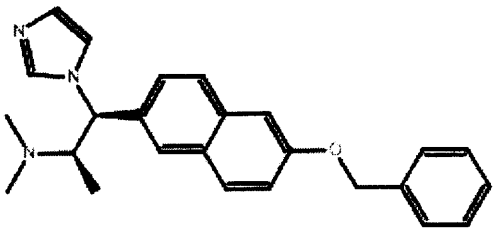

50 nM[161]

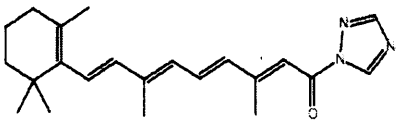

51.67 nM[159]

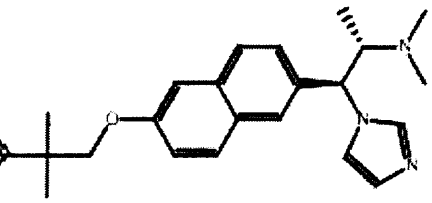

54 nM[161]

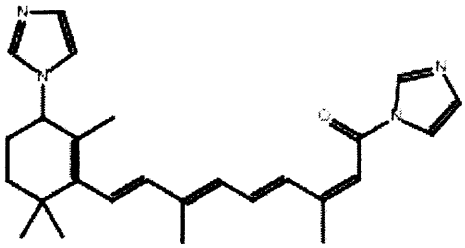

57.5 nM[159]

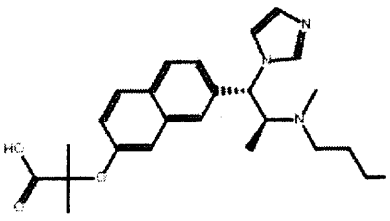

60 nM[161]

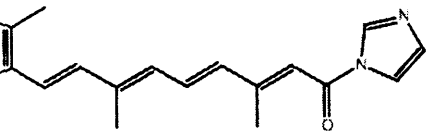

61.25 nM[159]

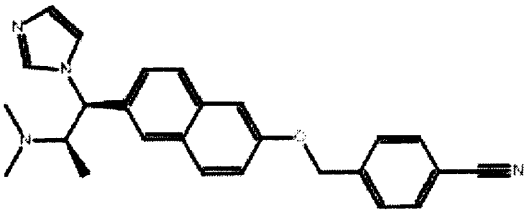

71 nM[161]

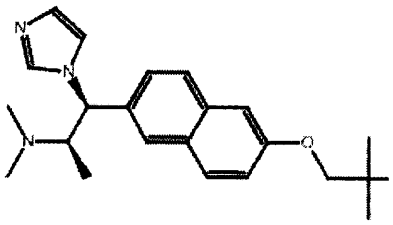

73 nM[161]

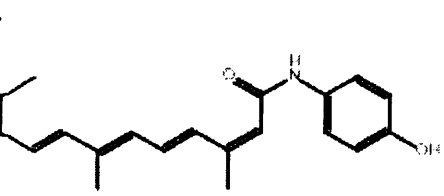

76.67 nM[159]

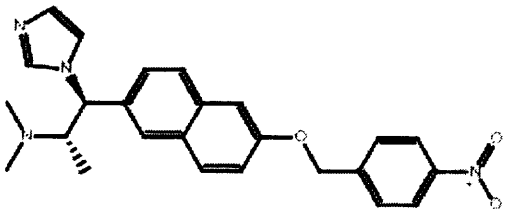

77 nM[161]

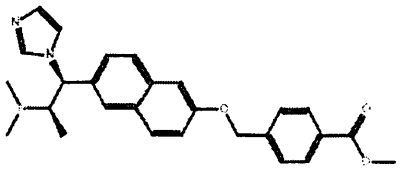

85 nM[161]

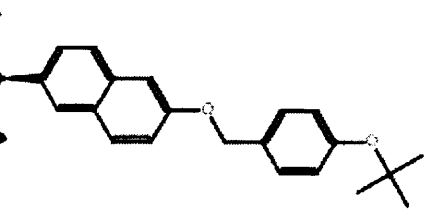

86 nM[161]

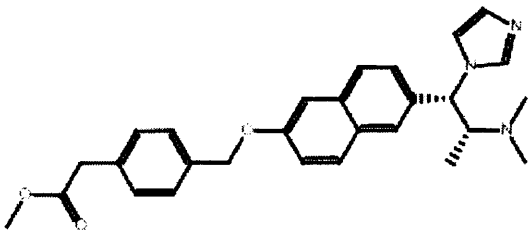

100 nM[161]

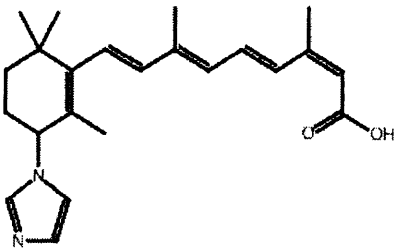

119 nM[159]

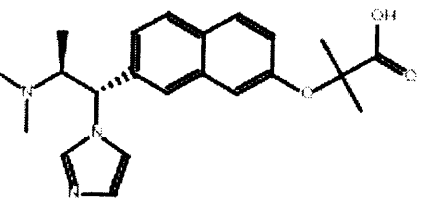

125 nM[161]

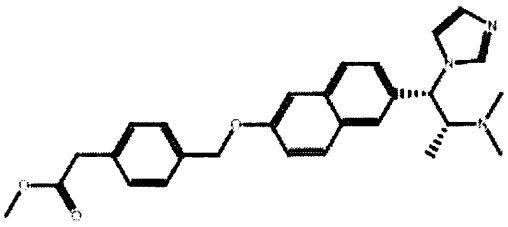

153 nM[161]

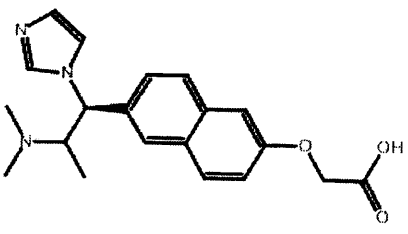

335 nM[161]

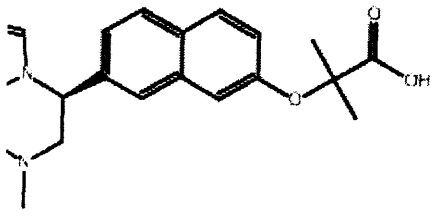

403 nM[161]

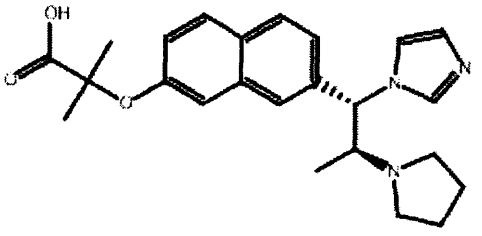

583 nM[161]

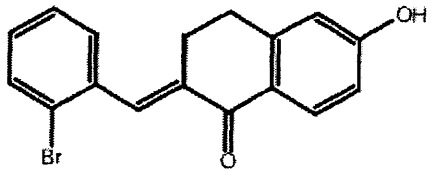

4.53 μM[160]

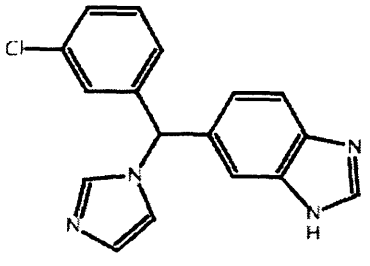

6 μM (Liarozole)[151]

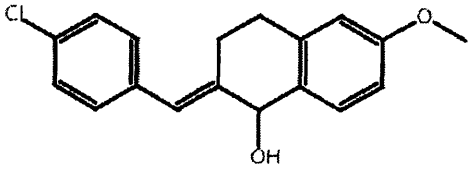

13.56 μM[153]

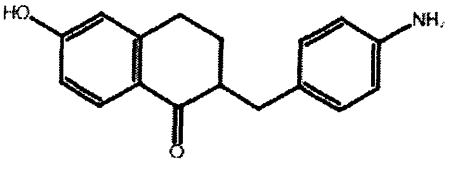

19.65 μM[157]

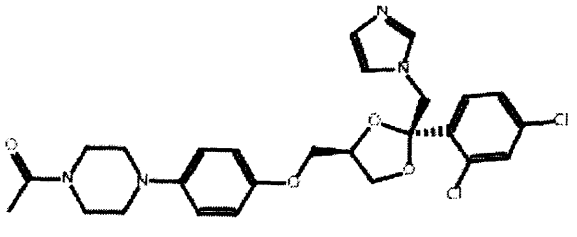

34 μM (Ketoconazole) [150]

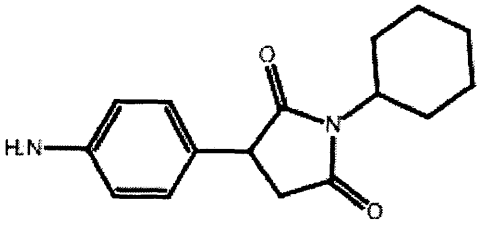

15.17 μM[156]

Table 3.1.1. Structures of the database training set.

(2) Aligning active molecules:

There are two ways in MOE programme to build the pharmacophore from the available database, one is the pharmacophore elucidation and the other is the alignment followed by using the pharmacophore consensus. As the training set contains 71 compounds of very diverse structures, it was very difficult to depend on the pharmacophore elucidation method, and that is why alignment/pharmacophore consensus method was chosen.

For alignment, the two most active compounds (**a**) and (**b**) in the database have been chosen and the partial charges have been calculated for these compounds. Then, alignment using the flexible alignment application available in the MOE programme was performed with the iteration limit set to 100, the failure limit to 20 and the energy cut-off to 10. The stochastic conformational search was enabled to allow a random conformation to be generated for each molecule prior to alignment. The resulting database was sorted according to the objective function (**S**) then by the similarity (**F**) to give the aligned compounds shown in **Figure 3.1.1** with the best value.

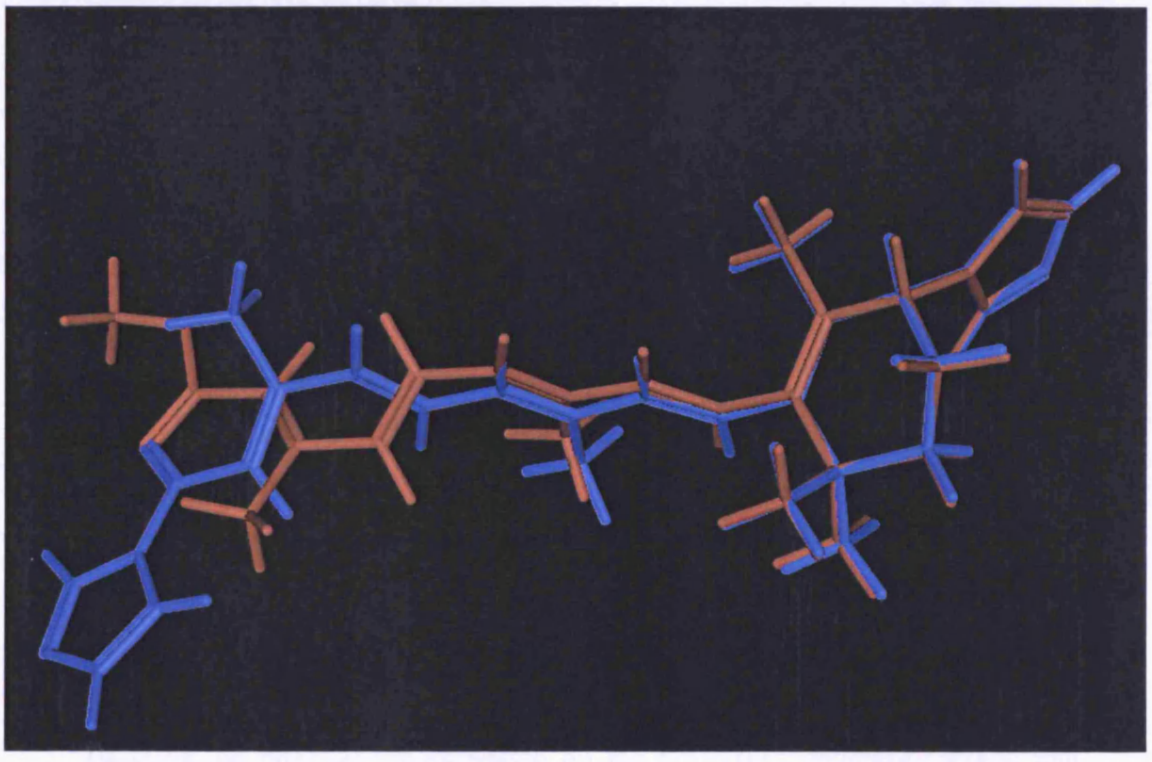

Figure 3.1.1. The alignment of the most 2 active compounds (**a**) and (**b**).

(3) Running the Pharmacophore consensus:

From the pharmacophore query editor in MOE the consensus on the aligned molecules was run, using the **PCH_All** scheme, the tolerance parameter was chosen to be 1 and the threshold to be 100%. This resulted in a pharmacophore with 8 features, as shown in **Figure 3.1.2**.

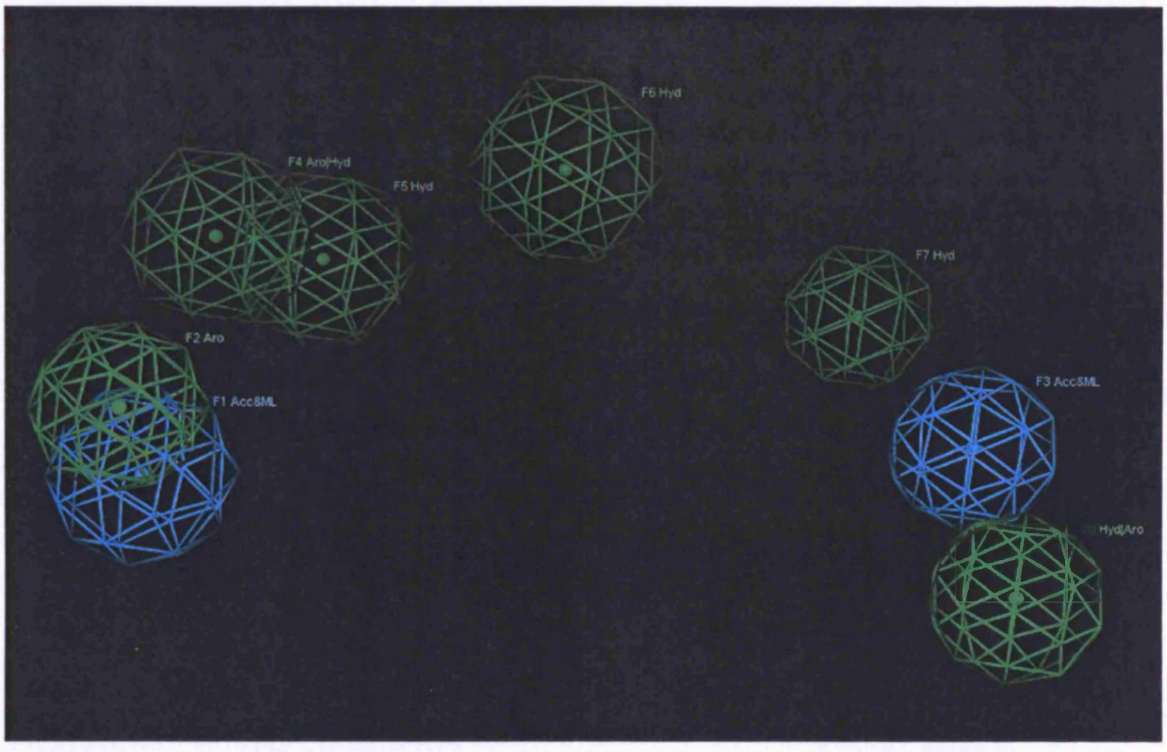

Figure 3.1.2. The suggested pharmacophore from the consensus.

The 8 features are:

1) F1: Acceptor and metal ligator.
2) F2: Aromatic ring centre.
3) F3: Acceptor and metal ligator.
4) F4: Aromatic or hydrophobic region.
5) F5-F7: Hydrophobic regions.
6) F8: Hydrophobic or aromatic regions.

(4) Focusing the query:

Running the pharmacophore search on the CYP26A1 database showed that only 18 compounds out of 71 have a full hit for the entire features. Therefore, a partial match was allowed, which resulted in 62 matches with partial hit to the pharmacophore out of the 71 active compounds in the database.

(5) Refining the query:

The final pharmacophore obtained had the same features as the original one with the 8 features, but with different diameters.

Also the distances between different features have been found to be as shown in the following **Figure 3.1.3**:

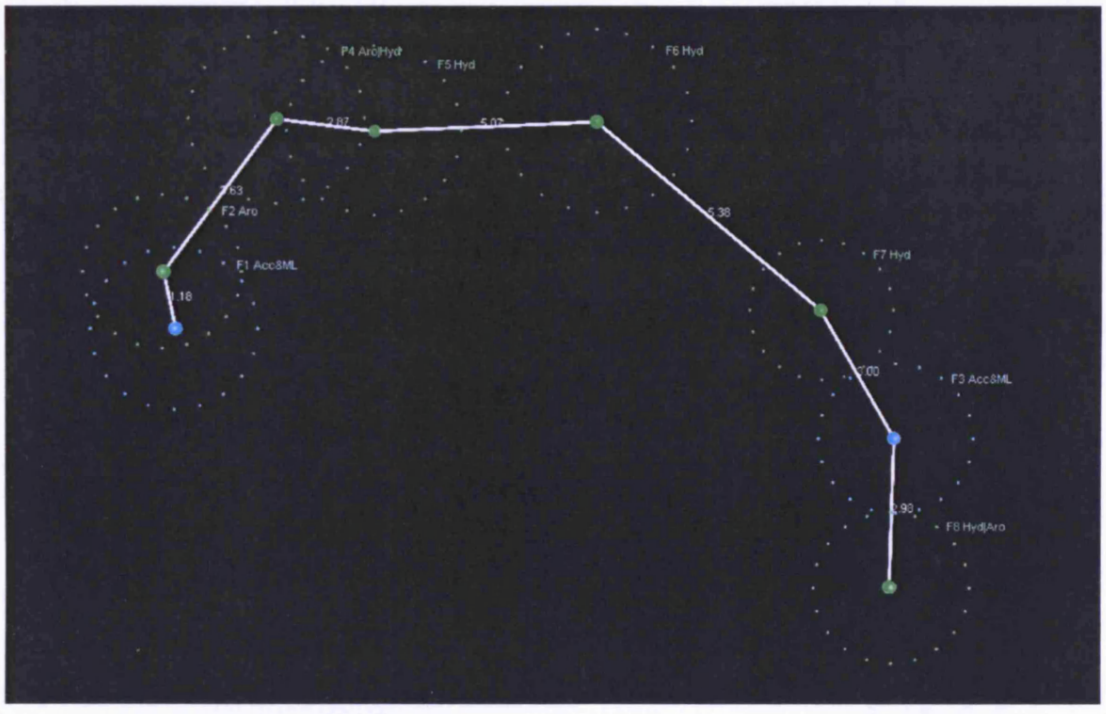

Figure 3.1.3. Showing the distances between different pharmacophoric features.

The distances are:

1) F1-F2: 1.17 Å.
2) F2-F4: 3.63 Å.
3) F4-F5: 2.87 Å.
4) F5-F6: 5.07 Å.
5) F6-F7: 5.38 Å.
6) F7-F3: 3.00 Å.
7) F3-F8: 2.98 Å.

- **Conclusion**:

In conclusion the CYP26A1 inhibitor pharmacophore has 8 features, of which only 5 features should be fulfilled to have an active inhibitor. Those five features are:

1) F1: Acceptor and metal ligator.
2) F2: Aromatic ring centre.

3) F4: Aromatic or hydrophobic region.

4) F5: Hydrophobic regions.

5) F6: Hydrophobic regions.

Therefore, a partial match could be allowed, so long as these 5 features are fulfilled from the 8 features identified.

3.1.4. Uses of CYP26A1 inhibitors pharmacophore model:

The produced CYP26A1 inhibitors pharmacophore investigate if the changes of the lead compound would be tolerated or not and also to search for new molecules that could be active as CYP26A1 inhibitors (**Table 3.1.2**).

Structure	Hits	NAME
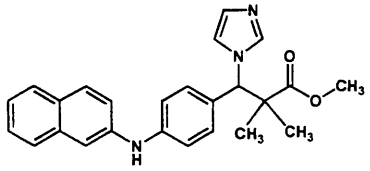	F1, F2, F4, F5, F6	**Lead compd.***
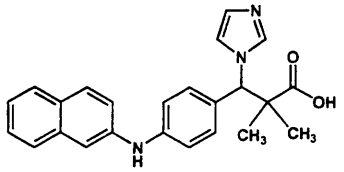	F1, F2, F4, F5, F6	**MCC 186***
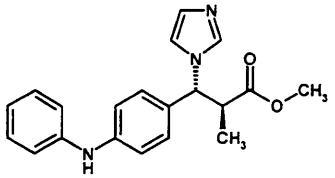	F1, F2, F4, F5, F6	**14**
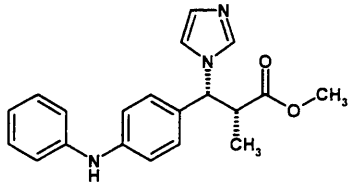	F1, F2, F4, F5, F6	**15**
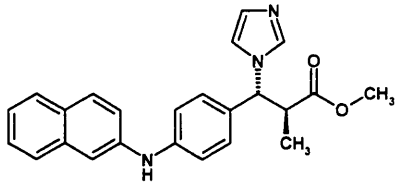	F1, F2, F4, F5, F6	**19**

Structure	Hits	NAME
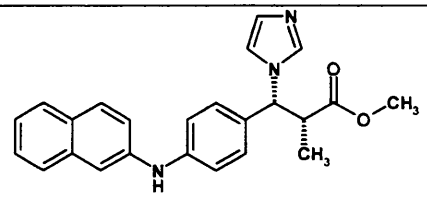	F1, F2, F4, F5, F6	**20**
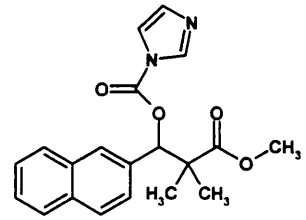	F1, F2, F5	**24**
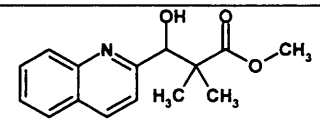	F1, F4	**28**
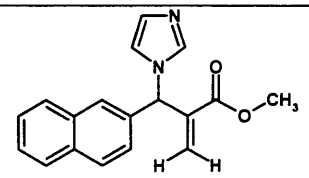	F1, F2, F4	**34**
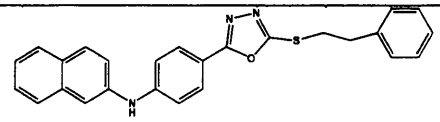	F1, F2, F4, F5, F6	**52**
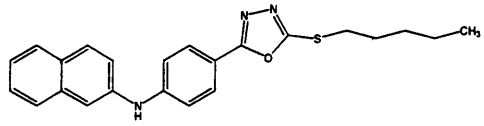	F1, F2, F4, F5, F6	**56**
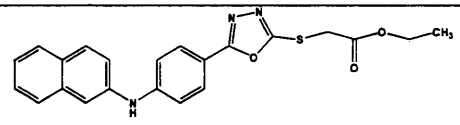	F1, F2, F4, F5, F6	**60**

Table 3.1.2. A table shows the hits of the investigated compounds and the new molecules.

Investigation of the match of the lead compound with the CYP26A1 inhibitors pharmacophore shows that the lead compound has a very good hit with the essential pharmacophoric features, i.e. F1, F2, F4, F5, F6 (**Figure 3.1.4**). As for the changes in the lead compound structure, some changes seem to be tolerated within the pharmacophore, such as replacement of the dimethyl groups with mono methyl (compounds (**14-15**) and (**19-20**)) or replacement of the naphthyl moiety with a

phenyl one (compounds (**14-15**)). Whereas, other changes in the lead compound, such as removing of the imidazole ring (compound (**28**)) or replacing the imidazole moiety with imidazolyl carbonyloxy one (compound (**24**)) do not seem to be tolerated within the pharmacophore as shown from decreased number of the pharmacophoric hits to the essential pharmacophoric features (**Table 3.1.2**).

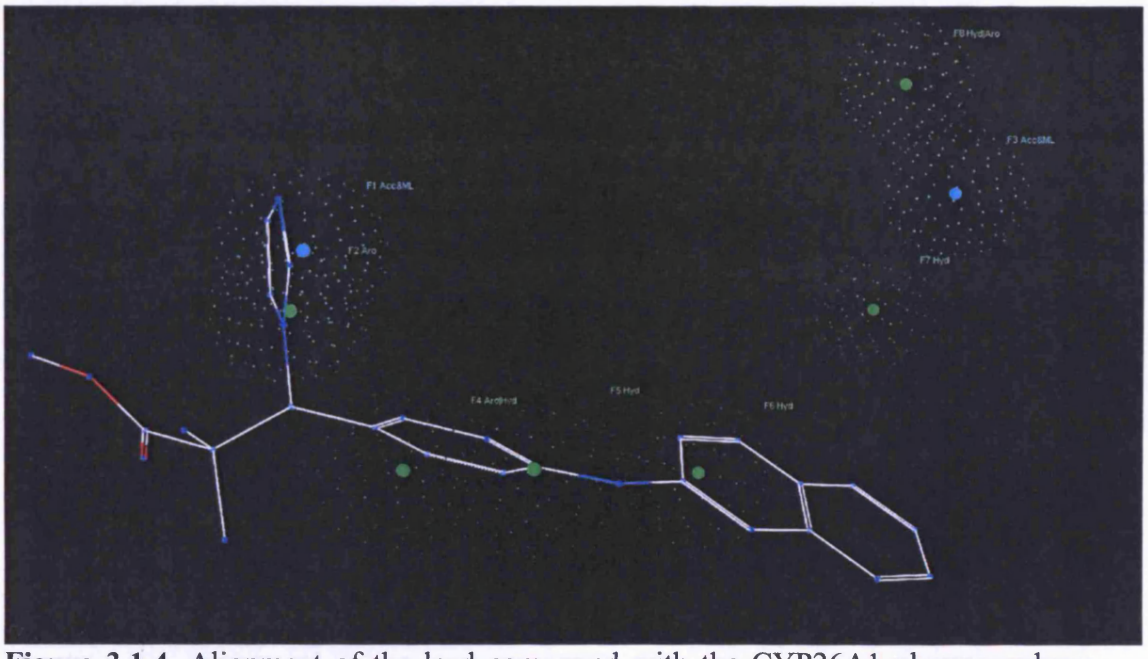

Figure 3.1.4. Alignment of the lead compound with the CYP26A1 pharmacophore model.

As for the search for new molecules which could have activity as inhibitors of CYP26A1, the National Cancer Institute (NCI) database was used to perform this search and using different fragments from this search (**Appendix I**) resulted in the design of some new molecules with different structures than the lead compound (as could be seen in **Table 3.1.2** in compounds (**52, 56** and **60**)). These fragments were chosen to fulfil at least the previously mentioned five main features and at the same time those fragments should be linked in a manner that keeps the mentioned distances between these features (**Figure 3.1.3**). For this purpose, these fragments could be such as the following:

1) F1: Acceptor and metal ligator: in this region we could have something like a nitrogen or oxygen atom as part of a heterocyclic ring.
2) F2: Aromatic ring centre: this should be an aromatic ring either heterocyclic or normal aromatic, this ring should contain the previously mentioned heteroatom either as a part of the ring or attached directly to the ring to keep

the distance between F1 and F2.

3) F3: Acceptor and metal ligator: as previously mentioned this feature is not one of the main features, so it could be excluded when thinking about building our compounds. However, if it is fulfilled then it should have either a heteroatom alone not included in a ring system, or a heteroatom inside a ring.
4) F4: Aromatic or hydrophobic region:, again this is one of the main features, so to fulfil it requires either an aromatic ring; aryl/biaryl or heteroaryl or a hydrophobic aliphatic chain.
5) F5 and F6: Hydrophobic regions. These two main features should be fulfilled, to do so would require, for example, either an aliphatic chain or halogen.
6) F7: Hydrophobic regions: this feature is not essential, but could be dealt with like F5 and F6.
7) F8: Hydrophobic or aromatic regions: again this feature is not essential, but could be treated like F4.

The newly designed compounds shows very good alignment to the essential pharmacophoric features, i.e. F1, F2, F4, F5, F6. **Figure 3.1.4** shows the alignment of compound (**60**), one of the new molecules with the pharmacophore model.

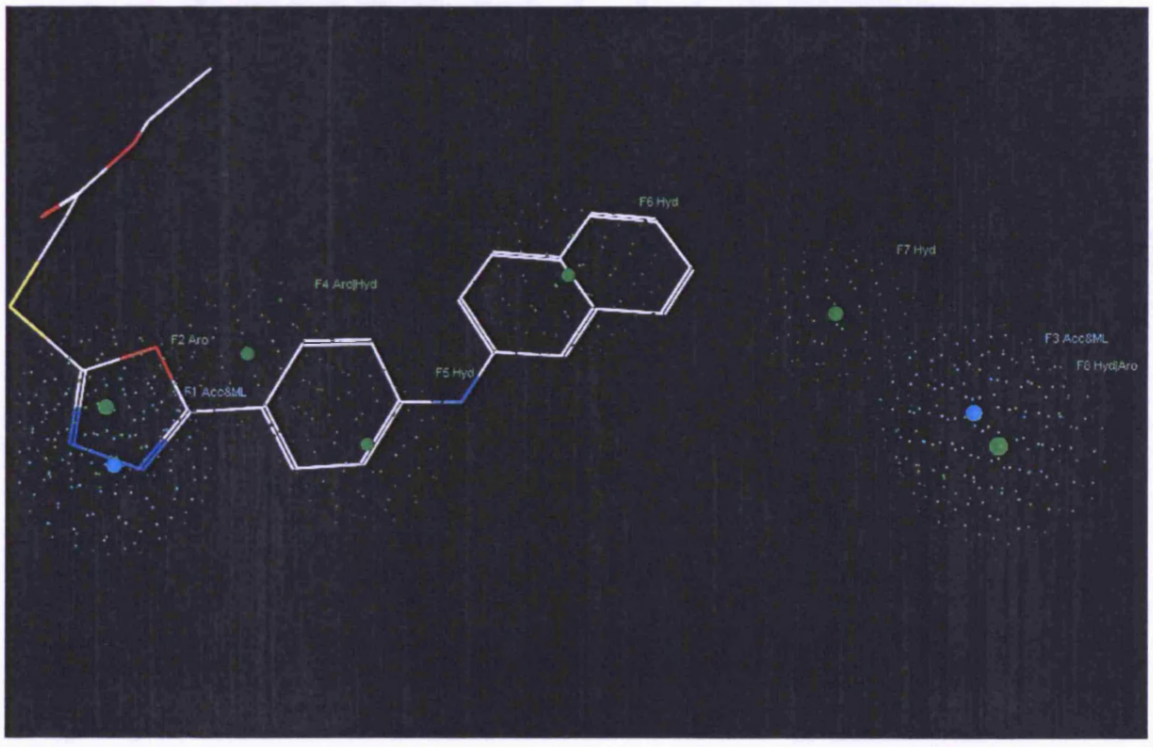

Figure 3.1.4. Alignment of a new molecule with the CYP26A1 pharmacophore model.

3.2. Chemistry of CYP26A1 inhibitors

3.2.1. Introduction:

As a continuation of the effort made within our group to develop CYP26A1 inhibitors with good potency and selectivity, many compounds have been designed as CYP26A1 inhibitors, taking R115866 [83] **(Figure 3.2.1)**, the most potent clinically evaluated CYP26A1 inhibitor, as a lead compound combined with a pharmacophore model search and docking studies with a CYP26A1 homology model, which was published by our group [163].

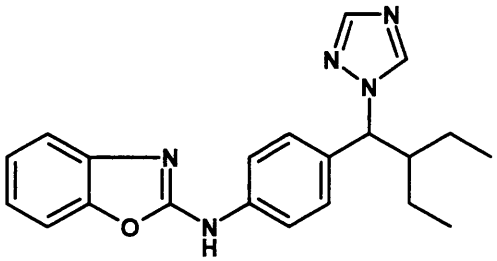

R115866

Figure 3.2.1. R115866.

3.2.2. Docking studies:

As yet no one has published a crystal structure for CYP26A1, possibly because CYP26A1 is hard to crystallise, as it is a membrane bound enzyme. As a result of this, the published homology model of CYP26A1 [163] was used in the docking studies.

In general, there are two strategies for docking a ligand into a macromolecule. The first one is to use the whole molecule of a ligand as a starting point and then perform a particular search algorithm to explore the energy landscape of the ligand at the binding site, looking for optimal solutions (local energy minima). The search algorithms include molecular dynamics and genetic algorithms. The programmes AutoDock [164], Gold [165] and MOE Dock [166] are some examples in this group.

The second strategy, called fragment-based docking, is to start by placing one or several base fragments of the ligand into a binding pocket, and then to build the rest of the molecule in the site. DOCK4.0 [167], FlexX [168,169], LUDI [170], Hammer-head [171], GROWMOL [172] and HOOK [173] are programmes in this group, although some of these algorithms are mainly used in the area of *de novo* ligand design.

The fragment-based approach is faster than the whole molecule-based docking

method. However, only the local interactions between the protein binding site and the ligand fragments under construction are taken into account during the docking procedure. Thus it is difficult to evaluate if the global energy minimum has been found. The results from the fragment-based approach are also sensitive to the choice of the base fragment and its placement. Indeed, if the binding site has a deeply buried pocket with hydrogen bond donors or acceptors, this approach gives good results. However, if the pocket is dominated by lipophilic residues or characterised by a shallow pocket, not only is the placement of the base fragment not definite, but also it is difficult for the programme to decide where to add the next fragments. Consequently, the resulting docking structures can deviate from the real binding mode significantly. While the docking results from whole-molecule-based methods are not dependant on the choice of the base fragment, they require much more computation to find an optimal solution in general. For a large flexible ligand, the whole molecule-based docking approach may not find a good binding mode due to the vast space to be searched [174].

Ligands were docked within the active site of the homology model using the FlexX docking programme of SYBYL, performed with the default values. The FlexX docking programme of SYBYL was used as it is one of the most suitable software programmes to perform fragment-based docking and to do the virtual screening. The active site was defined by all the amino acid residues within a 6.5 Å distance from TRP112, VAL116, THR304, VAL370 and GLY373, including the haem in a heteroatom file. The output of FlexX docking was visualised in MOE and the scoring.svl script (Code, scoring.svl) was used to identify interaction types between ligand and protein.

The docking studies of CYP26A1 inhibitor (*S*)-R115866 **(Figure 3.2.2)** show that the triazole nitrogen is perpendicular to the haem iron of the CYP26A1 model at a distance of 2.6 Å. Furthermore (*S*)-R115688 establishes a hydrogen bond between the benzothiazole nitrogen and the NH of SER115, as well as several hydrophobic interactions with the side chains of TRP112, PHE374, PHE84, PHE299, VAL116, PRO371 and other residues.

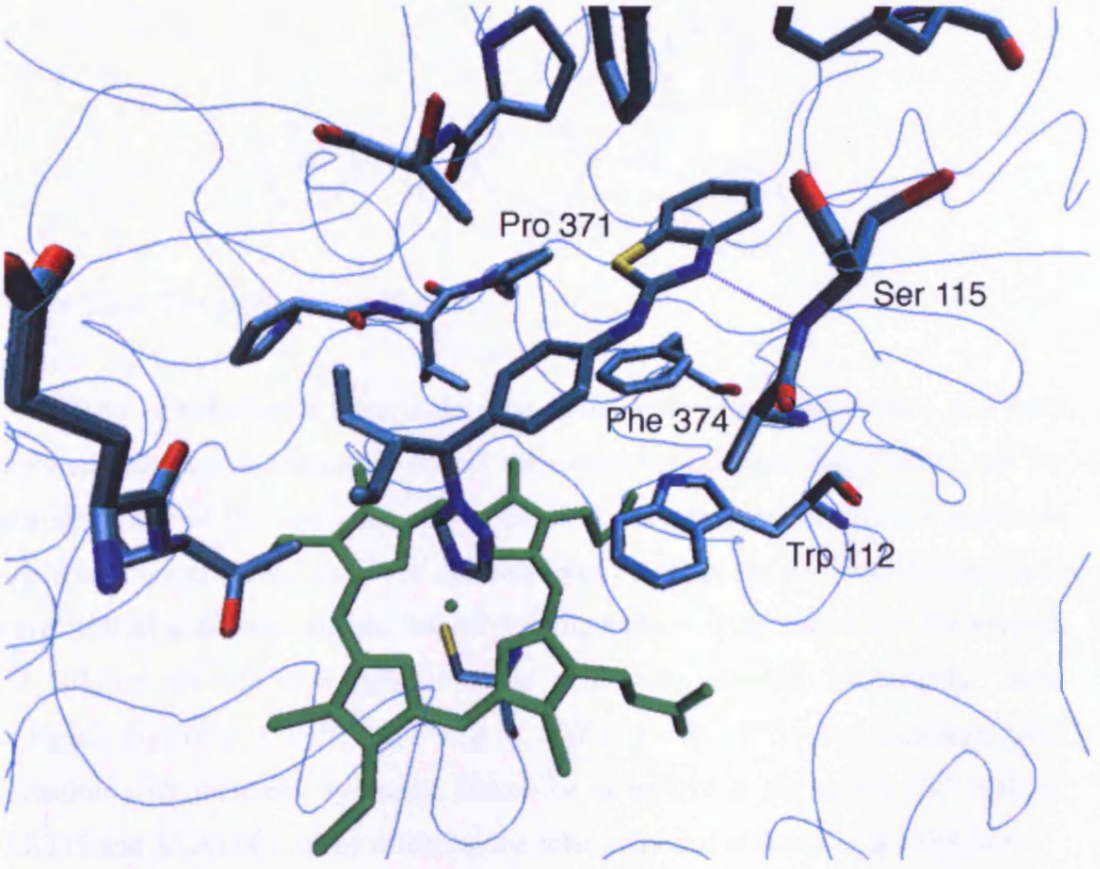

Fig. 3.2.2. Interactions between (*S*)-R115866 and the CYP26A1 active site [163].

3.2.3. Design of CYP26A1 inhibitors:

The compounds were designed by taking R115866 as a lead compound, and simplifying its structure to a scaffold that contains only the main part supposed to be crucial for enzyme inhibition. Also, the main part was chosen to coincide with the main features of the pharmacophore. The profile of the compounds was divided in three parts.

The scaffold **(Figure 3.2.3)** was chosen to be the imidazol-1-ylmethyl-phenylamine moiety. This moiety contains two essential components for the active binding of the molecule. The imidazole is essential for metal-ligand interaction with the haem part of the enzyme. The phenylamino group holds the inhibitor tightly in the active site with the phenyl ring forming hydrophobic bonds mainly with the haem, TRP112, PHE374 and the amino group forming hydrogen bonding with PRO113. The phenylamino also plays a role in positioning the imidazole in an optimal position from the haem.

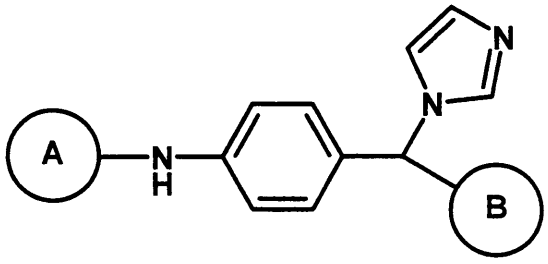

Figure 3.2.3. The proposed scaffold.

The A substituent, designed to be heteroaryl or aryl analogues, is a very important substituent because it affects the dimensions, the stereochemistry and the hydrophobicity of the molecule, and is therefore important in placing the imidazole ring in the right position just above the haem portion of the enzyme. The A substituent is also crucial in determining the overall binding pattern of the inhibitor to the enzyme and holding the inhibitor tightly in the active site through hydrophobic bond formation mainly with PHE374, PRO113, SER115 and PHE84 and hydrogen bond formation with different hydrogen donors or acceptors at the active site such as SER115 and ALA114 thereby affecting the selectivity and efficacy of the molecule.

The B substituent, which was chosen to be an acid substituent, since it was reported that the introduction of a carboxylic group to the structure of certain members of a group of CYP26A1 inhibitors was found to greatly increase the biological activity of the synthesised compounds [89]. Another reason is to mimic the natural substrate, retinoic acid, which contains a carboxylic group. The carboxylic moiety affects the binding of the molecule to the active site through hydrogen bonds it might form with different residues at the active site such as GLY300, GLU303 and THR304. The carboxylic moiety may also affect the movement and penetration of the molecule through biological membranes.

Also, compounds which do not contain the amino group, have been designed and docked to study the importance of the presence of the amino group, as the presence of this amino group in the para position represents synthetic difficulties in the synthesis of many derivatives.

3.2.3.1. Docking of the molecules and analysis of the results:

The FlexX programme was chosen as it is one of the most suitable software programmes to perform a virtual screening. Indeed, it can screen a large number of

molecules on a workstation computer within a few days. Other docking programmes such as those using a genetic algorithm or a Monte Carlo approach can screen a smaller number of molecules under the same conditions or require a more powerful computer to be applied to a large number of molecules [175].

In the database, the formal charges of all the constructed compounds in the library were first computed and their conformation energy minimised using MMFF94X as the force field. The database was then exported in Mol2 format to SYBYL databases and docked as multiple ligands in the active site using the same parameters applied in the docking of retinoic acid and R115866 [163].

The results of the docking were only analysed visually due to the lack of correlation between the FlexX scoring functions and the visual compound-active site interaction. The position of the imidazole ring from the haem was first evaluated. In the well docked compounds, the distance between the imidazole N3 and the iron of the haem should be around 3 Å thereby allowing the coordination bond to be formed. Secondly, the side chain A was assessed for its ability to form hydrophobic interactions with different residues at the active site especially TRP112 and PHE374. This part together with the position of side chain B is crucial in driving the imidazole ring in a conformation that allows good interaction with the haem. Finally, side chain B was evaluated for its capacity to offer the maximal hydrogen bonding and lipophilic interaction with the active site especially GLY300, thereby, holding the inhibitor tightly in the active site.

The docking study showed that the designed compounds **(Table 3.2.1)** can form a good coordinating bond with the haem centre of the CYP26A1 protein with a distance ranging from 1.83 Å to 3.88 Å. Most of the designed compounds form hydrophobic bonds with the forementioned amino acid residues of CYP26A1 protein. The absence of the amino group has not affected the docking of the designed compound to a high extent.

Table 3.2.1.:

Compound structure	Docking of the ligands with CYP26A1	Coordinating bond distance (Å)
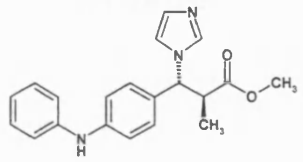		3.57
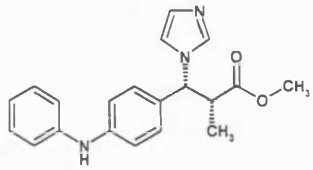	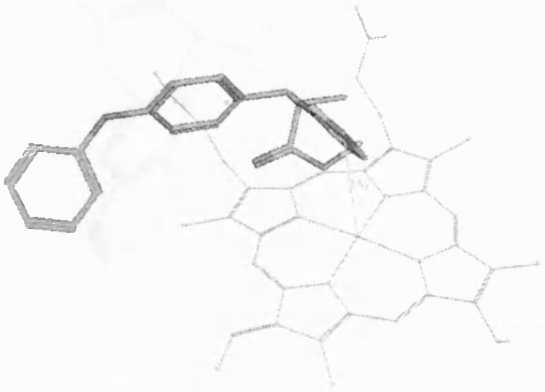	3.68
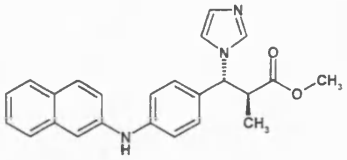	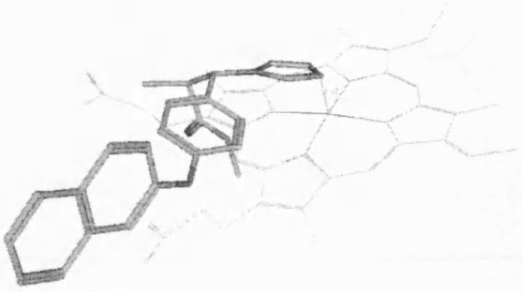	1.83
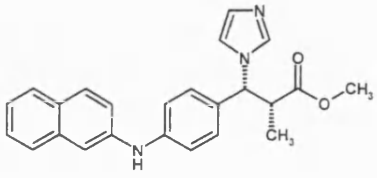	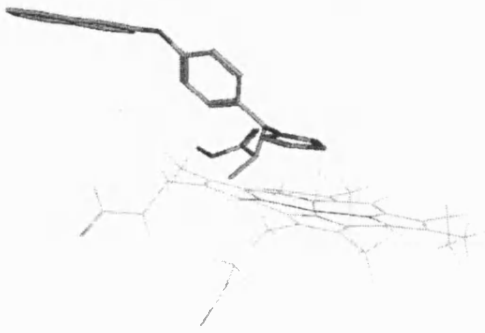	2.48

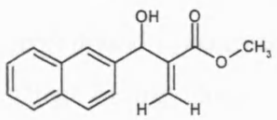 (*S*)-isomer	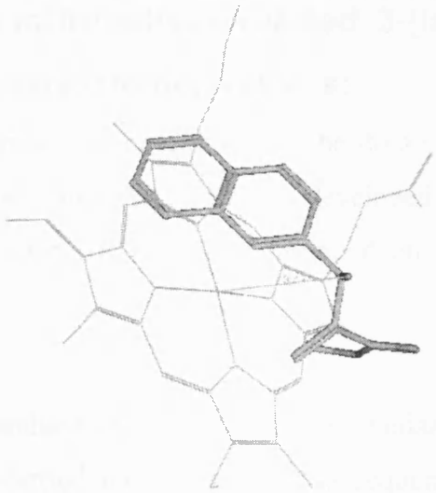	3.47
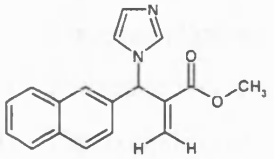 (*S*)-isomer	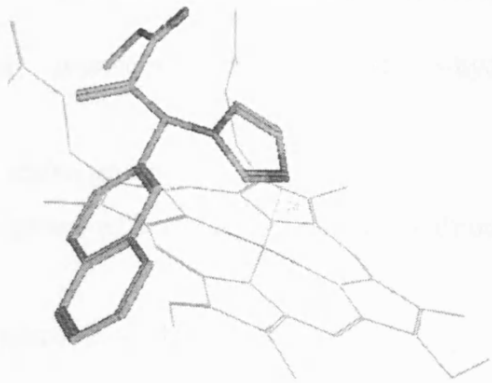	2.47
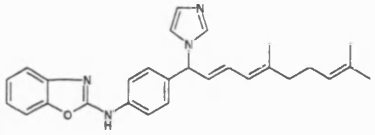	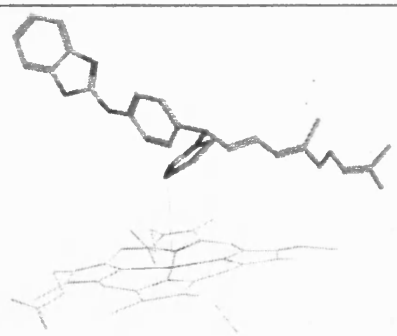	3.88
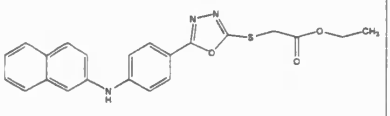		3.40

3.2.4. Synthesis of α-unsubstituted/substituted 3-(imidazol-1-yl)-4-(arylamino)phenyl propanoate derivatives:

Using the data from the pharmacophore model and the docking, beside the lead compound synthesised within our group, this series was developed to investigate the effect of the changes in the structure of the lead compound on the inhibitory activity.

• General chemistry:

The synthesis of α-unsubstituted/substituted 3-(imidazol-1-yl)-3-(4-(arylamino)phenyl)propanoates was carried out according to a sequence of 4 steps (**Scheme 3.2.1**):

1) The preparation of the α-unsubstituted/substituted 3-hydroxy-3-(4-nitrophenyl)propanoates.
2) The reduction of the nitro to amino group.
3) The coupling of the amino group with the aryl substituents through Suzuki coupling reaction.
4) The preparation of the 3-(imidazol-1-yl) derivatives.

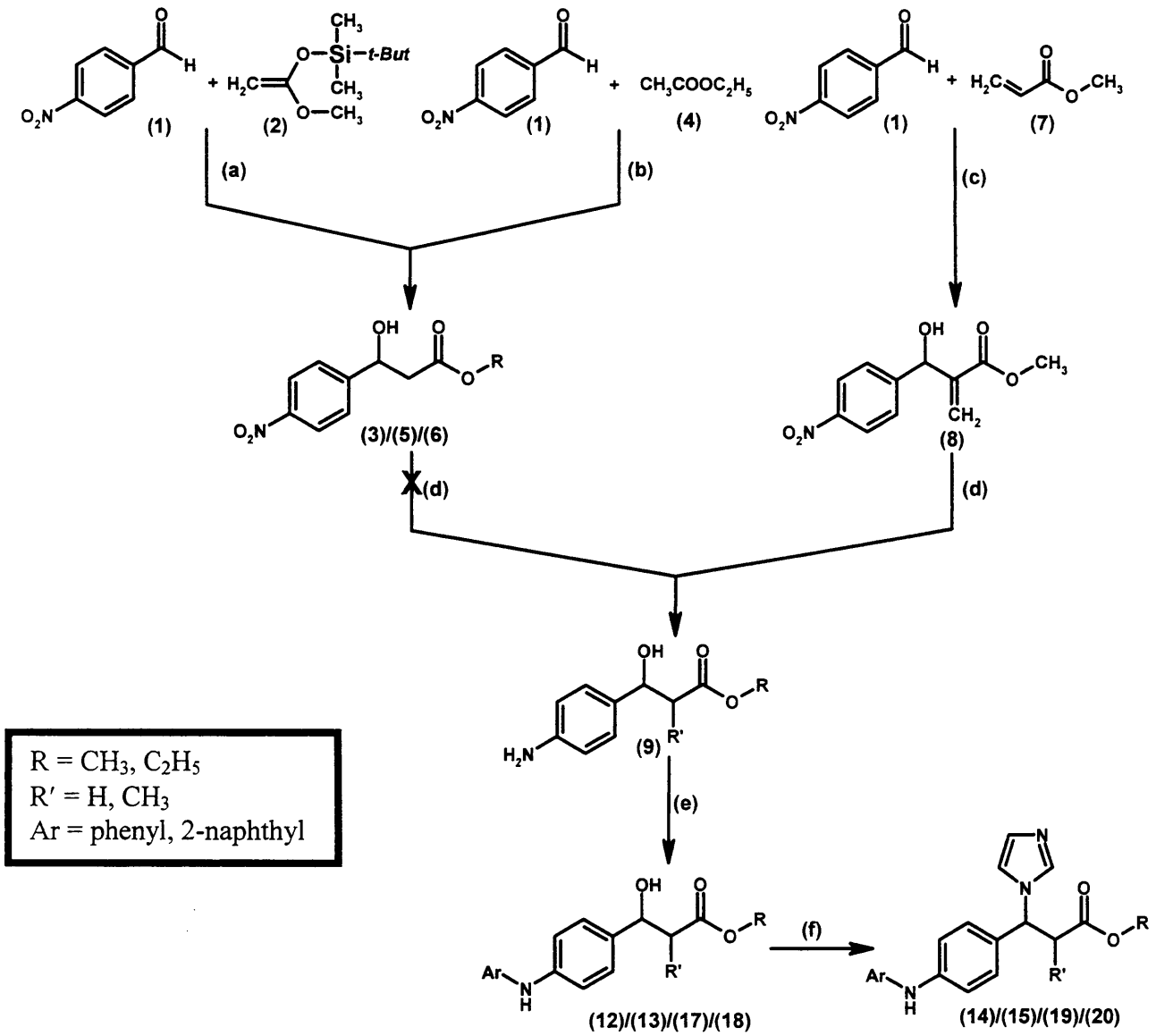

Scheme 3.2.1. Scheme of general chemistry: (a) Pyridine-*N*-oxide, LiCl, DMF, rt, 24 h; (b) $^{i}Pr_2NH$, n-BuLi, THF; (c) aqueous Me_3N, THF, 24 h; (d) Pd-C/ H_2, EtOAc, 1 h; (e) CuOAc, pyridine, CH_2Cl_2, 72 h; (f) Imidazole, 1,1'-carbonyldiimidazole, CH_3CN, 65 °C for 1h, then rt, 24 h.

3.2.4.1. Synthesis of α-unsubstituted/substituted 3-hydroxy-3-(4-nitrophenyl) propanoates:

1) Synthesis of methyl 3-hydroxy-3-(4-nitrophenyl)propanoate:

The synthesis of methyl 3-hydroxy-3-(4-nitrophenyl)propanoate was carried out through the aldol reaction of 4-nitrobenzaldehyde (**1**) with 1-(*t*-butyldimethylsilyloxy)-1-methoxyethene (**2**) **(Scheme 3.2.2)**.

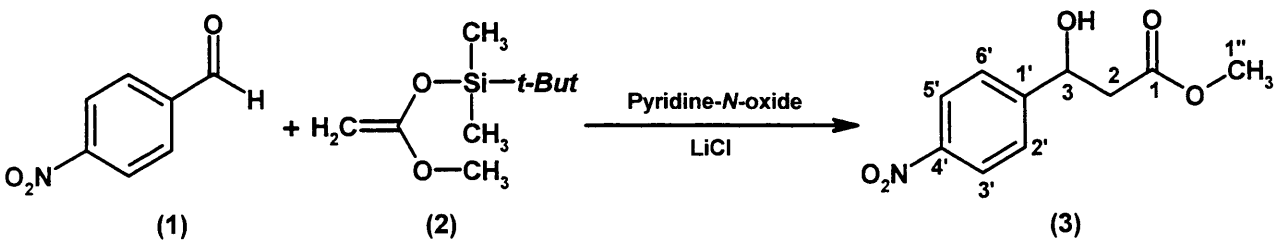

(1) (2) (3)

Scheme 3.2.2. Synthesis of methyl 3-hydroxy-3-(4-nitrophenyl)propanoate (**3**).

The aldol reaction is an important carbon-carbon bond-forming reaction [176]. Mukaiyama developed the aldol reaction of silyl enolate in the presence of a Lewis acid to solve the problem of generating an enol or enolate quantitatively [177].

The application of the aldol reaction in the synthesis of methyl 3-hydroxy-3-(4-nitrophenyl)propanoate, required milder conditions than that used in the Mukaiyama aldol reaction [178]. These conditions include the use of an amine *N*-oxide such as pyridine-*N*-oxide as an alternative candidate as an organomolecular Lewis basic catalyst in the presence of a catalytic amount of lithium chloride.

The general conditions for this reaction involve the addition of 5.0 equivalents of the silyl acetal (**2**) to 1.0 equivalent of the aldehyde (**1**), using catalytic amounts of pyridine-*N*-oxide and lithium chloride. The mixture was stirred at room temperature under nitrogen atmosphere for 24 h to give methyl 3-hydroxy-3-(4-nitrophenyl)propanoate in 34% yield.

The mechanism of the reaction **(Scheme 3.2.3)** [177] involves catalysis of the aldehyde with the Lewis acid, followed by the addition of the silyl enolate on the aldehydic carbonyl. The resulting intermediate undergoes rearrangement to form the silylether, which is then hydrolysed using 10% hydrochloric acid to form the desired compound.

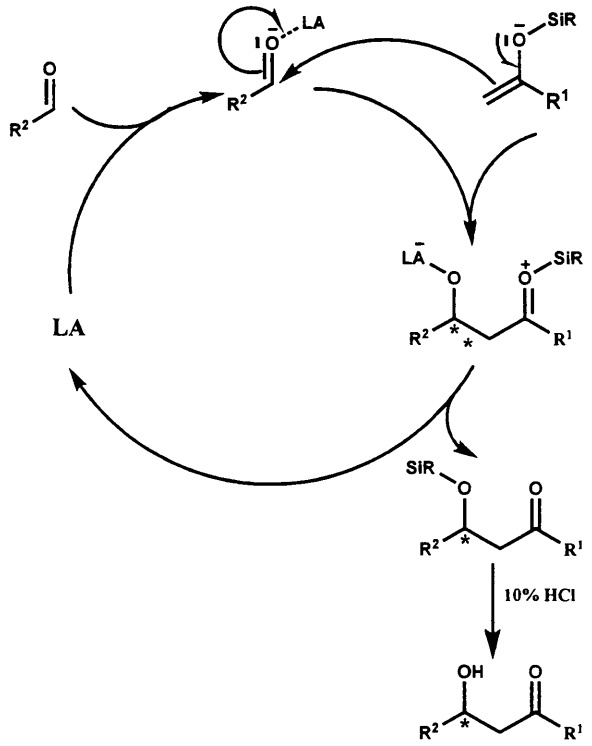

Scheme 3.2.3. Proposed mechanism of the aldol reaction between the aldehyde and the silyl enolate.

2) Synthesis of ethyl 3-hydroxy-3-(4-nitrophenyl)propanoate (5):

Another method for preparing the α-unsubstituted compounds is through the formation of the ester carbanion, which reacted with the 4-nitrobenzaldehyde to give the desired compound **(Scheme 3.2.4)**.

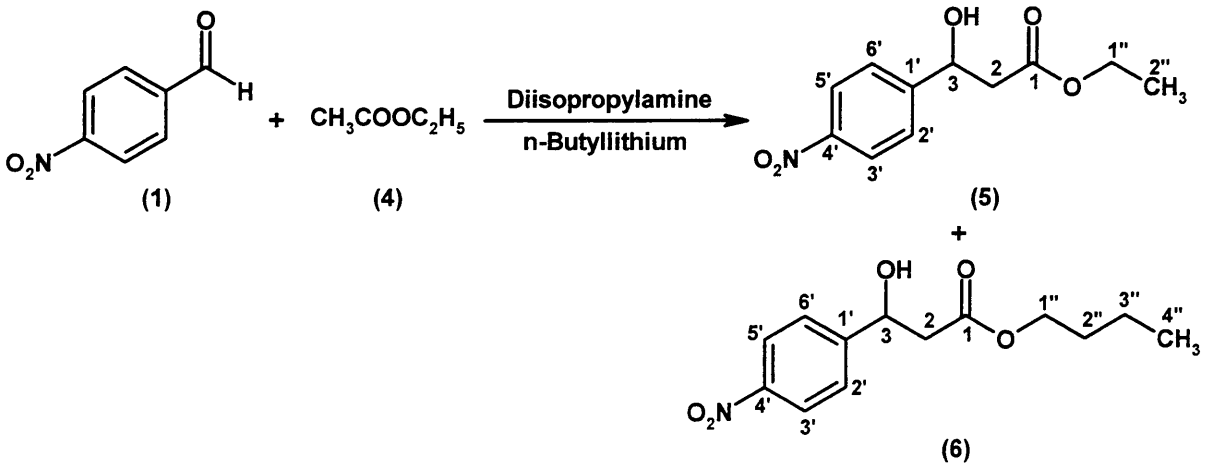

Scheme 3.2.4. Synthesis of ethyl 3-hydroxy-3-(4-nitrophenyl)propanoate (**5**).

The formation of ester carbanion can be afforded through the reaction of diisopropylamine with *n*-butyl lithium at -78 °C to form lithium diisopropylamide, which then deprotonates ethyl acetate through the known mechanism [179]. The formed carbanion then attacks the carbonyl carbon to form ethyl 3-hydroxy-3-(4-nitrophenyl)propanoate (**5**) **(Scheme 3.2.5)**.

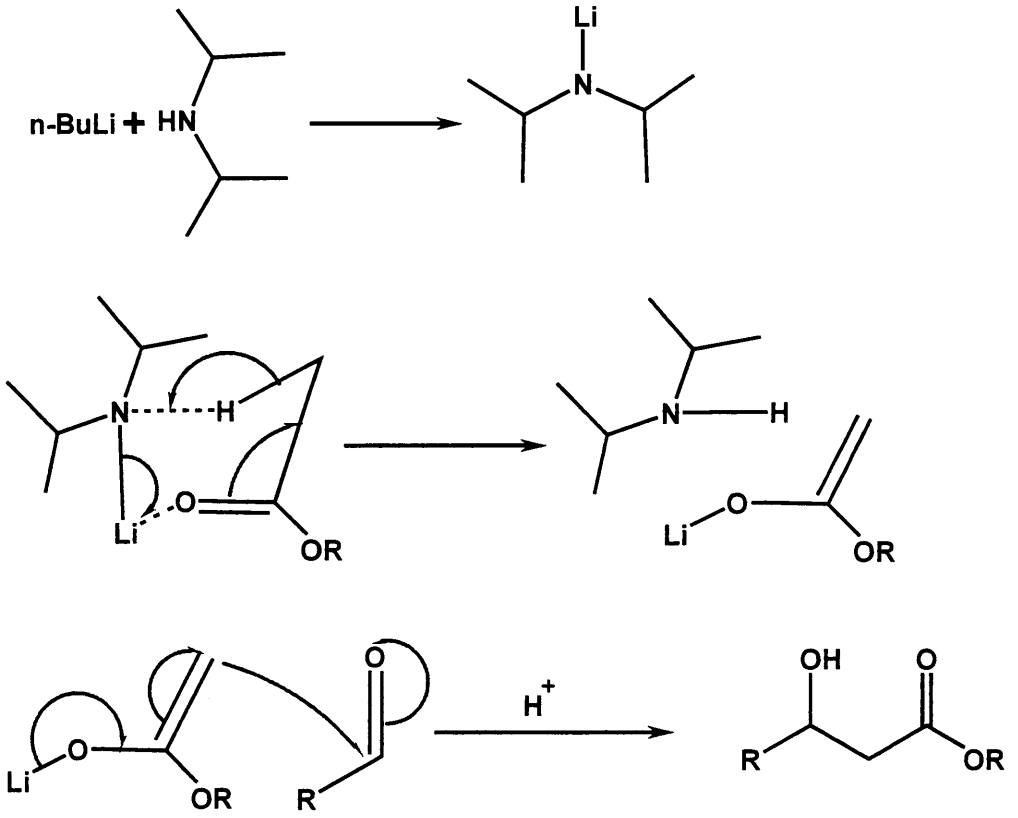

Scheme 3.2.5. Proposed mechanism for the preparation of ethyl 3-hydroxy-3-(4-nitrophenyl)propanoate (**5**).

The surprising result of this reaction was the unusual formation of the butyl ester (**6**) in addition to the required ethyl ester, which has been confirmed through NMR spectral data. The formation of the butyl ester indicated a possible replacement of the ethyl ester with a butyl species derived from the butyl lithium during the formation of the carbanion. The mechanism of this reaction is unknown.

3) **Synthesis of methyl 3-hydroxy-2-methylene-3-(4-nitrophenyl)propanoate (8):**

The formation of methyl 3-hydroxy-2-methylene-3-(4-nitrophenyl)propanoate (**8**) was carried out using the Baylis–Hillman reaction.

The Baylis-Hillman reaction was first reported in 1972 [180] and has great synthetic utility as it converts simple starting materials into densely functionalised products [181]. The Baylis-Hillman reaction is a reaction between an aldehyde and an α,β-unsaturated electron-withdrawing group. These reactions usually require Lewis bases as catalysts, such as tertiary phosphanes or tertiary amines, such as 1,4-diazabicyclo[2.2.2]octane (DABCO) [182] and diaza(1,3)bicyclo[5.4.0]undecane (DBU). The major problem associated with this reaction is its slow reaction rate. Numerous methods, including chemical [183-186] as well as physical attempts [182, 187-188] have been made to accelerate the reaction with some success.

The best yield for preparation of methyl 3-hydroxy-2-methylene-3-(4-nitrophenyl) propanoate was found by using aqueous trimethylamine as the basic catalyst [189], and 4-nitrobenzaldehyde (**1**) and methyl acrylate (**7**) **(Scheme 3.2.6)**. This reaction gave a very high yield (98%) of the desired product.

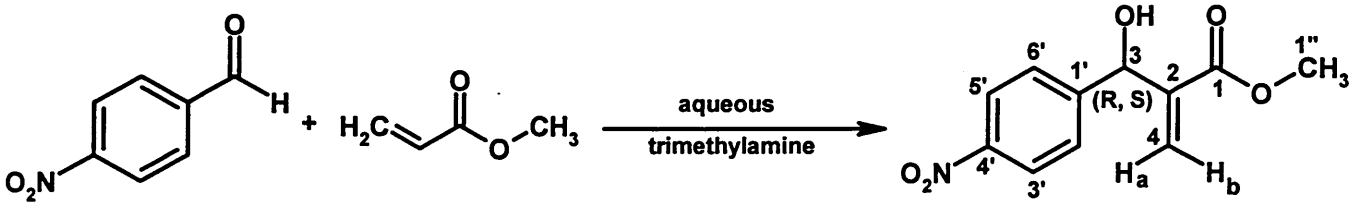

(1) **(7)** **(8)**

Scheme 3.2.6. Synthesis of methyl 3-hydroxy-2-methylene-3-(4-nitrophenyl) propanoate (**8**).

The Baylis-Hillman is initiated by the Michael type nucleophilic addition of tertiary amine (trimethylamine) to the activated alkene (methyl acrylate) resulting in a transient zwitter ionic enolate, which subsequently makes a nucleophilic attack on the electrophile (4-nitrobenzaldehyde) to produce the zwitter ionic adduct. The dipolar adduct gives the final product after proton migration followed by the elimination of the tertiary amine [190] **(Scheme 3.2.7)**.

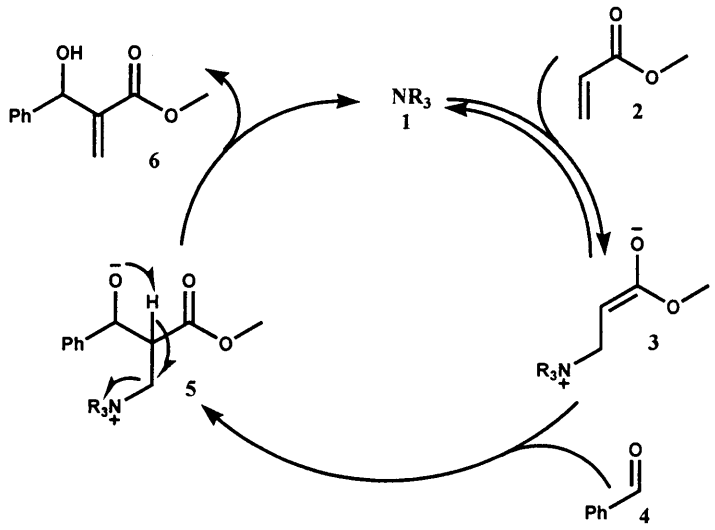

Scheme 3.2.7. Proposed mechanism of Baylis-Hillman reaction.

3.2.4.2. Reduction of the α-unsubstituted/substituted 3-hydroxy-3-(4-nitro phenyl)propanoates:

1) Reduction of the α-unsubstituted 3-hydroxy-3-(4-nitrophenyl) propanoates:

Unfortunately, all efforts made to reduce the α-unsubstituted 3-hydroxy-3-(4-nitrophenyl)propanoates (**3** & **5**) failed as the compounds were found to be completely unstable.

2) Reduction of the α-substituted 3-hydroxy-3-(4-nitrophenyl) propanoate (8):

Reduction of methyl 3-hydroxy-2-methylene-3-(4-nitrophenyl) propanoate (**8**) to the corresponding methyl 3-(4-aminophenyl)-3-hydroxy-2-methylpropanoate (**9**)-*anti* and (**9**)-*syn* was achieved in one step, using 5% Pd-C and hydrogen atmosphere **(Scheme 3.1.8)**.

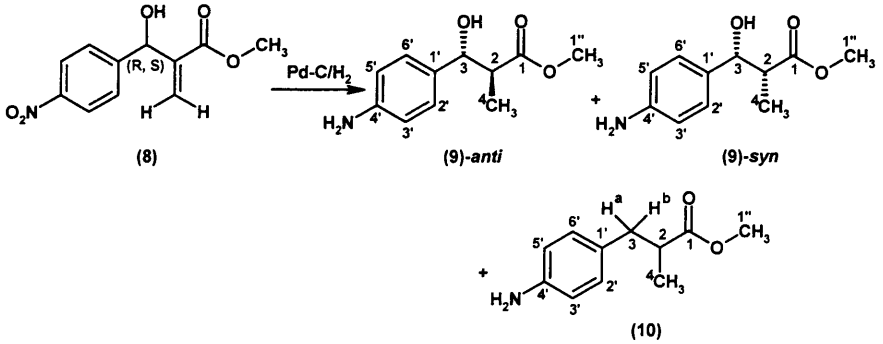

Scheme 3.2.8. Synthesis of methyl 3-(4-aminophenyl)-3-hydroxy-2-methylpropanoate (**9**)-*anti* and (**9**)-*syn*.

The reduction of the methylene to the methyl during the reduction of the nitro-group to the amine agreed with literature data [191]. The yield of the reduction reaction was not poor (48%), as a hydrogenolysis process occurred simultaneously in about 50% of the product. This hydrogenolysis process could not be avoided even with varying the time of the reduction. The hydrogenolysis product (**10**) has the same R_F as the starting compound (**8**), but they stained differently with ninhydrin stain.

Although, the diastereoisomers of methyl 3-(4-aminophenyl)-3-hydroxy-2-methylpropanoate could not be separated, the NMR spectral data indicated that the *syn* and *anti* forms were present in a ratio of 5:8.5 respectively.

• **Ninhydrin test for the amine compounds:**

The ninhydrin reagent is prepared by dissolving 0.35 g of ninhydrin in 100 mL ethanol. The primary amine compounds give a purple stain on the TLC plate when immersed in ninhydrin reagent (**Scheme 3.2.9**).

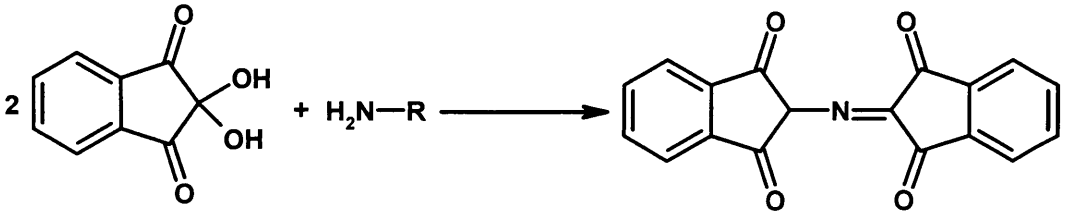

Ninhydrin **Purple complex**

Scheme 3.2.9. Ninhydrin reaction with the amine compounds.

3.2.4.3. Synthesis of the substituted 4-(arylamino)phenylpropanoates derivatives (12)/(13)/(17)/(18):

This synthesis involves the formation of an aromatic C-N bond. Despite the importance of aromatic amines and their use in pharmaceutical and agrochemical industries, few methods have been found in the literature for C-N coupling.

The traditional methods to prepare these compounds are through copper-catalysed Ullmann-type reactions [192], which involve the condensation of an aromatic amine and an unactivated aryl halide with catalysis by copper in the presence of a base. Strongly aggressive conditions involving high temperature and extended reaction times are generally needed to secure at best moderate yields.

The most popular C-N coupling methods have utilised the palladium- or nickel-catalysed coupling of amines with aryl halides in the presence of a hydroxide base [193-194]. The major drawback of this reaction is its incompatibility with base

sensitive functional groups such as esters and ketones. As our compounds contain an ester group, this reaction was not suitable.

The most suitable way for the arylation of NH in our compounds is the use of arylboronic acids in a Suzuki coupling reaction [195]. This reaction has been found to be successful in the synthesis of our compounds [129]. This reaction is performed in the presence of a stoichiometric amount of copper and a tertiary amine base such as triethylamine or pyridine. It should be noted that the yield of the reaction is quite dependent on the nature of the substrate, the substitution on the boronic acid and the choice of the tertiary amine base. The reaction is performed in air allowing oxygen uptake and therefore more efficient oxidation of a reduced copper intermediate [196]. This can be done by using vigorous stirring in flasks with a large volume relative to that of the solvent volume. This is more important during the first few hours of the reaction since it was found that the reaction proceeded smoothly to 35-45% conversion in the first 4-5 h, and catalytic activity rapidly diminished over the next 20 h [197]. The use of molecular sieves has been found important to obtain the best yield [195].

The general conditions for this coupling reaction **(Scheme 3.2.10)** involved the addition of 2.0 equivalents of arylboronic acid (**11**) and 2.0 equivalents of base (pyridine) to 1.0 equivalent of amine in anhydrous dichloromethane (8 mL/0.5g of the substrate) followed by (1-2) equivalents of anhydrous cupric acetate and 4Å molecular sieves. The mixture was stirred under air atmosphere at room temperature for 3 days and then chromatographed on silica gel to give the desired N-arylated amine.

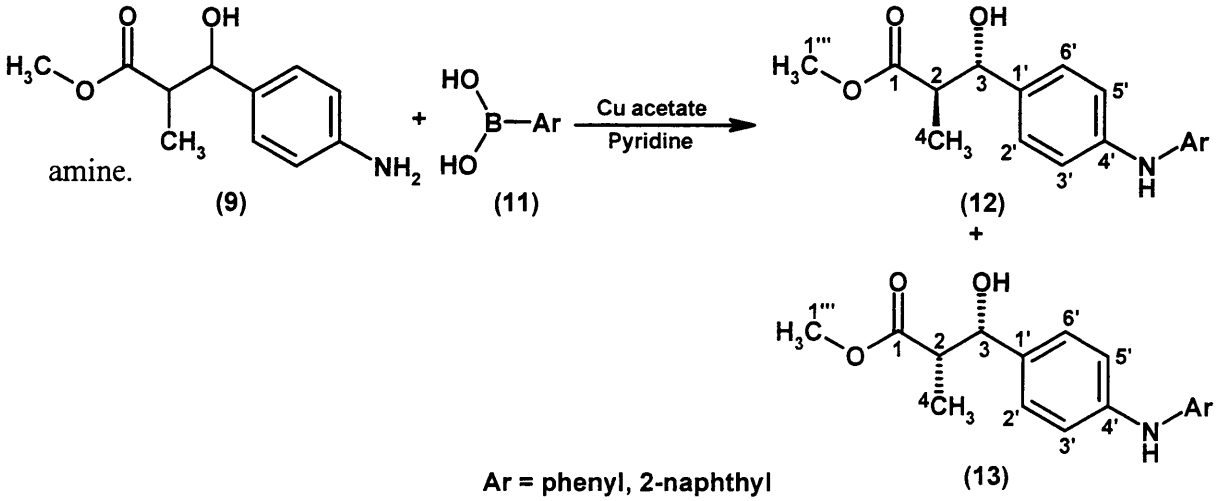

(9) (11) (12) + (13)

Scheme 3.2.10. Synthesis of the substituted 4-(arylamino)phenylpropanoate derivatives.

Table 3.2.2. Yields and melting points of different isomers.

	Ar	Yield (%)	m.p. (°C)
anti	phenyl	44	98-101
syn	phenyl	22	oil
anti	naphthyl	40	124-126
syn	naphthyl	20	oil

At this point separation of the diastereoisomers was achieved using the flash column chromatography. Although the two forms of the diastereoisomers have not been confirmed which is *syn* and which is *anti*, it is more likely that the *syn* and ~~which is~~ *anti* forms were obtained in a ratio of 1:2 respectively, as might be concluded from the NMR spectra comparison with very similar compounds that was mentioned in the literature [182]. The difference between the two diastereoisomers the ^{1}H-NMR spectral data was mainly at the CH in position 3. The CH at position 3 appeared as a doublet with higher coupling constant value which -in accordance with the literature- might be the *anti* form while CH at position 3 in the proposed *syn* form appeared also as a doublet but with lower coupling constant value (**table 3.2.3**).

Table 3.2.2. Coupling constants of the CH at position 3:

	Ar	CHOH J value
anti	phenyl	8.8 Hz
syn	phenyl	5.5 Hz
anti	naphthyl	8.8 Hz
syn	naphthyl	3.8 Hz

The mechanism of the reaction **(Scheme 3.2.11)** is believed to be analogous to that of the bismuth arylation proposed by Barton, with the arylboronic acid playing a role similar to the triarylbismuth [198]. It involves cupric acetate forming a complex with the amine and transmetallation with arylboronic acid. Reductive elimination of the resulting amine/copper/aryl complex affords the N-arylated amine. The role of the base in the catalytic cycle is to increase the carbanion character of the phenyl groups in organoboranes by their coordination with the boron atoms. This will then facilitate the transfer of phenyl groups from the boron to the copper complexes in the transmetallation step to form Ar-NH-Cu-Ar'.

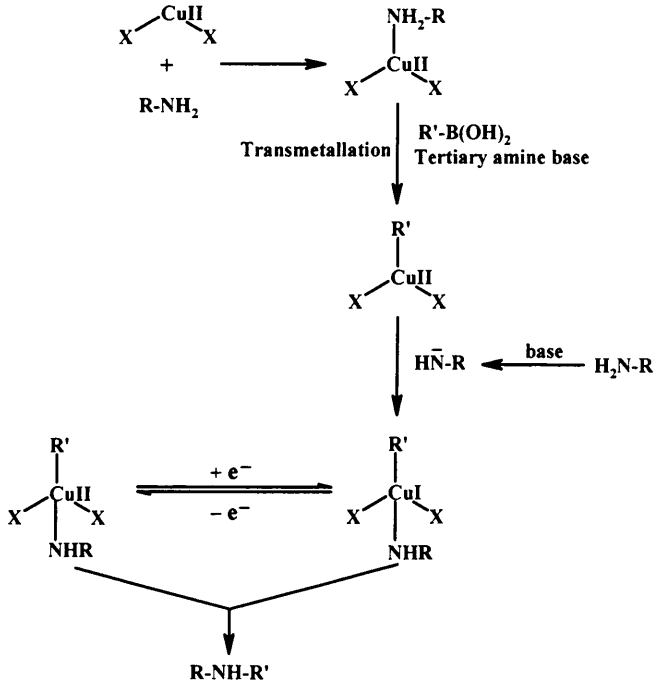

Scheme 3.2.11. Proposed mechanism of action of the Suzuki coupling reaction of aryl boronic acids with amines.

3.2.4.4. Synthesis of α-substituted 3-(imidazol-1-yl)-3-(4-(arylamino) phenyl) propanoates (14)/(15)/(19)/(20):

The synthesis of the imidazole compounds was carried out through the direct reaction of the carbinol compounds with 1,1′-carbonyldiimidazole in the presence of excess imidazole as reported [86]. The reaction was heated at reflux for one hour. An excess of imidazole was necessary to reduce the formation of a side product arising from the competitive attack of the exocyclic amino atom, instead of imidazole, on the intermediate imidazolide. The mechanism of the reaction involves two nucleophilic substitution reactions. The carbinol compounds reacted with 1,1′-carbonyldiimidazole to produce an intermediate which undergoes a second nucleophilic substitution by the excess imidazole to give the products **(Scheme 3.2.12)**.

The imidazole derivatives of both the *anti* and *syn* compounds have been synthesised with different yields, and from the NMR spectral data (**Figures 3.2.3** and **3.2.4**), we have found that the reaction of imidazole with these compounds is more likely to be a S_N1 nucleophilic substitution reaction.

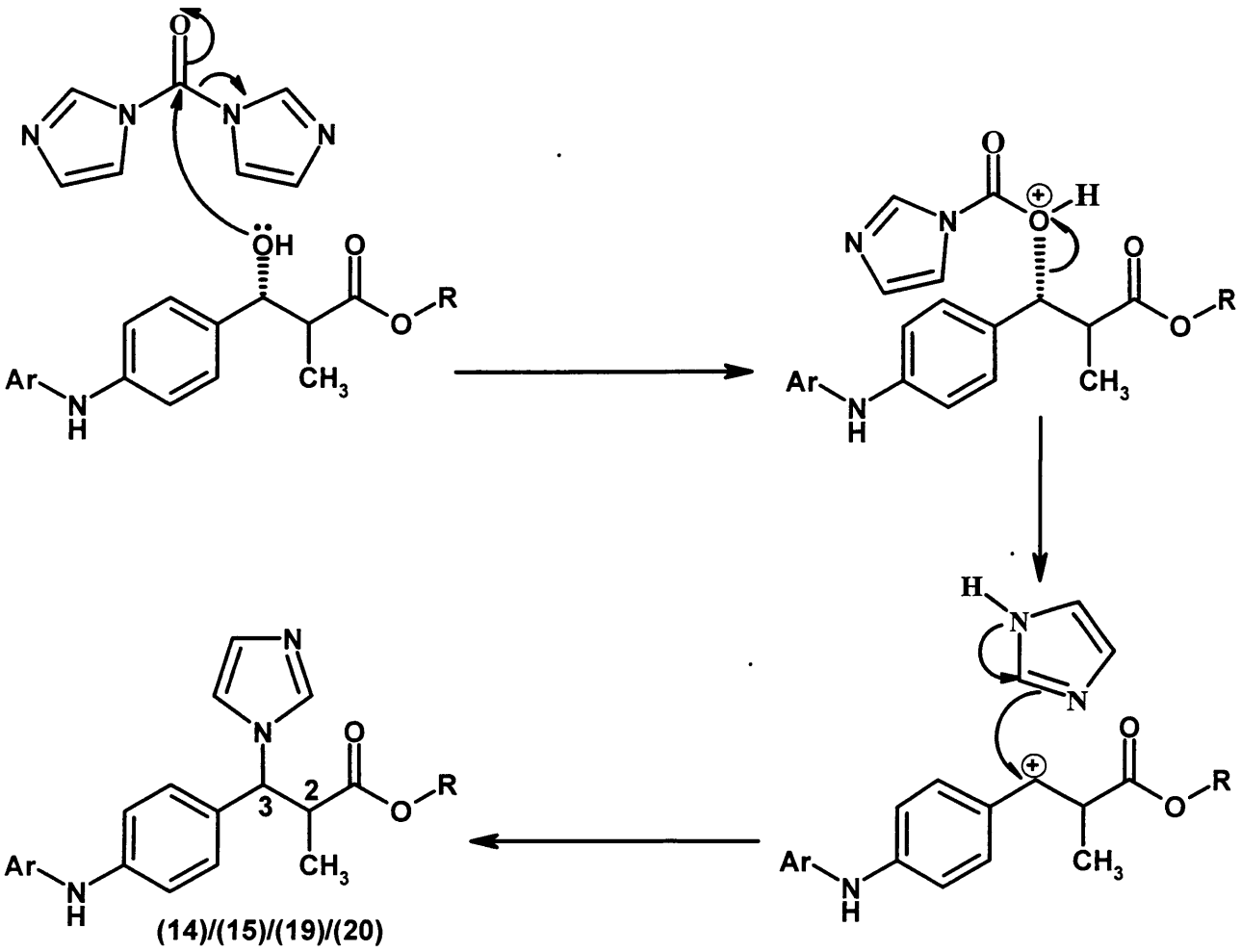

Scheme 3.2.12. Proposed mechanism of formation of α-substituted 3-(imidazol-1-yl)-3-(4-(arylamino)phenyl)propanoates: (**14**) Ar = phenyl, *anti*; (**15**) Ar = phenyl, *syn*; (**19**) Ar = naphthyl, *anti*; (**20**) Ar = naphthyl, *syn*.

This suggestion might be explained as there is no complete inversion of configuration of either of the compounds, and also, what could be seen clearly from **Figures 3.2.3** marked area; that is for each compound, in the same reaction a percentage from a second product with different configuration was found which suggests a small degree of racemisation, a characteristic feature of a S_N1 nucleophilic substitution reaction. What also may support this assumption is the presence of the methyl group at position 2 which may restrict with its steric effect the formation of bimolecular intermediate for the reaction to be performed through S_N2 nucleophilic substitution reaction.

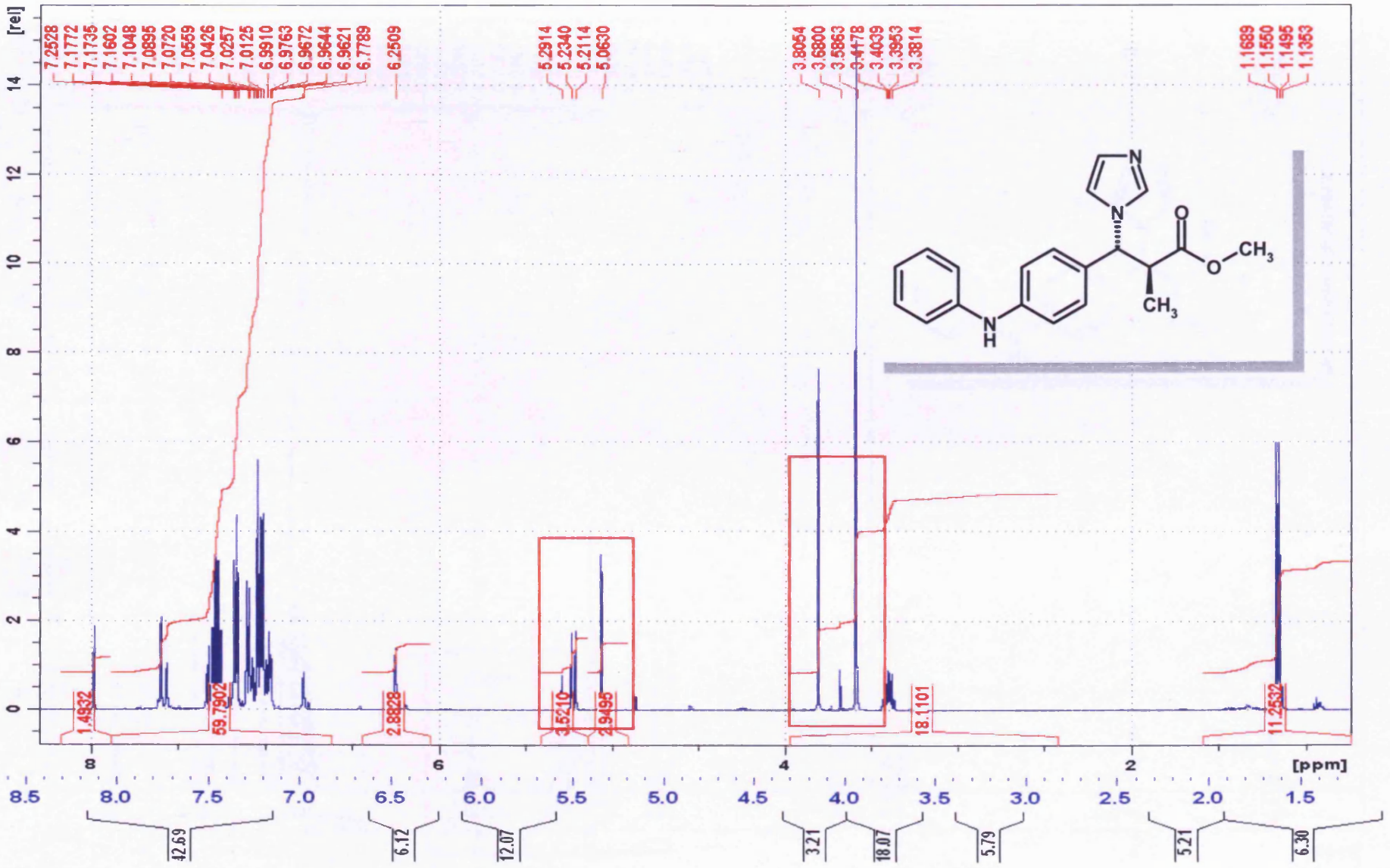

Figure 3.2.3. NMR of methyl *anti*-3-(1*H*-1-imidazolyl)-3-[4-(phenylamino)phenyl]-2-methylpropanoate (**14**).

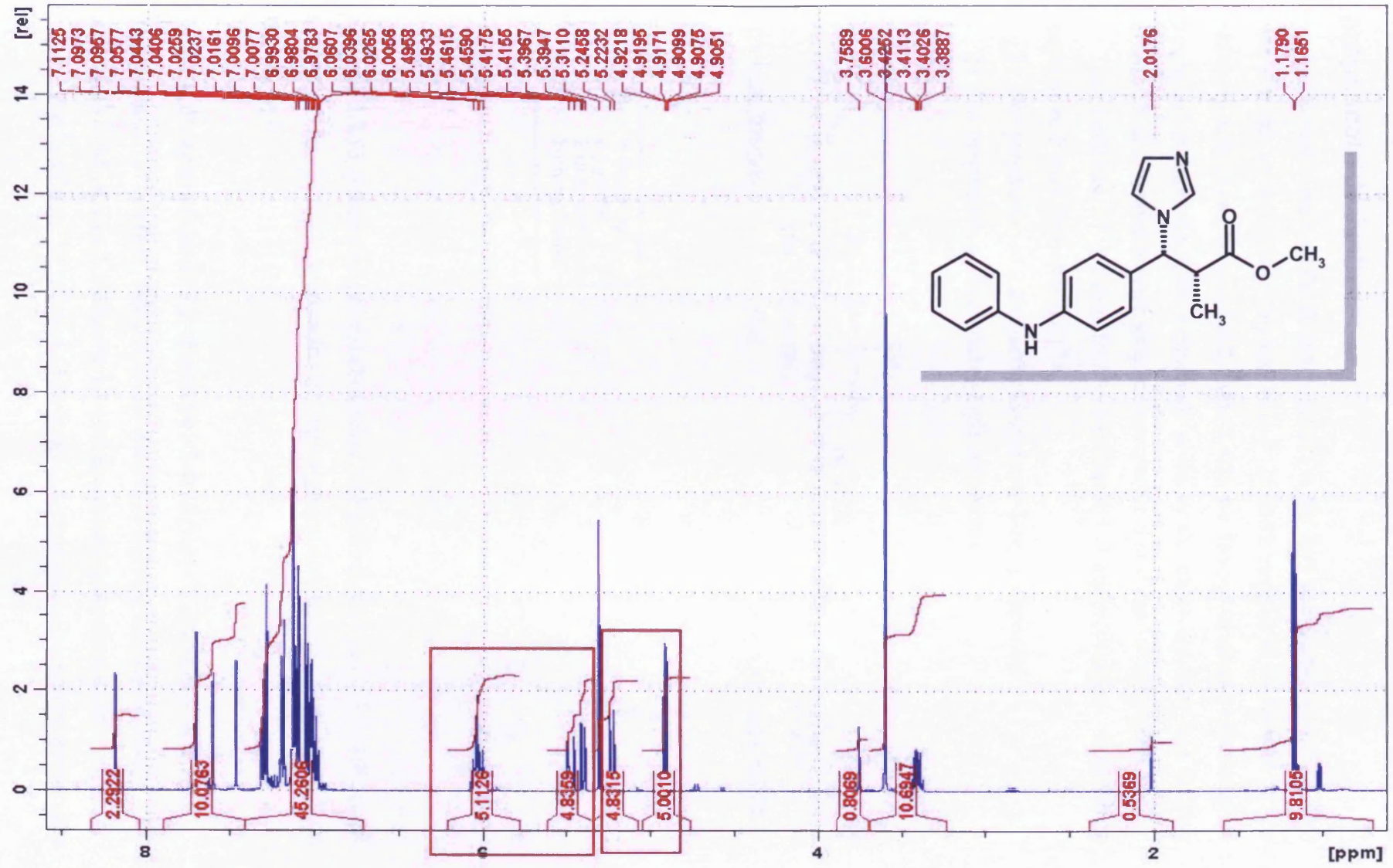

Figure 3.2.4. NMR of *syn*-3-(1*H*-1-imidazolyl)-3-[4-(phenylamino)phenyl]-2-methylpropanoate (**15**).

3.2.5. Synthesis of 2,2-dimethyl-3-(1-imidazolyl)-3-aryl propanoate derivatives:

As the replacement of the dimethyl groups in our lead compound (IC_{50} = 2.8 nM) with a mono methyl group (highest IC_{50} = 26 nM) resulted in a decrease in the inhibitory activity (see section **3.4.2, table 3.4.2**), we decided to return to the dimethyl groups and prepare the other compounds given by the pharmacophore and docking results. These compounds were simpler to prepare and also had lower lipophilicity.

The synthesis of 2,2-dimethyl-3-(1-imidazolyl)-3-arylpropanoates involved a sequence of 2 steps (**Scheme 3.2.13**):

1) The preparation of 2,2-dimethyl-3-hydroxy-3-arylpropanoate.
2) The preparation of 3-(imidazol-1-yl) derivatives.

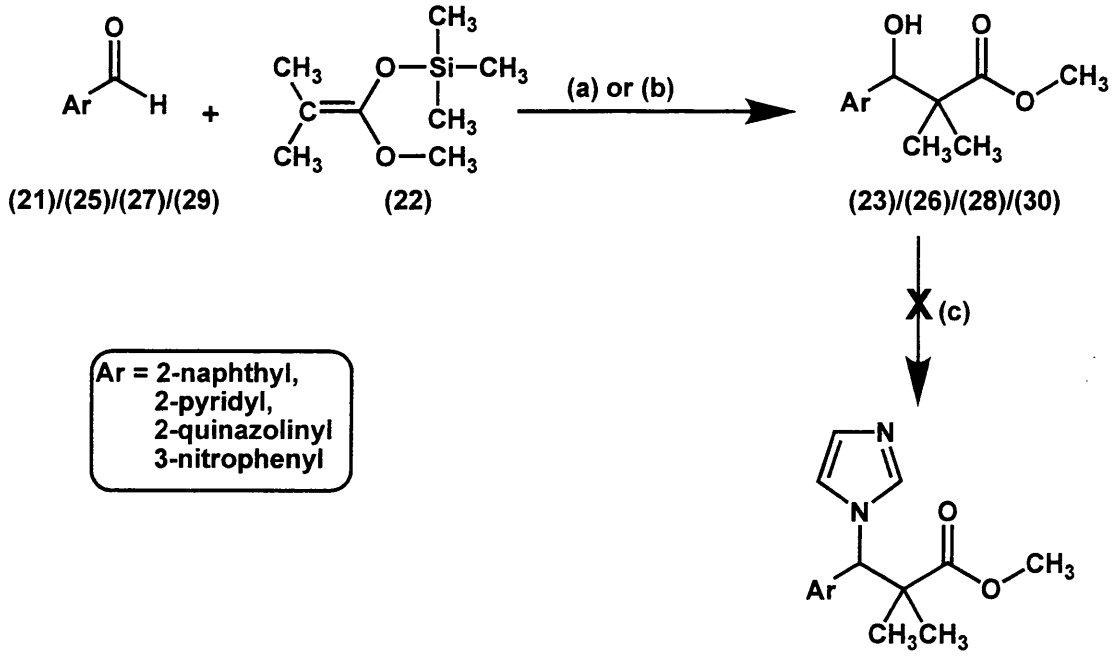

Scheme 3.2.13. Scheme of general chemistry: (a) Pyridine-*N*-oxide, LiCl, DMF, rt, 24 h; (b) H_2O, rt, 24 h; (c) Imidazole, 1,1'-carbonyldiimidazole, CH_3CN, 65 °C for 1h, then rt, 24 h.

3.2.5.1. Preparation of 2,2-dimethyl-3-hydroxy-3-arylpropanoate:

1) Synthesis of methyl 3-hydroxy-2,2-dimethyl-3-(2-naphthyl)propanoate (23) and Methyl 3-hydroxy-2,2-dimethyl-3-(3-nitrophenyl) propanoate (30):

The synthesis of methyl 3-hydroxy-2,2-dimethyl-3-(2-naphthyl)propanoate

(**23**) and methyl 3-hydroxy-2,2-dimethyl-3-(3-nitrophenyl) propanoate (**30**) was carried out through the aldol reaction of 2-naphthaldehyde (**21**) and 3-nitrobenzaldehyde (**29**) respectively with methyl trimethylsilyldimethyl ketene acetal (**22**) **(Scheme 3.2.14)** using the same method used before for the preparation of compound (**3**).

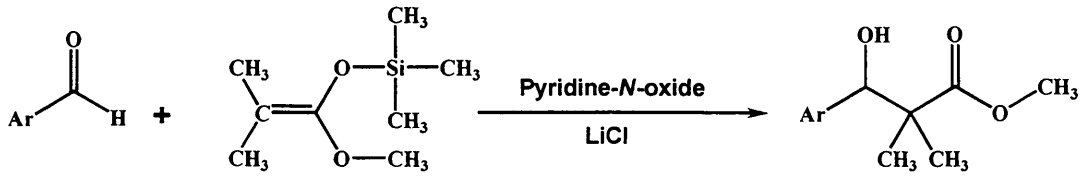

(21)/(29) **(22)** **(23)/(30)**

Ar = (**21**)/(**23**) 2-Naphthyl, (**23**)/(**30**) 3-Nitrophenylbenzaldehyde

Scheme 3.2.14. Synthesis of methyl 3-hydroxy-2,2-dimethyl-3-(2-naphthyl)propanoate (**23**) and methyl 3-hydroxy-2,2-dimethyl-3-(3-nitrophenyl) propanoate (**30**).

2) Synthesis of methyl 3-hydroxy-2,2-dimethyl-3-(2-pyridyl/quinolinyl) propanoate (26/28):

Aldol reaction using water at ambient temperature and without Lewis acid catalysis or any special activation has been used by many chemists [199-202]. Although the true mechanism of this reaction is unknown, the yield is completely dependent on the reactivity of the aldehyde [202].

The method involved the reaction (**Scheme 3.2.15**) between methyl trimethylsilyldimethyl ketene acetal (**22**) and pyridyl-2-carboxaldehyde (**25**) and quinazoline-2-carboxaldehyde (**27**) to give methyl 3-hydroxy-2,2-dimethyl-3-(2-pyridyl)propanoate (**26**) (Yield: 85%) and methyl 3-hydroxy-2,2-dimethyl-3-(2-quinolyl)propanoate (**28**) (Yield: 62%) respectively.

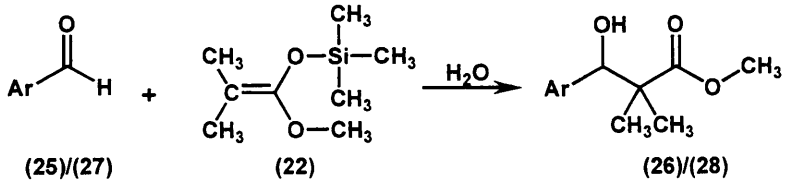

(25)/(27) (22) (26)/(28)

Ar = (**25**)/(**27**) 2-Pyridyl, (**26**)/(**28**) 2-Quinolinyl

Scheme 3.2.15. Synthesis of methyl 3-hydroxy-2,2-dimethyl-3-(2-pyridyl)propanoate and methyl 3-hydroxy-2,2-dimethyl-3-(2-quinolyl)propanoate.

3.2.5.2. Preparation of 3-(imidazol-1-yl) derivatives:

Unfortunately, all the methods that have been tried to obtain the imidazole derivatives from compounds (**23, 26, 28** and **31**) were unsuccessful, and the reaction stops at the point of formation of the intermediate with the 1,1'-carbonyldiimidazole as in the case of compound (**23**), which formed 3-methoxy-2,2-dimethyl-1-(2-naphthyl)-3-oxopropyl-1*H*-1-imidazolecarboxylate (**24**) **(Scheme 3.2.16).**

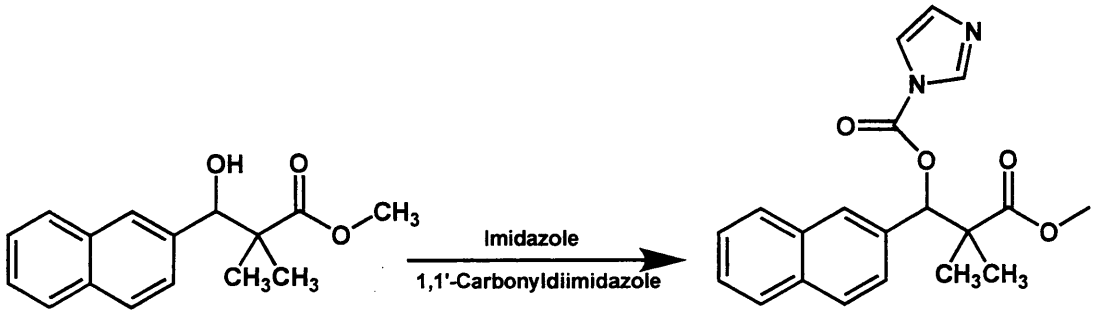

(23) (24)

Scheme 3.2.16. Formation of the intermediate with 1,1'-carbonyldiimidazole.

Also, another approach had been tried through conversion of the hydroxyl group to the more active bromo group, using either *N*-bromosuccinimide or PBr_3 in the presence of pyridine, but all these methods failed to replace the hydroxyl group with the bromide.

3.2.6. Synthesis of methyl 3-(1*H*-1-imidazolyl)-2-methylene-3-(2-naphthyl)propanoate (34):

As a result of the failure of the introduction of the imidazole in the previous series, we investigated the effect of the presence of a methylene group in place of the dimethyl groups.

The synthesis of methyl 3-(1*H*-1-imidazole)-2-methylene-3-(2-naphthyl)propanoate was carried out through two simple steps:

1) Firstly, the formation of methyl 3-hydroxy-2-methylene-3-(2-naphthyl)propanoate (**33**) through Baylis-Hillman reaction of 2-naphthaldehyde (**21**) and methyl acrylate (7) [203] **(Scheme 3.2.17)** which was also used as the solvent. The catalyst used in this reaction is DABCO, as the aqueous trimethylamine could not be used as it did not form a homogenous solution. The yield of this reaction was good (79%).

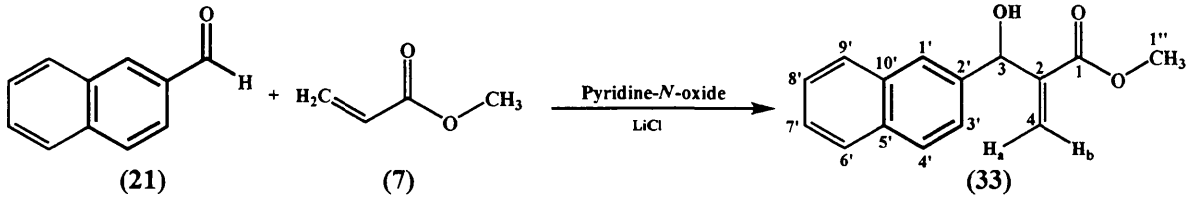

(21) (7) (33)

Scheme 3.2.17. Synthesis of methyl 3-hydroxy-2-methylene-3-(2-naphthyl)prapanoate (**33**).

2) Secondly, the reaction of methyl 3-hydroxy-2-methylene-3-(2-nephthyl) prapanoate (**33**) with 1,1'-carbonyldiimidazole in the presence of excess imidazole as stated before [86] **(Scheme 3.2.18)**.

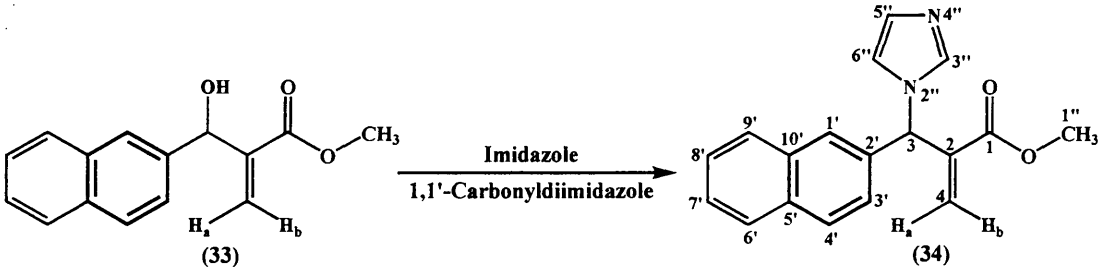

(33) (34)

Scheme 3.2.18. Synthesis of methyl 3-(1*H*-1-imidazole)-2-methylene-3-(2-naphthyl) propanoate (**34**).

Although the introduction of the methylene group retained the inhibitory activity (see section **3.4.1, table 3.4.1**), no more derivatives were made due to the expected irreversible enzyme inhibition that could result from the presence of the exposed methylene group which makes the dimethyl substituents still favourable.

3.2.7. Synthesis of 4-[(2-benzoxazolyl)amino]phenyl derivatives:

Based on previous work within our group [129] combined with our pharmacophore and docking results, a new series containing the benzoxazole heterocycle was developed.

• General chemistry:

The synthesis of the benzoxazoles series was carried out according to the following **Scheme 3.2.18**:

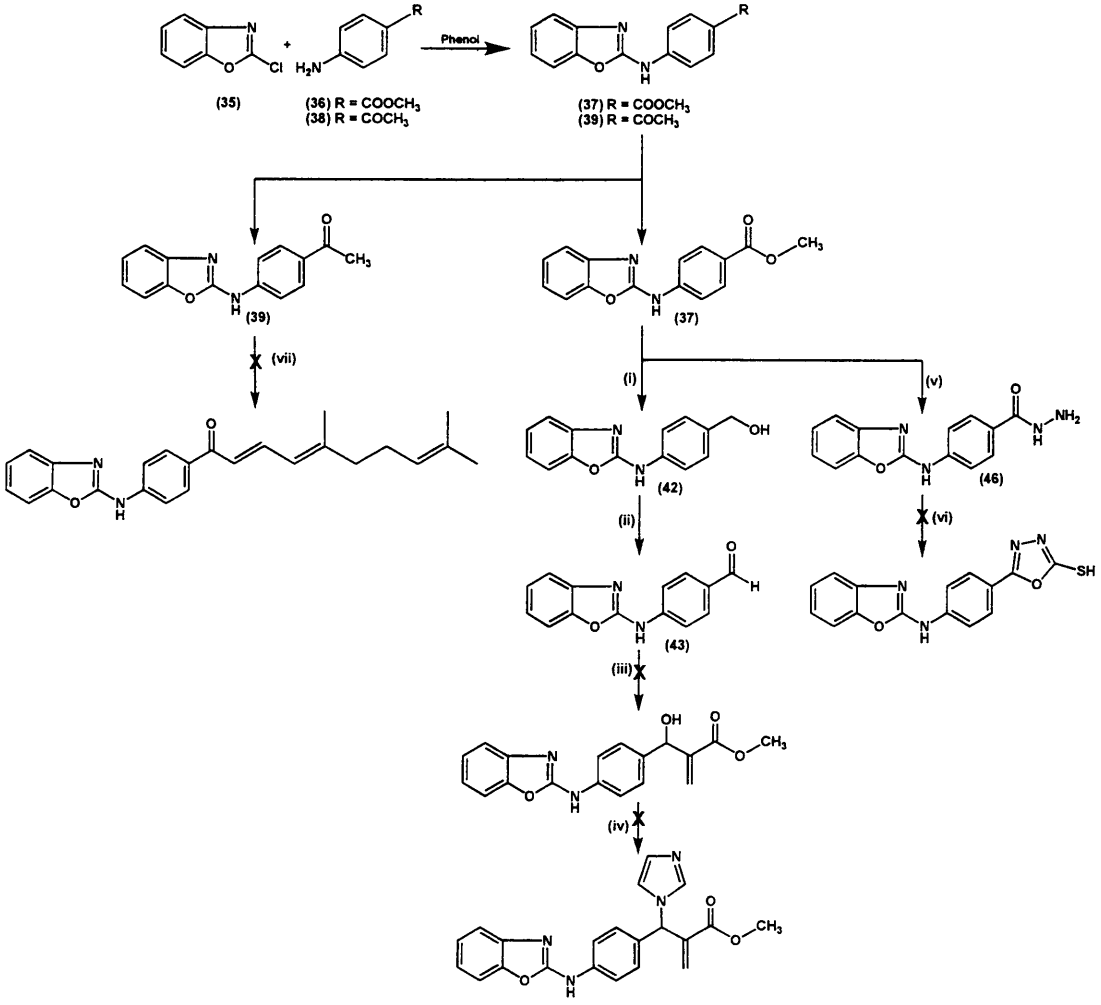

Scheme 3.2.18. General scheme for the synthesis of the benzoxazole series: (i) $LiAlH_4$, 20 min; (ii) SO_3-Py, DMSO, 0 °C, 5 min then rt, 25 min; (iii) Methyl acrylate, DABCO; (iv) Imidazole, 1,1'-carbonyldiimidazole, CH_3CN, 65 °C for 1h, then rt, 24 h; (v) $NH_2NH_2.H_2O$, reflux 3 h; (vi) CS_2, KOH, Δ, 24 h; (vii) Citral, NaOEt.

3.2.7.1. Coupling of the 4-aminophenyl derivatives with 2-chlorobenzoxazole:

The formation of 4-[(2-benzoxazolyl)amino]phenyl derivatives involved a nucleophilic substitution reaction between 4-amino phenyl derivatives and the 2-chlorobenzoxazole (**35**) in the presence of phenol **(Scheme 3.2.19)**.

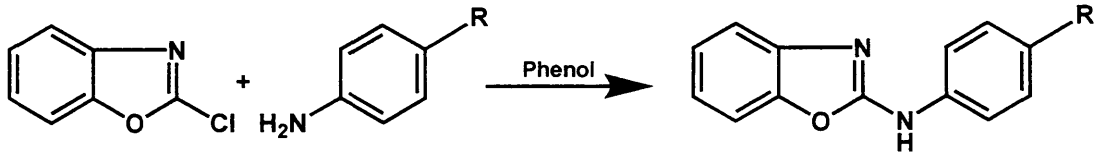

(35) **(36) R = $COOCH_3$** **(37) R = $COOCH_3$**
(38) R = $COCH_3$ **(39) R = $COCH_3$**

Scheme 3.2.19. Synthesis of 4-[(2-benzoxazolyl)amino]phenyl derivatives.

Unfortunately this reaction is not common; although it seems theoretically a very simple reaction. The reported method for this reaction [204] using methyl 4-aminobenzoate and 2-chlorobenzoxazole in benzene as a solvent did not work. The method using phenol is not a reported method for the preparation of benzoxazoles compounds, but it was reported for the preparation of benzothiazoles [205]. The role of phenol, other than solvation, is unclear although it may act as a Lewis acid. The reaction of 4-aminobenzylalcohol **(40)** with the 2-chlorobenzoxazole (**35**) **(Scheme 3.2.20)** led to the formation *N*-(1,3-benzoxazol-2-yl)-*N*-[4-(phenoxymethyl)phenyl] amine (**41**) as a white solid through the protonation of the alcohol which was then attacked by the phenolate anion **(Scheme 3.2.21)**.

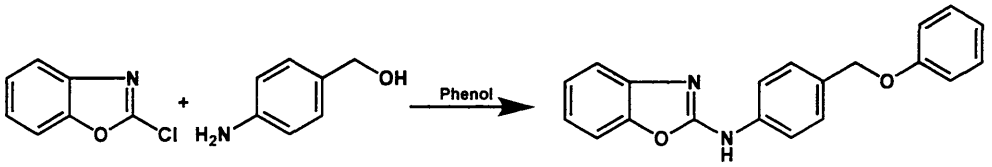

(35) **(40)** **(41)**

Scheme 3.2.20. The reaction between 4-aminobenzylalcohol **(40)** with the 2-chlorobenzoxazole (**35**).

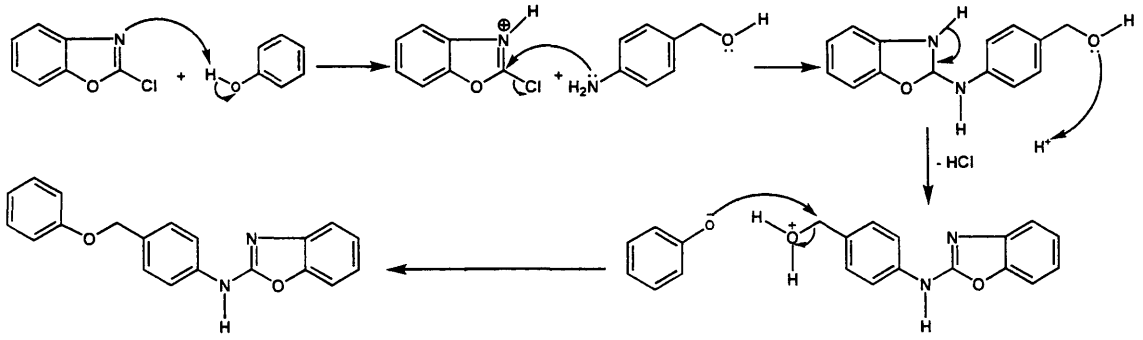

Scheme 3.2.21. Proposed mechanism for the reaction between 4-aminobenzylalcohol **(40)** with 2-chlorobenzoxazole (**35**).

3.2.7.2. Uses of the benzoxazole acetophenone (39):

The main reaction planned for the acetophenone derivative was the aldol condensation with citral to form a long alkyl chain that resembles vitamin A **(Scheme 3.2.22)**.

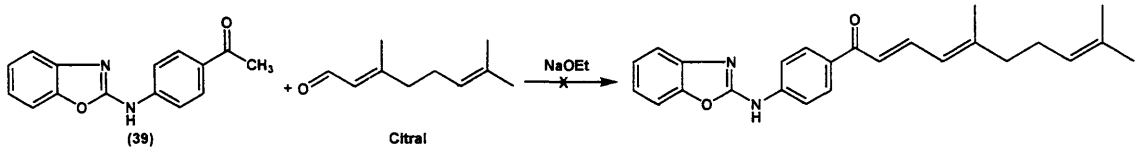

Scheme 3.2.22. Proposed reaction of the acetophenone derivative with citral.

However, because of the lability of the bond between the amino group and the benzoxazoles and the reduced reactivity of the ketone, the reaction did not work. It was thought that, protection of the amino group with BOC-anhydride **(Scheme 3.2.23)** may reduce the electron-donating ability of the amino group and possibly stabilise the bond between the NH and benzoxazole.

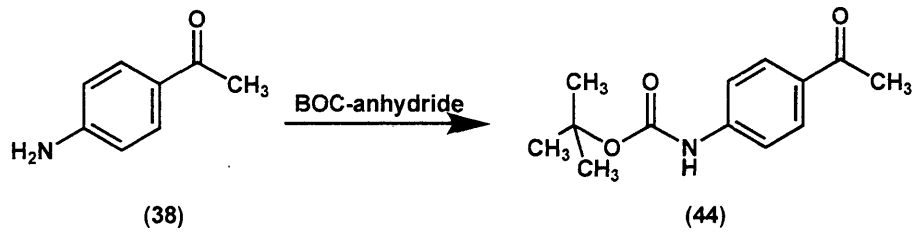

Scheme 3.2.23. Protection of 4-aminoacetophenone with BOC-anhydride

The next step was to form the methyl bromide to make the reaction with citral

easier and to avoid drastic conditions **(Scheme 3.2.24)**.

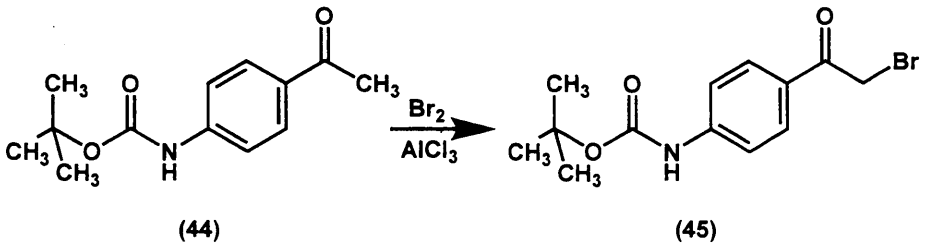

(44) (45)

Scheme 3.2.24. Formation of the bromide (**45**).

In spite of the protection of the amino group, the NH-benzoxazole bond was still very labile and the formation of the branched compound failed.

3.2.7.3. Uses of the benzoxazole ester (37):

1) Synthesis of Baylis Hillman products:

The key intermediate in these reactions is the preparation of the aldehyde which was prepared through the following **Schemes 3.2.25**:

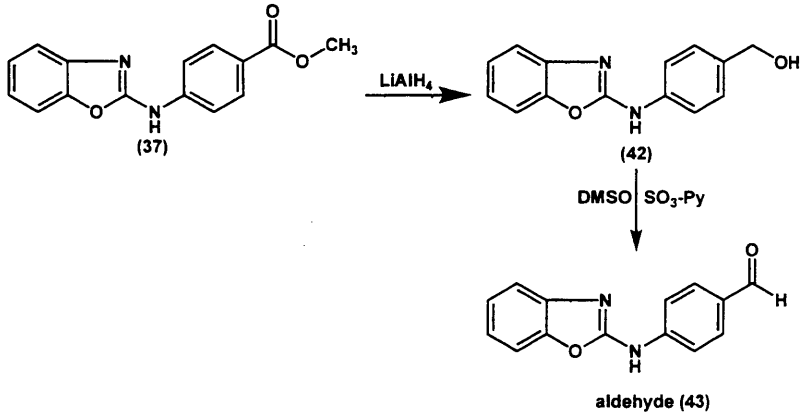

(37) (42) aldehyde (43)

Scheme 3.2.25. Preparation of the key aldehyde intermediate

The aldehyde (**43**) was prepared in two steps from the benzoxazole ester (**37**). As mentioned before the alcohol could not be synthesised using the phenol method and that is why the ester (**37**) has been used for this reaction. The ester was reduced with $LiAlH_4$ to give the alcohol (**42**) in 72 % yield, after extraction, and was pure enough for use in the next reaction step. The alcohol was insoluble in every solvent except DMSO, therefore the Parikh-Doering [206] oxidation was chosen as it uses DMSO as the reaction solvent and reagent, using this method the aldehyde was obtained as a pale yellow solid in low yield (19%). The major material was baseline by TLC and corresponded to the pyridine-SO_3 complex. The low yield may be owing

to either decomposition of the starting material under the reaction conditions or possibly N-oxidation; however isolation of either decomposition and/or by-product was not attempted from the DMSO/aqueous extraction layer.

The mechanism of the oxidation process using DMSO-SO_3 reagent, proceeds via an intermediary sulphonium ion, which collapses to a carbonyl compound (the aldehyde in our reaction) and dimethyl sulphide by a cyclic mechanism [207] **(Scheme 3.2.26)**.

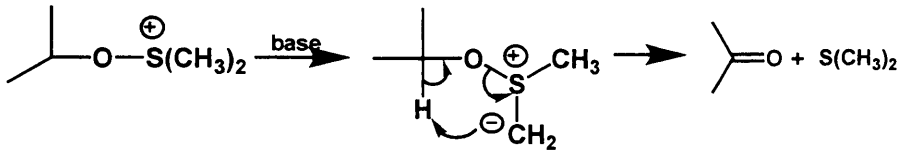

Scheme 3.2.26. Proposed mechanism for the oxidation of alcohol with DMSO.

Unfortunately, all the reactions that were planned using the aldehyde (e.g. Baylis-Hillman reaction **Scheme 3.2.27)** did not work, as the bond between the amino group and the benzoxazole is very labile under basic or acidic conditions. Also, the presence of the amino group in the *para* position reduces the reactivity of the carbonyl group.

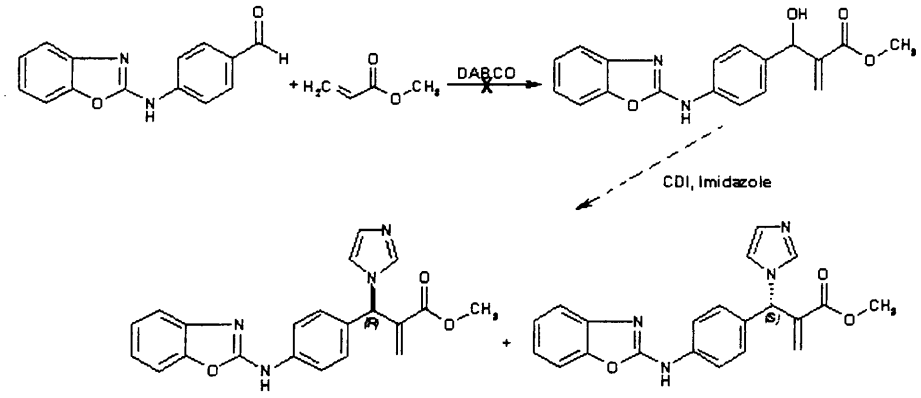

Scheme 3.2.27. Baylis-Hillman product.

2) Synthesis of 1,3,4-oxadiazole derivatives:

With the difficulty in introducing the imidazole group in our compounds, it was thought that replacing the whole imidazole methyl portion with 1,3,4-oxadiazole (**Figure 3.2.5**) might result in retaining inhibitory activity; specially with the previous data from the pharmacophore search and the docking (**Figure 3.1.3** and **Table 3.2.1**) with the CYP26A1 model, which showed very good interaction.

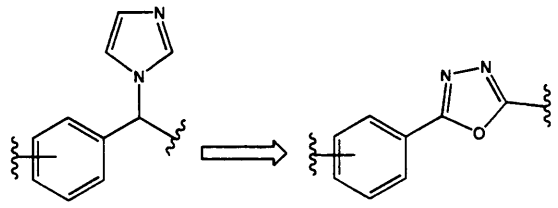

Figure 3.2.5. Replacement of the triazole by the oxadiazole.

The key intermediate of this reaction is the formation of the hydrazide which was prepared using the following reaction **(Scheme 3.2.28)**.

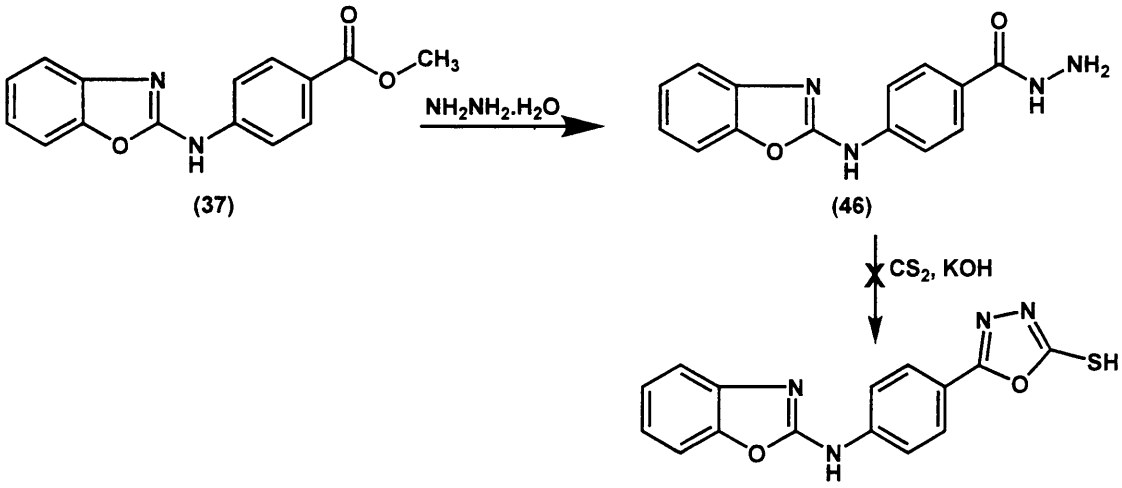

Scheme 3.2.28. Synthesis of the hydrazide (**46**).

The hydrazide (**46**) was prepared through the reaction of the ester (**37**) with excess hydrazine hydrate. The hydrazide was obtained in a fair yield of 45% after recrystallisation from aqueous ethanol.

Again due to the lability of the bond between the amino group and the benzoxazole, the formation of the 1,3,4-oxadiazole using CS_2 and KOH with reflux for about 20 h, was unsuccessful.

3.2.8. Synthesis of 2-[(4-arylamino)phenyl]-5-(aralkyl/aryl or alkoxycarbonylalkylsulfanyl)-1,3,4-oxadiazole:

As we previously discussed, this was a trial to replace the troubled imidazole ring with a more achievable oxadiazole ring, which showed good interaction with both the pharmacophore and the CYP26A1 homology model.

The synthesis of 2-[(4-arylamino)phenyl]-5-(aralkyl/aryl or alkoxycarbonyl alkylsulfanyl)-1,3,4-oxadiazole involves a sequence of 4 steps (**Scheme 3.2.29**):

1) Preparation of 5-(4-nitrophenyl)-1,3,4-oxadiazoline-2-thione.
2) Coupling of 5-(4-nitrophenyl)-1,3,4-oxadiazoline-2-thione with arylalkyl/aryl or bromoalkyl ester chains.
3) The reduction of the nitro to an amino group.
4) The coupling of the amino group with the aryl substituents through a Suzuki coupling reaction.

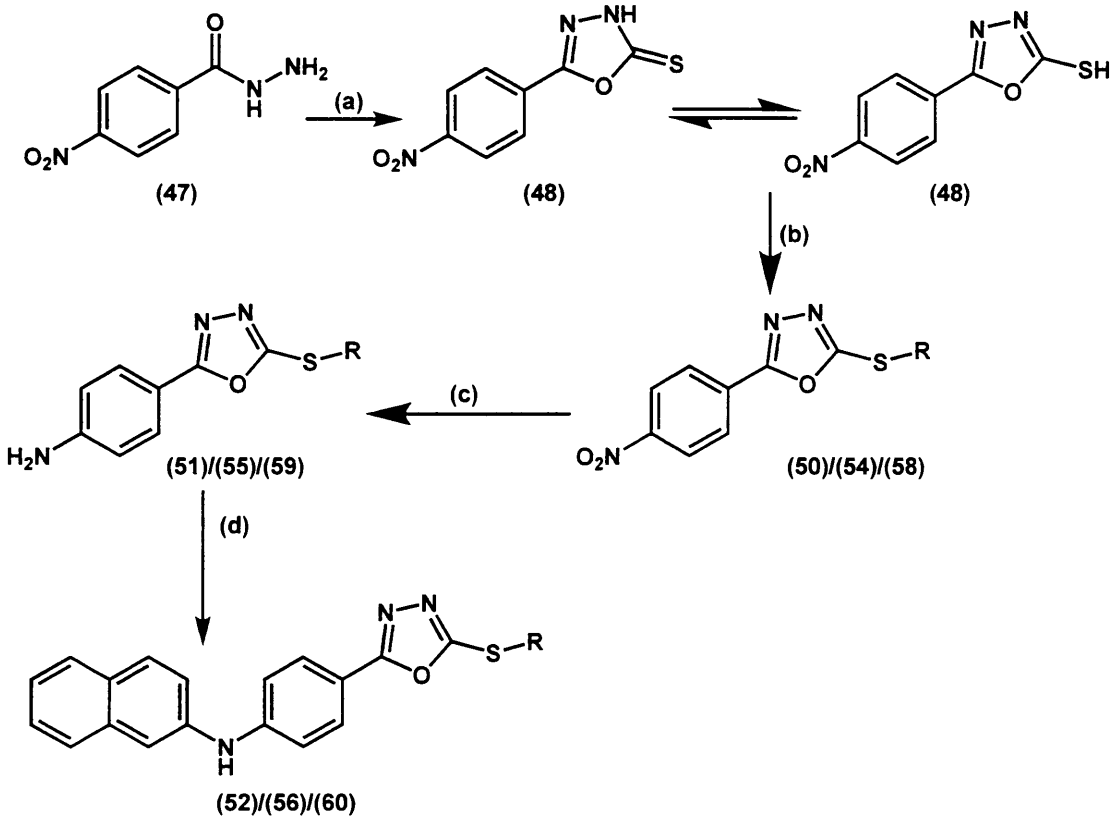

Scheme 3.2.29. Scheme of general chemistry: (a) CS_2, KOH, Δ, 24 h; (b) arylalkyl/alkyl bromide, K_2CO_3, rt, 24h; (c) Fe, NH_4Cl, EtOH, 3 h; (d) naphthyl-2-boronic acid, CuOAc, pyridine, CH_2Cl_2, 72 h.

3.2.8.1. Synthesis of 5-(4-nitrophenyl)-1,3,4-oxadiazoline-2-thione (48):

Different methods have been reported for the preparation of 5-aryl-2,3-dihydro-1,3,4-oxadiazole-2-thione where N-acylaminoiminophosphoranes were treated with carbon disulfide and the resulting isocyanates were cyclised without isolation to give 5-aryl-2,3-dihydro-1,3,4-oxadiazole-2-thiones in high yields [208].

It was also reported that 5-aryl-2,3-dihydro-1,3,4-oxadiazole-2-thiones were obtained by reaction of the acid hydrazides with an equivalent amount of

thiophosgene [209-211].

Moreover, 5-aryl-2,3-dihydro-1,3,4-oxadiazole-2-thiones were obtained by reaction of acid hydrazides and 1,1'-thiocarbonyldiimidazole in the presence of 3 equivalents of diisopropylethylamine (DIPEA) [212].

The most common method for the preparation of 5-aryl-2,3-dihydro-1,3,4-oxadiazole-2-thione is the reaction of acid hydrazides with CS_2 in the presence of a base, such as triethylamine, imidazole, NaOH, KOH, K_2CO_3 or Na_2CO_3, in preferably, alcoholic solvents such as, EtOH, MeOH, ^iPrOH or THF [213-215].

For preparation of 5-(4-nitrophenyl)-1,3,4-oxadiazoline-2-thione (**48**) (**Scheme 3.2.30**), 4-nitrobenzoylhydrazide (**37**) was refluxed with CS_2 in the presence of KOH for 24 h. The resulting residue was dissolved in H_2O ant treated with 1N HCl to give the desired compound in a yield of 75%.

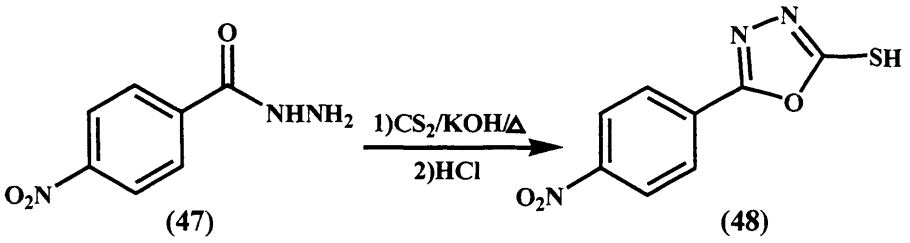

Scheme 3.2.30. Synthesis of 5-(4-nitrophenyl)-1,3,4-oxadiazoline-2-thione (**48**).

The mechanism of this reaction was proposed to be as follows; nucleophilic attack of the enolate ion **(i)** of the hydrazide on CS_2 forming a xanthate type salt **(ii)**. This salt might rearrange, through intramolecular acylation of the neighbouring amino function, to the potassium salt of 3-acyldithiocarbazinic acid **(iv)** via an intermediate oxadiazoline **(iii)**. It is possible that as equilibrium exists between **(v)** and **(viii)**, the position of which could be influenced by the relative nucleophilic character of oxygen versus sulphur or by steric hindrance around the carbonyl carbon. The 5-aryl-2,3-dihydro-1,3,4-oxadiazole-2-thione **(ix)** would be produced with concomitant loss of hydrogen sulfide, (**Scheme 3.2.31**) [214].

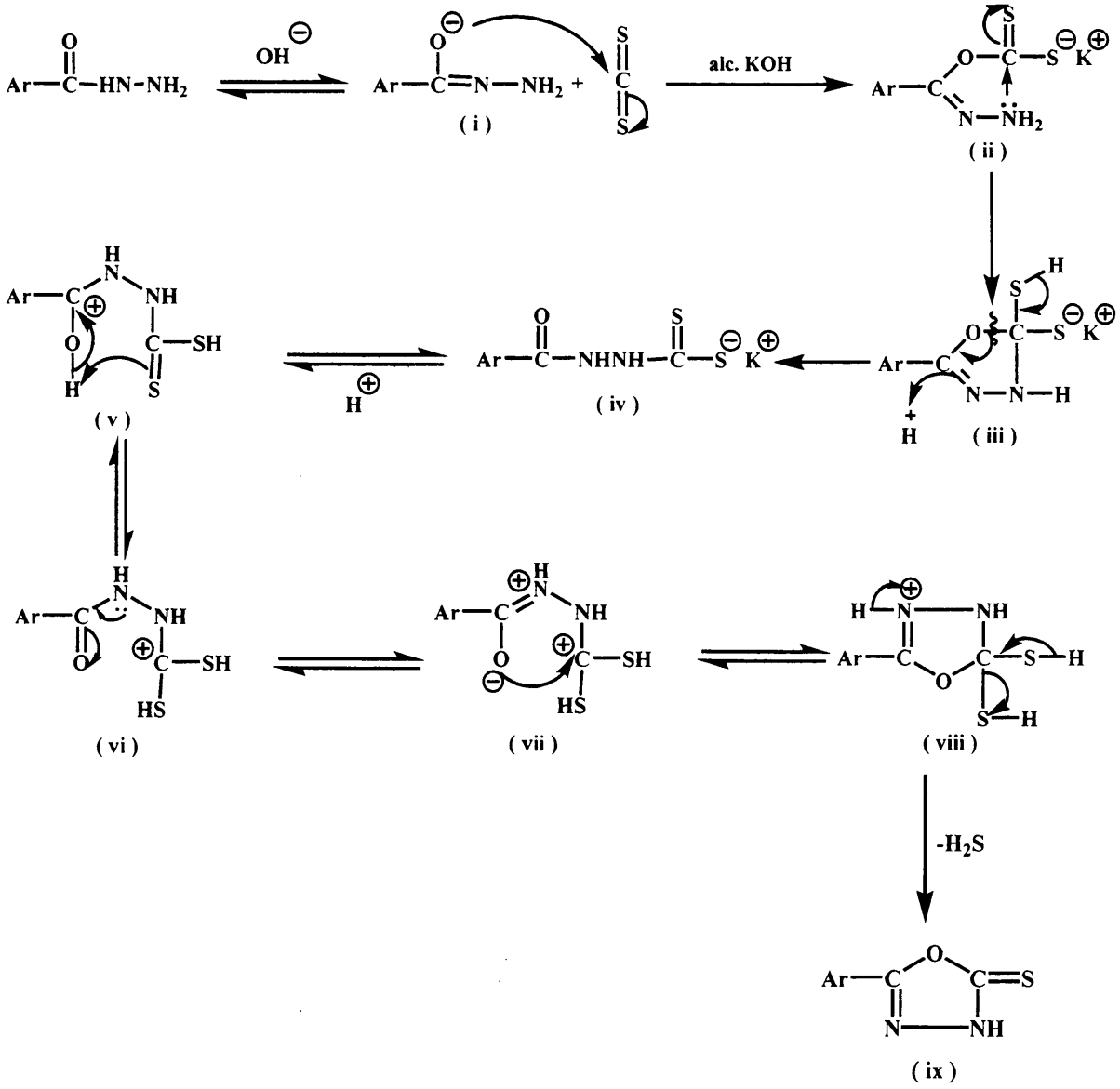

Scheme 3.2.31. Proposed mechanism for the formation of 5-aryl-1,3,4-oxadiazoline-2-thione [214].

3.2.8.2. Synthesis of 2-(4-nitrophenyl)-5-(alkyl/arylalkyl or alkoxycarbonylalkylsulfanyl)-1,3,4-oxadiazole:

For the preparation of 2-(4-nitrophenyl)-5-(alkyl/arylalkyl or alkoxycarbonyl alkyl sulfanyl)-1,3,4-oxadiazole, the 5-(4-nitrophenyl)-1,3,4-oxadiazoline-2-thione (**48**) was reacted with the arylalkyl/alkyl bromides bromoalkyl ester (**Scheme 3.2.32**) in the presence of K_2CO_3, at room temperature. Three representatives have been synthesised: 2-(4-nitrophenyl)-5-(phenethylsulfanyl)-1,3,4-oxadiazole (**50**) from 1-(2-bromoethyl)benzene (**49**), 2-(4-nitrophenyl)-5-(pentylsulfanyl)-1,3,4-oxadiazole (**54**) from 1-bromopentane (**53**) in yields of 69% for both reactions and ethyl 2-{[5-(4-

nitrophenyl)-1,3,4-oxadiazol-2-yl]sulfanyl}acetate (**58**) from ethyl 2-bromoacetate (**57**) in a yield of 62%.

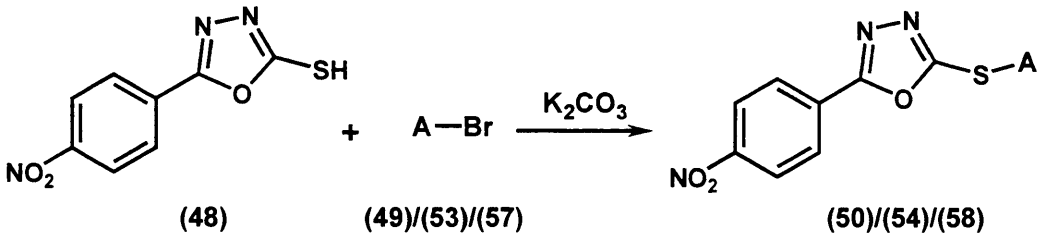

(48) (49)/(53)/(57) (50)/(54)/(58)

A = (**49**)/(**50**) Phenethyl

(**53**)/(**54**) pentyl

(**57**)/(**58**) $-CH_2COOCH_2CH_3$

Scheme 3.2.32. Synthesis of 2-(4-nitrophenyl)-5-(alkyl/aralkyl or alkoxycarbonyl alkyl sulfanyl)-1,3,4-oxadiazole.

3.2.8.3. Reduction of 2-(4-nitrophenyl)-5-(alkyl/arylalkylsulfanyl)-1,3,4-oxadiazole:

Reduction of 2-(4-nitrophenyl)-5-(alkyl/arylalkyl or alkoxycarbonyl alkyl sulfanyl)-1,3,4-oxadiazole to the corresponding 4-[5-(alkyl/arylalkyl or alkoxycarbonyl alkyl sulfanyl)-1,3,4-oxadiazol-2-yl]aniline was tried using 5% Pd-C and hydrogen atmosphere. The low yield of 34% obtained in this reduction is probably due to poisoning of the catalyst through complexation with the sulphur atom.

Another method of reduction using iron in the presence of NH_4Cl (**Scheme 3.2.33.**) has been used to give 4-[5-(alkyl/arylalkyl or alkoxycarbonyl alkyl sulfanyl)-1,3,4-oxadiazol-2-yl]anilines in much better yields of 89%, 79% and 78% respectively.

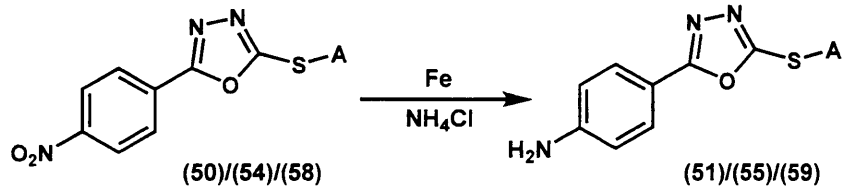

(50)/(54)/(58) (51)/(55)/(59)

A = (**50**)/(**51**) Phenethyl

(**54**)/(**55**) pentyl

(**58**)/(**59**) $-CH_2COOCH_2CH_3$

Scheme 3.2.33. Reduction of 2-(4-nitrophenyl)-5-(alkyl/arylalkyl or alkoxycarbonyl alkyl sulfanyl)-1,3,4-oxadiazole (**50**)/(**54**)/(**58**).

3.2.8.4. Synthesis of *N*-(2-naphthyl)-*N*-{4-[5-(alkyl/arylalkyl or alkoxycarbonyl alkyl sulfanyl)-1,3,4-oxadiazol-2-yl]phenyl} amine (52)/(56)/(60):

The Suzuki coupling reaction was used as before for the synthesis of *N*-(2-naphthyl)-*N*-{4-[5-(alkyl/arylalkyl or alkoxycarbonyl alkyl sulfanyl)-1,3,4-oxadiazol-2-yl]phenyl}amine (**52**)/(**56**)/(**60**) through the reaction between naphthylboronic acid (**16**) and 4-[5-(alkyl/arylalkyl or alkoxycarbonyl alkyl sulfanyl)-1,3,4-oxadiazol-2-yl]aniline (**51**)/(**55**)/(**59**) (**Scheme 3.2.34.**) to give the product in a yield of 71%, 65% and 78% respectively.

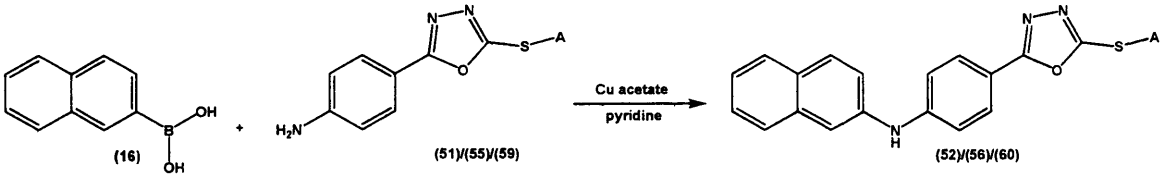

A = (**51**)/(**52**) Phenethyl

(**55**)/(**56**) pentyl

(**59**)/(**60**) $-CH_2COOCH_2CH_3$

Scheme 3.2.34. *N*-(2-naphthyl)-*N*-{4-[5-(alkyl/arylalkyl or alkoxycarbonyl alkyl sulfanyl)-1,3,4-oxadiazol-2-yl]phenyl}amine (**52**)/(**56**)/(**60**).

3.3. Chemistry of CYP24A1 inhibitors

(1) Azoles CYP24A1 inhibitors:

The idea behind this was to combine **VID 400**, a described potent CYP24A1 inhibitor, with calcitriol as the lead compound for this series (**Figure 3.3.1**).

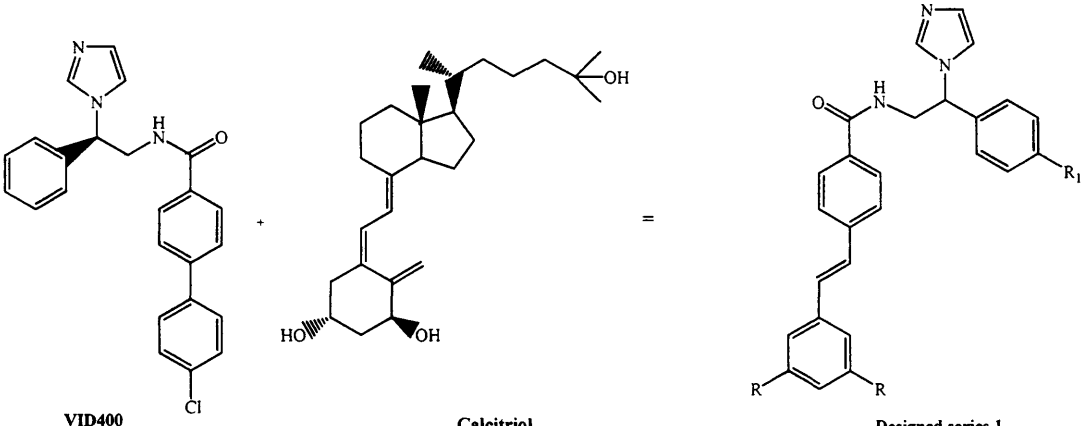

Figure 3.3.1. Design of the CYP24A1 first series.

3.3.1. Synthesis of *N*-[2-(1*H*-1-imidazolyl)-2-phenyl/flourophenylethyl]-4-[(*E*)-2-(3,5-unsubstituted/disubstitutedphenyl)-1-ethenyl]benzamide:

The synthesis of *N*-[2-(1*H*-1-imidazolyl)-2-phenyl/flourophenylethyl]-4-[(*E*)-2-(3,5-unsubstituted/disubstitutedphenyl)-1-ethenyl]benzamide was carried out according to the following steps (**Scheme 3.3.1**):

1) Synthesis of the 1,3-unsubstituted/disubstituted-5-vinylbenzene.

2) Preparation of 4-[(*E*)-2-(3,5-unsubstituted/dimethoxyphenyl)-1-ethenyl] benzoic acid.

3) Synthesis of *N*-(2-hydroxy-2-phenylethyl)-4-[(*E*)-2-(3,5-unsubstituted/ dimethoxyphenyl)-1-ethenyl]benzamide.

4) Synthesis of 2-4-[(*E*)-2-(3,5-unsubstituted/dimethoxyphenyl)-1-ethenyl] phenyl-5-phenyl-4,5-dihydro-1,3-oxazole.

5) Synthesis of *N*-[2-(1*H*-1-imidazolyl)-2-phenylethyl]-4-[(*E*)-2-(3,5-unsubstituted/dimethoxyphenyl)-1-ethenyl]benzamide.

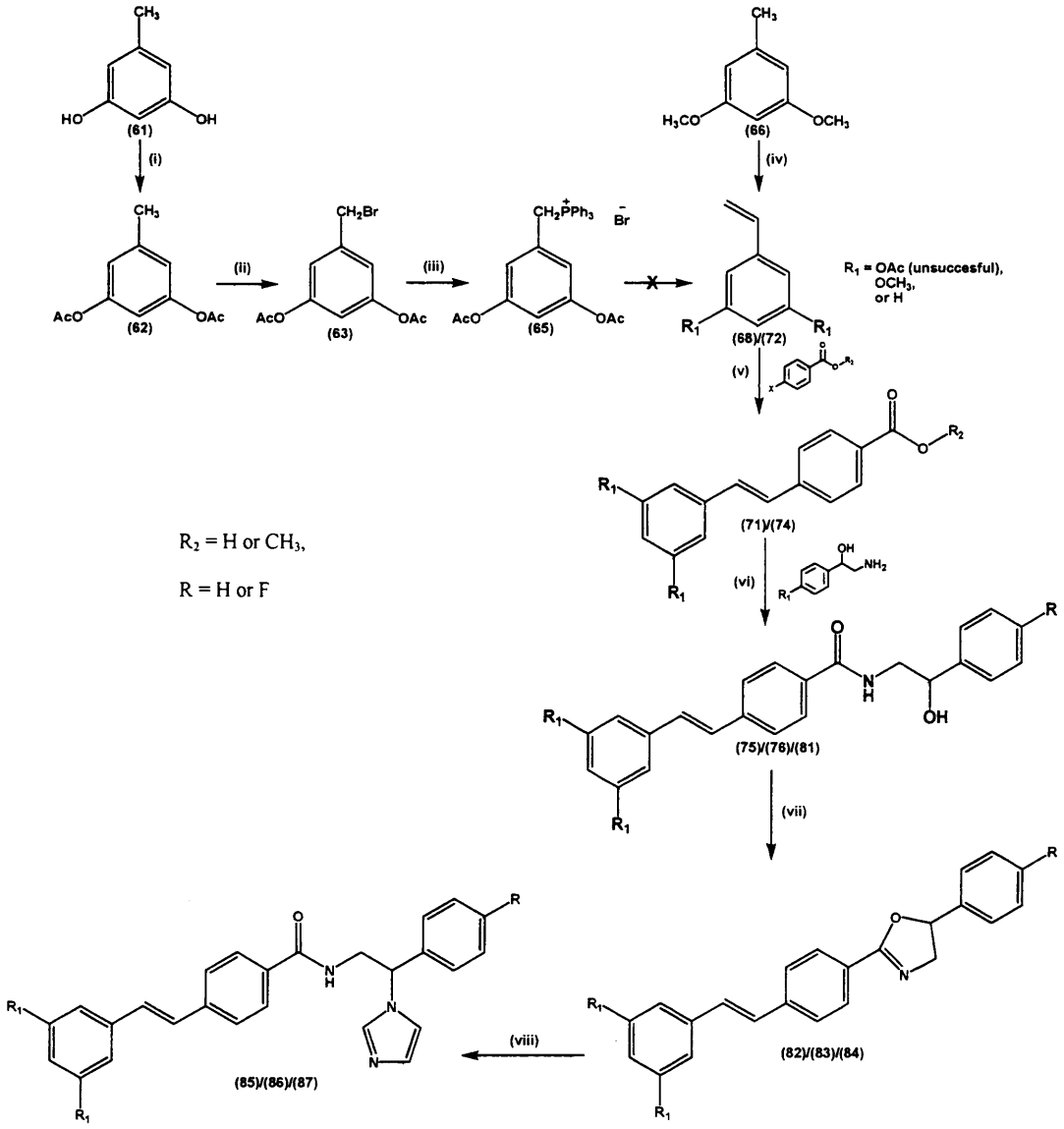

Scheme 3.3.1. Synthesis of the azole derivatives: (i) Ac_2O, rt, 17 h; (ii) *N*-bromosuccinimide, benzoyl peroxide, reflux 3 h; (iii) PPh_3, reflux 6 h; (iv) Ph_3PCH_3Br, *t*-BuOK, rt, 2 h; (v) $Pd(OAc)_2$, ToP, Et_3N, 80 °C, 2 h; (vi) 1,1'-carbonyldiimidazole, rt, overnight; (vii) methanesulphonic anhydride, NEt_3, 0 °C in the fridge overnight; (viii) imidazole, 24 h, 125 °C.

3.3.1.1. Synthesis of 4-[(*E*)-2-(3,5-diacyl/alkyloxyphenyl)-1-ethenyl]benzoic acid:

(1) Preparation of 3-(acetyloxy)-5-methylphenyl acetate (62):

The first step in the preparation of 4-[(*E*)-2-(3,5-diacyl/alkyloxyphenyl)-1-ethenyl]benzoic acid was to obtain the vinylbenzene compound.

In this reaction [215], orcinol (**61**) was used as the starting material, and the two hydroxyl groups were protected using acetic anhydride. The reaction took a long time

(17 h) at room temperature, however it gave the acetylated (**62**) product in almost quantitative yield (99%) **(Scheme 3.3.2)**.

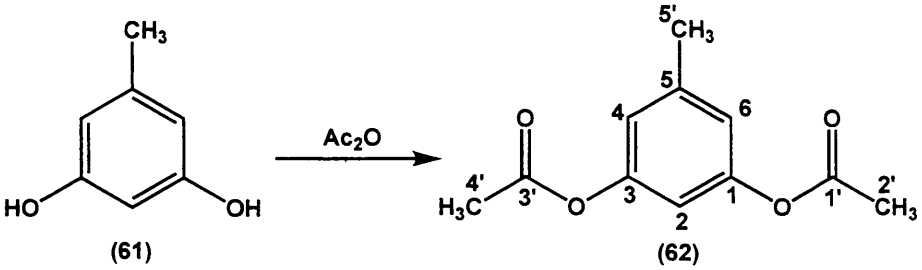

Scheme 3.3.2. Preparation of 3-(acetyloxy)-5-methylphenyl acetate (**62**).

(2) Preparation of 3-(acetyloxy)-5-(bromomethyl)phenyl acetate (63):

Bromination of 3-(acetyloxy)-5-methylphenyl acetate (**62**) was performed using Wohl–Ziegler bromination [215]. In Wohl–Ziegler bromination, *N*-bromosuccinimide (NBS) was used in the presence of benzoyl peroxide as a catalyst, and CCl_4 as the solvent **(Scheme 3.3.3)**.

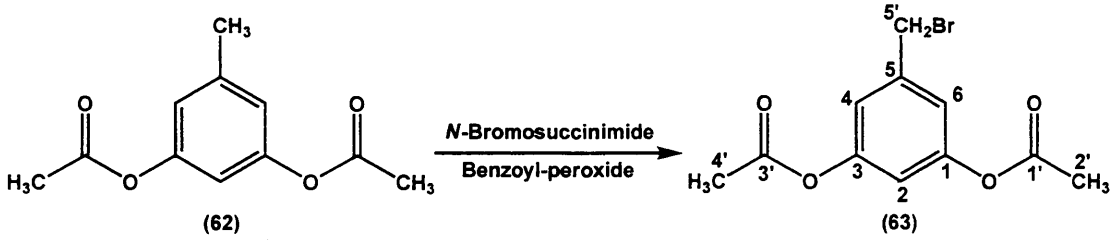

Scheme 3.3.3. Preparation of 3-(acetyloxy)-5-(bromomethyl)phenyl acetate (**63**).

The mechanism of bromination with NBS involves a free radical process [216]. Thermal decomposition of benzoyl peroxide provides the radical initiator (Step 1). Reaction with molecular bromine (present as an impurity in the NBS) affords the bromine radical (Step 2) which abstracts a proton from the benzylic methyl (Step 3). An ionic reaction between NBS and the HBr formed in Step 3 affords molecular bromine (Step 4) which reacts with the benzylic radical to give the product and a bromine radical (Step 5). Propagation occurs when the bromine atom reinserts itself into Step 3 **(Scheme 3.3.4)**.

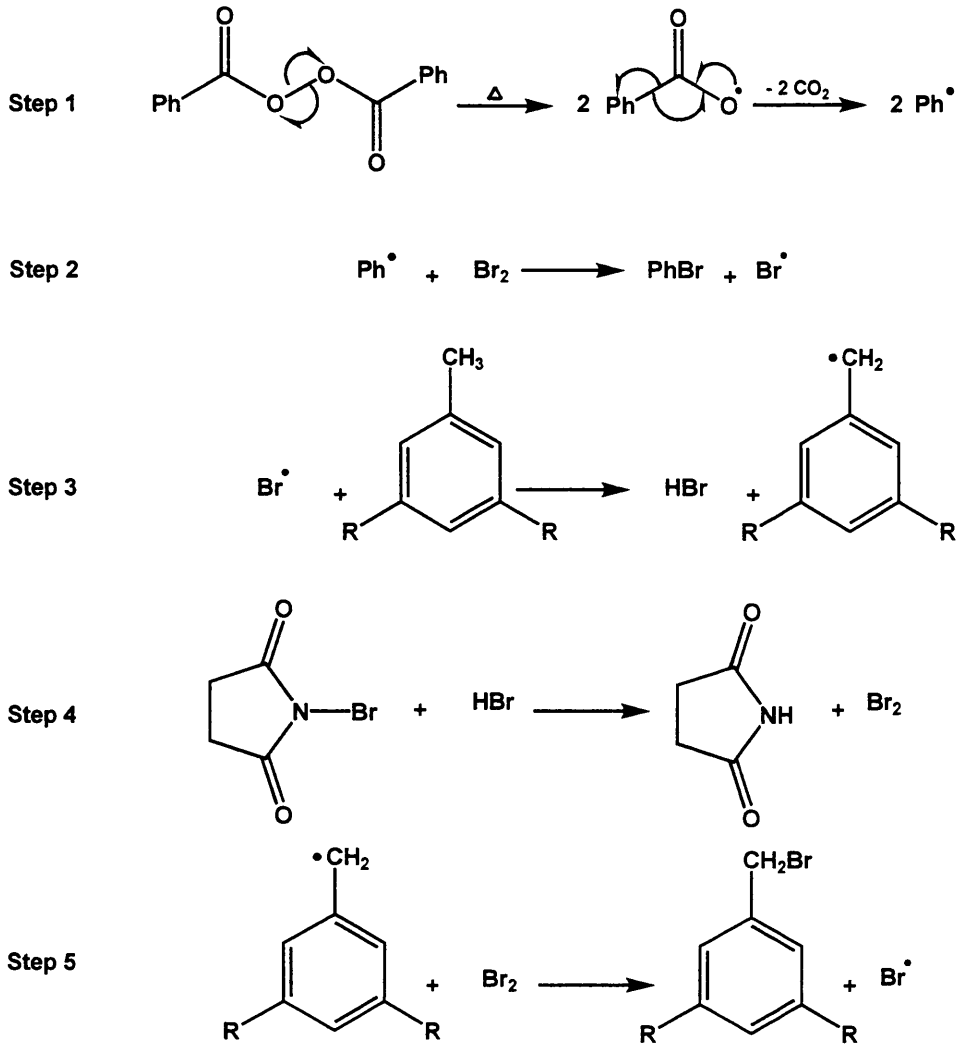

Scheme 3.3.4. Proposed mechanism for NBS bromination.

(3) Preparation of 3,5-diacetoxybenzyl-(triphenyl)phosphonium bromide (65):

The preparation of this phosphonium salt was an important step for the preparation of the Wittig reagent to proceed to the vinyl benzene. The reaction [215] was performed by refluxing 3-(acetyloxy)-5-(bromomethyl)phenyl acetate (**63**) with triphenylphosphine (**64**) **(Scheme 3.3.5)** to give the phosphonium bromide salt in a yield of 57%.

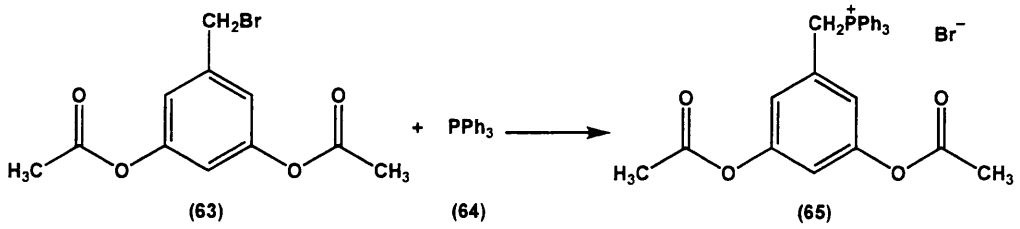

Scheme 3.3.5. Preparation of 3,5-diacetoxybenzyl-(triphenyl)phosphonium bromide (**65**).

Unfortunately, all attempts to generate the Wittig reagent from the phosphonium salt, using strong base, e.g. NaH, was not successful, and that is why an alternative pathway was taken.

(4) Preparation of 1,3-dimethoxy-5-vinylbenzene (68):

The synthesis of 1,3-dimethoxy-5-vinylbenzene (**68**) [217] was performed using the simple Wittig reaction. Methyl triphenylphosphonium bromide (**67**) and *t*-BuOK were used to generate the Wittig reagent which was then reacted with 3,5-dimethoxybenzaldehyde (**66**) to form 1,3-dimethoxy-5-vinylbenzene (**68**) **(Scheme 3.3.6)** as a colourless oil in a yield of 70%.

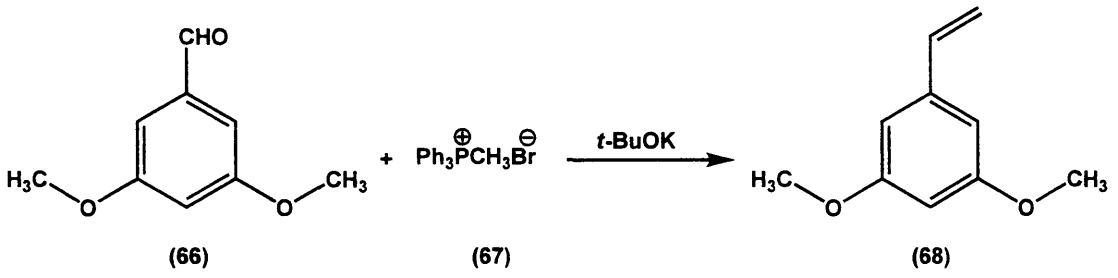

Scheme 3.3.6. Preparation of 1,3-dimethoxy-5-vinylbenzene (**68**).

The mechanism of the Wittig reaction [218] **(Scheme 3.3.7)** begins with the generation of the Wittig reagent. This is followed by cycloaddition of the Wittig reagents to the aldehyde to form a heterocycle called an oxaphosphetane. The oxaphosphetane then decomposes to give triphenylphosphine oxide and an alkene.

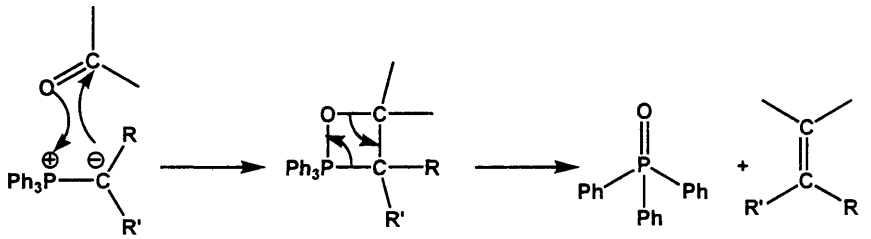

Scheme 3.3.7. Mechanism of the Wittig reaction [218].

(5) Preparation of methyl 4-[(*E*)-2-(3,5-dimethoxyphenyl)-1-ethenyl]benzoate (70):

The synthesis of methyl 4-[(*E*)-2-(3,5-dimethoxyphenyl)-1-ethenyl]benzoate (**68**) involves the coupling of 1,3-dimethoxy-5-vinylbenzene (**66**) with 4-iodo-methylbenzyl ester (**69**) via palladium-catalysed Heck reaction **(Scheme 3.3.8)**. The

reaction was performed in a basic medium using Et_3N at 80 °C for 24 h to give the desired compound in a yield of 86%.

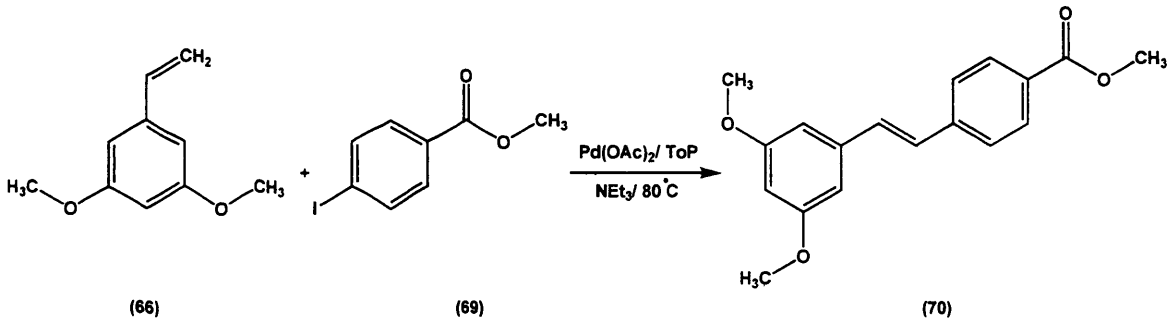

(66) (69) (70)

Scheme 3.3.8. Preparation of methyl 4-[(*E*)-2-(3,5-dimethoxyphenyl)-1-ethenyl]benzoate (**70**).

The mechanism of the Heck reaction [219] **(Scheme 3.3.9)** involves a catalytic cycle with a series of transformations around the palladium catalyst. The palladium compound required in this cycle is generally prepared *in situ* from palladium(II) acetate as a palladium(II) precursor which was reduced by tri(*o*-tolyl)phosphine to di(tri(*o*-tolyl)phosphine)palladium(0) and tri(*o*-tolyl)phosphine is oxidized to tri(*o*-tolyl)phosphine oxide in step I. Step II is an oxidative addition in which palladium inserts itself in the aryl iodide bond. In step III, palladium forms a π complex with the alkene and in step IV the alkene inserts itself in the palladium - carbon bond in a *syn* addition step. Step V is a β-hydride elimination step with the formation of a new palladium - alkene π complex. This complex is destroyed in step VI. The palladium(0) compound which is regenerated by reductive elimination of the palladium(II) compound by a base in the final step VII.

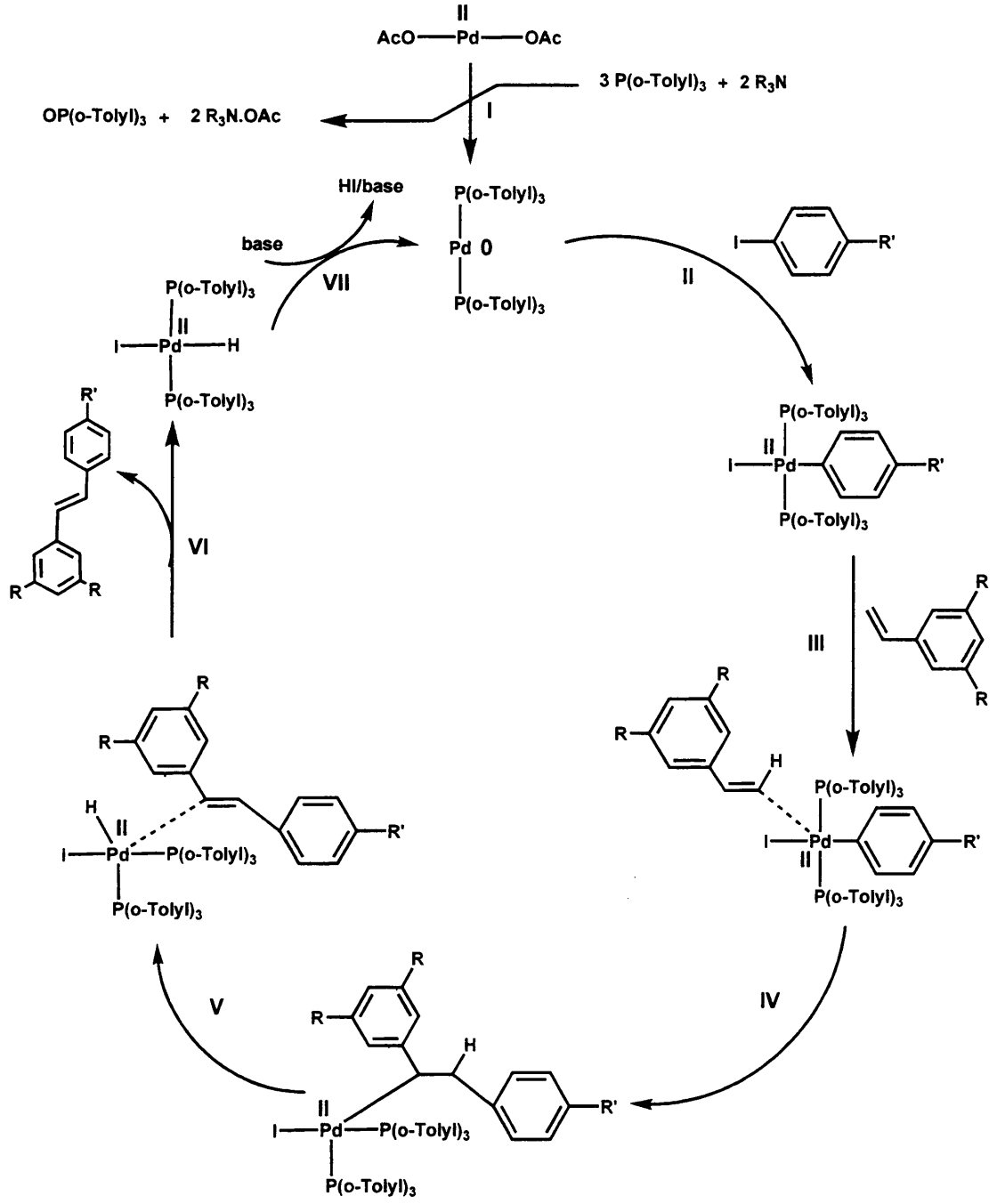

Scheme 3.3.9. Mechanism of the Heck reaction

(6) Preparation of 4-[(*E*)-2-(3,5-unsubstituted/dimethoxyphenyl)-1-ethenyl]benzoic acid

a) Preparation of 4-[(*E*)-2-(3,5-dimethoxyphenyl)-1-ethenyl]benzoic acid (71):

The synthesis of 4-[(*E*)-2-(3,5-dimethoxyphenyl)-1-ethenyl]benzoic acid (**71**) **(Scheme 3.3.10a)** from methyl 4-[(*E*)-2-(3,5-dimethoxyphenyl)-1-ethenyl]benzoate

(**70**) was a simple alkaline hydrolysis of the ester using 2M NaOH in EtOH as a solvent to give the desired free acid in 100% yield.

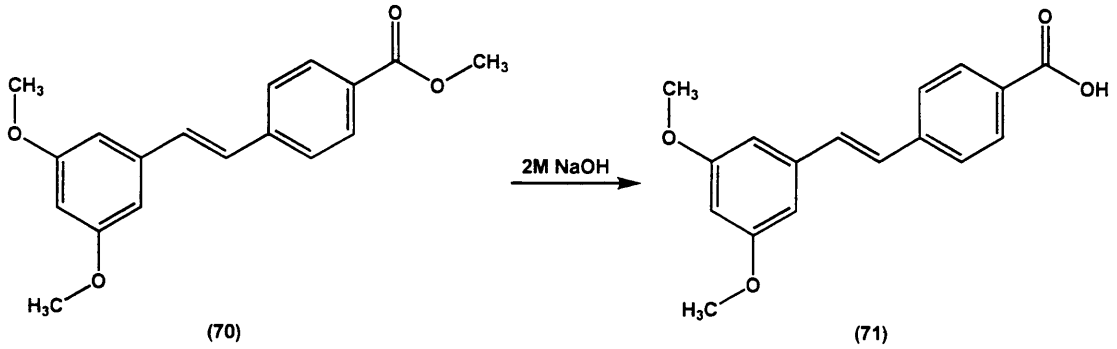

(70) (71)

Scheme 3.3.10a. Preparation of 4-[(*E*)-2-(3,5-dimethoxyphenyl)-1-ethenyl]benzoic acid (**71**).

b) Preparation of 4-[(*E*)-2-Phenyl-1-ethenyl]benzoic acid (74):

The same method used for the preparation of 4-[(*E*)-2-(3,5-dimethoxyphenyl)-1-ethenyl]benzoic acid (**71**) was tried for the preparation of 4-[(*E*)-2-phenyl-1-ethenyl]benzoic acid (**74**), but unfortunately the yield was not good (28%).

Another method has been used for the preparation of 4-[(*E*)-2-phenyl-1-ethenyl]benzoic acid (**74**) (**Scheme 3.3.10b**), which has been mentioned in the literature [220] using 4-bromobenzoic acid (**73**) and styrene (**72**) to give 4-[(*E*)-2-phenyl-1-ethenyl]benzoic acid (**74**) in a yield of 85%.

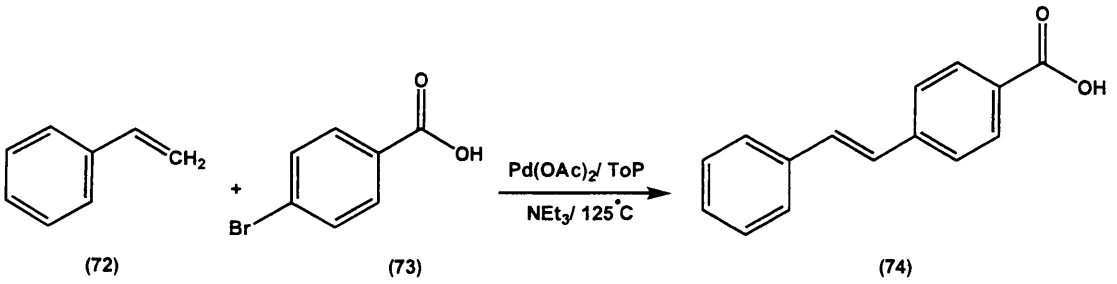

(72) (73) (74)

Scheme 3.3.10b. Preparation of 4-[(*E*)-2-phenyl-1-ethenyl]benzoic acid (**74**).

3.3.1.2. Synthesis of 4-[(*E*)-2-(3,5-unsubstituted/dimethoxyphenyl)-1-ethenyl] benzamide derivatives (75)/(76)/(81):

The synthesis of *N*-(2-hydroxy-2-phenylethyl)-4-[(*E*)-2-(3,5-dimethoxy/unsubstitutedphenyl)-1-ethenyl]benzamide (**75**)/(**76**) and *N*-[2-(4-fluorophenyl)-2-hydroxyethyl]-4-[(*E*)-2-(3,5-dimethoxy/unsubstitutedphenyl)-1-ethenyl]benzamide (**81**) was carried out using the reagent 1,1'-carbonyldiimidazole with the corresponding 4-unsubstituted/fluoro-2-amino-1-phenylethanol **(Scheme 3.3.11)**.

1,1'-Carbonyldiimidazole was used as a coupling reagent in the synthesis of the amide compound (**75, 76 and 81**). The products were isolated as pure white solids in different yields as shown in **Table 3.3.1**.

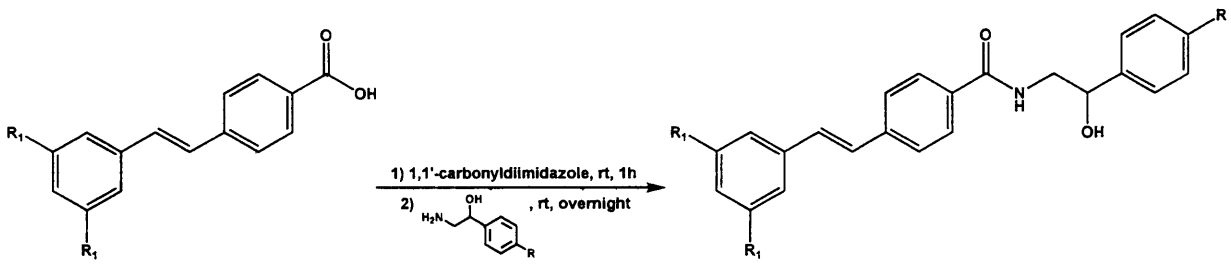

Scheme 3.3.11. Synthesis of 4-[(*E*)-2-(3,5-dimethoxy/unsubstitutedphenyl)-1-ethenyl]benzamide derivatives(**75**)/(**76**)/(**81**).

Table 3.3.1.

Compd. No.	R	R_1	Yield (%)
(**75**)	H	OCH_3	94
(**76**)	H	H	87
(**81**)	F	OCH_3	73

3.3.1.3. Synthesis of 2-{4-[(*E*)-2-(3,5-unsubstituted/dimethoxyphenyl)-1-ethenyl]phenyl}-5-phenyl-4,5-dihydro-1,3-oxazole derivatives (82)/(83)/(84):

This synthesis involved formation of an oxazole ring structure in which the oxazole compounds (**82-84**) were prepared by the reaction of the amide-containing compounds (**75, 76 and 81**) with methanesulphonic anhydride and a base (Et_3N) [221-222] **(Scheme 3.3.12)**. The yield of the oxazole compounds was very good for all of the compounds as shown in **Table 3.3.2**.

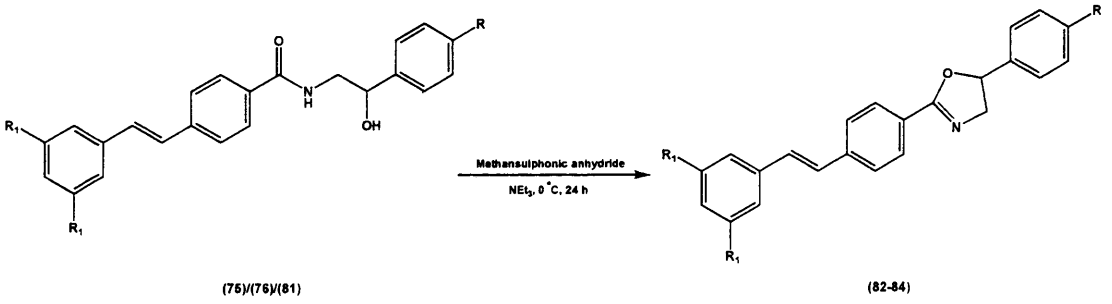

Scheme 3.3.12. Synthesis of 2-{4-[(*E*)-2-(3,5-dimethoxy/unsubstitutedphenyl)-1-ethenyl]phenyl}-5-phenyl-4,5-dihydro-1,3-oxazole derivatives (**82**)/(**83**)/(**84**).

Table 3.3.2.

Compd. No.	R	R_1	Yield (%)
(**82**)	H	OCH_3	100
(**83**)	H	H	97
(**84**)	F	OCH_3	98

The mechanism of this reaction involved nucleophilic attack by the hydroxyl group at the sulphur atom of methanesulphonic anhydride to form the intermediate (**a**). The activation of the carboxyl-oxygen as a nucleophile occurs as a result of the abstraction of the amido proton by the base; Et_3N [222] **(Scheme 3.3.13)**.

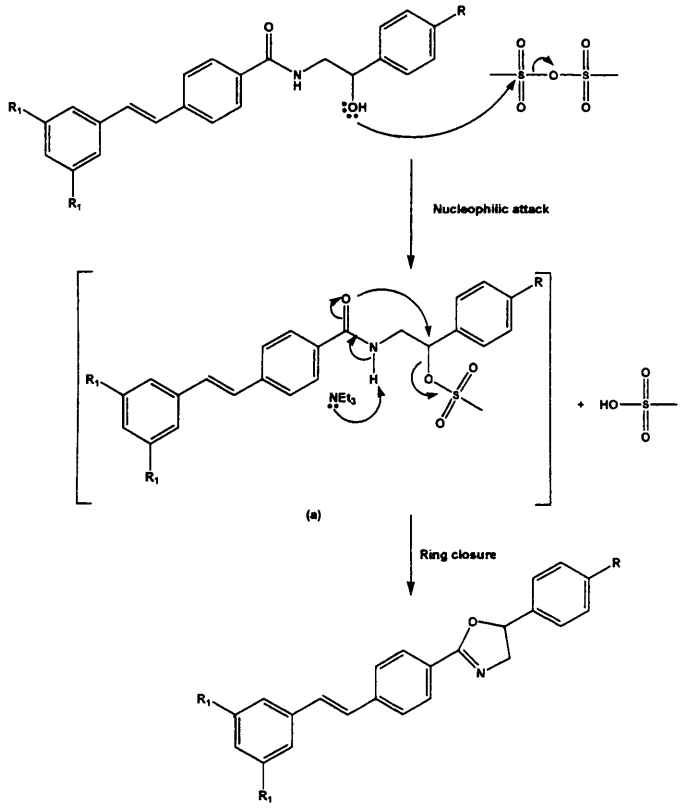

Scheme 3.3.13. Mechanism of formation of the oxazole ring.

3.3.1.4. Synthesis of *N*-[2-(1*H*-1-imidazolyl)-2-phenylethyl]-4-[(*E*)-2-(3,5-dimethoxy/unsubstitutedphenyl)-1-ethenyl]benzamide derivatives (85)/(86)/(87):

In this last step, heating of the oxazole compounds (**82-84**) in the presence of imidazole opened the oxazole ring by nucleophilic displacement [223] **(Scheme 3.3.14)**.

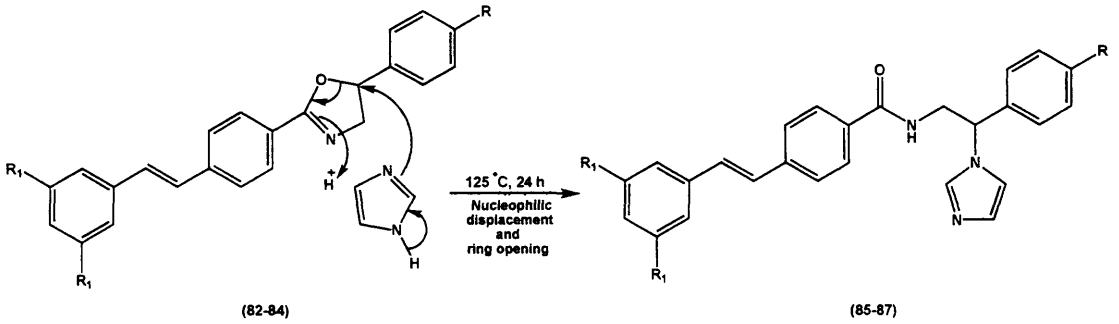

Scheme 3.3.14. Synthesis of the final compounds (**85-87**).

A reasonable yield of compounds (**85**)/(**86**) was produced 68%/47% respectively, while the flouro derivative (**87**) was not produced in a very good yield 35% (**Table 3.3.3**). All compounds were recrystallised from aqueous EtOH.

Table 3.3.2.

Compd. No.	R	R_1	Yield (%)
(**85**)	H	OCH_3	68
(**86**)	H	H	47
(**87**)	F	OCH_3	35

(2) Tetralones CYP24A1 inhibitors:

This series was designed based on previous work in our group on the 2-substituted-3,4-dihydro-2*H*-naphthalen-1-one derivatives (tetralones) [224]. The most potent tetralones in the previous series were the 2-methyl and 2-phenyl substituted benzyl tetralones (**Figure 3.3.2**) with IC_{50} values of 0.9 and 2.1 μM respectively in a rat mitochondrial CYP24 assay.

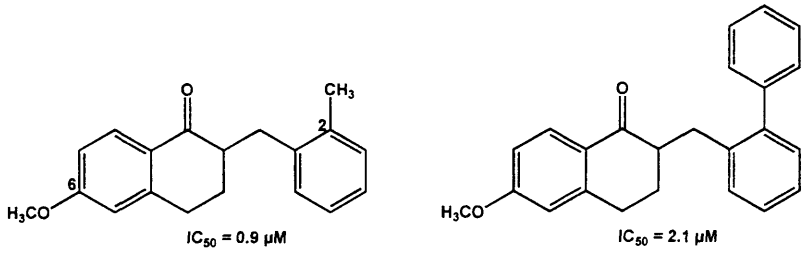

Figure 3.3.2. The structure of the lead compounds.

The target compounds (**Figure 3.3.3**) were planned to develop the lead compounds to explore the effect of varying the 2-substituents on IC_{50}. Also, a slight

preference for a 6-methoxy rather than a 6-hydroxy substituent in the naphthalene ring was noted; therefore the 6-methoxy has been included.

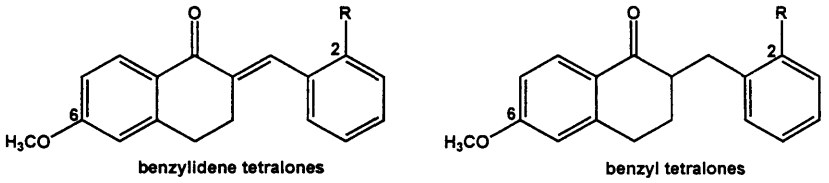

Figure 3.3.3. The target compounds.

The drawing of the benzylidene tetralones in the *E*-form at the double bond at the position of attachment between the tetralone and benzyl ring depends on previous x-ray crystallography of compound (**96**) that has been made and published before by our group [96].

3.3.2. Synthesis of the (*E*)-2-(2-substitutedbenzylidene)-6-methoxytetralone derivatives (90)/(93) and their reduced 2-(benzyl)-tetralones (91)/(94):

This synthesis involved direct condensation of commercially available 6-methoxytetralone (tetralone) (**88**) with the appropriate benzaldehyde (**89** and **92**) in ethanolic KOH solution (**Scheme 3.3.15**) [225].

The reduced 2-(benzyl)-tetralones (**91**)/(**94**) were readily obtained by hydrogenation of 2-benzylidenetetralone derivatives (**90**)/(**93**) with 10% Pd/C catalyst for 1 h, at approximately 30 psi (Parr hydrogenator) (**Scheme 3.3.15**).

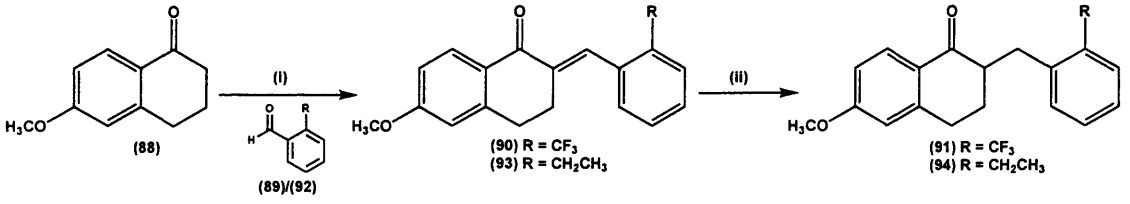

Scheme 3.3.15. Synthesis of the (*E*)-2-(2-substitutedbenzylidene)-6-methoxytetralone derivatives (**90**)/(**93**) and their reduced 2-(benzyl)-tetralones (**91**)/(**94**): (i) 4 % ethanolic KOH, rt, 1 h; (ii) Pd-C/ H_2, MeOH, 1 h.

The mechanism of the formation of 2-benzylidenetetralone derivatives (**90**)/ (**93**) is illustrated in **Scheme 3.3.16**. In this base-catalysed condensation between two carbonyl compounds, the hydroxide ion (from KOH) abstracts a proton from the α-carbon of the tetralone to form the carbanion [226]. The carbanion attacks the

electrophilic carbonyl carbon atom of the benzaldehyde to gives the unstable alkoxide, which abstracts a hydrogen ion from water to form intermediary aldol. The elimination of water from the aldol forms a carbon-carbon double bond which is conjugated to the aromatic ring, giving stability to the molecule [227].

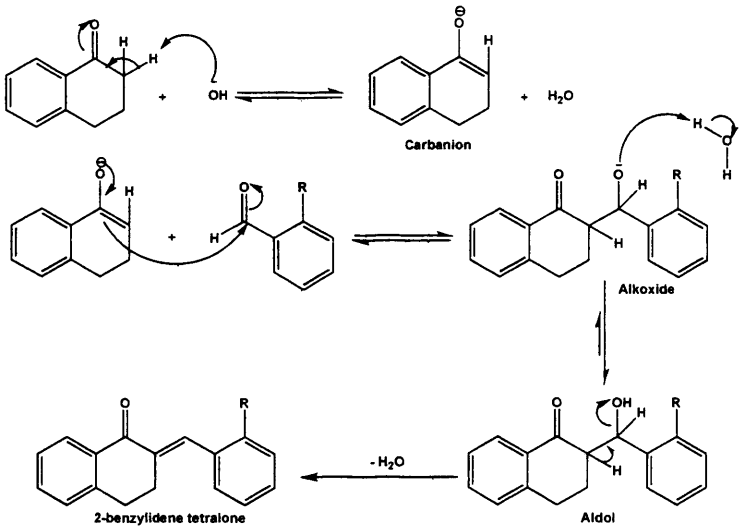

Scheme 3.3.16. Mechanism of the formation of the 2-benzylidene tetralones.

3.3.3. Synthesis of 6-methoxy-2-(1-{2-[(*E*)-2-phenyl-1-ethenyl]phenyl}methylidene)-1,2,3,4-tetrahydro-1-naphthalenone (98) and its reduced compound (99):

The 6-methoxy-2-(1-{2-[(*E*)-2-phenyl-1-ethenyl]phenyl}methylidene)-1,2,3,4-tetrahydro-1-naphthalenone (**98**) were prepared by Suzuki coupling of the 2-bromo-benzylidene tetralone [224] (**96**) with *trans*-2-phenylvinylboronic acid (**97**) (**Scheme 3.3.17**).

The 2-bromo-benzylidene tetralone (**96**) was prepared according to the same general procedure mentioned before for the synthesis 2-benzylidenetetralone derivatives (**90**)/(**93**) using 2-bromobenzaldehyde (**95**) and 6-methoxytetralone (tetralone) (**88**) in ethanolic KOH solution. This reaction was followed by Suzuki coupling of 2-bromo-benzylidene tetralone [224] (**96**) with *trans*-2-phenylvinylboronic acid (**97**) in the presence of $Pd(PPh_3)_4$ catalyst [228] (**Scheme 3.3.17**).

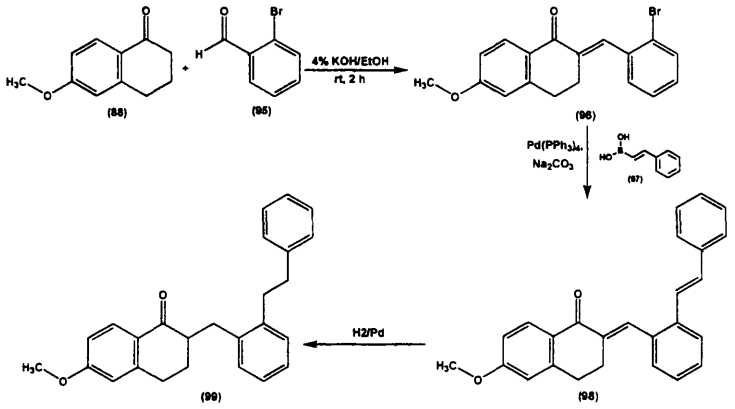

Scheme 3.3.17. Synthesis of compounds (**98**) and (**99**).

Reduction of (**98**) by hydrogenation with 10% Pd/C catalyst for 1 h, at approximately 30 psi (Parr hydrogenator), gave the reduced compound (**99**) (**Scheme 3.3.17**).

3.3.4. Synthesis of 6-methoxy-2-[2-[(*E*)-3,5-unsubstituted/dimethoxy-2-phenyl-1-ethenyl]benzyl]-1,2,3,4-tetrahydro-1-naphthalenone (105)/(106):

• General chemistry:

The synthesis of 6-methoxy-2-[2-[(*E*)-2-unsubstituted/substituted phenyl-1-ethenyl]benzyl]-1,2,3,4-tetrahydro-1-naphthalenone was carried out according to a sequence of 4 steps (**Scheme 3.3.18**):

1) The preparation ethyl 6-methoxy-1-oxo-1,2,3,4-tetrahydro-2-naphthalene-carboxylate.
2) The preparation of ethyl 2-(2-bromobenzyl)-6-methoxy-1-oxo-1,2,3,4-tetrahydro-2-naphthalenecarboxylate.
3) The decarboxylation of ethyl 2-(2-bromobenzyl)-6-methoxy-1-oxo-1,2,3,4-tetrahydro-2-naphthalenecarboxylate.
4) Suzuki coupling of the decarboxylated compound with boronic acid compound.

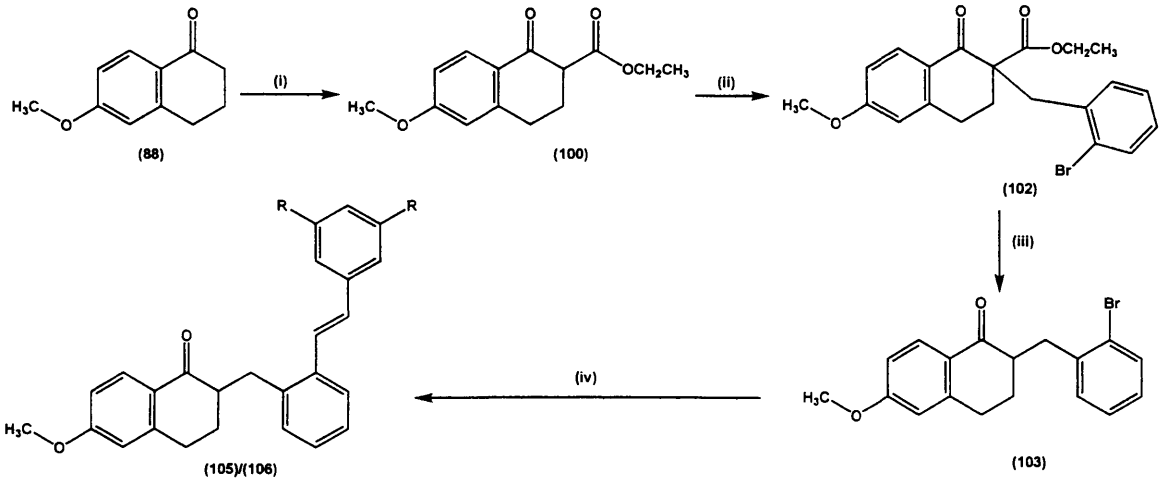

(**105**) R = H (**106**) R = OCH_3.

Scheme 3.3.18. Scheme for synthesis of 6-Methoxy-2-[2-[(*E*)-3,5-unsubstituted/dimethoxy-2-phenyl-1-ethenyl]benzyl]-1,2,3,4-tetrahydro-1-naphthalenone (**105**)/(**106**): (i) NaH, diethyl carbonate; (ii) NaH, 2-bromobenzyl bromide; (iii) 48% HBr, 96% AcOH; (iv) (**95**) $Pd(PPh_3)_4$, *trans*-2-phenylvinylboronic acid, Na_2CO_3, (**96**) ToP, $Pd(OAC)_2$, Et_3N, 80 °C.

(1) Preparation of ethyl 6-methoxy-1-oxo-1,2,3,4-tetrahydro-2-naphthalene carboxylate (100):

6-Methoxy-1-oxo-1,2,3,4-tetrahydro-2-naphthalenecarboxylate (**100**) was synthesised (**Scheme 3.3.19**) through the reaction between 6-methoxy-1-tetralone (**88**) and diethyl carbonate in the presence of NaH as a strong base to abstract the acidic proton from the tetralone ring. The desired compound was produced in a yield of 70%.

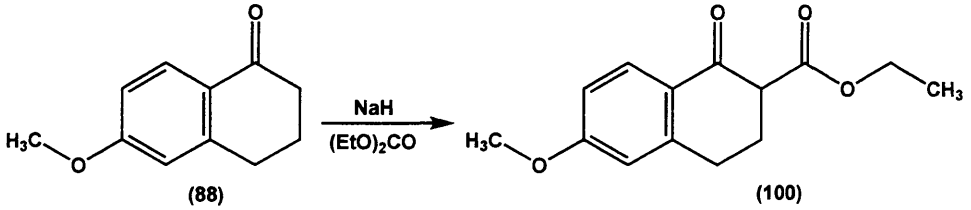

Scheme 3.3.19. Preparation of ethyl 6-methoxy-1-oxo-1,2,3,4-tetrahydro-2-naphthalene carboxylate (**100**).

(2) Preparation of ethyl 2-(2-bromobenzyl)-6-methoxy-1-oxo-1,2,3,4-tetrahydro-2-naphthalenecarboxylate (102):

Once again NaH was used to abstract acidic proton at the 2-position of the tetralone, and hence this position was attacked by 2-bromobenzyl bromide (**101**) to

form ethyl 2-(2-bromobenzyl)-6-methoxy-1-oxo-1,2,3,4-tetrahydro-2-naphthalenecarboxylate (**102**) (**Scheme 3.3.20**) in a yield of 69%.

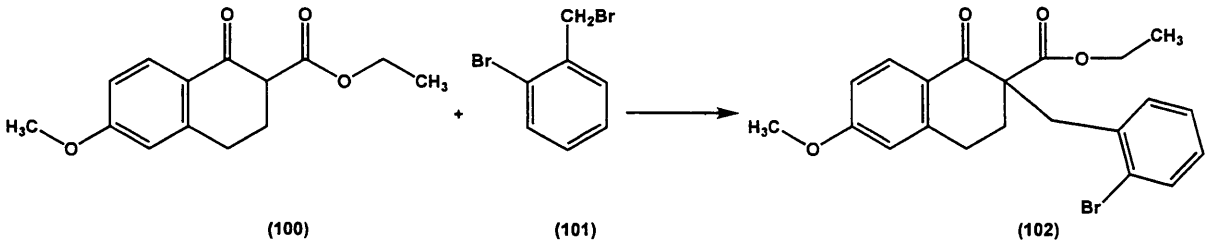

Scheme 3.3.20. Preparation of ethyl 2-(2-bromobenzyl)-6-methoxy-1-oxo-1,2,3,4-tetrahydro-2-naphthalenecarboxylate (**102**).

(3) Preparation of 2-(2-bromobenzyl)-6-methoxy-1,2,3,4-tetrahydro-1-naphthalenone (103):

This synthesis involved a decarboxylation of 2-(2-bromobenzyl)-6-methoxy-1-oxo-1,2,3,4-tetrahydro-2-naphthalenecarboxylate (**102**) using 48% HBr and 96% AcOH. Unfortunately, while these conditions decarboxylate compound (**102**); they also demethylated the methoxy group (**Scheme 3.3.21**). The two compounds were separated using flash chromatography, and they were produced in a ratio of 1.45:1 of 2-(2-bromobenzyl)-6-hydroxy-1,2,3,4-tetrahydro-1-naphthalenone (**104**) to 2-(2-bromobenzyl)-6-methoxy-1,2,3,4-tetrahydro-1-naphthalenone (**103**) respectively.

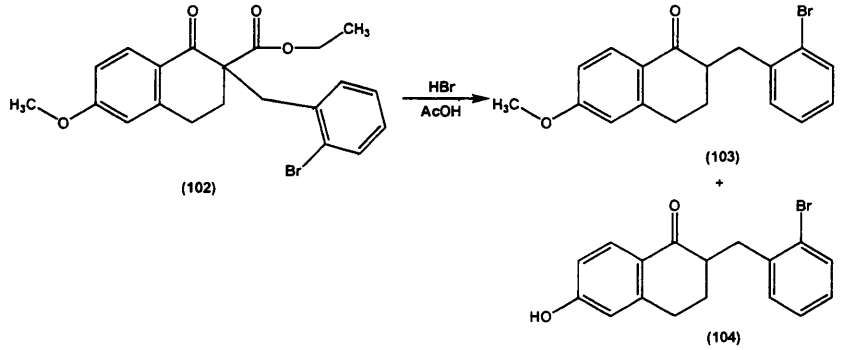

Scheme 3.3.21. Synthesis of 2-(2-bromobenzyl)-6-methoxy-1,2,3,4-tetrahydro-1-naphthalenone (**103**) and 2-(2-bromobenzyl)-6-hydroxy-1,2,3,4-tetrahydro-1-naphthalenone (**104**).

The 2-(2-bromobenzyl)-6-hydroxy-1,2,3,4-tetrahydro-1-naphthalenone (**104**) was remethylated using MeI in the presence of K_2CO_3 (**Scheme 3.3.22**).

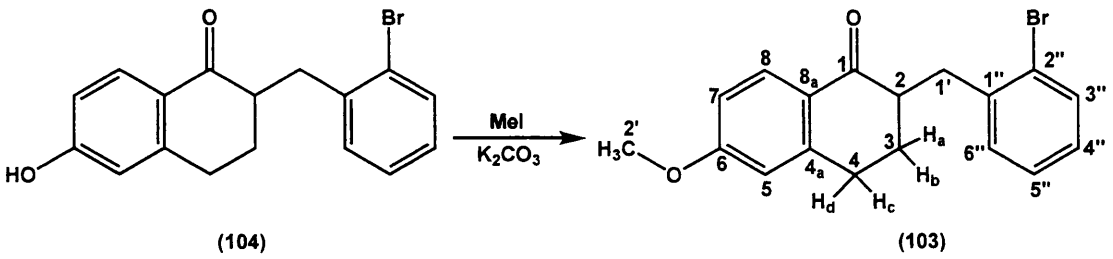

(104) (103)

Scheme 3.3.22. Methylation of 2-(2-bromobenzyl)-6-hydroxy-1,2,3,4-tetrahydro-1-naphthalenone (**104**).

(4a) Preparation of 6-methoxy-2-[2-[(*E*)-2-phenyl-1-ethenyl]benzyl]-1,2,3,4-tetrahydro-1-naphthalenone (105):

This synthesis was performed by Suzuki reaction using *trans*-2-phenylvinylboronic acid (**7 (Scheme 3.3.23)**. The cross-coupling of boronic acid with aryl bromide was reported [228] in the presence of palladium catalysts and base. After the reaction was complete, 30% H_2O_2, as an oxidizing agent, was added to remove the residual boronic acid.

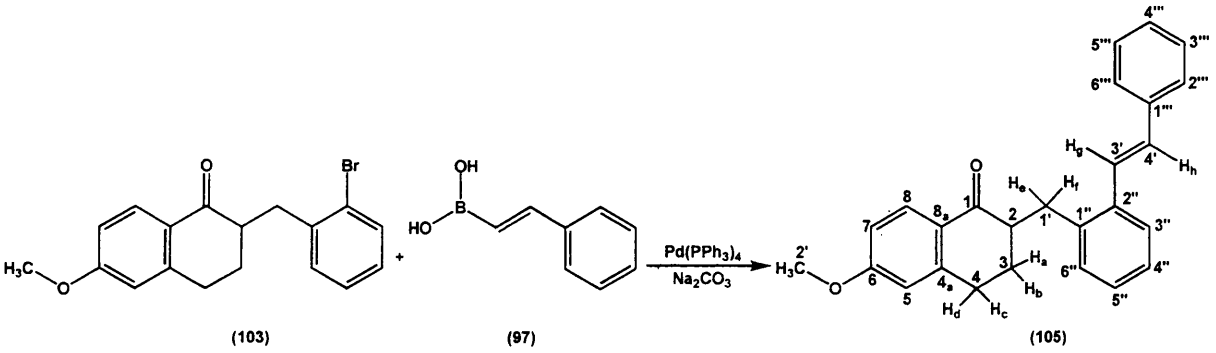

(103) (97) (105)

Scheme 3.3.23. Preparation of 6-methoxy-2-[2-[(*E*)-2-phenyl-1-ethenyl]benzyl]-1,2,3,4-tetrahydro-1-naphthalenone (**105**).

(4b) Preparation of 2-{2-[(*E*)-2-(3,5-dimethoxyphenyl)-1-ethenyl]benzyl}-6-methoxy -1,2,3,4-tetrahydro-1-naphthalenone (106):

The synthesis of 2-{2-[(*E*)-2-(3,5-dimethoxyphenyl)-1-ethenyl]benzyl}-6-methoxy -1,2,3,4-tetrahydro-1-naphthalenone (**106**) involves the coupling of 1,3-dimethoxy-5-vinylbenzene (**68**) with 2-(2-bromobenzyl)-6-methoxy-1,2,3,4-tetrahydro-1-naphthalenone (**103**) via palladium-catalysed Heck reaction **(Scheme 3.3.24)**. The reaction was performed in a basic medium using Et_3N and at 80 °C for 72 h to give the desired compound in a yield of 64%.

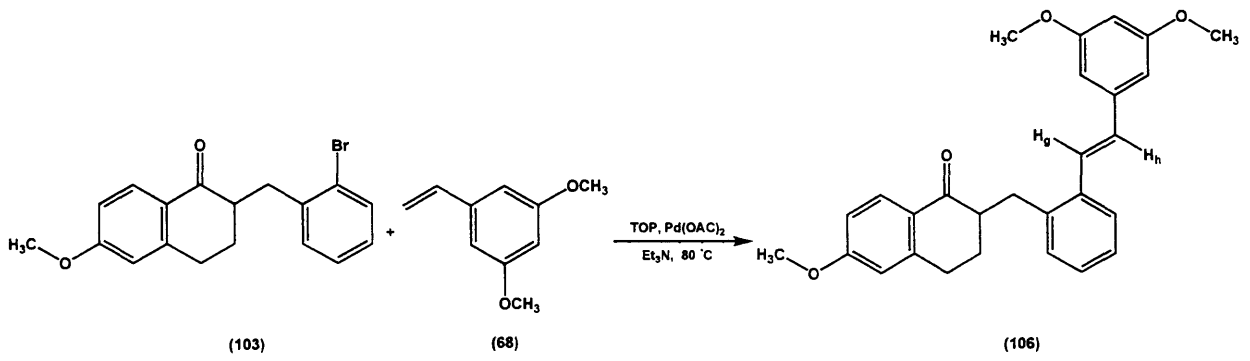

(103) (68) (106)

Scheme 3.3.24. Preparation of 2-{2-[(*E*)-2-(3,5-dimethoxyphenyl)-1-ethenyl]benzyl}-6-methoxy -1,2,3,4-tetrahydro-1-naphthalenone (**106**).

3.4.CYP26A1 Biological results

3.4.1. Cell Based Assay:

Initially, the CYP26A1 cell based assay was done in our labs using methods previously developed by our group.

The IC_{50} of final compounds was measured using HPLC linked to a β-RAM detector and Laura software. Two major peaks can be observed on the HPLC. The first peak (retention time 1.5-2.5 min) corresponds to the metabolites of ATRA (4-oxo-ATRA, 4-hydroxy-ATRA and other polar metabolites), which are metabolised by the action of CYP26A1 on ATRA and the second peak (retention time 5-6.5 min) corresponds to ATRA itself.

Consequently, disappearance of the first peak would be observed if an inhibitor was added to the medium. The separated metabolites were quantitatively calculated from the area under the curves and the percentage inhibition was calculated from: 100[(%metabolites (control) – %metabolites (inhibitors) / %(metabolites control)]. The results of the assay are summarised in **Table 3.4.1.**

Table 3.4.1.: IC_{50} of the tested compounds:

Structure	IC_{50}	ClogP	NAME
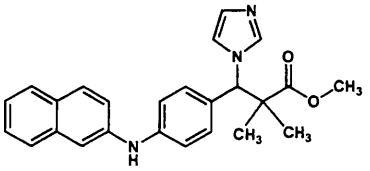	30 nM	4.92	**Lead compd.***
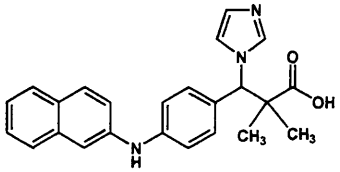	>20 μM	4.46	**MCC 186***
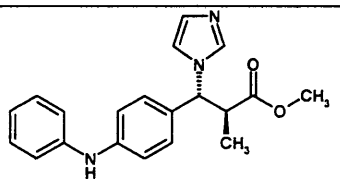	>10 μM	3.35	**14**
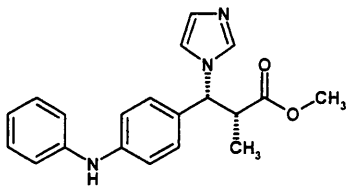	>10 μM	3.35	**15**

Structure	IC_{50}	ClogP	NAME
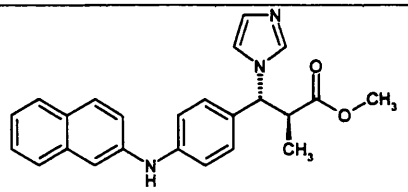	0.84 μM	4.52	**19**
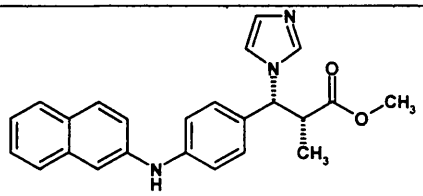	0.85 μM	4.52	**20**
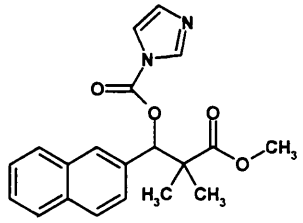	> 10 μM	3.49	**24**
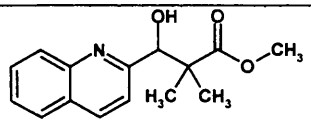	>10 μM	1.69	**28**
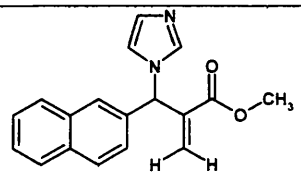	0.45 μM	3.00	**34**
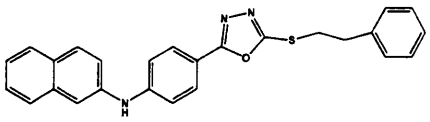	>10 μM	6.56	**52**
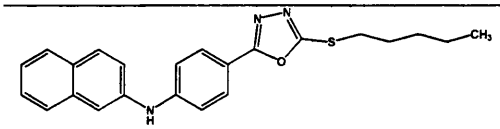	>10 μM	6.58	**56**
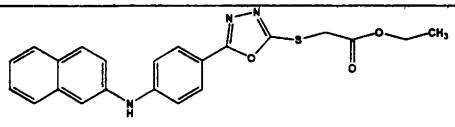	8.8 μM	4.55	**60**

* previously synthesised within our group [129].

From these results, and by comparing the IC_{50} of the lead compound and compounds (**14**), (**15**), (**19**) and (**20**); it seems that the dimethyl substitution at the α-carbon is much more preferable than the mono-methyl substitution as can be seen from the huge decrease in inhibitory activity by about 30 fold. As the free acid seems

not to be the active form of our compounds, it may be the presence of the dimethyl group has a steric effect that restrains the attack of the esterase enzyme. Of course, this steric effect decreases with the introduction of the mono-methyl group resulting in more rapid removal of the esters to give the free acid, this may explain the loss in inhibitory activity. Also from the IC_{50} of the compounds (**14**), (**15**), (**19**) and (**20**), it appears that the difference in the diastereoisomerism does not affect the inhibitory activity.

The presence of the imidazole is essential for the inhibitory activity, removal of the imidazole as in compound (**28**) or replacement with the 1,3,4-oxadiazole ring, such as compounds (**52, 56** and **60**) or introducing of a link between the imidazole and the β-carbon such as compound (**24**), dramatically decreases the activity. Introduction of a link between the imidazole and the β-carbon may make the compound too big to enter the active site cavity of the enzyme. As for the replacement of the imidazole with the 1,3,4-oxadiazole part, although these compounds dock very well in the CYP26A1 homology model, the decrease in the flexibility of the molecules could explain the decrease in the activity. The non-conformity between the biological results and the modelling suggest a limitation of the CYP26A1 model.

3.4.2. Biochemical Assay:

The CYP26A1 biochemical assay of the most promising compounds (**14, 15, 19 and 20**) versus CYP26A1 was performed by Dr Caroline Bridgens, Northern Institute for Cancer Research, Newcastle University, Newcastle, United Kingdom. Microsomes were prepared by differential centrifugation of MCF-7 homogenised cells. The results of the assay are presented in **table 3.4.2.**

Table 3.4.2.: IC_{50} of the tested compounds:

Structure	IC_{50}	ClogP	NAME
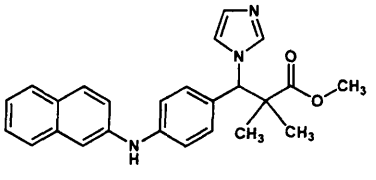	2.8 nM	4.92	**Lead compd.***

Structure	IC_{50}	ClogP	NAME
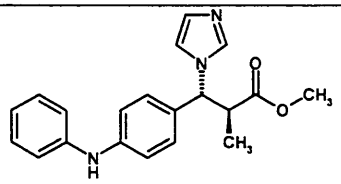	26 nM	3.35	14
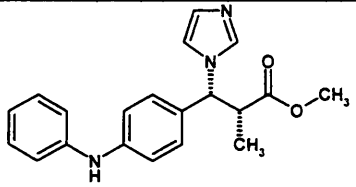	50 nM	3.35	15
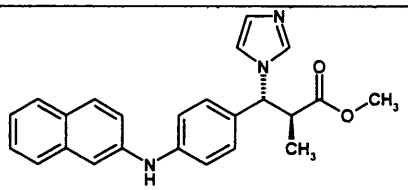	100 nM	4.52	19
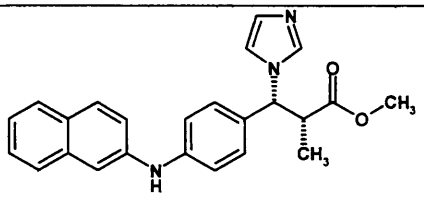	120 nM	4.52	20
Liarozole	6 μM	3.24	-
R115866	4 nM	5.78	-

These results showed that compounds **14, 15, 19** and **20** are good CYP26A1 inhibitors being about 70-100 times more active than the well-known CYP26A1 inhibitor liarazole (IC_{50}= 6 μM). However, they were still less active than R115866. Also, these compounds are much less active than our lead compound which showed an IC_{50} of 2.8 nM. The non-conformity of the cell based assay and the biochemical assay, in which the phenyl and the naphthyl derivatives were more active, could be explained in terms of the easier uptake of compounds (**19** and **20**) by the cells than compounds (**14** and **15**) due to the higher lipophilicity. Although those results were surprising, they were favourable, as there was not a huge difference between the lead compound with the dimethyl groups and the mono-methyl phenyl derivatives (**14** and **15**) in terms of the CYP26A1 inhibitory activity. These results were favourable, because compounds (**14** and **15**) are more preferred in terms of synthesis and yield.

3.5.CYP24A1 Biological results

3.5.1. V79-CYP24 Assay:

The inhibitory activity of the novel compounds versus CYP24A1 was performed by Anna Robotham and Bart Makowski in the labs of Professor Glen Jones, Queen's University Kingston, Ontario, Canada. The results of the assay are presented in **table 3.5.1.**

Table 3.5.1.

Structure	CYP24A1 IC_{50}	CYP27A1 IC_{50}	NAME
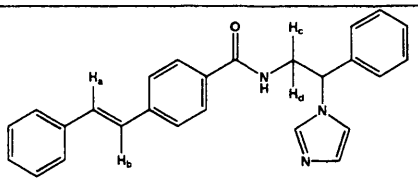	0.3 μM	-	**86**
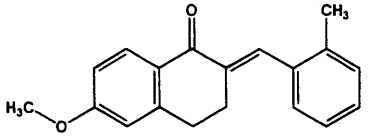	480.1 μM	-	**MCC 173***
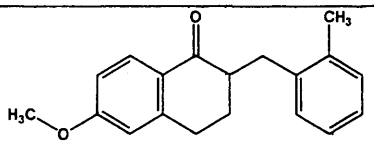	126.9 μM	-	**MCC 174***
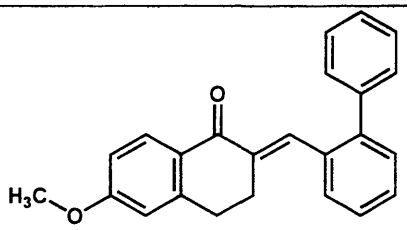	111.1 μM	-	**MCC 179***
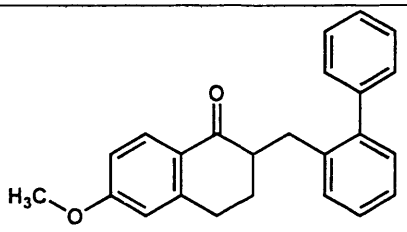	127.6 μM	-	**MCC 180***
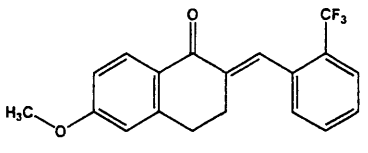	11.22 μM	-	**90**

Structure	CYP24A1 IC_{50}	CYP27A1 IC_{50}	NAME
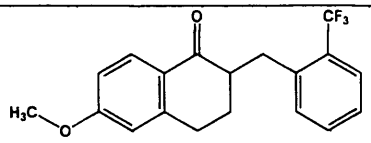	2.08 μM	-	**91**
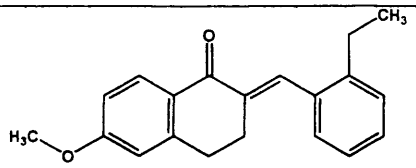	10.76 μM	-	**93**
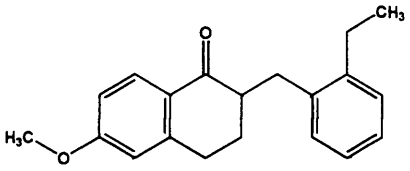	1.92 μM	8.32 μM	**94**
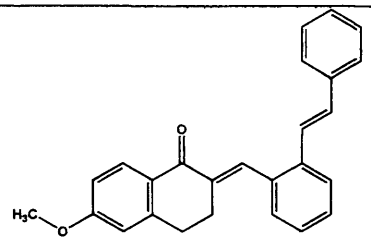	5.08 μM	5.96 μM	**98**
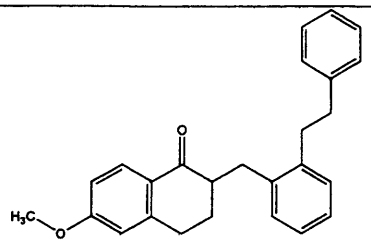	25.57	-	**99**
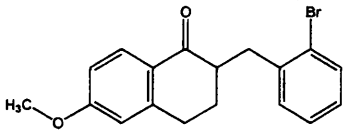	16.3 μM	0.059 μM	**103**
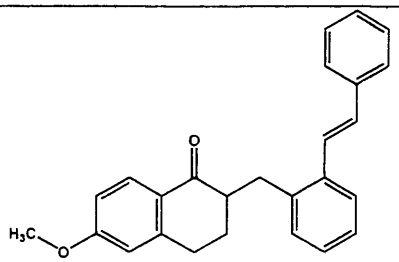	5.08 μM	-	**105**
Ketoconazole	0.52 μM.	-	-

* previously synthesised within our group [224].

The results showed that the inclusion of a double bond at the position of

attachment between the tetralone and benzyl ring appeared to reduce the inhibitory effect of the inhibitors. For example, **(94)** (IC_{50} = 1.92 μM) was more potent than its double bond counterpart, **(93)** (IC_{50} =10.76 μM). The double bond will conjugate with the adjacent phenyl group resulting in decreased conformational flexibility of the structure. This loss of flexibility could inhibit the entrance of the inhibitor through the access channel of CYP24A1 (**Figure 3.5.1**), thus decreasing its access to the enzyme cavity where it would exert its inhibitory effect. Alternatively, the loss of conformational flexibility could prevent a favourable conformation that stabilises the inhibitor inside the enzyme cavity.

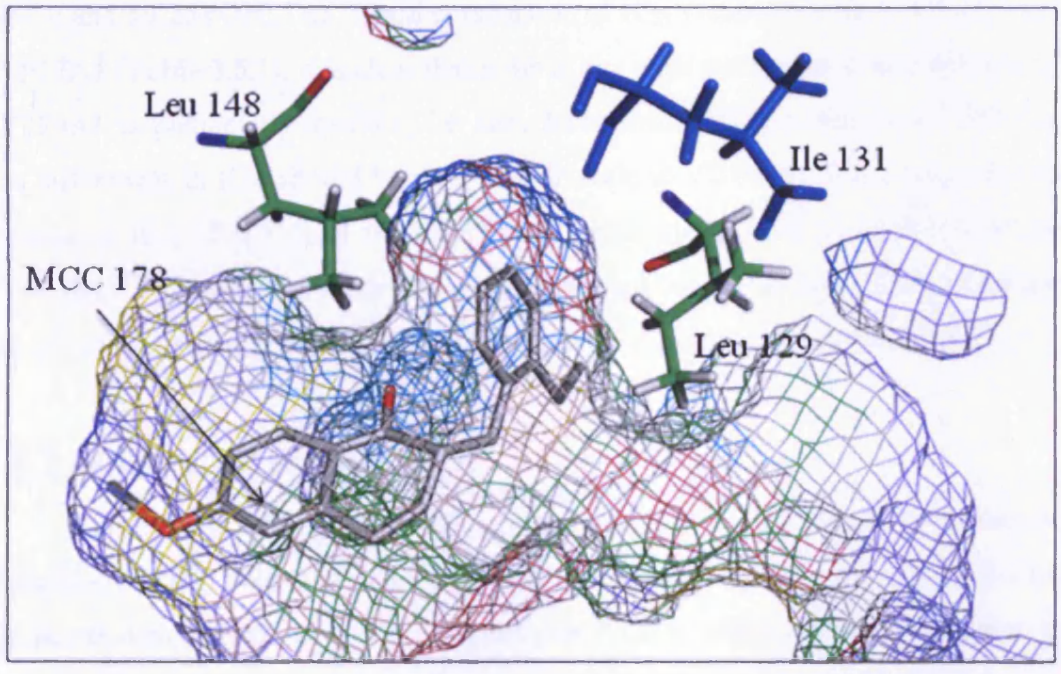

Figure 3.5.1. Docking of compound **(94)**, **MCC178** with CYP24A1 homology model (129).

The strong inhibitory capacity of **(91)** could reflect a trend observed in inhibitor design; the addition of fluorine groups increases the inhibitory capacity of a compound. It has been suggested that this increase is not caused by a stronger enzyme-inhibitor complex, but by increasing the cell-membrane penetrating capacity and thus increasing the bio-availability. However, many of the compounds appear to be hydrophobic and should have little problem penetrating cell membranes. As such, the fluorination may have a stabilising effect on the inhibitor inside the enzyme resulting in more effective inhibition.

As for the azoles, from the results, it seems that the azoles would be much

more active than the tetralone derivative with compound (**86**) displaying greater inhibitory activity than the standard ketoconazole. This activity may also be attributed to the resemblance between the structure of these azoles and calcitriol. At the time of submitting this thesis the CYP24/CYP27 data for compounds (**85, 87** and **96**) were not available.

CYP27A1 Assays

A potent and specific inhibitor of CYP24A1 would display a low IC_{50} value towards CYP24A1 and a high IC_{50} value towards related cytochrome P450s. CYP27A1 is a good enzyme to test for specificity because of its structural similarity to CYP24A1, as well as the structural similarity of their respective substrates (1α-OH-D_3 and 1α,25-$(OH)_2D_3$). Upon comparison of IC_{50} values between CYP24A1 and CYP27A1 (**Table 3.5.1**), it is clear that none of the most potent tetralone inhibitors of CYP24A1 is particularly specific, i.e. they have similar IC_{50} values for CYP27A1. The differences in IC_{50} should be on a similar scale to VID-400, which was reported to have an IC_{50} of 0.015μM for CYP24A1, while having an IC_{50} of 0.616μM for CYP27B1 [115]. Surprisingly, the 2-bromo-substituted benzyl tetralone (**103**) displayed a much greater potency towards CYP27A1 than CYP24A1 (276-fold selectivity).

3.5.2. VitD3 CLL Study:

Recent gene expression profiling experiments of B-cell chronic lymphocytic leukemia (B-CLL) cells have identified that the VDR is highly expressed in B-CLL compared with normal B and T lymphocytes [229]. It was therefore of interest to evaluate our compounds in these cells.

The activity of the novel compounds versus these cells was performed by Dr Chris Pepper, University of Wales College of Medicine, Cardiff, United Kingdom. The results of the assay are presented in **table 3.5.2.**

Table 3.5.2.

Structure	LD_{50}	NAME
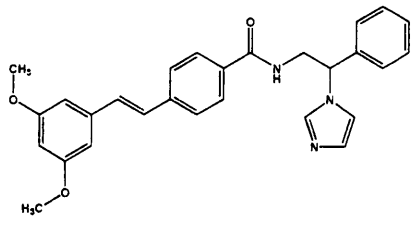	37 nM	**85**

Structure	LD_{50}	NAME
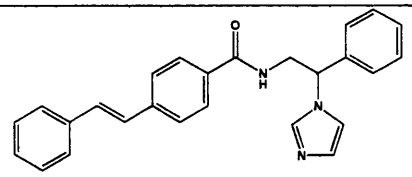	66 nM	**86**
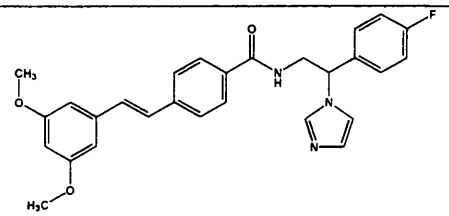	34 nM	**87**
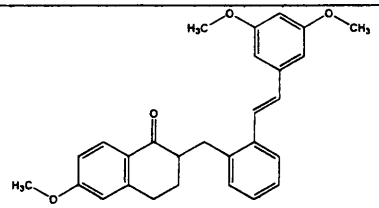	19 μM	**96**

The results showed that the azole compounds had very good antiproliferative activity against B-CLL. Introduction of the dimethoxy groups did not greatly affect the activity, with only a fold increase in the activity which was the same case for the introduction of the fluorine group, as both compounds with or without the fluorine group (**85** and **87**) showed comparable activity. Also, from the results, the tetralones seem to be much less active than the azoles, which suggest the low antiproliferative activity of these tetralones, this may reflect the difference in CYP24 inhibitory activity.

4. Experimental

■ General considerations:

All reactions were carried out under an atmosphere of nitrogen when necessary. All reagents and solvents employed were of general purpose or analytical grade and purchased from Sigma-Aldrich Chemical Company, Fluka and Acros Chemicals. Solvents were appropriately dried over molecular sieves (3Å).

^{1}H and ^{13}C-NMR spectra were recorded on a Bruker Avance DP500 spectrometer at 500 MHz and 125 MHz respectively. The NMR solvent was $CDCl_3$ for all cases unless mentioned otherwise. Each resonance signal was reported according to the following convention:

5) chemical shifts are given in parts per million (ppm) relative to the internal standard tetramethyl silane (Me_4Si).

6) coupling constants [J in hertz (Hz)].

7) multiplicity are denoted as s (singlet), d (doublet), t (triplet), m (multiplet) or combinations thereof.

Mass spectra were determined under EI (Electron Impact) or CI (Chemical Ionisation) conditions at the EPSRC National Mass Spectrometry Service Centre, University of Wales, Swansea. Accurate mass measurement was also performed at the EPSRC National Mass Spectrometry Service Centre. Microanalysis data were performed by Medac Ltd., Brunel Science Centre, Surrey.

For column chromatography, a glass column was slurry packed in the appropriate eluent with silica gel (Fluka Kieselgel 60). Flash column chromatography was performed with the aid of a pump. Analytical thin layer chromatography (TLC) was carried out on pre-coated silica plates (Merck Kieselgel 60 F_{254}) with visualisation *via* UV light (254 nm), ninhydrin and/or vanillin stains.

Melting points were determined using a Gallenkamp melting point apparatus and are uncorrected.

All NMR characterisations were made by comparison with previous NMR spectra of the appropriate structure class and/or predictions from ACD/HNMR and ACD/CNMR (Advanced Chemistry Development Inc., Version 2.51, 1997) and ChemDraw Ultra™ 7.0 (CambridgeSoft).

4.1. Synthesis of CYP26A1 inhibitors

4.1.1. Methyl 3-hydroxy-3-(4-nitrophenyl)propanoate (3) [178].

(Mol. Formula: $C_{10}H_{11}NO_5$, M. W.: 225.2)

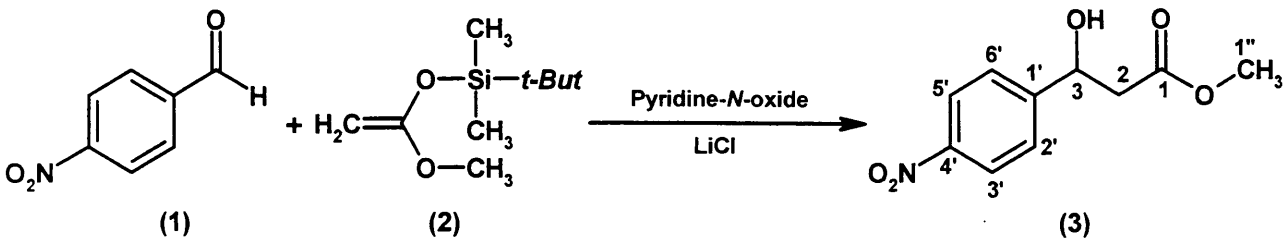

(1) (2) (3)

To a stirred solution of pyridine-*N*-oxide (50 mg, 0.53 mmol) and LiCl (50 mg, 1.2 mmol) in *N,N*-dimethylformamide (DMF) (3 mL) were added 4-nitrobenzaldehyde (**1**) (1 g, 6.6 mmol) and 1-(*t*-butyldimethylsilyloxy)-1-methoxyethene (**2**) (7 mL, 33 mmol) at room temperature under nitrogen atmosphere and left for 24 h. The product was isolated by direct flash column chromatography of the crude reaction mixture (petroleum ether – EtOAc 50:50 v/v) to give methyl 3-hydroxy-3-(4-nitrophenyl)propanoate (**3**) as a colourless oily product. Yield: 0.5 g (34%), t.l.c. system: petroleum ether – EtOAc 1:1 v/v, R_F: 0.55, vanillin stain positive.

^{1}H-NMR ($CDCl_3$), δ: 2.64 (d, 2H, J = 6.5 Hz, CH_2), 3.60 (s, 3H, CH_3), 3.93 (d, 1H, J = 2.6 Hz, OH), 5.13-5.16 (m, 1H, CH), 7.46 (d, 2H, J = 8.6 Hz, H-2', H-6'), 8.05 (d, 2H, J = 8.8 Hz, H-3', H-5').

^{13}C NMR ($CDCl_3$), δ: 42.94 (CH_2, C-2), 52.30 (CH_3, C-1''), 69.51 (CH, C-3), 123.93 (CH, C-3', C-5'), 126.88 (CH, C-2', C-6'), 147.26 (C, C-1'), 150.14 (C, C-4'), 172.10 (C, C-1).

4.1.2. Ethyl 3-Hydroxy-3-(4-nitrophenyl)propanoate (5) [230] and butyl 3-hydroxy-3-(4-nitrophenyl)propanoate (6).

(Compound (**5**): Mol. Formula: $C_{11}H_{13}NO_5$, M. W.: 239.2)

(Compound (**6**): Mol. Formula: $C_{13}H_{17}NO_5$, M. W.: 267.2)

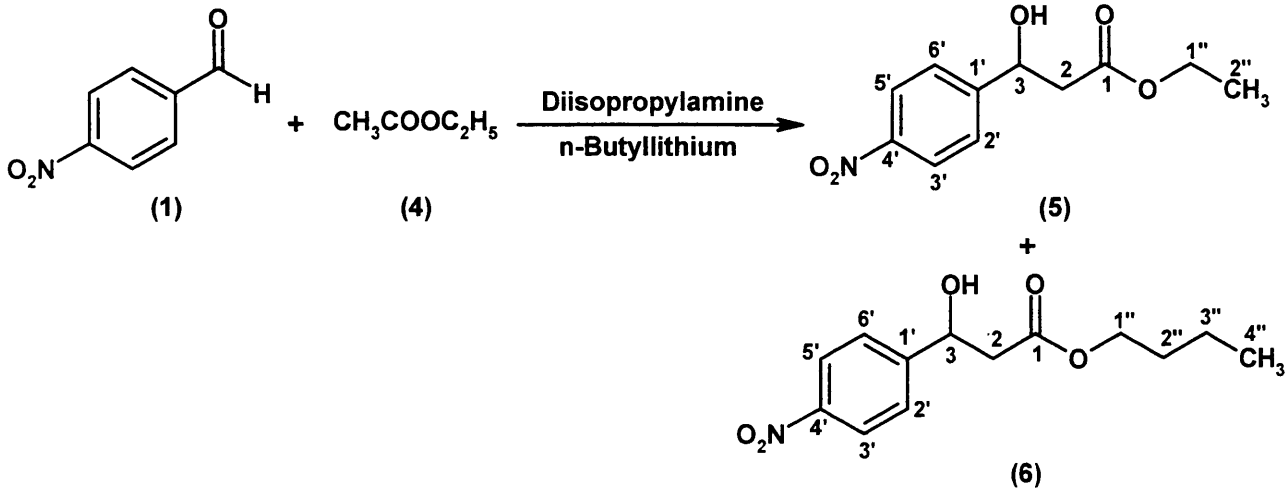

To a cooled (-78 °C) solution of diisopropylamine (2.8 mL, 20 mmol) in THF (25 mL) was added *n*-butyllithium (18.2 mL, 30 mmol) dropwise over a period of 5 min under nitrogen atmosphere. After the addition of *n*-butyllithium, the reaction mixture was stirred at -78 °C for 30 min.

EtOAc (**4**) (1.8 g, 20 mmol) in THF (10 mL) was added and stirring continued at -78 °C for 10 min. Then a solution of 4-nitrobenzaldehyde (**1**) (3.02 g, 20 mmol) in THF (10 mL) was added dropwise over a period of 10 min and the reaction stirred at room temperature overnight. The reaction was quenched with 10% aqueous HCl (20 mL) and the product was extracted with Et_2O (2 x 50 mL). The organic layer was washed with H_2O (2 x 50 mL), dried ($MgSO_4$) and concentrated under reduced pressure. The product was purified by column chromatography (petroleum ether – EtOAc 100:0 increasing to 70:30 v/v) to give ethyl 3-hydroxy-3-(4-nitrophenyl)propanoate (**5**) as a colourless oily product. Yield: 1.5 g (31%), t.l.c. system: petroleum ether – EtOAc 3:1 v/v, R_F: 0.48, vanillin stain positive. Butyl 3-hydroxy-3-(4-nitrophenyl)propanoate (**6**) was obtained as a side product as a yellow oily product, Yield: 1.6 g (30%), R_F: 0.77, vanillin stain positive.

• Ethyl 3-hydroxy-3-(4-nitrophenyl)propanoate (**5**):

^{1}H-NMR ($CDCl_3$), δ: 1.14 (t, 3H, J = 7.2 Hz, CH_3), 2.65 (d, 2H, J = 6.5 Hz, O-CH_2-CH_3), 4.04-4.08 (m, 3H, OH + CO-CH_2), 5.13-5.18 (m, 1H, CH), 7.48 (d, 2H, J = 8.7 Hz, H-2', H-6'), 8.05 (d, 2H, J = 8.8 Hz, H-3', H-5').

^{13}C NMR ($CDCl_3$), δ: 14.01 (CH_3, C-2''), 43.48 (CH_2, C-2), 61.33 (CH_2, C-1''), 69.33 (CH, C-3), 123.84 (CH, C-3', C-5'), 126.34 (CH, C-2', C-6'), 147.19 (C, C-1'), 150.29 (C, C-4'), 171.42 (C, C-1).

• Butyl 3-hydroxy-3-(4-nitrophenyl)propanoate (**6**):

HRMS (EI): Calculated mass: 267.1101 $[M+H]^+$, Measured mass: 267.1098 $[M+H]^+$.

^{1}H-NMR ($CDCl_3$), δ: 8.85 (t, J = 6.9 Hz, 3H, CH_3), 1.24-1.31 (m, 2H, CH_2-CH_3), 1.51-1.56 (m, 2H, CH_2- CH_2- CH_2), 2.69 (d, 2H, J = 1.8 Hz, CH- CH_2), 3.98 (d, 1H, J = 3.4 Hz, OH), 4.05 (t, 2H, J = 6.8, O-CH_2), 5.17-5.21 (m, 1H, CH-OH), 7.51 (dt, 2H, J = 2.0 Hz, 8.7 Hz, H-2', H-6'), 8.11 (dt, 2H, J = 2.3 Hz, 8.8 Hz, H-3', H-5').

^{13}C NMR ($CDCl_3$), δ: 13.54 (CH_3, C-4''), 18.98 (CH_2, C-3''), 30.44 (CH_2, C-2''), 43.09 (CH_2, C-1''), 65.26 (CH_2, C-2), 69.54 (CH, C-3), 123.85 (CH, C-3', C-5'), 126.55 (CH, C-2', C-6'), 147.27 (C, C-1'), 150.14 (C, C-4'), 171.82 (C, C-1).

4.1.3. Methyl 3-hydroxy-2-methylene-3-(4-nitrophenyl) propanoate (8) [189].

(Mol. Formula: $C_{11}H_{11}NO_5$, M. W.: 237.1)

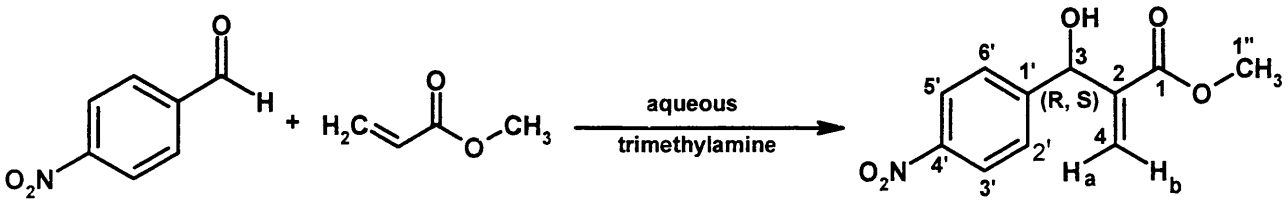

(1) (7) (8)

To a stirred solution of 4-nitrobenzylaldehyde (**1**) (3.02 g, 20 mmol) and aqueous trimethylamine (5 mL, 25 mmol) in THF (20 mL) was added methylacrylate (**7**) (5.4 mL, 60 mmol) and the resulting clear mixture was stirred at room temperature for 24 h. Then $CHCl_3$ (40 mL) and H_2O (25 mL) were added

and the mixture was stirred for another 2 min. The organic phase was separated and the H_2O phase was extracted with chloroform (2 x 30 mL). The combined organic layers were dried ($MgSO_4$) and concentrated under reduced pressure. The crude product was purified by column chromatography (petroleum ether – EtOAc 100:0 increasing to 70:30 v/v) to afford the pure adduct, methyl 3-hydroxy-2-methylene-3-(4-nitrophenyl)propanoate (**8**) as a pale yellow solid. Yield: 4.7 g (98%), t.l.c. system: petroleum ether – EtOAc 3:1 v/v, R_F: 0.77, vanillin stain positive.

Melting point: 71-73 °C (lit. m.p. 72-73 °C) [189].

^{1}H-NMR ($CDCl_3$), δ: 3.34 (s, 1H, OH), 3.68 (s, 3H, CH_3), 5.56 (s, 1H, CH), 5.81 (s, 1H, H_a), 6.32 (s, 1H, H_b), 7.50 (d, 2H, J = 8.5 Hz, H-2', H-6'), 8.12 (d, 2H, J = 8.8 Hz, H-3', H-5').

^{13}C NMR ($CDCl_3$), δ: 51.49 (CH_3, C-1''), 74.18 (CH, C-3), 121.10 (CH, C-3',C-5'), 122.93 (CH_2, C-4), 127.94 (CH, C-2', C-6'), 140.28 (C, C-2), 147.35 (C, C-4'), 149.78 (C, C-1'), 171.25 (C, C-1).

4.1.4. Methyl 3-(4-aminophenyl)-3-hydroxy-2-methylpropanoate (9) and methyl 3-(4-aminophenyl)-2-methylpropanoate (10) [182].

(Compound (**9**): Mol. Formula: $C_{11}H_{15}NO_3$, M. W.: 209.2)

(Compound (**10**): Mol. Formula: $C_{11}H_{15}NO_2$, M. W.: 193.3)

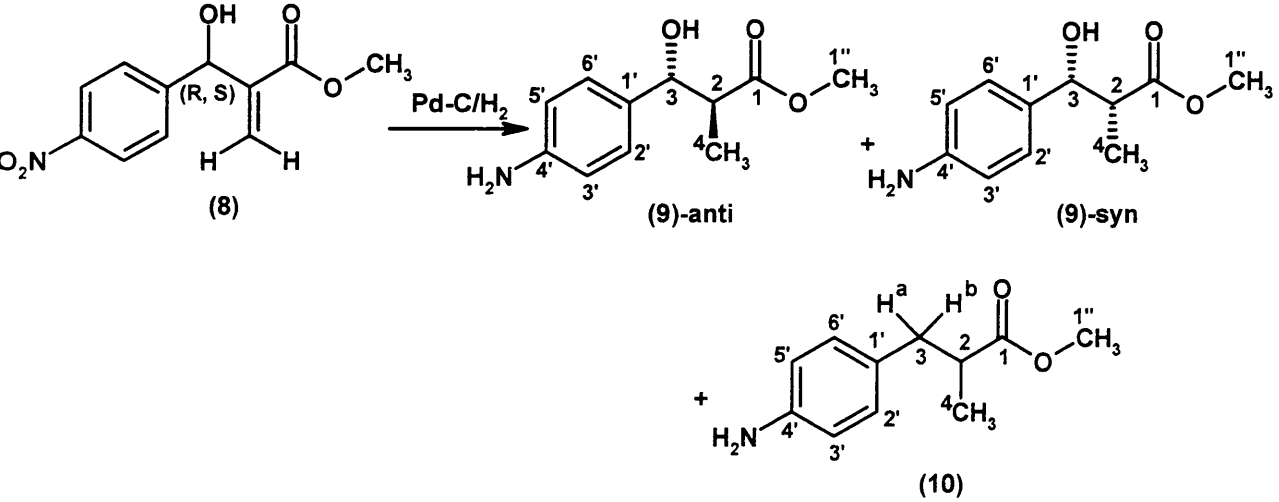

To a suspension of 5% Pd-C (10 mol %) in EtOAc (5 mL) was added, under

nitrogen, a solution of methyl 3-hydroxy-2-methylene-3-(4-nitrophenyl) propanoate (**8**) (2.4 g, 10 mmol) in EtOAc (30 mL). Then, the reaction atmosphere was changed to hydrogen and the reaction mixture stirred at room temperature. After a period of 1 h, the suspension was filtered over a pad of celite and the solvent removed under reduced pressure. The product was purified by column chromatography (petroleum ether – EtOAc 100:0 increasing to 70:30 v/v) to give a mixture of the (**9**)-*anti* and (**9**)-*syn* diastereoisomers of methyl 3-(4-aminophenyl)-3-hydroxy-2-methylpropanoate (in a ratio of 8.5:5 respectively) as a brown solid. Yield: 1.0 g (48%), t.l.c. system: petroleum ether – EtOAc 3:1 v/v, R_F: 0.23, ninhydrin stain positive and the hydrogenolysis product methyl 3-(4-aminophenyl)-2-methylpropanoate (**10**) as a colourless oily product. Yield: 0.8 g (43%), R_F: 0.76, ninhydrin stain positive.

• Methyl 3-(4-aminophenyl)-3-hydroxy-2-methylpropanoate (**9**)

Melting point: 116-118 °C (lit. m.p. 116-118 °C) [182].

Microanalysis: Calculated for $C_{11}H_{15}NO_3$ (209.2), Theoretical: %C= 63.14, %H= 7.23, %N= 6.69, Found: %C= 63.45, %H= 7.33, %N= 6.31.

^{1}H-NMR ($CDCl_3$), δ: 0.90 (d, 3H, J = 7.2 Hz, *anti*-CH-C<u>H</u>$_3$), 1.09 (d, 3H, J = 7.1 Hz, *syn*-CH-C<u>H</u>$_3$), 2.65-2.73 (m, 2H, *anti* and *syn* C<u>H</u>-CH$_3$), 3.57 (s, 3H, *syn*-O-CH$_3$), 3.66 (s, 3H, *anti*-O-CH$_3$), 4.57 (d, 1H, J = 8.9 Hz, *anti*-C<u>H</u>-OH), 4.87 (d, 1H, J = 4.9 Hz, *syn*-C<u>H</u>-OH), 6.57-6.60 (m, 4H, *anti* and *syn* H-2', H-6'), 7.04-7.06 (m, 4H, *anti* and *syn* H-3', H-5').

^{13}C NMR ($CDCl_3$), δ: 11.31 (CH_3, *syn*-C-4), 14.50 (CH_3, *anti*-C-4), 46.69 (CH, *syn*-C-2), 47.20 (CH, *anti*-C-2), 51.75 (CH_3, *syn*-C-1''), 51.86 (CH_3, *anti*-C-1''), 73.85 (CH, *syn*-C-3), 76.32 (CH, *anti*-C-3), 114.91 (CH, *syn*-C-3', *syn*-C-5'), 115.05 (CH, *anti*-C-3', *anti*-C-5'), 127.10 (CH, *syn*-C-2', *syn*-C-6'), 127.82 (CH, *anti*-C-2', *anti*-C-6'), 131.54 (C, *syn*-C-1'), 131.60 (C, *anti*-C-1'), 145.81 (C, *syn*-C-4'), 146.32 (C, *anti*-C-4'), 176.12 (C, *syn*-C-1), 176.45 (C, *anti*-C-1).

• Methyl 3-(4-aminophenyl)-2-methylpropanoate (**10**)

^{1}H-NMR ($CDCl_3$), δ: 1.05 (s, CH_3, 3H, O-CH$_3$), 2.45-2.49 (m, 1H, H_a), 2.56-2.60 (m, 1H, C<u>H</u>-CH$_3$), 2.80-2.84 (m, 1H, H_b), 3.41-3.50 (bs, 2H, NH_2), 3.55 (s, 3H, O-CH$_3$), 6.52 (d, 2H, J = 8.4 Hz, H-2', H-6'), 6.85 (d, 2H, J = 8.4 Hz, H-3', H-5').

^{13}C NMR ($CDCl_3$), δ: 16.62 (CH_3, C-4), 38.98 (CH_2, C-3), 41.70 (CH, C-2),

51.48 (CH_3, C-1''), 115.17 (CH, C-3', C-5'), 129.27 (C, C-1'), 129.77 (CH, C-2', C-6'), 144.74 (C, C-4'), 176.76 (C, C-1).

4.1.5. Methyl 3-[4-(phenylamino)phenyl]-3-hydroxy-2-methyl propanoate (12 and 13).

(Mol. Formula: $C_{17}H_{19}NO_3$, M. W.: 285.3)

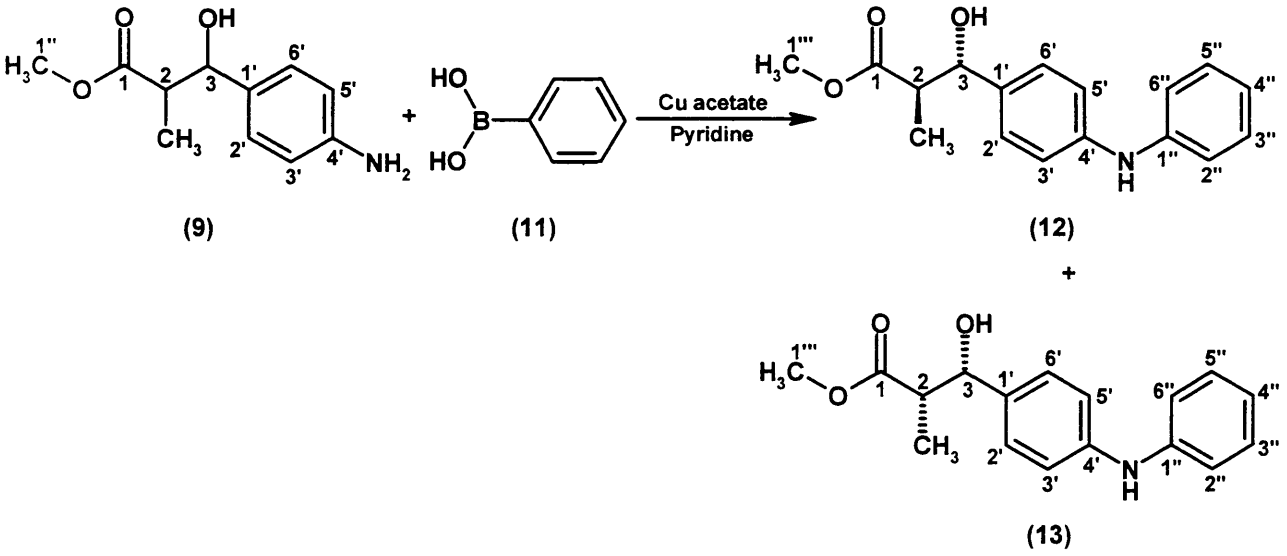

(9) (11) (12)

+

(13)

To phenylboronic acid (**11**) (0.854 g, 7 mmol), methyl 3-(4-aminophenyl)-3-hydroxy-2-methylpropanoate (**9**) (1 g, 3.5 mmol), anhydrous cupric acetate (1.176 g, 7 mmol), pyridine (0.553 g, 7 mmol) and 250 mg activated 4Å molecular sieves under an atmosphere of air was added anhydrous CH_2Cl_2 (20 mL) and the reaction stirred under air atmosphere at ambient temperature for 3 days. The product was isolated by flash column chromatography (petroleum ether – EtOAc 100:0 v/v increasing to 70:30 v/v) to give methyl 3-[4-(phenylamino)phenyl]-3-hydroxy-2-methylpropanoate in two forms: *anti* form as a brown solid (**12**) and the *syn* form as a colourles oily product (**13**) in a ratio of 2:1 respectively. Yield: 0.66 g (0.44 g *anti* (44%) and 0.22 g *syn* (22%)), t.l.c. system: petroleum ether – EtOAc 3:1 v/v, R_F: *anti* = 0.55 and *syn* = 0.62, vanillin stain positive.

• *anti*-form:

Melting point for the *anti* form: 98-101 °C.

Microanalysis for the *anti* form: Calculated for $C_{17}H_{19}NO_3$. $0.1H_2O$ (287.1),

Theoretical: %C= 71.11, %H= 6.74, %N= 4.88, Found: %C= 71.19, %H= 6.75, %N= 4.67.

^{1}H-NMR ($CDCl_3$), δ: 0.90 (d, 3H, J = 7.2 Hz, CH-C<u>H</u>$_3$), 2.62-2.71 (m, 1H, C<u>H</u>-CH$_3$), 2.95 (bs, 1H, OH), 3.58 (s, 3H, O-CH$_3$), 4.57 (d, 1H, J = 8.8 Hz, C<u>H</u>-OH), 5.77 (s, 1H, NH), 6.77-6.82 (m, 1H, H-aromatic), 6.88-6.96 (m, 4H, H-aromatic), 7.05-7.16 (m, 2H, H-aromatic), 7.18-7.20 (m, 2H, H-aromatic).

^{13}C NMR ($CDCl_3$), δ: 14.50 (CH_3, C-4), 47.26 (CH, C-2), 51.95 (CH_3, C-1'''), 76.21 (CH, C-3), 117.16, 118.29, 121.19, 127.60, 129.59 (CH, aromatic), 133.79 (C, C-1'), 142.95 (C, C-4'), 143.21 (C, C-1''), 176.49 (C, C-1).

• *syn*-form:

HRMS (EI) for the *syn* form: Calculated mass: 308.1257 $[M+Na]^+$, Measured mass: 308.1260 $[M+Na]^+$.

^{1}H-NMR (DMSO-d_6), δ: 1.07 (d, 3H, J = 6.9 Hz, CH-C<u>H</u>$_3$), 2.34-2.70 (m, 1H, C<u>H</u>-CH$_3$), 3.51 (s, 3H, O-CH$_3$), 4.74 (d, 1H, J = 5.5 Hz, C<u>H</u>-OH), 5.33 (d, 1H, J = 4.9 Hz, OH), 6.79-6.81 (m, 1H, H-aromatic), 7.00-7.05 (m, 4H, H-aromatic), 7.14-7.17 (m, 2H, H-aromatic), 7.20-7.23 (m, 2H, H-aromatic), 8.08 (s, 1H, NH).

^{13}C NMR (DMSO-d_6), δ: 11.87 (CH_3, C-4), 47.23 (CH, C-2), 51.14 (CH_3, C-1'''), 73.15 (CH, C-3), 116.41, 119.37, 126.89, 127.89, 129.10 (CH, aromatic), 135.06 (C, C-1'), 142.14 (C, C-4'), 143.61 (C, C-1''), 174.18 (C, C-1).

4.1.6. Methyl *anti*-3-(1*H*-1-imidazolyl)-3-[4-(phenylamino)phenyl]-2-methylpropanoate (14).

(<u>Mol. Formula</u>: $C_{20}H_{21}N_3O_2$, <u>M. W.</u>: 335.4)

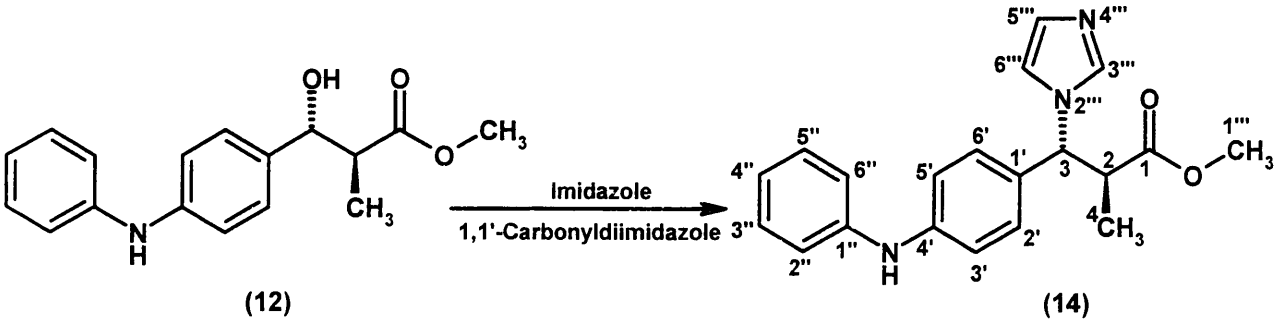

(12) (14)

To a solution of methyl *anti*-3-[4-(phenylamino)phenyl]-3-hydroxy-2-methylpropanoate (**12**) (0.42 g, 1.47 mmol) in anhydrous CH_3CN (20 mL) was added imidazole (0.294 g, 4.41 mmol) and 1,1'-carbonyldiimidazole (0.356 g, 2.20 mmol). The mixture was then heated at 65 °C for 1h and stirred afterwards for 24 h at room temperature. The reaction mixture was allowed to cool and then extracted with CH_2Cl_2 (3 x 50 mL) and H_2O (3 x 100 mL). The organic layer was dried ($MgSO_4$) and reduced *in vacuo*. The product was then purified by flash column chromatography (CH_2Cl_2 – MeOH 99:1 v/v increasing to 97:3 v/v) to give methyl *anti*-3-(1*H*-1-imidazolyl)-3-[4-(phenylamino)phenyl]-2-methylpropanoate (**14**) as a brown solid. Yield: 0.32 g (65 %), t.l.c. system: CH_2Cl_2 – MeOH 90:10 v/v, R_F: 0.4, vanillin stain positive.

Melting point: 118-122 °C.

Microanalysis: Calculated for $C_{20}H_{21}N_3O_2$. $0.2H_2O$ (339.01), Theoretical: %C= 70.86%, %H= 6.36%, %N= 12.39%, Found: %C= 70.72, %H= 6.24, %N= 12.31.

^{1}H-NMR ($CDCl_3$), δ: 1.11 (d, 3H, J = 6.9 Hz, CH-C<u>H</u>$_3$), 3.33-3.39 (m, 1H, C<u>H</u>-CH$_3$), 3.52 (s, 3H, OCH_3), 5.18 (s, 1H, C<u>H</u>-imidazole), 7.79 (s, 1H, NH), 6.87-6.95 (m, 1H, H-aromatic), 6.97-7.01 (m, 4H, H-aromatic), 7.04-7.07 (m, 2H, H-aromatic), 7.20-7.24 (m, 2H, H-aromatic), 7.20-7.24 (m, 2H, H-aromatic), 7.57 (s, 1H, H-aromatic).

^{13}C NMR ($CDCl_3$), δ: 15.98 (CH_3, C-4), 44.95 (CH, C-2), 52.07 (CH_3, C-1'''), 63.98 (CH, C-3), 116.78, 118.91, 121.89, 128.49, 129.54 (CH, aromatic), 128.22 (C, C-1'), 142.51 (C, C-4'), 144.28 (C, C-1''), 174.54 (C, C-1).

4.1.7. Methyl *syn*-3-(1*H*-1-imidazolyl)-3-[4-(phenylamino)phenyl]-2-methylpropanoate (15).

(Mol. Formula: $C_{20}H_{21}N_3O_2$, M. W.: 335.4)

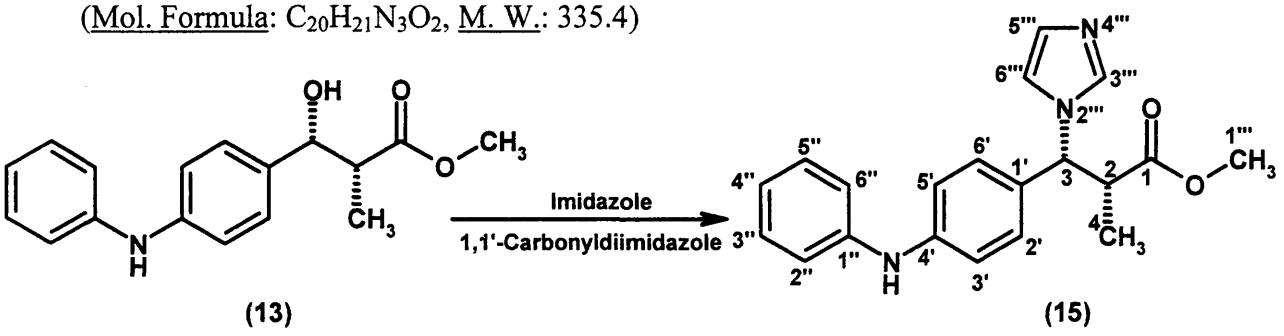

(13) (15)

To a solution of methyl *syn*-3-[4-(phenylamino)phenyl]-3-hydroxy-2-methylpropanoate (**13**) (0.21 g, 0.735 mmol) in anhydrous CH_3CN (20 mL) was added imidazole (0.294 g, 2.20 mmol) and 1,1'-carbonyldiimidazole (0.356 g, 1.10 mmol). The mixture was then heated at 65 °C for 1h and stirred afterwards for 24 h at room temperature. The reaction mixture was allowed to cool and then extracted with CH_2Cl_2 (3 x 50 mL) and H_2O (3 x 100 mL). The organic layer was dried over $MgSO_4$, filtered and reduced *in vacuo*. The product was then purified by flash column chromatography (CH_2Cl_2 – MeOH 99:1 v/v increasing to 97:3 v/v) to give methyl *syn*-3-(1*H*-1-imidazolyl)-3-[4-(phenylamino)phenyl]-2-methylpropanoate (**15**) as a colourless oily product. Yield: 0.14 g (57 %), t.l.c. system: CH_2Cl_2 – MeOH 90:10 v/v, R_F: 0.52, vanillin stain positive.

HRMS (EI): Calculated mass: 336.1707 $[M+H]^+$, Measured mass : 336.1709 $[M+H]^+$.

^{1}H-NMR ($CDCl_3$), δ: 1.15 (d, 3H, J = 2.8 Hz, CH-C<u>H</u>$_3$), 3.33-3.43 (m, 1H, C<u>H</u>-CH$_3$), 3.59 (s, 3H, OCH_3), 5.22 (d, 1H, J = 11.3 Hz, C<u>H</u>-imidazole), 6.25 (s, 1H, NH), 6.96-6.99 (m, 1H, H-aromatic), 7.01-7.05 (m, 4H, H-aromatic), 7.07-7.11 (m, 2H, H-aromatic), 7.15-7.20 (m, 2H, H-aromatic), 7.25-7.33 (m, 2H, H-aromatic), 7.61 (s, 1H, H-aromatic).

^{13}C NMR ($CDCl_3$), δ: 16.02 (CH_3, C-4), 44.99 (CH, C-2), 52.11 (CH_3, C-1'''), 63.98 (CH, C-3), 116.90, 119.39, 122.18, 128.55, 129.92 (CH, aromatic), 124.76 (C, C-1'), 142.28 (C, C-4'), 144.15 (C, C-1''), 174.52 (C, C-1).

4.1.8. Methyl 3-[4-(2-naphthylamino)phenyl]-3-hydroxy-2-methyl propanoate (17 and 18).

(Mol. Formula: $C_{21}H_{21}NO_3$, M. W.: 335.4)

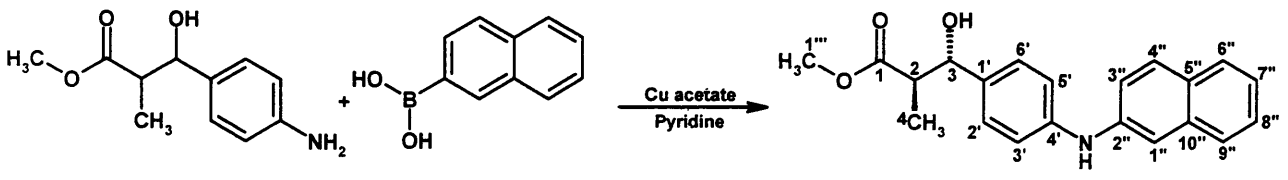

(9) (16) (17)

(18)

To naphthylboronic acid (**16**) (1.8 g, 10.5 mmol), methyl 3-(4-aminophenyl)-3-hydroxy-2-methylpropanoate (**9**) (1 g, 3.5 mmol), anhydrous cupric acetate (1.176 g, 7 mmol), pyridine (0.553 g, 7 mmol) and 250 mg activated 4Å molecular sieves under an atmosphere of air was added anhydrous CH_2Cl_2 (20 mL) and the reaction stirred under air atmosphere at ambient temperature for 3 days. The product was isolated by direct flash column chromatography (petroleum ether – EtOAc 100:0 v/v increasing to 70:30 v/v) to give methyl 3-[4-(2-naphthylamino)phenyl]-3-hydroxy-2-methylpropanoate in two forms: *anti* form as a brown solid (**17**) and the *syn* form (**18**) as a colourless oily product in a ratio of 2:1 respectively. Yield: 0.60 g (0.4 g *anti* (40%) and 0.2 g *syn* (20%)), t.l.c. system: petroleum ether – EtOAc 3:1 v/v, R_F: *anti* = 0.74 and *syn* = 0.8, vanillin stain positive.

• *anti*-form:

Melting point for the *anti* form: 124-126 °C.

Microanalysis for the *anti* form: Calculated for $C_{21}H_{21}NO_3$. $0.8H_2O$ (349.80), Theoretical: %C= 72.10, %H= 6.51, %N= 4.00, Found: %C= 72.14, %H= 6.44, %N= 3.64, N.b. this compound is very hygroscopic, and this microanalysis is the best one obtained after five days drying in the oven.

^{1}H-NMR ($CDCl_3$), δ: 0.97 (d, 3H, J = 7.2 Hz, CH-C$\underline{H}_3$), 2.73-2.79 (m, 2H, C$\underline{H}$-CH_3, OH), 3.68 (s, 3H, O-CH_3), 4.65 (d, 1H, J = 8.8 Hz, C$\underline{H}$-OH), 5.83 (s, 1H, NH), 7.05-7.08 (m, 2H, H-aromatic), 7.15 (dd, 1H, J = 2.3 Hz, 8.7 Hz, H-aromatic), 7.18-7.25 (m, 3H, H-aromatic), 7.32-7.37 (m, 2H, H-aromatic), 7.58 (d, 1H, J = 8.3 Hz, H-aromatic), 7.66-7.68 (m, 2H, H-aromatic).

^{13}C NMR ($CDCl_3$), δ: 14.56 (CH_3, C-4), 47.14 (CH, C-2), 51.94 (CH_3, C-1'''), 76.21 (CH, C-3), 112.08, 117.90, 120.15, 123.66, 126.52, 127.66, 127.89, 129.24 (CH, aromatic), 129.33 (C, C-5''), 134.24 (C, C-1'), 134.59 (C, C-10''), 140.54 (C, C-4'), 142.98 (C, C-2''), 176.37 (C, C-1).

• *syn*-form:

HRMS (EI) for the *syn* form: Calculated mass: 336.1594 $[M+H]^+$, Measured mass: 336.1597 $[M+H]^+$.

^{1}H-NMR ($CDCl_3$), δ: 1.11 (d, 3H, J = 7.2 Hz, CH-C$\underline{H}_3$), 2.69-2.75 (m, 1H,

C<u>H</u>-CH_3), 2.78 (d, 1H, J = 3.3 Hz, OH), 3.59 (s, 3H, O-CH_3), 4.74 (d, 1H, J = 3.8 Hz, C<u>H</u>-OH), 5.80 (s, 1H, NH), 7.02-7.05 (m, 2H, H-aromatic), 7.11 (dd, 1H, J = 2.3 Hz, 8.8 Hz, H-aromatic), 7.16-7.23 (m, 3H, H-aromatic), 7.29-7.32 (m, 2H, H- aromatic), 7.55 (d, 1H, J = 8.2 Hz, H-aromatic), 7.60-7.71 (m, 2H, H-aromatic).

<u>^{13}C NMR ($CDCl_3$), δ</u>: 10.15 (CH_3, C-4), 45.52 (CH, C-2), 50.83 (CH_3, C-1'''), 72.64 (CH, C-3), 110.67, 116.90, 119.01, 122.51, 125.45, 126.14, 126.62, 128.16 (CH, aromatic), 128.20 (C, C-5''), 133.32 (C, C-1'), 133.59 (C, C-10''), 139.74 (C, C-4'), 141.35 (C, C-2''), 175.14 (C, C-1).

4.1.9. Methyl *anti*-3-(1*H*-1-imidazolyl)-3-[4-(2-naphthylamino)phenyl]-2-methylpropanoate (19).

(<u>Mol. Formula</u>: $C_{24}H_{23}N_3O_2$, <u>M. W.</u>: 385.47)

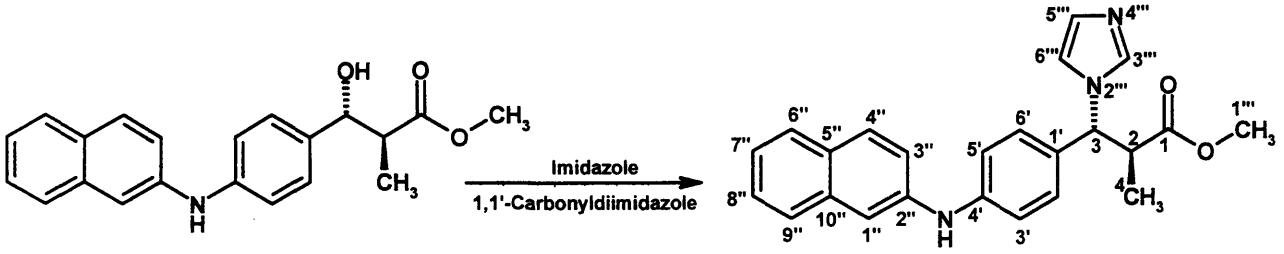

(17) (19)

To a solution of methyl *anti*-3-[4-(2-naphthylamino)phenyl]-3-hydroxy-2-methylpropanoate **(17)** (0.4 g, 1.19 mmol) in anhydrous CH_3CN (20 mL) was added imidazole (0.238 g, 3.57 mmol) and 1,1'-carbonyldiimidazole (0.29 g, 1.79 mmol). The mixture was then heated at 65 °C for 1h and stirred afterwards for 24 h at room temperature. The reaction mixture was allowed to cool and then extracted with CH_2Cl_2 (3 x 50 mL) and H_2O (3 x 100 mL). The organic layer was dried ($MgSO_4$) and reduced *in vacuo*. The product was then purified by flash column chromatography (CH_2Cl_2 – MeOH 99:1 v/v increasing to 97:3 v/v) to give methyl *anti*-3-(1*H*-1-imidazolyl)-3-[4-(2-naphthylamino)phenyl]-2-methylpropanoate **(19)** as a brown solid. Yield: 0.28 g (61%), t.l.c. system: CH_2Cl_2 – MeOH 90:10 v/v, R_F: 0.62, vanillin stain positive.

<u>Melting point:</u> 131-133 °C.

<u>HRMS (EI)</u>: Calculated mass: 386.1863 $[M+H]^+$, Measured mass: 386.1858 $[M+H]^+$..

^{1}H-NMR ($CDCl_3$), δ: 1.09 (d, 3H, J = 7.0 Hz, CH-C<u>H</u>$_3$), 3.29-3.37 (m, 1H, C<u>H</u>-CH$_3$), 3.52 (s, 3H, O-CH$_3$), 5.16 (s, 1H, C<u>H</u>-imidazole), 5.96 (s, 1H, NH), 6.95-7.04 (m, 2H, H-aromatic), 7.12-7.18 (m, 2H, H-aromatic), 7.24-7.27 (m, 3H, H-aromatic), 7.32-7.36 (m, 1H, H-aromatic), 7.38-7.39 (m, 2H, H-aromatic), 7.53 (s, 1H, H-aromatic), 7.59 (d, 1H, J = 8.2 Hz, H-aromatic), 7.67-7.69 (m, 2H, H-aromatic).

^{13}C NMR ($CDCl_3$), δ: 16.04 (CH_3, C-4), 44.99 (CH, C-2), 52.23 (CH_3, C-1'''), 64.00 (CH, C-3), 113.16, 117.52, 120.47, 123.96, 126.61, 127.68, 128.66, 129.32 (CH, aromatic), 129.16 (C, C-5''), 129.60 (C, C-1'), 134.50 (C, C-10''), 139.81.54 (C, C-4'), 143.84 (C, C-2''), 174.47 (C, C-1).

4.1.10. Methyl *syn*-3-(1*H*-1-imidazolyl)-3-[4-(2-naphthylamino)phenyl]-2-methylpropanoate (20).

(<u>Mol. Formula</u>: $C_{24}H_{23}N_3O_2$, <u>M. W.</u>: 385.47)

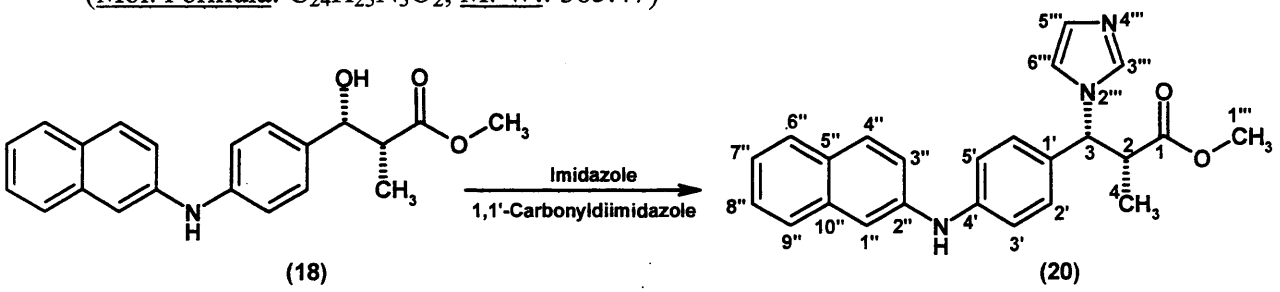

(18) (20)

To a solution of methyl *syn*-3-[4-(2-naphthylamino)phenyl]-3-hydroxy-2-methylpropanoate (**18**) (0.2 g, 0.595 mmol) in anhydrous CH_3CN (20 mL) was added imidazole (0.119 g, 1.785 mmol) and 1,1'-carbonyldiimidazole (0.144 g, 0.893 mmol). The mixture was then heated at 65 °C for 1h and stirred afterwards for 24 h at room temperature. The reaction mixture was allowed to cool and then extracted with CH_2Cl_2 (3 x 50 mL) and H_2O (3 x 100 mL). The organic layer was dried ($MgSO_4$) reduced *in vacuo*. The product was then purified by flash column chromatography (CH_2Cl_2 – MeOH 99:1 v/v increasing to 97:3 v/v) to give methyl *syn*-3-(1*H*-1-imidazolyl)-3-[4-(2-naphthylamino)phenyl]-2-methylpropanoate (**20**) as a yellow oily product. Yield: 0.13 g (57%), t.l.c. system: CH_2Cl_2 – MeOH 90:10 v/v, R_F: 0.66, vanillin stain positive.

<u>HRMS (EI):</u> Calculated mass: 386.1863 $[M+H]^+$, Measured mass: 386.1862 $[M+H]^+$.

^{1}H-NMR ($CDCl_3$), δ: 1.08 (d, 3H, J = 7.0 Hz, CH-C<u>H</u>$_3$), 3.29-3.37 (m, 1H,

C<u>H</u>-CH_3), 3.52 (s, 3H, O-CH_3), 4.47 (d, 1H, J = 11.3 Hz, C<u>H</u>-imidazole), 5.90 (s, 1H, NH), 6.94-7.05 (m, 2H, H-aromatic), 7.13-7.19 (m, 2H, H-aromatic), 7.24-7.27 (m, 3H, H-aromatic), 7.33-7.36 (m, 1H, H-aromatic), 7.39-7.41 (m, 2H, H-aromatic), 7.52 (s, 1H, H-aromatic), 7.60 (d, 1H, J = 8.2 Hz, H-aromatic), 7.67-7.70 (m, 2H, H-aromatic).

<u>^{13}C NMR ($CDCl_3$), δ</u>: 16.05 (CH_3, C-4), 44.99 (CH, C-2), 52.24 (CH_3, C-1'''), 63.99 (CH, C-3), 113.19, 117.52, 120.47, 123.98, 126.61, 127.68, 128.66, 129.32 (CH, aromatic), 129.16 (C, C-5''), 129.60 (C, C-1'), 134.50 (C, C-10''), 139.81.54 (C, C-4'), 143.84 (C, C-2''), 174.47 (C, C-1).

4.1.11. Methyl 3-hydroxy-2,2-dimethyl-3-(2-naphthyl) propanoate (37) [231].

(<u>Mol. Formula</u>: $C_{16}H_{18}O_3$, <u>M. W.</u>: 258.32)

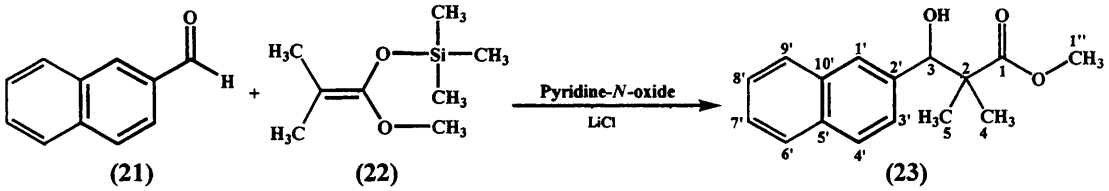

(21) (22) (23)

To a stirred solution of pyridine-*N*-oxide (61 mg, 0.64 mmol) and LiCl (54 mg, 1.28 mmol) in DMF (15 mL) was added naphthalene-2-carboxaldehyde (**21**) (1 g, 6.4 mmol) and methyl trimethylsilyldimethyl ketene acetal (**22**) (5.2 mL, 25.6 mmol) at room temperature under nitrogen atmosphere and left for 48 h. The product was isolated by direct flash column chromatography of the crude reaction mixture (petroleum ether – EtOAc 70:30 v/v) to give methyl 3-hydroxy-2,2-dimethyl-3-(2-naphthyl)propanoate (**23**) as a colourless oily product. Yield: 1.21 g (73%), t.l.c. system: petroleum ether – EtOAc 3:1 v/v, R_F: 0.47, vanillin stain positive.

<u>^{1}H-NMR ($CDCl_3$), δ</u>: 1.20 (s, 3H, C-C<u>H</u>$_3$), 1.22 (s, 3H, C-C<u>H</u>$_3$), 3.24 (d, 1H, J = 4.0 Hz, O<u>H</u>), 3.77 (s, 3H, O-C<u>H</u>$_3$), 5.10 (d, 1H, J = 4.0 Hz, C<u>H</u>-OH), 7.48 (m, 3H, H-aromatic), 7.8 (s, 1H, H-aromatic), 7.85 (m, 3H, H-aromatic).

<u>^{13}C NMR ($CDCl_3$), δ</u>: 19.23 (CH_3, C-4), 23.16 (CH_3, C-5), 47.98 (C, C-2), 52.14 (CH_3, C-1''), 78.85, 125.68, 125.96, 126.07, 126.72, 127.32, 127.60, 128.06 (CH, aromatic), 132.87 (C, C-5'), 133.06 (C, C-10'), 137.55 (C, C-2'), 178.23 (C, C-1).

4.1.12. 3-Methoxy-2,2-dimethyl-1-(2-naphthyl)-3-oxopropyl-1*H*-1-imidazolecarboxylate (38).

(Mol. Formula: $C_{20}H_{20}N_2O_4$, M. W.: 252.39)

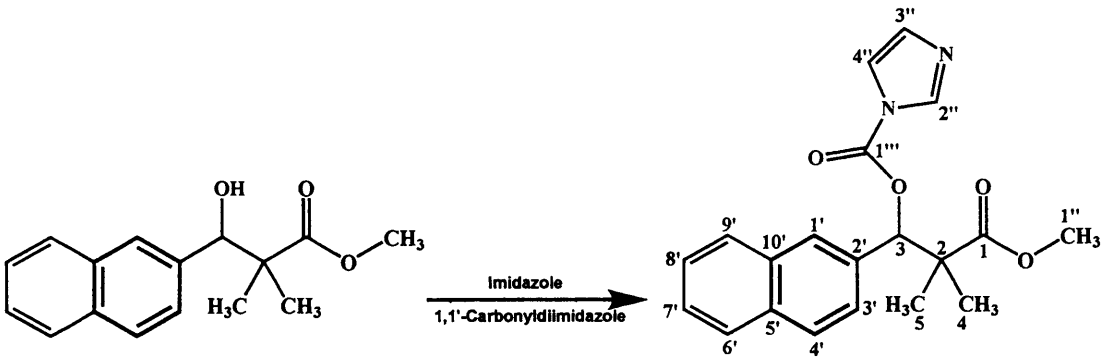

(23) (24)

To a solution of methyl 3-hydroxy-2,2-dimethyl-3-(2-naphthyl)propanoate (**23**) (0.904 g, 3.5 mmol) in anhydrous CH_3CN (20 mL) was added imidazole (0.714 g, 10.5 mmol) and 1,1'-carbonyldiimidazole (0.851 g, 5.25 mmol). The mixture was then heated at 65 °C for 1h and stirred afterwards for 24 h at room temperature. The reaction mixture was allowed to cool and then extracted with CH_2Cl_2 (3 x 50 mL) and H_2O (3 x 100 mL). The organic layer was dried over $MgSO_4$, filtered and reduced *in vacuo*. The product was then purified by flash column chromatography (CH_2Cl_2 – MeOH 99:1 v/v increasing to 97:3 v/v) to give 3-methoxy-2,2-dimethyl-1-(2-naphthyl)-3-oxopropyl-1*H*-1-imidazolecarboxylate (**24**) as a yellow oily product. Yield: 0.39 g (44 %), t.l.c. system: CH_2Cl_2 – MeOH 90:10 v/v, R_F: 0.12, vanillin stain negative.

HRMS (EI): Calculated mass: 353.14 $[M+H]^+$, Measured mass: 353.30 $[M+H]^+$.

^{1}H-NMR ($CDCl_3$), δ: 1.13 (s, 3H, C-C<u>H</u>$_3$), 1.29 (s, 3H, C-C<u>H</u>$_3$), 3.60 (s, 3H, O-C<u>H</u>$_3$), 6.28 (s, 1H, C<u>H</u>), 7.00 (s, 1H, H-aromatic), 7.32 (m, 2H, H-aromatic), 7.36 (s, 1H, H-aromatic), 7.40 (m, 2H, H-aromatic), 7.70 (s, 1H, H-aromatic), 7.72 (m, 3H, H-4', H-aromatic), 8.10 (s, 1H, H-aromatic).

^{13}C NMR ($CDCl_3$), δ: 19.90 (CH_3, C-4), 22.63 (CH_3, C-5), 47.50 (C, C-2), 52.41 (CH_3, C-1"), 83.87, 117.13, 124.73, 126.72, 126.94, 127.23, 127.72, 128.0, 128.15, 128.47, 130.90 (CH, aromatic), 132.45 (C, C-10'), 132.73 (C, C-5'), 133.02 (C, C-2'), 147.53 (C, C-1"), 175.34 (C, C-1).

4.1.13. Methyl 3-hydroxy-2,2-dimethyl-3-(2-pyridyl)propanoate (26) [202].

(Mol. Formula: $C_{11}H_{15}NO_3$, M. W.: 209.24)

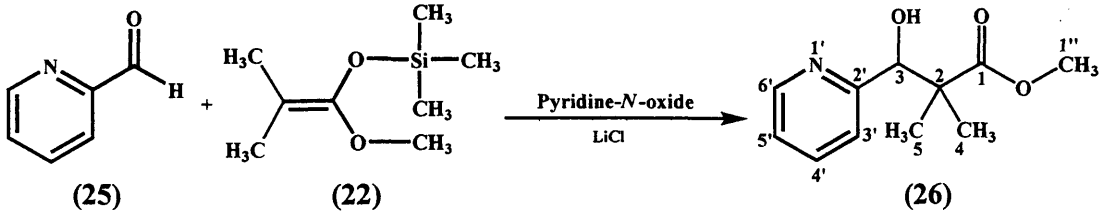

(25) (22) (26)

2-Pyridinecarboxaldehyde (**25**) (0.48 mL, 5 mmol) was added to a suspension of methyl trimethylsilyldimethyl ketene acetal (**22**) (2 mL, 10 mmol) in H_2O (20 mL). The suspension was stirred for 24 h at room temperature. The reaction mixture was extracted with EtOAc (3 x 50 mL). The combined organic layers were washed with brine (50 mL), dried over anhydrous $MgSO_4$, and the solvent evaporated *in vacuo* to give methyl 3-hydroxy-2,2-dimethyl-3-(2-pyridyl)propanoate (**26**) as a colourless oil. Yield: 0.89 g (85%), t.l.c. system: petroleum ether – EtOAc 3:1 v/v, R_F: 0.44, vanillin stain positive.

^{1}H-NMR ($CDCl_3$), δ: 0.94 (s, 3H, C-CH_3), 1.02 (s, 3H, C-CH_3), 3.59 (s, 3H, O-CH_3), 4.50 (s, 1H, O*H*), 4.81 (s, 1H, C*H*), 7.08 (m, 2H, H-aromatic), 7.51 (m, 1H, H-aromatic), 8.40 (d, 1H, J = 4.5 Hz, H-aromatic).

^{13}C NMR ($CDCl_3$), δ: 20.84 (CH_3, C-4), 20.91 (CH_3, C-5), 48.47 (C, C-2), 51.89 (CH_3, C-1''), 77.05 (CH, C-3), 122.12, 122.79, 136.16, 148.09 (CH, aromatic), 158.43 (C, C-2'), 177.14 (C, C-1).

4.1.14. Methyl 3-hydroxy-2,2-dimethyl-3-(2-quinolyl) propanoate (28).

(Mol. Formula: $C_{15}H_{17}NO_3$, M. W.: 259.30)

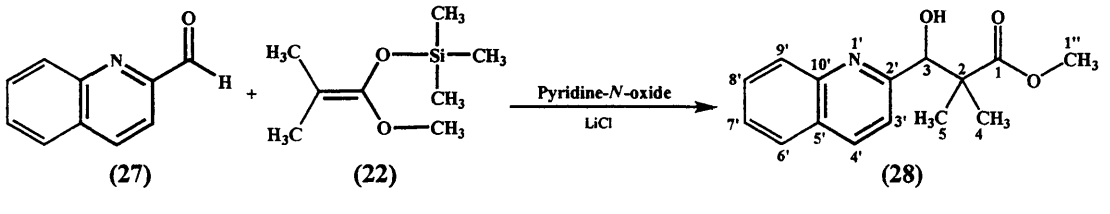

(27) (22) (28)

2-Quinolinecarboxaldehyde (**27**) (0.786 g, 5 mmol) was added to the suspension of methyl trimethylsilyldimethyl ketene acetal (**22**) (2 mL, 10 mmol) in a mixture of H_2O / MeOH (3:1, 20 mL). The suspension was stirred for 24 h at room temperature. The reaction mixture was extracted with EtOAc (3X50 ml). The

combined organic layers were washed with brine (50 mL), dried over anhydrous $MgSO_4$, and the solvent evaporated *in vacuo*. Purification of crude product by flash chromatography (petroleum ether – EtOAc 100:0 v/v increasing to 70:30 v/v) gave methyl 3-hydroxy-2,2-dimethyl-3-(2-quinolyl)propanoate (**28**) as a colourless oil. Yield: 0.80 g (62%), t.l.c. system: petroleum ether – EtOAc 3:1 v/v, R_F: 0.44, vanillin stain positive.

HRMS (EI): Calculated mass: 260.1281 $[M+H]^+$, Measured mass: 260.1283 $[M+H]^+$.

^{1}H-NMR ($CDCl_3$), δ: 1.00 (s, 3H, C-CH_3), 1.12 (s, 3H, C-CH_3), 3.60 (s, 3H, O-CH_3), 5.15 (s, 2H, CH, OH), 7.12 (d, 1H, J = 8.5 Hz, H-aromatic), 7.35 (t, 1H, J = 7.5 Hz, H-aromatic), 7.52 (t, 1H, J = 7.8 Hz, H-aromatic), 7.61 (d, 1H, J = 8.0 Hz, H-aromatic), 7.90 (m, 2H, H-aromatic).

^{13}C NMR ($CDCl_3$), δ: 19.50 (CH_3, C-4), 20.29 (CH_3, C-5), 47.51 (C, C-2), 50.83 (CH_3, C-1''), 76.21, 118.79, 125.48, 126.49, 127.83, 128.46, 135.44 (CH, aromatic), 126.54 (C, C-5'), 145.39 (C, C-10'), 157.98 (C, C-2'), 176.07 (C,C-1).

4.1.15. Methyl 3-hydroxy-2,2-dimethyl-3-(3-nitrophenyl) propanoate (30) [178]

(Mol. Formula: $C_{12}H_{15}NO_5$, M. W.: 253.25)

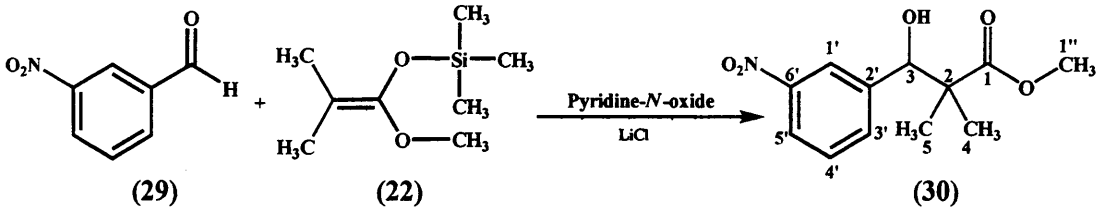

(29) (22) (30)

To a stirred solution of pyridine-*N*-oxide (61 mg, 0.64 mmol) and LiCl (54 mg, 1.28 mmol) in DMF (15 mL) was added 3-nitrobenzaldehyde (**29**) (1 g, 6.62 mmol) and methyl trimethylsilyldimethyl ketene acetal (**22**) (2.2 mL, 19.85 mmol) at room temperature under nitrogen atmosphere and left for 24 h. The product was isolated by direct flash column chromatography of the crude reaction mixture (petroleum ether – EtOAc 70:30 v/v) to give methyl 3-hydroxy-2,2-dimethyl-3-(3-nitrophenyl) propanoate (**30**) as a colourless oily product. Yield: 1.65 g (98%), t.l.c. system: petroleum ether – EtOAc 3:1 v/v, R_F: 0.44, vanillin stain positive.

^{1}H-NMR ($CDCl_3$), δ: 1.01 (s, 3H, C-CH_3), 1.05 (s, 3H, C-CH_3), 3.61 (s, 3H, O-CH_3), 3.7 (s, 1H, OH), 4.92 (s, 1H, CH), 7.41 (t, 1H, J = 8.0 Hz, H-aromatic), 7.52 (d, 1H, J = 8.0 Hz, H-aromatic), 8.01 (d, 1H, J = 8.5 Hz, H-aromatic), 8.05 (s, 1H, H-2').

^{13}C NMR ($CDCl_3$), δ: 19.30 (CH_3, C-4), 22.19 (CH_3, C-5), 47.78 (C, C-2), 52.21 (CH_3, C-1''), 77.50 (CH, C-3), 122.40, 122.60, 128.64, 133.51 (CH, aromatic), 142.46 (C, C-1'), 147.79 (C, C-3'), 177.53 (C, C-1).

4.1.16. Methyl 3-(3-aminophenyl)-3-hydroxy-2,2-dimethyl propanoate (31).

(Mol. Formula: $C_{12}H_{17}NO_3$, M. W.: 223.27)

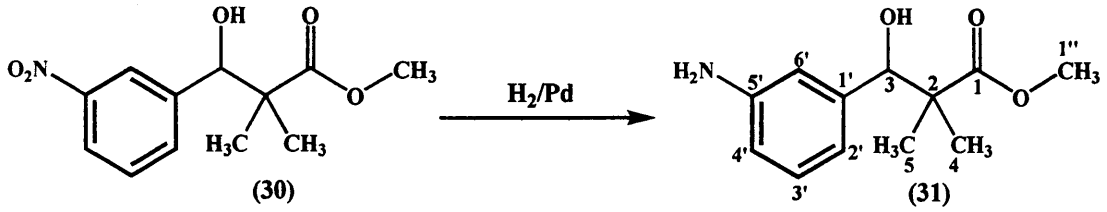

To a suspension of 5% Pd-C (10 mol %) in EtOH (5 mL) was added, under nitrogen, a solution of 3-hydroxy-2,2-dimethyl-3-(3-nitrophenyl) propanoate (**30**) (1.65 g, 6.52 mmol) in EtOH (20 mL). Then, the reaction atmosphere was changed to hydrogen and the reaction mixture stirred at room temperature. After a period of 3 h, the suspension was filtered over a pad of celite and the solvent removed under reduced pressure to give methyl 3-(3-aminophenyl)-3-hydroxy-2,2-dimethyl propanoate (**31**) as a white solid. Yield: 1.5 g (99%), t.l.c. system: petroleum ether – EtOAc 3:1 v/v, R_F: 0.20, vanillin stain positive.

Melting point: 173-176 °C.

Microanalysis: Calculated for $C_{12}H_{17}NO_3$ (223.27), Theoretical: %C= 64.55, %H= 7.67, %N= 6.27, Found: %C= 64.31, %H= 7.74, %N= 5.98.

^{1}H-NMR ($CDCl_3$), δ: 1.01 (s, 3H, C-CH_3), 1.08 (s, 3H, C-CH_3), 3.29 (s, 3H, OH, NH_2), 3.62 (s, 3H, O-CH_3), 4.72 (s, 1H, CH), 6.51 (d, 1H, J = 8.0 Hz, H-aromatic), 6.60 (m, 2H, H-aromatic), 7.01 (t, 1H, J = 7.5 Hz, H-aromatic).

^{13}C NMR ($CDCl_3$), δ: 19.15 (CH_3, C-4), 23.13 (CH_3, C-5), 47.68 (C, C-2), 52.06 (CH_3, C-1''), 78.73 (CH, C-3), 114.46, 114.66, 118.28, 128.63 (CH, aromatic), 141.33 (C, C-1'), 145.80 (C, C-3'), 178.26 (C, C-1).

4.1.17. Methyl 3-hydroxy-2,2-dimethyl-3-[3-(2-naphthylamino) phenyl]propanoate (32).

(Mol. Formula: $C_{22}H_{23}NO_3$, M. W.: 349.42)

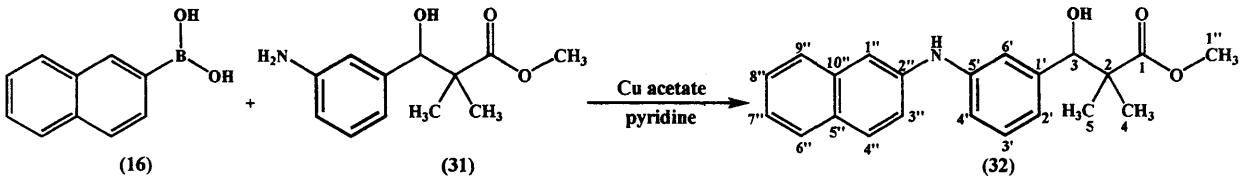

To naphthylboronic acid (**16**) (3.47 g, 20.15 mmol), methyl 3-(3-aminophenyl)-3-hydroxy-2,2-dimethyl propanoate (**31**) (1.5 g, 6.72 mmol), anhydrous cupric acetate (2.44 g, 13.44 mmol), pyridine (1.09 mL, 13.44 mmol) and 250 mg activated 4Å molecular sieves under an atmosphere of air was added anhydrous CH_2Cl_2 (20 mL) and the reaction stirred under air atmosphere at ambient temperature for 3 days. The product was isolated by direct flash column chromatography (petroleum ether – EtOAc 100:0 v/v increasing to 70:30 v/v) to give methyl 3-hydroxy-2,2-dimethyl-3-[3-(2-naphthylamino)phenyl]propanoate (**32**) as a colourless oily product. Yield: 1.3 g (57%), t.l.c. system: petroleum ether – EtOAc 3:1 v/v, R_F: 0.50, vanillin stain positive.

HRMS (EI): Calculated mass: 350.1751 $[M+H]^+$, Measured mass: 350.1749 $[M+H]^+$.

^{1}H-NMR ($CDCl_3$), δ: 1.09 (s, 3H, C-C<u>H</u>$_3$), 1.11 (s, 3H, C-C<u>H</u>$_3$), 3.00 (s, 1H, O<u>H</u>,), 3.62 (s, 3H, O-C<u>H</u>$_3$), 4.78 (s, 1H, C<u>H</u>), 5.81 (s, 1H, N<u>H</u>), 6.82 (d, 1H, J = 8.0 Hz, H-aromatic), 7.00 (d, 1H, J = 7.0 Hz, H-aromatic), 7.02 (s, 1H, H-aromatic), 7.11 (d, 1H, J = 8.8 Hz, H-aromatic), 7.17 (m, 1H, H-aromatic), 7.21 (t, 1H, J = 6.8 Hz, H-aromatic), 7.32 (m, 2H, H-aromatic), 7.54 (d, 1H, J = 8.0 Hz, H-aromatic), 7.65 (d, 2H, J = 8.5 Hz, H-aromatic).

^{13}C NMR ($CDCl_3$), δ: 19.33 (CH_3, C-4), 23.16 (CH_3, C-5), 47.80 (C, C-2), 52.14 (CH_3, C-1''), 78.73 (CH, C-3), 111.63 (CH, C-4'), 117.61 (CH, C-2, C-aromatic), 120.05, 120.83, 126.48, 126.50, 127.65, 128.82, 129.20 (CH, aromatic), 123.54 (C, C-6), 129.23 (C, C-5'), 134.62 (C, C-10''), 140.82 (C, C-1'), 141.49 (C, C-2''), 142.57 (C, C-3'), 178.17 (C, C-1).

4.1.18. Methyl 3-hydroxy-2-methylene-3-(2-naphthyl)propanoate (33) [203].

(Mol. Formula: $C_{15}H_{14}O_3$, M. W.: 242.28)

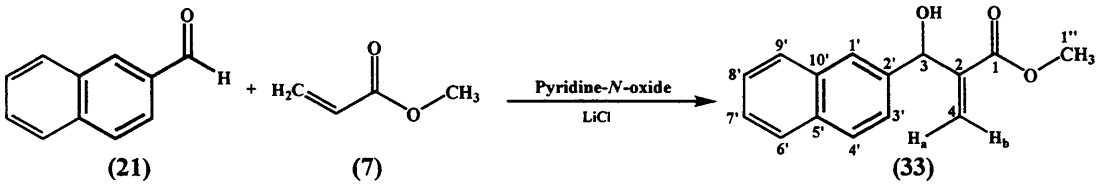

(21) (7) (33)

DABCO (0.275 g, 2.5 mmol) was added to a solution containing 2-naphthaldehyde (**21**) (1.3 g, 8.3 mmol) in methyl acrylate (**7**) (1.5 mL, 16.66 mmol) and the mixture was allowed to stir for 72 h at 25 °C. The reaction was then diluted in CH_2Cl_2 (50 mL), washed with 5% aqueous HCl (25 mL) and H_2O (25 mL), dried with $MgSO_4$, and concentrated under reduced pressure. The solid residue obtained was purified using flash column chromatography (CH_2Cl_2 – MeOH 99:1 v/v increasing to 97:3 v/v) to give methyl 3-hydroxy-2-methylene-3-(2-naphthyl)propanoate (**33**) as a white solid. Yield: 1.6 g (79%), t.l.c. system: petroleum ether – EtOAc 3:1 v/v, R_F: 0.63, vanillin stain positive.

Melting point: 97-99 °C (lit. m.p. 97-99 °C) [203].

^{1}H-NMR ($CDCl_3$), δ: 3.18 (d, 1H, J = 5.6 Hz, OH), 3.75 (s, 3H, O-CH_3), 5.77 (d, 1H, J = 5.6 Hz, CH-OH), 5.90-5.91 (m, 1H, H_a), 6.40-6.41 (m, 1H, H_b), 7.48-7.51 (m, 3H, H-aromatic), 7.84-7.89 (m, 4H, H-aromatic).

^{13}C NMR ($CDCl_3$), δ: 51.99 (CH_3, C-1''), 73.38 (CH, C-3), 124.59, 125.54, 126.06, 126.16, 127.66, 128.13, 128.20 (CH, aromatic), 126.35 (CH_2, C-4), 133.06 (C, C-5'), 133.27 (C, C-10'), 138.63 (C, C-2'), 141.93 (C, C-2), 166.81 (C, C-1).

4.1.19. Methyl 3-(1*H*-1-imidazolyl)-2-methylene-3-(2-naphthyl) propanoate (34).

(Mol. Formula: $C_{18}H_{16}N_2O_2$, M. W.: 292.34)

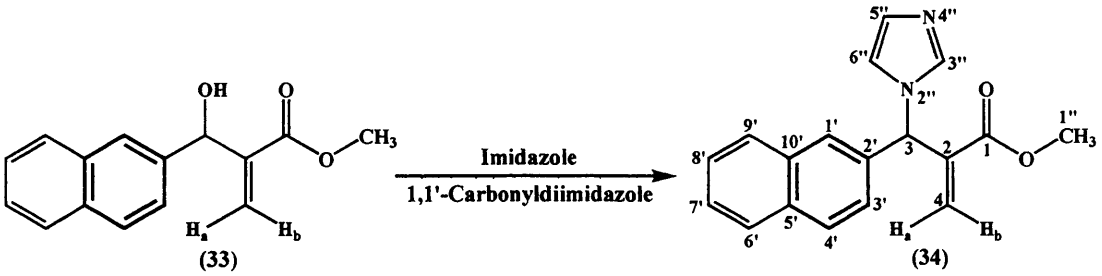

To a solution of methyl 3-hydroxy-2-methylene-3-(2-naphthyl)propanoate (**33**) (0.824 g, 3.4 mmol) in anhydrous CH_3CN (30 mL) was added imidazole (0.68 g, 10.2 mmol) and 1,1'-carbonyldiimidazole (0.822 g, 5.1 mmol). The mixture was then heated at 65 °C for 1h and stirred afterwards for 24 h at room temperature. The reaction mixture was allowed to cool and then extracted with CH_2Cl_2 (3 x 50 mL) and H_2O (3 x 100 mL). The organic layer was dried ($MgSO_4$) and reduced *in vacuo*. The product was then purified by flash column chromatography (CH_2Cl_2 – MeOH 99:1 v/v increasing to 97:3 v/v) to give methyl 3-(1*H*-1-imidazolyl)-2-methylene-3-(2-naphthyl) propanoate (**34**) as a white solid. Yield: 0.62 g (70%), t.l.c. system: CH_2Cl_2 – MeOH 90:10 v/v, R_F: 0.43, vanillin stain positive.

Melting point: 99-101 °C.

Microanalysis: Calculated for $C_{18}H_{16}N_2O_2$ (349.8), Theoretical: %C= 73.96, %H= 5.52, %N= 9.58, Found: %C= 73.59, %H= 5.46, %N= 9.71.

^{1}H-NMR ($CDCl_3$), δ: 3.77 (s, 1H, CH_3), 4.97 (s, 2H, N-CH, H_a), 5.21 (s, 1H, H_b), 6.82-6.83 (m, 1H, H-aromatic), 6.94-6.99 (m, 1H, H-aromatic), 7.43-7.48 (m, 3H, H-aromatic), 7.70 (s, 1H, H-aromatic), 7.74-7.82 (m, 3H, H-aromatic), 8.11 (s, 1H, H-aromatic).

^{13}C NMR ($CDCl_3$), δ: 43.10 (CH_2, C-4), 52.54 (CH_3, C-1"), 118.76, 125.66, 127.01, 127.47, 127.67, 127.79, 128.44, 128.86, 129.49, 144.97 (CH, aromatic), 127.19 (C, C-5'), 131.39 (C, C-10'), 133.04 (C, C-2'), 133.47 (C, C-2), 167.05 (C, C-1).

4.1.20. Methyl 4-[(2-benzoxazolyl)amino]benzoate (37).

(Mol. Formula: $C_{15}H_{12}N_2O_3$, M. W.: 268.27)

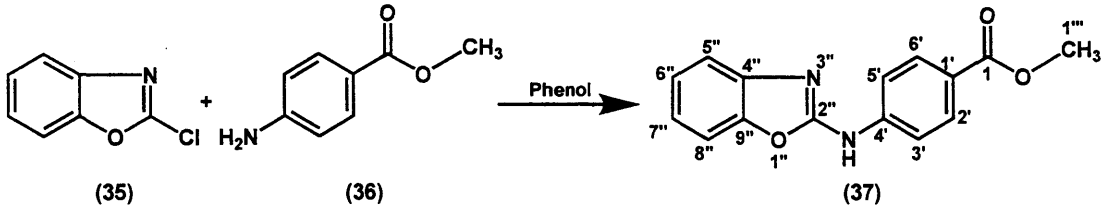

(35) (36) (37)

A mixture of 2-chlorobenzoxazole (**35**) (1.2 mL, 10 mmol) and phenol (6 g) was heated at 100 °C under nitrogen. When 2-chlorobenzoxazole was dissolved in phenol, methyl 4-aminobenzoate (**36**) (1.5 g, 10 mmol) was introduced into the reaction mixture. The mixture was stirred at 80 °C for 4 h, cooled to room temperature and poured into H_2O (25 mL). The precipitate was then filtered, washed well with H_2O and recrystallised from EtOH to give methyl 4-[(2-benzoxazolyl)amino]benzoate (**37**) as white crystals. Yield: 2.4 g (90%), t.l.c. system: petroleum ether – EtOAc 3:1 v/v, R_F: 0.58, vanillin stain positive.

Melting point: 214-216 °C.

Microanalysis: Calculated for $C_{15}H_{12}N_2O_3$ (268.27), Theoretical: %C= 67.16, %H= 4.51, %N= 10.44, Found: %C= 67.32, %H= 4.50, %N= 10.28.

^{1}H-NMR (DMSO-d_6), δ: 3.84 (s, 3H, CH_3), 7.17-7.20 (t, 1H, J = 7.8 Hz, H-aromatic), 7.25-7.28 (t, 1H, J = 7.6 Hz, H-aromatic), 7.52-7.54 (m, 2H, H-aromatic), 7.89 (d, 2H, J = 8.8 Hz, H-aromatic), 7.99 (d, 2H, J = 8.7 Hz, H-aromatic), 11.07 (s, 1H, NH).

^{13}C NMR (DMSO-d_6), δ: 51.71 (CH_3, C-1'''), 109.16, 116.90, 117.00, 122.21, 124.16, 130.53 (CH, aromatic), 122.76 (C, C-1'), 141.97 (C, C-4''), 143.07 (C, C-4'), 146.96 (C, C-9''), 157.25 (C, C-2''), 165.85 (C, C-1).

4.1.21. 4-[(2-Benzoxazolyl)amino]acetophenone (39).

(Mol. Formula: $C_{15}H_{12}N_2O_2$, M. W.: 252.28)

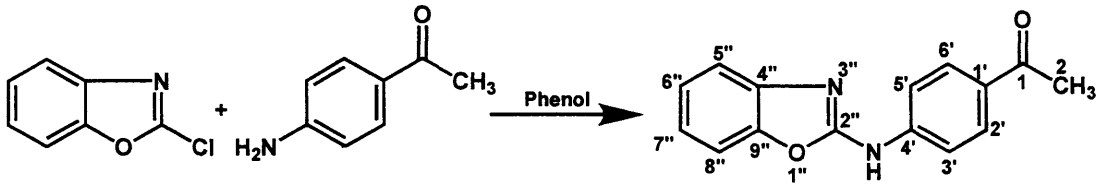

(35) (38) (39)

A mixture of 2-chlorobenzoxazole (**24**) (1.2 mL, 10 mmol) and phenol (6 g) was heated at 100 °C under nitrogen. When the 2-chlorobenzoxazole was dissolved in phenol, 4-aminoacetophenone (**27**) (1.35 g, 10 mmol) was introduced into the reaction mixture. The mixture was stirred at 80 °C for 4 h, cooled to room temperature and poured into H_2O. The precipitate was then filtered, washed with H_2O and recrystallised from EtOH to give 4-[(2-benzoxazolyl)amino]acetophenone (**28**) as yellow crystals. Yield: 1.4 g (56%), t.l.c. system: petroleum ether – EtOAc 3:1 v/v, R_F: 0.38, vanillin stain positive.

Melting point: 205-207 °C.

Microanalysis: Calculated for $C_{15}H_{12}N_2O_2$ (252.28), Theoretical: %C= 71.42, %H= 4.79, %N= 11.10, Found: %C= 71.35, %H= 4.82, %N= 10.94.

^{1}H-NMR (DMSO-d_6), δ: 2.54 (s, 3H, CH_3), 7.17-7.20 (dt, 1H, J = 1.2 Hz, 7.8 Hz, H-aromatic), 7.25-7.28 (dt, 1H, J = 1.1 Hz, 7.7 Hz, H-aromatic), 7.52-7.54 (m, 2H, H-aromatic), 7.89 (d, 2H, J = 8.8 Hz, H-aromatic), 8.00 (d, 2H, J = 8.7 Hz, H-aromatic), 11.07 (s, 1H, NH).

^{13}C NMR (DMSO-d_6), δ: 26.32 (CH_3, C-2), 109.16, 116.77, 117.01, 122.21, 124.17, 129.75 (CH, aromatic), 130.69 (C, C-1'), 141.98 (C, C-4"), 143.01 (C, C-4'), 146.97 (C, C-9"), 157.27 (C, C-2"), 196.24 (C, C-1).

4.1.22. *N*-(1,3-Benzoxazol-2-yl)-*N*-[4-(phenoxymethyl)phenyl]amine (41).

(Mol. Formula: $C_{20}H_{16}N_2O_2$, M. W.: 316.36)

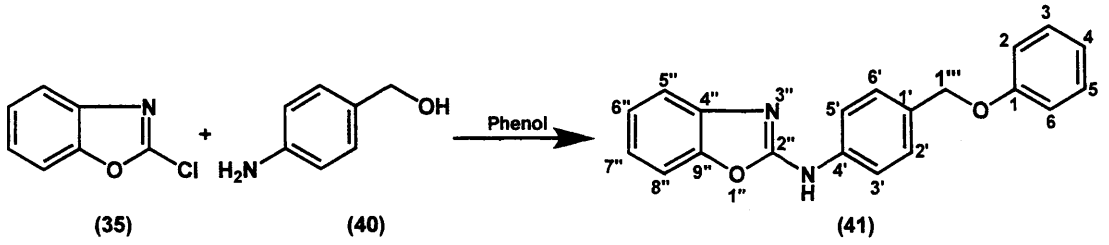

(35) (40) (41)

A mixture of 2-chlorobenzoxazole (**24**) (1.2 mL, 10 mmol) and phenol (6 g) was heated at 100 °C under nitrogen. When the 2-chlorobenzoxazole was dissolved in phenol, 4-aminobenzylalcohol **(29)** (1.23 g, 10 mmol) was introduced into the reaction mixture. The mixture was stirred at 80 °C for 4 h, cooled to room temperature and poured into H_2O. The precipitate was then filtered, washed with H_2O and the product was isolated by flash column chromatography (petroleum ether – EtOAc 100:0 v/v increasing to 70:30 v/v) to give *N*-(1,3-benzoxazol-2-yl)-*N*-[4-(phenoxymethyl)phenyl]amine as white solid (**30**). Yield: 0.9 g (28%), t.l.c. system: petroleum ether – EtOAc 3:1 v/v, R_F: 0.64, vanillin stain positive.

Melting point: 151-156 °C.

HRMS (EI): Calculated mass: 317.1285 $[M+H]^+$, Measured mass: 317.1289 $[M+H]^+$.

^{1}H-NMR (DMSO-d_6), δ: 3.79 (s, 2H, CH_2), 6.68 (d, 2H, J = 7.4 Hz, H-aromatic), 7.1 (d, 2H, J = 8.5 Hz, H-aromatic), 7.12 (t, J = 7.5 Hz, H-aromatic), 7.19 (m, 3H, H-aromatic), 8.00 (d, 2H, J = 8.7 Hz, H-aromatic), 11.07 (s, 1H, NH).

^{13}C NMR (DMSO-d_6), δ: 71.72 (CH_2, C-1'''), 108.84, 115.11, 116.46, 117.75, 121.48, 123.70, 129.03, 129.43 (CH, aromatic), 131.64 (C, C-1'), 135.73 (C, C-4'), 142.49 (C, C-4''), 147.00 (C, C-9''), 155.44 (C, C-2''), 158.09 (C, C-1).

4.1.23. 4-[(2-Benzoxazolyl)amino]benzyl alcohol (42).

(Mol. Formula: $C_{15}H_{12}N_2O_2$, M. W.: 252.28)

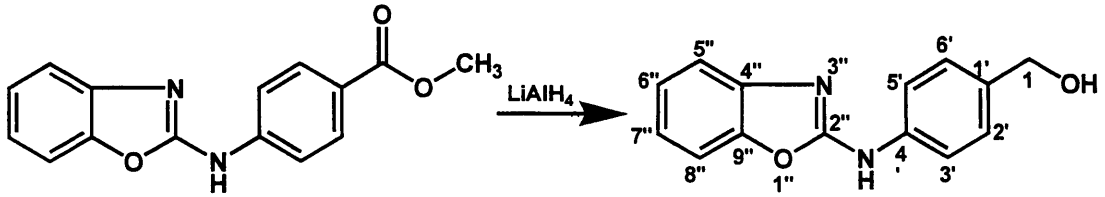

(37) (42)

To a cooled (ice) solution of methyl 4-[(2-benzoxazolyl)amino]benzoate (**26**) (1.85 g, 6.9 mmol) in anhydrous THF (60 mL) was added 1M (THF) $LiAlH_4$ (14.0 mL, 14.0 mmol) dropwise. Once addition was complete the reaction was stirred at room temperature for 20 min then EtOAc (20 mL) added slowly, with cooling, to quench the reaction. H_2O (20 mL) was added to dissolve the lithium salts, and then the organic layer separated. The organic layer was washed with H_2O (2 x 100 mL), then the combined aqueous washes back extracted with EtOAc (2 x 100 mL). The combined organic layers were dried ($MgSO_4$) and concentrated under reduced pressure to give a pale orange/brown residue. The residue was washed with EtOH, filtered and dried *in vacuo* at 70 °C to give 4-[(2-benzoxazolyl)amino]benzyl alcohol (**31**) as a cream coloured solid, pure enough for use in the next reaction. Yield: 1.194 g (72 %), t.l.c. system: petroleum ether- EtOAc 1:1 v/v, R_F: 0.18.

Melting point: 205-207 °C.

^{1}H-NMR (DMSO-d_6), δ: 4.47 (d, 2H, J = 5.3 Hz, CH_2OH), 5.14 (t, 1H, J = 5.6 Hz, CH_2OH), 7.12 (dt, 1H, J = 1.2 Hz, 7.8 Hz, H-aromatic), 7.22 (dt, 1H, J = 1.1 Hz, 7.7 Hz, H-aromatic), 7.47 (dd, 2H, J = 7.7 Hz, 12.2 Hz, H-aromatic), 7.52-7.54 (m, 2H, H-aromatic), 7.72 (d, 2H, J = 8.6 Hz, H-aromatic), 10.59 (s, 1H, NH).

^{13}C NMR (DMSO-d_6), δ: 62.6 (CH_2, C-1), 108.9, 116.5, 117.3, 121.5, 127.3 (CH, aromatic), 123.9 (C, C-1'), 136.3 (C, C-1'), 137.3 (C, C-4"), 142.5 (C, C-4'), 147.0 (C, C-9"), 158.0 (C, C-2").

4.1.24. 4-[(2-Benzoxazol)amino]benzaldehyde (43).

(Mol. Formula: $C_{14}H_{10}N_2O_2$, M. W.: 238.07)

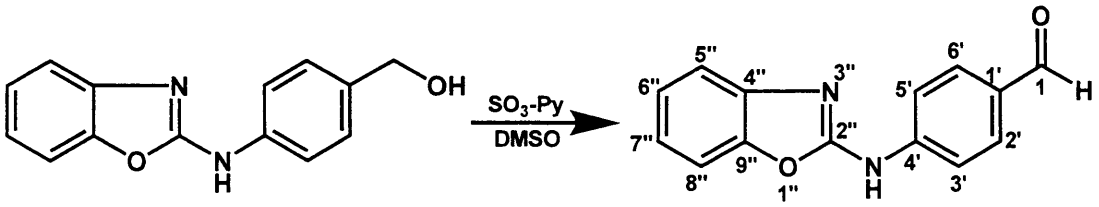

(42) (43)

To a cooled (ice) solution of 4-[(2-benzoxazolyl)amino]benzyl alcohol (**31**) (0.5 g, 2.08 mmol) in dry DMSO (5 mL) and Et_3N (2.9 mL, 20.8 mmol) was added a solution of pyridine-sulphur trioxide complex (1.40 g, 8.8 mmol) in dry DMSO (5 mL) dropwise. The reaction was stirred at 0 °C for 5 min then at room temperature for 25 min. The reaction was cooled in ice and quenched by the dropwise addition of 1M aqueous HCl (~ 10 mL) to pH5. H_2O (50 mL) was added and this solution extracted with EtOAc (2 x 100 mL). The organic layers were combined, washed with aq. $NaHCO_3$ solution (100 mL), H_2O (100 mL), dried ($MgSO_4$) and concentrated under reduced pressure. The resulting residue was washed with Et_2O to give 4-[(2-benzoxazol)amino]benzaldehyde (**32**) as a pale yellow solid which was dried *in vacuo* at 70 °C. Yield: 96 mg (19%), t.l.c. system: petroleum ether- EtOAc 1:2 v/v, R_F: 0.89.

Melting point: 183-186 °C.

^{1}H-NMR (DMSO-d_6), δ: 7.25 (t, 1H, J = 7.8 Hz, H-aromatic), 7.33 (ψt, 1H, J = 7.2 Hz, 8.0 Hz, H-aromatic), 7.60 (dd, 2H, J = 2.9 Hz, 7.9 Hz, H-aromatic), 8.01 (m, 4H, H-aromatic), 9.94 (s, 1H, NH), 11.28 (s, 1H, CHO).

^{13}C NMR (DMSO-d_6), δ: 109.2, 117.1, 117.2, 122.4, 130.3 (CH, aromatic), 124.2 (C, C-1'), 131.1 (C, C-1'), 141.9 (C, C-4"), 144.2 (C, C-4'), 147.0 (C, C-9"), 158.1 (C, C-2"), 191.24 (C, C-1).

4.1.25. *tert*-Butyl *N*-(4-acetylphenyl)carbamate (44) [232].

(Mol. Formula: $C_{13}H_{17}NO_3$, M. W.: 235.29)

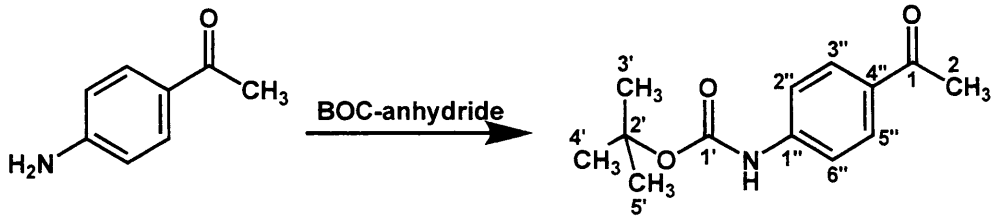

(38) (44)

4-Aminoacetophenone **(38)** (1.096 g, 8.12 mmol) was dissolved in a mixture of dioxane (5 mL), H_2O (5 mL), and 1N aqueous NaOH (8 mL) and cooled in an ice bath. Di-tert-butyl pyrocarbonate (BOC-anhydride, 2.66 g, 12.18 mol) was added in one portion, and stirring was continued at room temperature for 48 h. The dioxane was removed *in vacuo* and the aqueous layer chilled, acidified with 1N aqueous HCl. The precipitate was then filtered and washed with H_2O to give *tert*-butyl *N*-(4-acetylphenyl)carbamate (**44**) as a white solid which was dried *in vacuo* at 70 °C. Yield: 1.1 g (58%) t.l.c. system: petroleum ether – EtOAc 3:1 v/v, R_F: 0.71, vanillin stain positive.

Melting point: 137-139 °C (lit. m.p. 137-138 °C) [232].

^{1}H-NMR (DMSO-d_6), δ: 1.50 (s, 9H, C(CH_3)$_3$), 2.5 (s, 3H, CO-CH_3), 7.58 (d, 2H, J = 9.0 Hz, H-aromatic), 7.88 (d, 2H, J = 9.0 Hz, H-aromatic), 9.76 (s, 1H, NH).

^{13}C NMR (DMSO-d_6), δ: 26.28 (CH_3, C-2), 27.99 (CH_3, C-3', C-4', C-5'), 79.72 (C, C-2'), 117.15, 129.41 (CH, aromatic), 130.69 (C, C-4''), 144.07 (C, C-1''), 152.47 (C, C-1'), 196.38 (C, C-1).

4.1.26. *tert*-Butyl *N*-[4-(2-bromoacetyl)phenyl]carbamate (45) [232].

(Mol. Formula: $C_{13}H_{17}NO_3$, M. W.: 235.29)

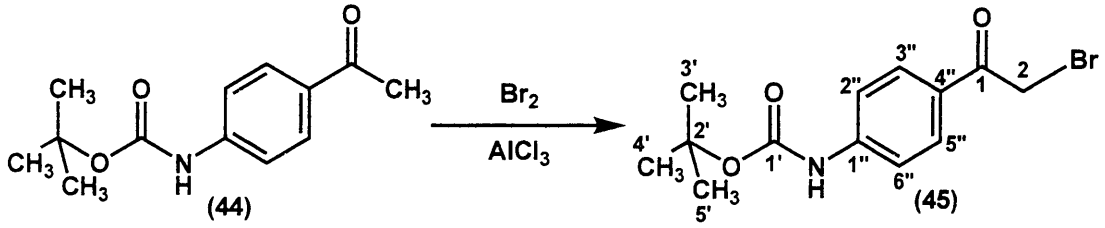

(44) (45)

To a solution of *tert*-butyl *N*-(4-acetylphenyl)carbamate (**44**) (0.943g, 3 mmol) in THF (30 mL) containing a catalytic amount of $AlCl_3$ (20 mg, 0.15 mmol) was

added Br_2 (0.2 mL, 3.9 mmol in 5 mL THF) dropwise for 30 min at 0 °C. Then, the mixture was allowed to warm to room temperature. After 60 min, the solvent was removed *in vacuo*, followed by extraction of the resulting solid with EtOAc- H_2O (1:1, 50 mL). The aqueous layer was subsequently extracted with EtOAc (2 x 50 mL), and the organic layers were combined, concentrated, dried ($MgSO_4$) and purified using flash column chromatography (petroleum ether – EtOAc 100:0 v/v increasing to 70:30 v/v) to give *tert*-butyl *N*-[4-(2-bromoacetyl)phenyl]carbamate (**45**) as a white solid. Yield: 0.12 g (17%) t.l.c. system: petroleum ether – EtOAc 3:1 v/v, R_F: 0.54, vanillin stain positive.

Melting point: 164-167 °C (166-167 °C) [232].

^{1}H-NMR (DMSO-d_6), δ: 1.55 (s, 9H, C(CH_3)$_3$), 3.34 (s, 2H, CH_2), 7.65 (d, 2H, J = 9.0 Hz, H-aromatic), 7.99 (d, 2H, J = 9.0 Hz, H-aromatic), 9.87 (s, 1H, NH).

^{13}C NMR (DMSO-d_6), δ: 27.99 (CH_3, C-3', C-4', C-5'), 33.57 (CH_2, C-2), 79.88 (C, C-2'), 117.25, 130.15 (CH, aromatic), 127.58 (C, C-4''), 144.76 (C, C-1''), 152.42 (C, C-1'), 190.16 (C, C-1).

4.1.27. 4-(1,3-Benzoxazol-2-ylamino)-1-benzoylhydrazide (46).

(Mol. Formula: $C_{14}H_{12}N_4O_2$, M. W.: 268.28)

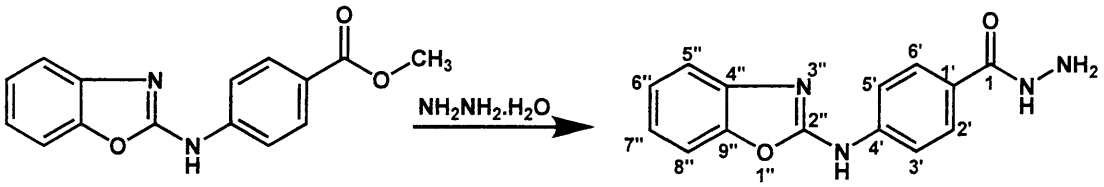

(37) (46)

Hydrazine hydrate (0.4 mL, 12.5 mol) was added to a stirred solution of methyl 4-[(2-benzoxazolyl)amino]benzoate (**37**) (1.34 g, 5 mmol) in EtOH (25 mL). The reaction mixture was refluxed for 3 h, diluted with H_2O and cooled in an ice bath. Diluted AcOH (30 mL, 10%) was added to the reaction mixture, where a yellow precipitate was formed, filtered, washed with cold EtOH then recrystallised from aqueous EtOH to give 4-(1,3-benzoxazol-2-ylamino)-1-benzenecarbohydrazide (**46**) as yellow crystals. Yield: 2.4 g (45%), t.l.c. system: petroleum ether – EtOAc 3:1 v/v, R_F: 0.2, vanillin stain positive.

Melting point: 213-216 °C.

HRMS (EI): Calculated mass: 269.1033 $[M+H]^+$, Measured mass: 269.1035 $[M+H]^+$.

^{1}H-NMR (DMSO-d_6), δ: 4.43 (s, 2H, NH_2), 7.16 (m, 1H, H-aromatic), 7.24 (t, 1H, J = 8.5 Hz, H-aromatic), 7.04 (t, 2H, J = 8.8 Hz, H-aromatic), 7.80 (d, 2H, J = 8.9 Hz, H-aromatic), 7.87 (d, 2H, J = 8.9 Hz, H-aromatic), 9.68 (s, 1H, Ar-NH-Ar), 10.91 (s, 1H, CO-NH-NH_2).

^{13}C NMR (DMSO-d_6), δ: 109.09, 116.70, 116.84, 122, 124.11 (CH, aromatic), 126.65 (C, C-1'), 128.03 (CH, C-2', C-6'), 141.14 (C, C-4'), 142.12 (C, C-4"), 146.94 (C, C-9"), 157.51 (C, C-2"), 165.54 (C, C-1).

4.1.28. 5-(4-Nitrophenyl)-1,3,4-oxadiazoline-2-thione (48) [233].

(Mol. Formula: $C_8H_5N_3O_3S$, M. W.: 223.21)

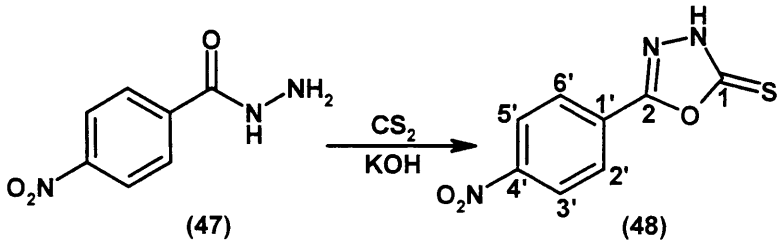

(47) (48)

To a solution of KOH (0.31 g, 5.5 mmol) in EtOH (20 mL), was added 4-nitrobenzoylhydrazide (**47**) (1 g, 5.5 mmol) with stirring. Then an excess of CS_2 (1.13 mL, 18.7 mmol) was added and the mixture refluxed until the evolution of H_2S ceases (about 20 h). The solvent was removed *in vacuo* and the residue dissolved in H_2O (20 mL), cooled in ice and acidified with 1N aqueous HCl to give 5-(4-nitrophenyl)-1,3,4-oxadiazoline-2-thione (**48**) as a yellow solid which was filtered off, dried and recrystallised from aqueous EtOH. Yield: 0.925 g (75%), t.l.c. system: petroleum ether – EtOAc 3:1 v/v, R_F: 0.1, vanillin stain negative.

Melting point: 202-205 °C (lit. m.p. 202-204 °C) [232].

^{1}H-NMR (DMSO-d_6), δ: 3.36 (s, 1H, NH), 8.11 (d, 2H, J = 9.0 Hz, H-3', H-5'), 8.40 (d, 2H, J = 9.0 Hz, H-2', H-6').

^{13}C NMR (DMSO-d_6), δ: 124.51 (CH, C-2', C-6'), 127.59 (CH, C-3', C-5'), 128.01 (C, C-1'), 149.11 (C, C-4'), 158.88 (C, C-2), 177.76 (C, C-1').

4.1.29. 2-(4-Nitrophenyl)-5-(phenethylsulfanyl)-1,3,4-oxadiazole (50).

(Mol. Formula: $C_{16}H_{13}N_3O_3S$, M. W.: 327.36)

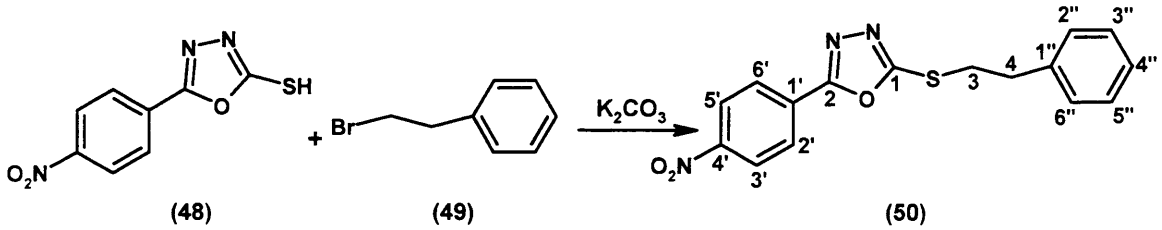

A mixture of 5-(4-nitrophenyl)-1,3,4-oxadiazoline-2-thione (**48**) (0.31 g, 1.39 mmol), 1-(2-bromoethyl)benzene (0.2 mL, 1.39 mmol) and K_2CO_3 (0.29 g, 2.09 mmol) in DMF (20 ml) was stirred for 24 h at room temperature. The reaction mixture was poured into H_2O (20 mL) and the precipitate formed filtered, washed with EtOH and recrystallised from aqueous EtOH to give 2-(4-nitrophenyl)-5-(phenethylsulfanyl)-1,3,4-oxadiazole (**50**) as yellow crystals. Yield: 0.31 g (69%), t.l.c. system: petroleum ether – EtOAc 3:1 v/v, R_F: 0.87, vanillin stain negative.

Melting point: 95-98 °C.

HRMS (EI): Calculated mass: 328.0751 $[M+H]^+$, Measured mass: 328.0749 $[M+H]^+$.

^{1}H-NMR (DMSO-d_6), δ: 3.11 (t, 2H, J = 7.0 Hz, S-CH_2-CH_2-Ar), 3.61 (t, 2H, J = 7.5 Hz, S-CH_2-CH_2-Ar), 7.3 (m, 5H, H-aromatic), 8.21 (d, 2H, J = 9.0 Hz, H-aromatic), 8.41 (d, 2H, J = 9.0 Hz, H-aromatic).

^{13}C NMR (DMSO-d_6), δ: 33.34 (CH_2, C-3), 34.93 (CH_2, C-3), 124.55, 126.53, 127.69, 128.35, 128.66 (CH, aromatic), 128.30 (C, C-1'), 139.08 (C, C-1''), 149.06 (C, C-4'), 163.71 (C, C-2), 165.10 (C, C-1).

4.1.30. 4-[5-(Phenethylsulfanyl)-1,3,4-oxadiazol-2-yl]aniline (51).

(Mol. Formula: $C_{16}H_{15}N_3OS$, M. W.: 297.37)

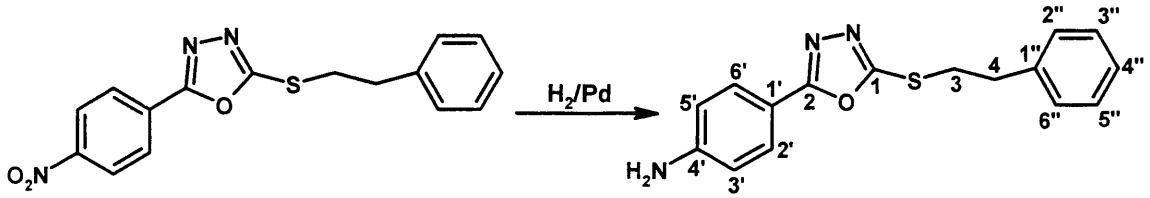

To a refluxed mixture of Fe (0.57 g, 10.23 mmol) and NH_4Cl (0.128 g, 2.39 mmol) in 10:1 of EtOH:H_2O (30 mL), 2-(4-nitrophenyl)-5-(phenethylsulfanyl)-1,3,4-oxadiazole (**50**) (1.11 g, 3.41 mmol) was added. The reaction mixture was stirred under reflux for 3 h and then allowed to cool to room temperature. The solution was filtered through celite and the solvent removed under reduced pressure. The residue then dissolved in CH_2CL_2 (50 mL), washed with saturated aq. $NaHCO_3$ (2 x 50 mL). The organic layer then dried ($MgSO_4$) and concentrated in *vacuo*. The product was isolated by flash column chromatography (petroleum ether – EtOAc 100:0 v/v increasing to 80:20 v/v) to give pure 4-[5-(phenethylsulfanyl)-1,3,4-oxadiazol-2-yl]aniline (**51**) as a yellow solid. Yield: 0.8 g (89%), t.l.c. system: CH_2Cl_2 – MeOH 9:1 v/v, R_F: 0.7, ninhydrin stain positive.

Melting point: 97-98 °C.

HRMS (EI): Calculated mass: 298.1009 $[M+H]^+$, Measured mass: 298.1007 $[M+H]^+$.

^{1}H-NMR ($CDCl_3$), δ: 3.02 (t, 2H, J = 7.0 Hz, S-CH_2-CH_2-Ar), 3.39 (t, J = 7.5 Hz, 2H, S-CH_2-CH_2-Ar), 4.10 (s, 2H, NH_2), 6.59 (d, J = 8.0 Hz, 2H, H-aromatic), 7.13 (m, 3H, H-aromatic), 7.2 (m, 2H, H-aromatic), 7.67 (d, 2H, J = 8.0 Hz, H-aromatic).

^{13}C NMR ($CDCl_3$), δ: 33.88 (CH_2, C-3), 35.73 (CH_2, C-3), 113.08 (C, C-1'), 114.65, 126.82, 128.38, 128.66, 128.72 (CH, aromatic), 139.19 (C, C-1''), 149.96 (C, C-4'), 162.71 (C, C-2), 166.30 (C, C-1).

4.1.31. *N*-(2-Naphthyl)-*N*-{4-[5-(phenethylsulfanyl)-1,3,4-oxadiazol-2-yl]phenyl}amine (52).

(Mol. Formula: $C_{26}H_{21}N_3OS$, M. W.: 423.53)

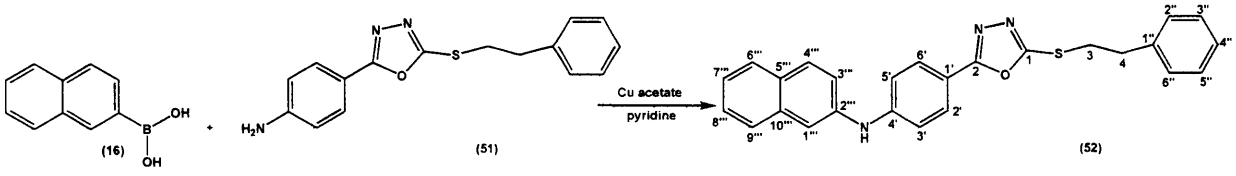

To naphthylboronic acid (**16**) (1.1 g, 6.4 mmol), 4-[5-(phenethylsulfanyl)-1,3,4-oxadiazol-2-yl]aniline (**51**) (0.63 g, 2.1 mmol), anhydrous cupric acetate (0.76 g, 4.2 mmol), pyridine (0.4 mL, 4.2 mmol) and 250 mg activated 4Å molecular sieves under an atmosphere of air was added anhydrous CH_2Cl_2 (30 mL) and the reaction stirred under air atmosphere at ambient temperature for 3 days. The product was isolated by direct flash column chromatography (petroleum ether – EtOAc 100:0 v/v increasing to 80:20 v/v) to give *N*-(2-naphthyl)-*N*-4-[5-(phenethylsulfanyl)-1,3,4-oxadiazol-2-yl]phenylamine (**52**) as a yellow solid. Yield: 0.63 g (71%), t.l.c. system: petroleum ether – EtOAc 3:1 v/v, R_F: 0.65, vanillin stain positive.

Melting point: 132-134 °C.

Microanalysis: Calculated for $C_{26}H_{21}N_3OS.\ 0.1H_2O$ (425.33), Theoretical: %C= 73.42, %H= 5.02, %N= 9.88, Found: %C= 73.20, %H= 4.72, %N= 9.51, N.b. this compound is very hygroscopic, and this microanalysis is the best one obtained after five days drying in the oven.

^{1}H-NMR ($CDCl_3$), δ: 3.19 (t, 2H, J = 7.9 Hz, -S-CH_2-CH_2-Ph), 3.55 (t, 2H, J = 7.4 Hz, -S-CH_2-CH_2-Ph), 6.27 (s, 1H, NH), 7.19 (d, 2H, J = 8.8 Hz, H-aromatic), 7.25-7.31 (m, 3H, H-aromatic), 7.33-7.37 (m, 3H, H-aromatic), 7.41 (m, 1H, H-aromatic), 7.49 (m, 1H, H-aromatic), 7.60 (d, 1H, J = 2.0 Hz, H-aromatic), 7.75 (d, 1H, J = 8.2 Hz, H-aromatic), 7.83 (t, 2H, J = 8.9 Hz, H-aromatic), 7.92 (d, 2H, J = 8.8 Hz, H-aromatic).

^{13}C NMR ($CDCl_3$), δ: 33.89 (CH_2, C-3), 35.72 (CH_2, C-4), 115.14 (C, C-2'''), 115.38, 115.98, 121.15, 124.53, 126.70, 126.82, 126.85, 127.73, 128.34, 128.65, 128.72, 129.47 (CH, aromatic), 130.13 (C, C-1'), 134.36 (C, C-5'''), 138.58 (C, C-10'''), 139.17 (C, C-1''), 146.77 (C, C-4'), 163.10 (C, C-2), 165.95 (C, C-1).

4.1.32. 2-(4-Nitrophenyl)-5-(pentylsulfanyl)-1,3,4-oxadiazole (54).

(Mol. Formula: $C_{13}H_{15}N_3O_3S$, M. W.: 293.34)

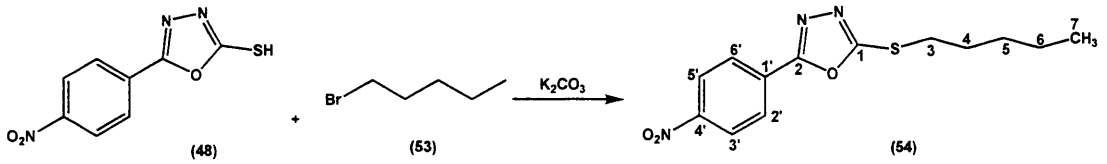

A mixture of 5-(4-nitrophenyl)-1,3,4-oxadiazoline-2-thione (**48**) (0.94 g, 4.21 mmol), 1-bromopentane (0.5 mL, 4.21 mmol) and K_2CO_3 (0.9 g, 6.31 mmol) in DMF (20 ml) was stirred for 24 h at room temperature. The reaction mixture was poured into H_2O and the precipitate formed filtered, washed with EtOH and recrystallised from aqueous EtOH to give 2-(4-nitrophenyl)-5-(pentylsulfanyl)-1,3,4-oxadiazole (**54**) as yellow crystals. Yield: 0.65 g (69%), t.l.c. system: petroleum ether – EtOAc 3:1 v/v, R_F: 0.86, vanillin stain negative.

Melting point: 80-82 °C.

Microanalysis: Calculated for $C_{13}H_{15}N_3O_3S$ (293.34), Theoretical: %C= 53.23, %H= 5.15, %N= 14.32, Found: %C= 53.30, %H= 5.33, %N= 13.93.

^{1}H-NMR ($CDCl_3$), δ: 0.83 (t, 3H, J = 7.5 Hz, $-CH_2-CH_3$), 1.31 (m, 2H, $-CH_2-CH_2-CH_3$), 1.39 (m, 2H, $-CH_2-CH_2-CH_3$), 1.81 (m, 2H, $S-CH_2-CH_2-CH_2$), 3.27 (m, 2H, $S-CH_2-CH_2-CH_2$), 8.11 (d, 2H, J = 9.0 Hz, H-2', H-6'), 8.30 (d, 2H, J = 9.0 Hz, H-3', H-5').

^{13}C NMR ($CDCl_3$), δ: 13.87 (CH_3, C-7), 22.10 (CH_2, C-6), 28.86 (CH_2, C-3), 30.70 (CH_2, C-5), 32.65 (CH_2, C-4), 124.38 (CH, C-2', C-6'), 127.46 (CH, C-3', C-5'), 129.18 (C, C-1'), 149.42 (C, C-4'), 163.87 (C, C-2), 166.40 (C, C-1).

4.1.33. 4-[5-(Pentylsulfanyl)-1,3,4-oxadiazol-2-yl]aniline (54).

(Mol. Formula: $C_{13}H_{17}N_3OS$, M. W.: 263.36)

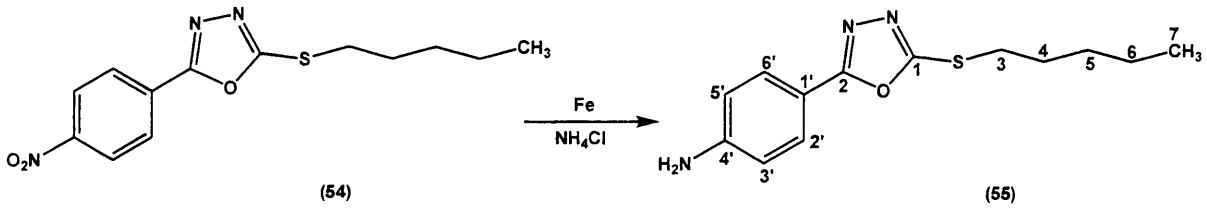

To a refluxed mixture of Fe (0.57 g, 10.23 mmol) and NH_4Cl (0.128 g, 2.39 mmol) in 10:1 of EtOH:H_2O (30 mL), 2-(4-nitrophenyl)-5-(pentylsulfanyl)-1,3,4-oxadiazole (**54**) (1.00 g, 3.41 mmol) was added. The reaction mixture was stirred under reflux for 3 h and then allowed to cool to room temperature. The solution was filtered through celite and the solvent removed under reduced pressure. The residue then dissolved in CH_2CL_2 (50 mL), washed with saturated aq. $NaHCO_3$ (2 x 50 mL). The organic layer then dried ($MgSO_4$) and concentrated in *vacuo*. The product was isolated by flash column chromatography (petroleum ether – EtOAc 100:0 v/v increasing to 80:20 v/v) to give pure 4-[5-(pentylsulfanyl)-1,3,4-oxadiazol-2-yl]aniline (**55**) as a white solid. Yield: 0.8 g (89%), t.l.c. system: CH_2Cl_2 – MeOH 9:1 v/v, R_F: 0.7, ninhydrin stain positive.

Melting point: 116-118 °C.

HRMS (EI): Calculated mass: 264.1166 $[M+H]^+$, Measured mass: 264.1169 $[M+H]^+$.

^{1}H-NMR ($CDCl_3$), δ: 0.93 (t, 3H, J = 7.5 Hz, -CH_2-CH_3), 1.34-1.42 (m, 2H, -CH_2-CH_2-CH_3), 1.43-1.49 (m, 2H, -CH_2-CH_2-CH_3), 1.81-1.87 (m, 2H, S-CH_2-CH_2-CH_2), 3.27 (t, 2H, J = 7.4 Hz, S-CH_2-CH_2-CH_2), 4.09 (s, 2H, NH_2), 6.73 (d, 2H, J = 9.0 Hz, H-3', H-5'), 7.80 (d, 2H, J = 8.6 Hz, H-2', H-6').

^{13}C NMR ($CDCl_3$), δ: 13.88 (CH_3, C-7), 22.11 (CH_2, C-6), 29.03 (CH_2, C-3), 30.71 (CH_2, C-5), 32.66 (CH_2, C-4), 113.47 (C, C-1'), 114.64 (CH, C-3', C-5'), 128.35 (CH, C-2', C-6'), 149.63 (C, C-4'), 163.09 (C, C-2), 166.09 (C, C-1).

4.1.34. *N*-(2-Naphthyl)-*N*-{4-[5-(pentylsulfanyl)-1,3,4-oxadiazol-2-yl]phenyl}amine (55).

(Mol. Formula: $C_{23}H_{23}N_3OS$, M. W.: 389.51)

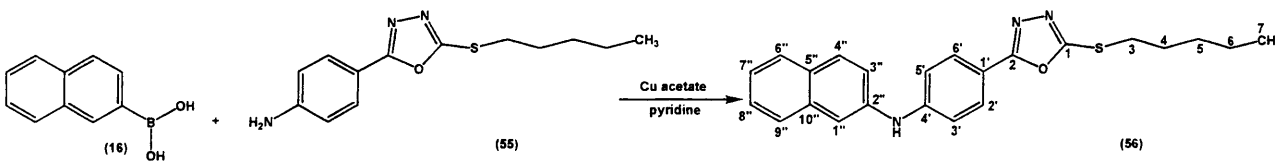

(16) (55) (56)

To naphthylboronic acid (**16**) (0.9 g, 5.2 mmol), 4-[5-(pentylsulfanyl)-1,3,4-oxadiazol-2-yl]aniline (**55**) (0.45 g, 1.74 mmol), anhydrous cupric acetate (0.63 g, 3.47 mmol), pyridine (0.3 mL, 3.47 mmol) and 250 mg activated 4Å molecular sieves under an atmosphere of air was added anhydrous CH_2Cl_2 (30 mL) and the reaction

stirred under air atmosphere at ambient temperature for 3 days. The product was isolated by direct flash column chromatography (petroleum ether – EtOAc 100:0 v/v increasing to 80:20 v/v) to give *N*-(2-naphthyl)-*N*-4-[5-(pentylsulfanyl)-1,3,4-oxadiazol-2-yl]phenylamine (**56**) as a yellow solid. Yield: 0.45 g (65%), t.l.c. system: petroleum ether – EtOAc 3:1 v/v, R_F: 0.7, vanillin stain positive.

Melting point: 138-139 °C.

HRMS (EI): Calculated mass: 390.1636 $[M+H]^+$, Measured mass: 390.1635 $[M+H]^+$.

^{1}H-NMR ($CDCl_3$), δ: 0.95 (t, 3H, J = 7.2 Hz, -CH_2-CH_3), 1.38-1.45 (m, 2H, -CH_2-CH_2-CH_3), 1.47-1.58 (m, 2H, -CH_2-CH_2-CH_3), 1.84-1.90 (m, 2H, S-CH_2-CH_2-CH_2), 3.30 (t, 2H, J = 7.5 Hz, S-CH_2-CH_2-CH_2), 6.21 (s, 1H, NH), 7.81 (d, 2H, J = 6.9 Hz, H-aromatic), 7.33 (d, 1H, J = 6.5 Hz, H-aromatic), 7.39-7.43 (m, 1H, H-aromatic), 7.47-7.50 (m, 1H, H-aromatic), 7.60 (d, 1H, J = 2.1 Hz, H-aromatic), 7.74 (d, 1H, J = 8.2 Hz, H-aromatic), 7.81-7.85 (m, 2H, H-aromatic), 7.92 (d, 2H, J = 5.1 Hz, H-aromatic).

^{13}C NMR ($CDCl_3$), δ: 13.89 (CH_3, C-7), 22.13 (CH_2, C-6), 29.03 (CH_2, C-3), 30.73 (CH_2, C-5), 32.68 (CH_2, C-4), 115.14 (C, C-2''), 115.33, 116.00, 121.11, 124.51, 126.69, 126.83, 127.72, 128.32, 129.47 (CH, aromatic), 130.12 (C, C-1'), 134.36 (C, C-5''), 138.60 (C, C-10''), 146.67 (C, C-4'), 163.09 (C, C-2), 166.09 (C, C-1).

4.1.35. Ethyl 2-{[5-(4-nitrophenyl)-1,3,4-oxadiazol-2-yl]sulfanyl}acetate (58).

(Mol. Formula: $C_{12}H_{11}N_3O_5S$, M. W.: 309.30)

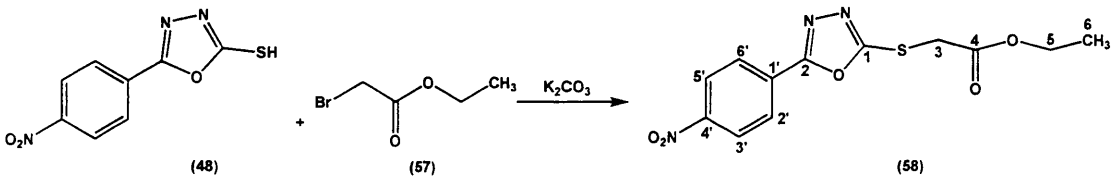

A mixture of 5-(4-nitrophenyl)-1,3,4-oxadiazoline-2-thione (**48**) (1.5 g, 6.7 mmol), ethyl 2-bromoacetate (**57**) (0.7 mL, 6.7 mmol) and K_2CO_3 (1.39 g, 10.05 mmol) in DMF (25 mL) was stirred for 24 h at room temperature. The reaction mixture is poured into H_2O and the precipitate formed filtered, washed with EtOH and

recrystallised from EtOH to give ethyl 2-{[5-(4-nitrophenyl)-1,3,4-oxadiazol-2-yl]sulfanyl}acetate (**58**) as yellow crystals. Yield: 1.3 g (62%), t.l.c. system: petroleum ether – EtOAc 3:1 v/v, R_F: 0.41, vanillin stain positive.

Melting point: 109-110 °C.

Microanalysis: Calculated for $C_{12}H_{11}N_3O_5S$ (309.30), Theoretical: %C= 46.60, %H= 3.58, %N= 13.58, Found: %C= 46.73, %H= 3.32, %N= 13.59.

^{1}H-NMR ($CDCl_3$), δ: 1.33 (t, 3H, J = 7.2 Hz, -CH_2-CH_3), 4.16 (s, 2H, S-CH_2-CO), 4.29 (q, 2H, J = 7.2 Hz, 21.4 Hz, -CH_2-CH_3), 8.21 (d, 2H, J = 9.0 Hz, H-2', H-6'), 8.38 (d, 2H, J = 9.0 Hz, H-3', H-5').

^{13}C NMR ($CDCl_3$), δ: 14.09 (CH_3, C-6), 34.42 (CH_2, C-3), 62.55 (CH_2, C-5), 124.42 (CH, C-2', C-6'), 127.59 (CH, C-3', C-5'), 128.91 (C, C-1'), 149.57 (C, C-4'), 164.32 (C, C-2), 164.67 (C, C-1), 167.15 (C, C-4).

4.1.36. Ethyl 2-{[5-(4-aminophenyl)-1,3,4-oxadiazol-2-yl]sulfanyl}acetate (59).

(Mol. Formula: $C_{12}H_{13}N_3O_3S$, M. W.: 279.07)

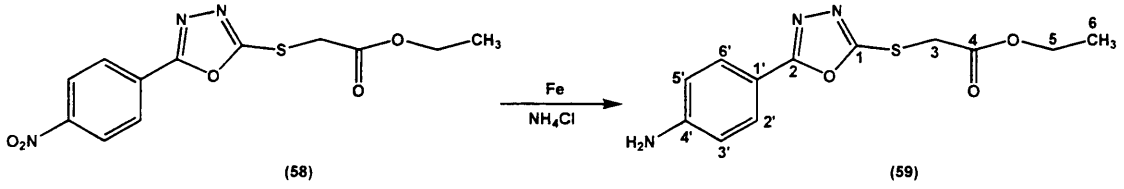

(58) (59)

To a refluxed mixture of Fe (0.54 g, 9.69 mmol) and NH_4Cl (0.121 g, 2.26 mmol) in 10:1 of EtOH:H_2O (30 mL), ethyl 2-{[5-(4-nitrophenyl)-1,3,4-oxadiazol-2-yl]sulfanyl}acetate (**58**) (1.00 g, 3.23 mmol) was added. The reaction mixture was stirred under reflux for 3 h and then allowed to cool to room temperature. The solution was filtered through celite and the solvent removed under reduced pressure. The residue then dissolved in CH_2CL_2 (50 mL), washed with saturated aq. $NaHCO_3$ (2 x 50 mL). The organic layer then dried ($MgSO_4$) and concentrated in *vacuo*. The product was isolated by flash column chromatography (petroleum ether – EtOAc 100:0 v/v increasing to 80:20 v/v) to give pure ethyl 2-{[5-(4-aminophenyl)-1,3,4-oxadiazol-2-yl]sulfanyl}acetate (**59**) as white solid. Yield: 0.7 g (78%), t.l.c. system: CH_2Cl_2 – MeOH 9:1 v/v, R_F: 0.35, ninhydrin stain positive.

Melting point: 146-148 °C.

Microanalysis: Calculated for $C_{12}H_{13}N_3O_3S$ (279.07), Theoretical: %C= 51.60, %H= 4.69, %N= 15.04, Found: %C= 51.32, %H= 4.81, %N= 14.80.

^{1}H-NMR (DMSO-d_6), δ: 1.19 (t, 3H, J = 7.1 Hz, -CH_2-CH_3), 4.15 (q, 2H, J = 7.1 Hz, 21.3 Hz, -CH_2-CH_3), 4.22 (s, 2H, S-CH_2-CO), 5.94 (s, 2H, NH_2), 6.67 (d, 2H, J = 8.6 Hz, H-3', H-5'), 7.61 (d, 2H, J = 8.6 Hz, H-2', H-6').

^{13}C NMR (DMSO-d_6), δ: 13.91 (CH_3, C-6), 33.83 (CH_2, C-3), 61.48 (CH_2, C-5), 109.19 (C, C-1'), 113.52 (CH, C-3', C-5'), 127.88 (CH, C-2', C-6'), 152.40 (C, C-4'), 160.53 (C, C-2), 166.04 (C, C-1), 167.79 (C, C-4).

4.1.37. Ethyl 2-({5-[4-(2-naphthylamino)phenyl]-1,3,4-oxadiazol-2-yl}sulfanyl)acetate (60).

(Mol. Formula: $C_{22}H_{19}N_3O_3S$, M. W.: 405.47)

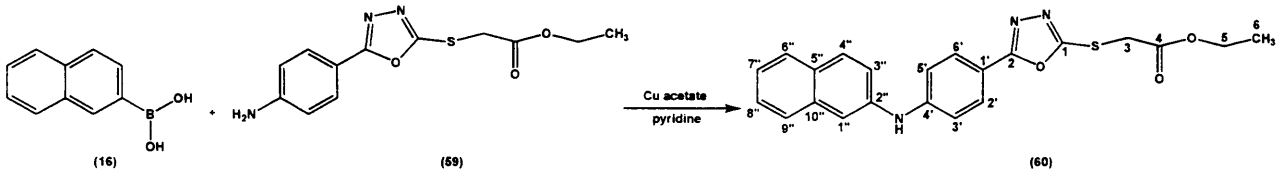

(16) (59) (60)

To naphthylboronic acid (**16**) (0.92 g, 5.37 mmol), ethyl 2-{[5-(4-aminophenyl)-1,3,4-oxadiazol-2-yl]sulfanyl}acetate (**59**) (0.5 g, 1.79 mmol), anhydrous cupric acetate (0.65 g, 3.58 mmol), pyridine (0.3 mL, 3.58 mmol) and 250 mg activated 4Å molecular sieves under an atmosphere of air was added anhydrous CH_2Cl_2 (30 mL) and the reaction stirred under air atmosphere at ambient temperature for 3 days. The product was isolated by direct flash column chromatography (petroleum ether – EtOAc 100:0 v/v increasing to 80:20 v/v) to give ethyl 2-({5-[4-(2-naphthylamino)phenyl]-1,3,4-oxadiazol-2-yl}sulfanyl)acetate (**60**) as a yellow solid. Yield: 0.45 g (65%), t.l.c. system: petroleum ether – EtOAc 3:1 v/v, R_F: 0.7, vanillin stain positive.

Melting point: 150-152 °C.

Microanalysis: Calculated for $C_{22}H_{19}N_3O_3S$ (405.47), Theoretical: %C= 65.17, %H= 4.72, %N= 10.36, Found: %C= 65.00, %H= 4.74, %N= 10.58.

^{1}H-NMR ($CDCl_3$), δ: 1.33 (t, 3H, J = 7.1 Hz, -CH_2-CH_3), 4.11 (s, 2H, S-CH_2-CO), 4.28 (q, 2H, J = 7.2 Hz, 21.4 Hz, -CH_2-CH_3), 6.25 (s, 1H, NH), 7.18 (d, 2H, J =

8.8 Hz, H-aromatic), 7.32-7.34 (m, 1H, H-aromatic), 7.40-7.43 (m, 1H, H-aromatic), 7.47-7.51 (m, 1H, H-aromatic), 7.60 (d, 1H, J = 1.8 Hz, H-aromatic), 7.75 (d, 1H, J = 8.2 Hz, H-aromatic), 7.81-7.85 (m, 2H, H-aromatic), 7.91 (d, 2H, J = 8.7 Hz, H-aromatic).

^{13}C NMR ($CDCl_3$), δ: 14.09 (CH_3, C-6), 34.48 (CH_2, C-3), 62.37 (CH_2, C-5), 114.89 (C, C-2''), 115.49, 115.91, 121.17, 124.56, 126.70, 126.86, 127.73, 128.41, 129.48 (CH, aromatic), 130.15 (C, C-1'), 134.34 (C, C-5''), 138.49 (C, C-10''), 146.90 (C, C-4'), 161.72 (C, C-2), 166.29 (C, C-1), 167.58 (C, C-4).

4.2. Synthesis of CYP24A1 inhibitors

4.2.1. 3-(Acetyloxy)-5-methylphenylacetate (62) [215].

(Mol. Formula: $C_{11}H_{12}O_4$, M. W.: 208.21)

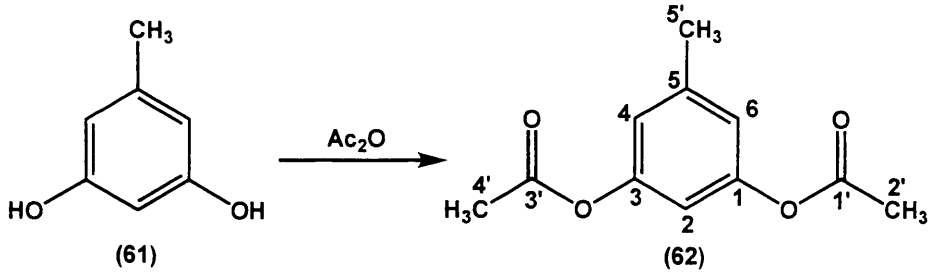

A solution of orcinol (5-methylresorcinol) (**61**) (2 g, 17.07 mmol) in pyridine (20 mL) and Ac_2O (8 mL, 84.6 mmol) was stirred at room temperature for 17 h then evaporated *in vacuo*. The residue was dissolved in CH_2Cl_2 (50 mL) and the solution was washed with saturated aqueous $NaHCO_3$ (50mL), H_2O (50 mL), dried ($MgSO_4$) and evaporated under reduced pressure giving 3-(acetyloxy)-5-methylphenyl acetate (**62**) as a colourless oil. Yield: 2.9 g (99%), t.l.c. system: petroleum ether – EtOAc 3:1 v/v, R_F: 0.54, vanillin stain positive.

^{1}H-NMR ($CDCl_3$), δ: 2.29 (s, 6H, 2 CO-CH_3), 2.37 (s, 3H, Ar-CH_3), 6.74 (t, 1H, J = 2.1 Hz, H-2), 6.81-6.82 (m, 2H, H-4, H-6).

^{13}C NMR ($CDCl_3$), δ: 21.33 (CH_3, C-2', C-4'), 22.13 (CH_3, C-5'), 112.45 (CH, C-2), 119.69 (CH, C-4, C-6), 140.34 (C, C-5), 150.90 (C, C-1, C-3), 169.09 (C, C-1', C-3').

4.2.2. 3-(Acetyloxy)-5-(bromomethyl)phenyl acetate (63) [215].

(Mol. Formula: $C_{11}H_{11}BrO_4$, M. W.: 287.11)

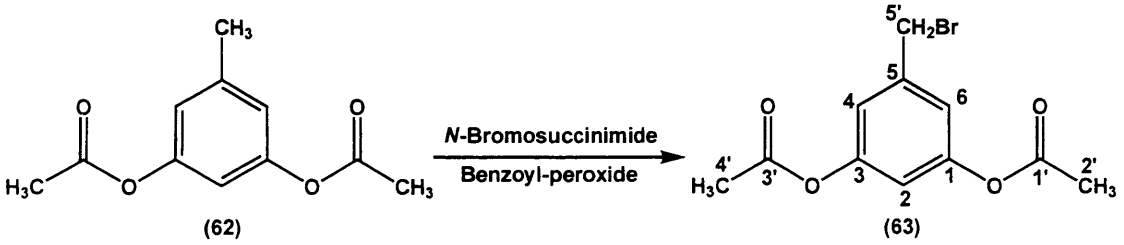

3,5-Diacetoxytoluene (**62**) (2.9 g, 14.07 mmol) was dissolved in dry CCl_4 (50 mL). After addition of freshly recrystallised *N*-bromosuccinimide (2.56 g, 14.38 mmol) and a catalytic amount of benzoyl peroxide (0.2 g, 0.83 mmol), the mixture was refluxed for 3 h. After the mixture had cooled, the succinimide was removed by

filtration, and the solvent was removed under reduced pressure to give 3-(acetyloxy)-5-(bromomethyl)phenyl acetate (**63**) as a colourless oil. Yield: 4 g (99%), t.l.c. system: petroleum ether – EtOAc 3:1 v/v, R_F: 0.43, vanillin stain positive.

^{1}H-NMR ($CDCl_3$), δ: 2.31 (s, 6H, 2 CO-CH_3), 4.45 (s, 2H, Ar-CH_2-Br), 6.91 (t, 1H, J = 2.2 Hz, H-2), 7.05-7.06 (m, 2H, H-4, H-6).

^{13}C NMR ($CDCl_3$), δ: 21.06 (CH_3, C-2', C-4'), 31.78 (CH_2, C-5'), 115.43 (CH, C-2), 119.55 (CH, C-4, C-6), 139.82 (C, C-5), 151.1 (C, C-1, C-3), 169.10 (C, C-1', C-3').

4.2.3. 3,5-Diacetoxybenzyl-(tripheny1)phosphonium bromide (65) [215].

(Mol. Formula: $C_{29}H_{26}BrO_4P$, M. W.: 549.39)

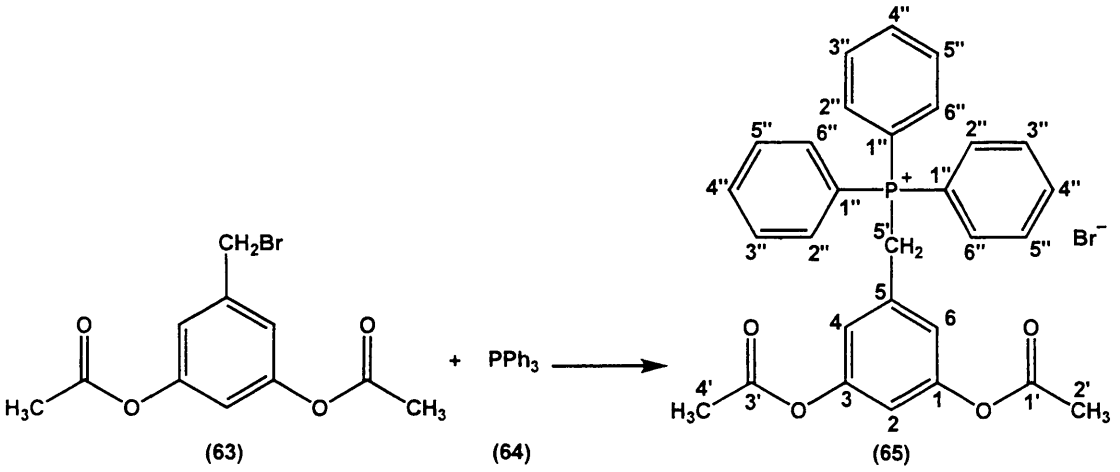

3,5-Diacetoxybenzyl bromide (**63**) (4 g, 14 mmol) and triphenylphosphine (**64**) (3.67 g, 14 mmol) were dissolved in dry benzene (25 mL). The mixture was then refluxed for 6 h, to form a precipitate which upon washing with benzene gave 3,5-diacetoxybenzyl-(tripheny1)phosphonium bromide (**65**) as a white solid. Yield: 4.38 g (57%), t.l.c. system: petroleum ether – EtOAc 3:1 v/v, R_F: 0.00, vanillin stain negative.

Melting point: 246-249 °C (lit. m.p. 247 °C) [215].

^{1}H-NMR (DMSO-d_6), δ: 2.21 (s, 6H, 2 CO-CH_3), 3.78 (d, 2H, J = 15.8 Hz), 6.68 (t, 2H, J = 2.3 Hz, H-aromatic), 7.00 (t, 1H, J = 2.1 Hz, H-aromatic), 7.66-7.71 (m, 6H, H-aromatic), 7.34-7.77 (m, 6H, H-aromatic), 7.91-7.94 (m, 3H, H-aromatic).

^{13}C NMR (DMSO-d_6), δ: 20.65 (CH_3, C-2', C-4'), 28.01 (CH_2, C-5'), 116.14, 121.75, 130.22, 134.06, 135.16 (CH, aromatic), 117.35 (C, C-1"), 130.32 (C, C-5),

150.75 (C, C-1, C-3), 168.58 (C, C-1', C-3').

4.2.4. 1,3-Dimethoxy-5-vinylbenzene (68) [217].

(Mol. Formula: $C_{10}H_{12}O_2$, M. W.: 164.2)

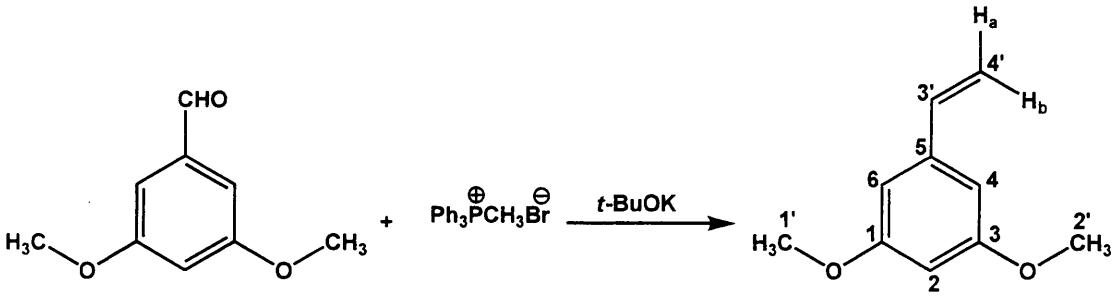

(66) (67) (68)

A solution of 3,5-dimethoxybenzaldehyde (**66**) (2.93 g, 17.5 mmol), methyl-triphenylphosphonium bromide (**67**) (6.95 g, 19.5 mmol) and *t*-BuOK (2.19 g, 19.5 mmol) in dry THF (50 mL) was stirred for 2 h at room temperature under nitrogen. Then, the reaction was quenched by adding 10 mL of a saturated aqueous solution of NH_4Cl. The solvents were removed under vacuum. The crude product was extracted with CH_2Cl_2 (50 mL) and the organic layer was washed with H_2O (50 mL), dried over $MgSO_4$ and the solvent removed under reduced pressure. The product then was isolated by flash column chromatography (petroleum ether – EtOAc 100:0 v/v increasing to 70:30 v/v) to give 1,3-dimethoxy-5-vinylbenzene (**68**) as a colourless oil. Yield: 2 g (70%), t.l.c. system: petroleum ether – EtOAc 3:1 v/v, R_F: 0.67, vanillin stain positive.

^{1}H-NMR ($CDCl_3$), δ: 3.83 (s, 6H, CH_3), 5.28 (d, 1H, J = 10.9 Hz, H_a), 5.76 (d, 1H, J = 17.2 Hz, H_b), 6.42 (t, 1H, J = 2.3 Hz, H-2), 6.60 (d, 2H, J = 2.3 Hz, H-4, H-6), 6.66 (dd, 1H, J = 10.8 Hz, 17.5 Hz, H-3').

^{13}C NMR ($CDCl_3$), δ: 55.32 (CH_3, C-1', C-2'), 100.11 (CH, C-2), 104.35 (CH, C-4, C-6), 114.31 (CH_2, C-4'), 136.88 (CH, C-3'), 139.64 (C, C-5), 160.94 (C, C-1,C-3).

4.2.5. Methyl 4-[(*E*)-2-(3,5-dimethoxyphenyl)-1-ethenyl]benzoate (70) [234].

(Mol. Formula: $C_{18}H_{18}O_4$, M. W.: 298.33)

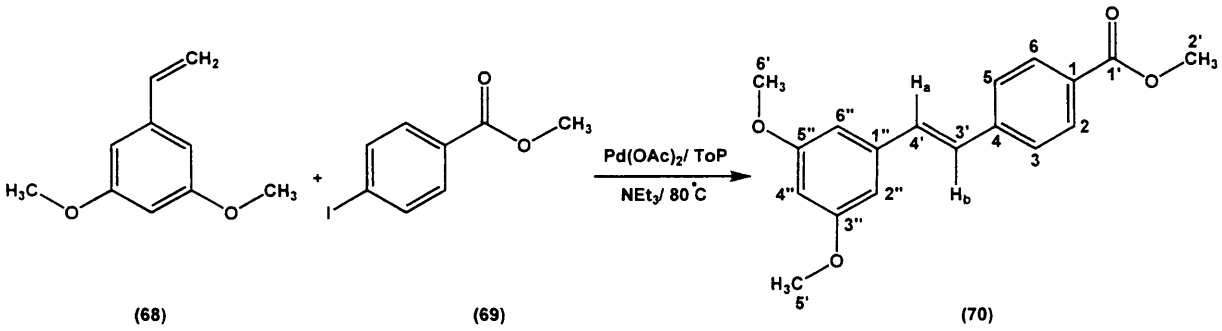

(68) (69) (70)

A solution of 1,3-dimethoxy-5-vinylbenzene (**68**) (2 g, 12.18 mmol), $Pd(OAc)_2$ (0.108 g, 0.48 mmol), tri(o-tolyl)phosphine (ToP, 0.22 g, 0.72 mmol) and 4-iodo-methylbenzyl ester (**69**) (2.88 g, 11 mmol) in dry Et_3N (25 mL) was stirred for 2 h at 60 °C under nitrogen. Then the mixture was stirred for 1 day at 80 °C. After the reaction was complete, the solvent was evaporated. The crude product was dissolved in CH_2Cl_2 (50 mL) and washed with H_2O (50 mL), dried over $MgSO_4$ and the solvent evaporated. The crude product was purified by flash column chromatography (petroleum ether – EtOAc 100:0 v/v increasing to 70:30 v/v) to give methyl 4-[(*E*)-2-(3,5-dimethoxyphenyl)-1-ethenyl] benzoate (**70**) as a colourless oil. Yield: 3.12 g (86%), t.l.c. system: petroleum ether – EtOAc 3:1 v/v, R_F: 0.65, vanillin stain positive.

^{1}H-NMR ($CDCl_3$), δ: 3.86 (s, 6H, 2 O-CH_3), 3.95 (s, 3H, COOCH_3), 6.46 (t, 1H, J = 2.0 Hz, H-aromatic), 6.71 (d, 2H, J = 2.1 Hz, H-aromatic), 7.14 (d, 2H, J = 9.7 Hz, H_a, H_b), 7.57 (d, 2H, J = 8.3 Hz, H-aromatic), 8.05 (d, 2H, J = 8.3 Hz, H-aromatic).

^{13}C NMR ($CDCl_3$), δ: 52.05 (CH_3, C-2'), 55.39 (CH_3, C-5', C-6'), 100.59 (CH, C-4"), 104.89, 126.38, 128.08, 130.02, 131.24 (CH, aromatic and alkene), 129.04 (C, C-1), 138.77 (C, C-1"), 141.65 (C, C-4), 161.07 (C, C-3", C-5"), 166.84 (C, C-1').

4.2.6. 4-[(*E*)-2-(3,5-Dimethoxyphenyl)-1-ethenyl]benzoic acid (71) [234].

(Mol. Formula: $C_{14}H_{16}O_4$, M. W.: 284.31)

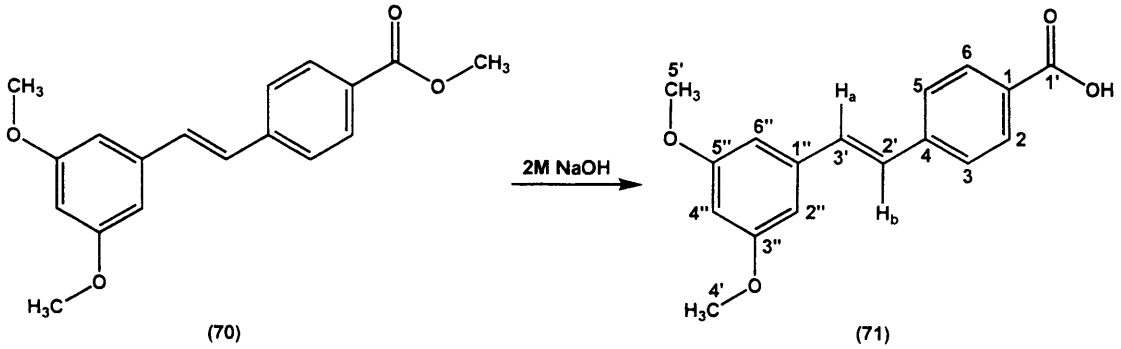

(70) (71)

A solution of methyl 4-[(*E*)-2-(3,5-dimethoxyphenyl)-1-ethenyl] benzoate (**70**) (1 g, 3.35 mmol) in EtOH (30 mL) was treated with 2M aqueous NaOH (7 mL) and stirred at room temperature. Progress of the reaction was monitored by observing the disappearance of methyl 4-[(*E*)-2-(3,5-dimethoxyphenyl)-1-ethenyl] benzoate (**71**) by t.l.c. After hydrolysis was complete (1 h), the reaction solution was acidified to pH 1 by the dropwise addition of concentrated HCl (3 mL). The solution was then extracted with Et_2O (3 x 50 mL) and the organic layer dried ($MgSO_4$) and concentrated under reduced pressure to give a crude brown solid. The crude product was washed with H_2O, dried and recrystallised from EtOH to give pure 4-[(*E*)-2-(3,5-dimethoxyphenyl)-1-ethenyl]benzoic acid (**69**) as transparent crystals. Yield: 0.95 g (100%), t.l.c. system: petroleum ether – EtOAc 2:3 v/v, R_F: 0.14, vanillin stain negative.

Melting point: 186-189°C (lit. m.p. 189 °C) [234].

^{1}H-NMR (DMSO-d_6), δ: 3.79 (s, 6H, 2 O-CH_3), 6.46 (t, 1H, J = 2.2 Hz, H-aromatic), 6.83 (d, 2H, J = 2.3 Hz, H-aromatic), 7.34 (d, 2H, J = 3.7 Hz, H_a, H_b), 7.71 (d, 2H, J = 8.5 Hz, H-aromatic), 7.94 (d, 2H, J = 8.5 Hz, H-aromatic), 11.91-13.42 (bs, 1H, COO**H**).

^{13}C NMR (DMSO-d_6), δ: 55.23 (CH_3, C-4', C-5'), 100.40, 104.81, 126.46, 128.08, 129.73, 130.97 (CH, aromatic and alkene), 129.52 (C, C-1), 138.63 (C, C-4), 141.95 (C, C-1''), 160.67 (C, C-3'', C-5''), 167.03 (C, C-1').

4.2.7. 4-[(*E*)-2-Phenyl-1-ethenyl]benzoic acid (74) [235].

(Mol. Formula: $C_{15}H_{12}O_2$, M. W.: 224.26)

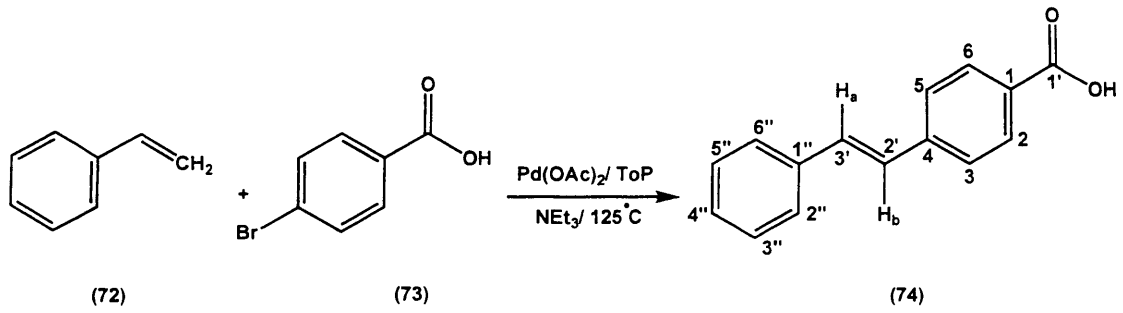

(72) (73) (74)

A mixture of 4-bromobenzoic acid (**73**) (2 g, 10 mmol), styrene (**72**) (1.4 mL, 12.5 mmol), triethylamine (3.5 mL, 25 mmol), $Pd(OAc)_2$ (0.022 g, 0.1 mmol), and tri(o-tolyl)phosphine (ToP, 0.122 g, 0.4 mmol) were heated in capped heavy-walled glass tubes under nitrogen at 100 °C for 3.5 h. After completion of the reaction as judged by the disappearance of one of the reactants by TLC, cold dilute hydrochloric acid (1 M, 10 mL) was added to the mixture. The crude solid was filtered and recrystallised from ethanol to give 4-[(*E*)-2-phenyl-1-ethenyl]benzoic acid (**74**) as white crystals. Yield: 1.9 g (85%), t.l.c. system: petroleum ether – EtOAc 1:1 v/v, R_F: 0.1, vanillin stain negative.

Melting point: 251-253 °C (lit. m.p. 254-255 °C) [235].

^{1}H-NMR (DMSO-d_6), δ: 7.28-7.34 (m, 3H, H_a, H_b, H-aromatic), 7.36-7.42 (m, 4H, H-aromatic), 7.72 (d, 2H, J = 8.4 Hz, H-aromatic), 7.95 (d, 2H, J = 6.8 Hz, H-aromatic), 11.91-13.42 (bs, 1H, COOH).

^{13}C NMR (DMSO-d_6), δ: 126.30, 126.44, 126.55, 127.35, 129.43, 130.25 (CH, aromatic and alkene), 128.47 (C, C-3'), 128.98 (C, C-1"), 136.56 (C, C-4), 141.37 (C, C-1), 167.07 (C, C-1').

4.2.8. *N*-(2-Hydroxy-2-phenylethyl)-4-[(*E*)-2-(3,5-dimethoxyphenyl)-1-ethenyl]benzamide (75).

(Mol. Formula: $C_{25}H_{25}NO_4$, M. W.: 403.47)

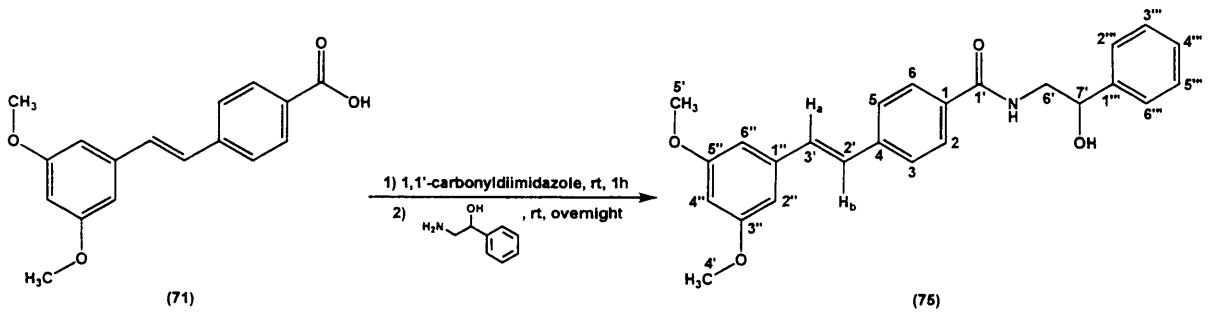

To a suspension of 4-[(*E*)-2-(3,5-dimethoxyphenyl)-1-ethenyl]benzoic acid (**71**) (0.6 g, 2.11 mmol) in anhydrous DMF (20 mL) was added 1,1'-carbonyldiimidazole (0.34 g, 2.11 mmol) and the reaction stirred at room temperature for 1 h. The reaction was then cooled to 0 °C and subsequently combined with a solution of 2-amino-1-phenylethanol (0.29 g, 2.11 mmol), in DMF (5 mL). The mixture was stirred at room temperature overnight. After the reaction was complete, ice was added into the flask to precipitate out the product which was then filtered and washed with ice-cold H_2O, dried under vacuum to give pure *N*-(2-hydroxy-2-phenylethyl)-4-[(*E*)-2-(3,5-dimethoxyphenyl)-1-ethenyl]benzamide (**75**) as a white solid. Yield: 0.8 g (94%), t.l.c. system: petroleum ether – EtOAc 3:1 v/v, R_F: 0.39, vanillin stain positive.

Melting point: 222-224 °C.

Microanalysis: Calculated for $C_{25}H_{25}NO_4$ (403.47), Theoretical: %C= 74.42, %H= 6.25, %N= 3.47, Found: %C= 74.15, %H= 6.21, %N= 3.53.

^{1}H-NMR (DMSO-d_6), δ: 3.34-3.53 (m, 2H, CH_2), 3.80 (s, 6H, 2 O-CH_3), 4.80-4.82 (m, 1H, CH-OH), 5.38 (d, 1H, J = 4.1 Hz, OH), 6.45 (s, 1H, H-aromatic), 6.82 (s, 2H, H-aromatic), 7.25-7.27 (m, 1H, H-aromatic), 7.32-7.40 (m, 6H, H_a, H_b, H-aromatic), 7.68 (d, 2H, J = 8.1 Hz, H-aromatic), 7.87 (d, 2H, J = 8.1 Hz, H-aromatic), 8.51 (t, 1H, J = 5.2 Hz, NH).

^{13}C NMR (DMSO-d_6), δ: 47.69 (CH_2, C-6'), 55.21 (CH_3, C-4', C-5'), 71.20 (CH, C-7'), 100.24, 104.81, 126.96, 126.20, 126.99, 127.67, 128.00, 128.05, 130.97 (CH, aromatic and alkene), 133.31 (C, C-1), 138.79 (C, C-1"), 139.62 (C, C-4), 143.77 (C, C-1'"), 160.67 (C, C-3", C-5"), 166.00 (C, C-1').

4.2.9. *N*-(2-Hydroxy-2-phenylethyl)-4-[(*E*)-2-phenyl-1-ethenyl]benzamide (76).

(Mol. Formula: $C_{23}H_{21}NO_2$, M. W.: 343.42)

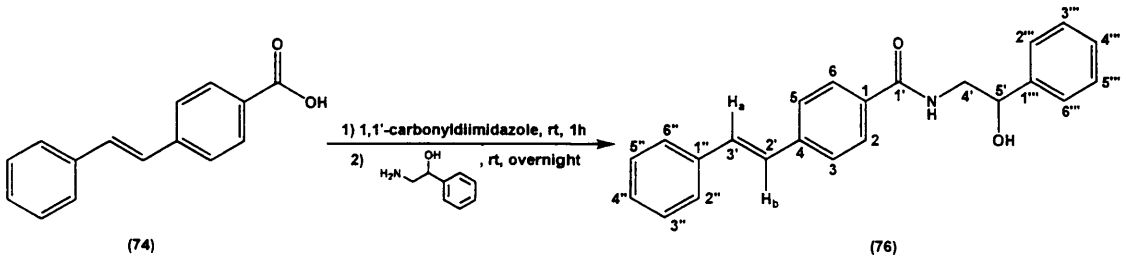

To a suspension of 4-[(*E*)-2-phenyl-1-ethenyl]benzoic acid (**74**) (0.6 g, 2.68 mmol) in anhydrous DMF (20 mL) was added 1,1'-carbonyldiimidazole (0.43 g, 2.68 mmol) and the reaction stirred at room temperature for 1 h. The reaction was then cooled to 0 °C and subsequently combined with a solution of 2-amino-1-phenylethanol (0.37 g, 2.68 mmol), in DMF (5 mL). The mixture was stirred at room temperature overnight. After the reaction was complete, ice was added into the flask to precipitate out the product which was then filtered and washed with ice-cold H_2O, dried under vacuum to give pure *N*-(2-hydroxy-2-phenylethyl)-4-[(*E*)-2-phenyl-1-ethenyl]benzamide (**76**) as a white solid. Yield: 0.8 g (87%), t.l.c. system: petroleum ether – EtOAc 3:1 v/v, R_F: 0.39, vanillin stain positive.

Melting point: 218-219 °C.

Microanalysis: Calculated for $C_{23}H_{21}NO_2$ (343.42), Theoretical: %C= 80.44, %H= 6.16, %N= 4.08, Found: %C= 80.27, %H= 6.21, %N= 3.88.

^{1}H-NMR (DMSO-d_6), δ: 3.34-3.43 (m, 2H, CH_2), 3.47-3.51 (m, 1H, CH-OH), 5.53 (s, 1H, OH), 7.25-7.42 (m, 10H, H-aromatic and alkene), 7.64 (d, 2H, J = 7.5 Hz, H-aromatic), 7.69 (d, 2H, J = 8.0 Hz, H-aromatic), 7.88 (d, 2H, J = 8.0 Hz, H-aromatic), 8.52 (s, 1H, NH).

^{13}C NMR (DMSO-d_6), δ: 47.72 (CH_2, C-4'), 71.21 (CH, C-5'), 125.96, 126.08, 126.18, 126.66, 126.99, 127.53, 127.67, 128.01, 128.73, 130.12 (CH, aromatic and alkene), 133.26 (C, C-1), 136.75 (C, C-1''), 139.71 (C, C-4), 143.78 (CH, C-1'''), 166.03 (C, C-1').

4.2.10. 1-(4-Fluorophenyl)-2-nitro-1-ethanol (79) [236].

(Mol. Formula: $C_8H_8FNO_3$, M. W.: 185.15)

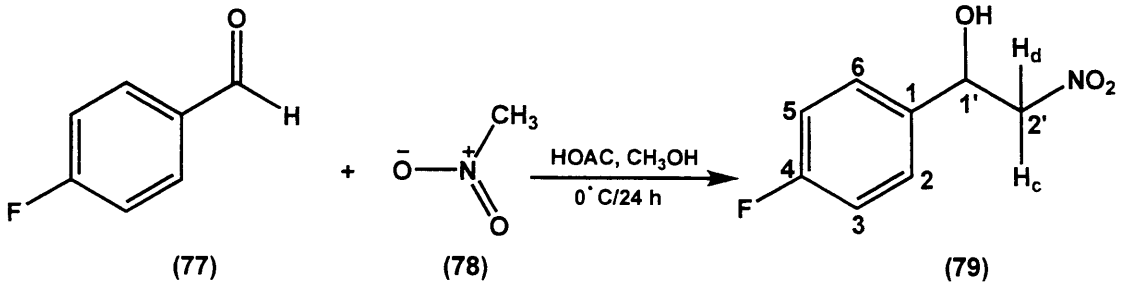

(77) (78) (79)

To a cooled solution (0 °C) of 4-fluorobenzaldehyde (**77**) (4.25mL, 40.29 mmol) in MeOH (75 mL) was added nitromethane (**78**) (4.35 mL, 80.57 mmol) and aq. NaOH (1.6 mL of a 100g/100mL solution). The resulting suspension was stirred at 0 °C for 3.5 h then left in the fridge overnight. The produced orange suspension was treated with a solution of AcOH (10 mL, 4.6 mL of AcOH in 10 mL H_2O) at 0 °C for 30 min. The solvent was removed under reduced pressure and the residue dissolved in CH_2Cl_2 (100 mL), washed with H_2O (75 mL) and brine (75 mL). The organic layer was dried ($MgSO_4$) and concentrated to give a brown syrup, which was purified by flash column chromatography (petroleum ether – EtOAc 100:0 v/v increasing to 70:30 v/v) to give pure 1-(4-fluorophenyl)-2-nitro-1-ethanol (**79**) as dark orange liquid. Yield: 6.5 g (87%), t.l.c. system: petroleum ether – EtOAc 3:1 v/v,, R_F: 0.33, vanillin stain positive.

^{1}H-NMR (DMSO-d_6), δ: 4.58 (dd, 1H, J = 2.8 Hz, 12.5 Hz, H_c), 4.84 (dd, 1H, J = 9.5 Hz, 12.5 Hz, H_d), 5.27-5.31 (m, 1H, H-1'), 6.14 (d, 1H, J = 5.0 Hz, OH), 7.18-7.23 (m, 2H, H-3, H-5), 7.47-7.51 (m, 2H, H-2, H-4).

^{13}C NMR (DMSO-d_6), δ: 69.26 (CH, C-1'), 81.72 (CH_2, C-2'), 114.99 and 115.16 (CH, C-3 and C-5), 128.26 and 128.32 (CH, C-2 and C-6), 136.61 and 136.63 (C, C-1), 160.75 and 162.69 (C, C-4).

4.2.11. 2-Amino-1-(4-fluorophenyl)-1-ethanol (80) [237].

(Mol. Formula: $C_8H_{10}FNO$, M. W.: 155.17)

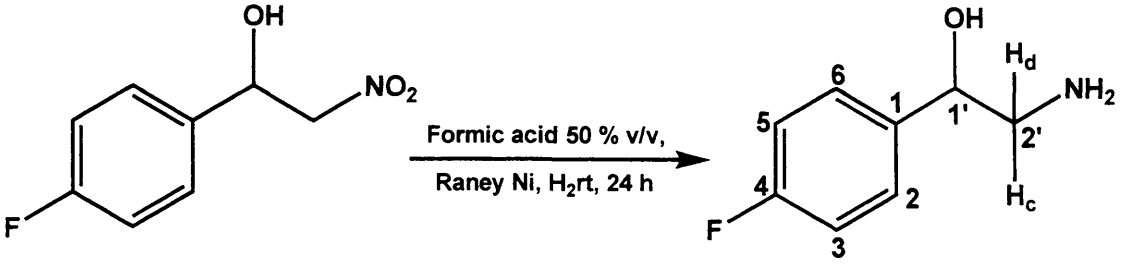

(79) **(80)**

Raney nickel (50 % slurry in H_2O, 6 mL), was added to a solution of 1-(4-fluorophenyl)-2-nitro-1-ethanol (**79**) (7.0 g, 37.83 mmol) in MeOH (100 mL) and aq. HCOOH (50 % v/v, 8 mL). The reaction flask was then degassed and purged with hydrogen. The reaction was carried out under 40 psi H_2 atmosphere using a Paar hydrogenator. The reaction flask was shaken at room temperature for 24 h until all starting material had been consumed. After removal of hydrogen the reaction mixture was filtered and the solvent removed in *vacuo*. The aqueous residue was made alkaline with NH_4OH (28 %) and extracted with EtOAc (2 x 100 mL). The organic layer was then washed with brine (2 x 50 mL), dried ($MgSO_4$), and concentrated under reduced pressure. The crude product was then purified by flash column chromatography (CH_2Cl_2-MeOH-Et_3N 100: 0: 0.05 v/v increasing to 95: 5 :0.05 v/v) to give pure 2-amino-1-(4-fluorophenyl)-1-ethanol (**80**) as a yellow solid. Yield: 2.60 g (47%), t.l.c. system: CH_2Cl_2 – MeOH 9:1 v/v, R_F: 0.08, vanillin stain positive.

Melting point: 59-61 °C (lit. m.p. 60-61 °C) [237].

^{1}H-NMR (DMSO-d_6), δ: 2.63 (dd, 1H, J = 2.8 Hz, 12.5 Hz, H_c), 2.76 (dd, 1H, J = 9.5 Hz, 12.5 Hz, H_d), 4.87 (dd, J = 4.5 Hz, 7.3 Hz, 1H, H-1'), 4.65 (t, 2H, J = 6.1 Hz, NH_2), 6.14 (d, 1H, J = 5.0 Hz, OH), 7.10-7.16 (m, 2H, H-3, H-5), 7.34-7.38 (m, 2H, H-2, H-4).

^{13}C NMR (DMSO-d_6), δ: 59.41 (CH_2, C-2'), 73.20 (CH, C-1'), 114.46 and 114.49 (CH, C-3 and C-5), 127.70 and 127.71 (CH, C-2 and C-6), 140.32 and 140.64 (C, C-1), 160.17 and 162.09 (C, C-4).

4.2.12. *N*-[2-(4-Fluorophenyl)-2-hydroxyethyl]-4-[(*E*)-2-(3,5-dimethoxyphenyl)-1-ethenyl]benzamide (81).

(Mol. Formula: $C_{25}H_{24}FNO_4$, M. W.: 421.46)

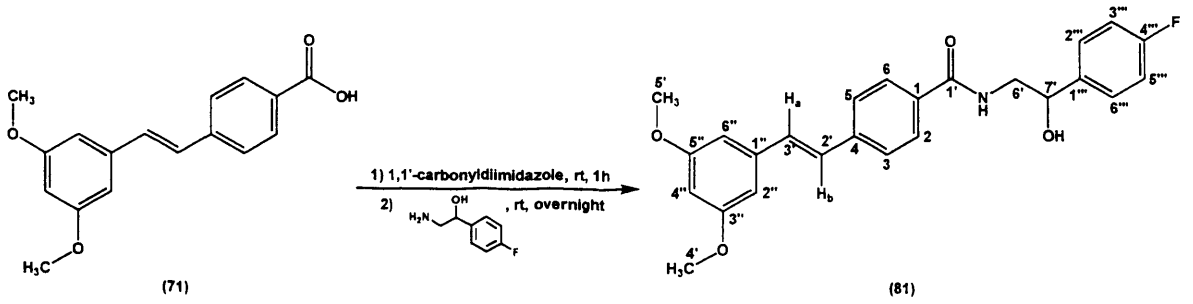

To a suspension of 4-[(*E*)-2-(3,5-dimethoxyphenyl)-1-ethenyl]benzoic acid (**71**) (0.6 g, 2.11 mmol) in anhydrous DMF (20 mL) was added 1,1'-carbonyldiimidazole (0.34 g, 2.11 mmol) and the reaction stirred at room temperature for 1 h. The reaction was then cooled to 0 °C and subsequently combined with a solution of 2-amino-1-(4-flourophenyl)ethanol (**80**) (0.33 g, 2.11 mmol), in DMF (5 mL). The mixture was stirred at room temperature overnight. After the reaction was complete, ice was added into the flask to precipitate out the product which was then filtered and washed with ice-cold H_2O, dried under vacuum to give pure *N*-(2-hydroxy-2-phenylethyl)-4-[(*E*)-2-(3,5-dimethoxyphenyl)-1-ethenyl]benzamide (**81**) as a white solid. Yield: 0.65 g (73%), t.l.c. system: petroleum ether – EtOAc 3:1 v/v, R_F: 0.38, vanillin stain positive.

Melting point: 202-205 °C.

Microanalysis: Calculated for $C_{25}H_{24}FNO_4$ (421.46), Theoretical: %C= 71.25, %H= 5.74, %N= 3.32, Found: %C= 71.05, %H= 5.77, %N= 3.32.

^{1}H-NMR (DMSO-d_6), δ: 3.34-3.51 (m, 2H, CH_2), 3.80 (s, 6H, 2 O-CH_3), 4.80-4.82 (m, 1H, CH-OH), 5.46 (s, 1H, OH), 6.45 (s, 1H, H-aromatic), 6.82 (d, 2H, J = 1.5 Hz, H-aromatic), 7.61 (t, 2H, J = 8.8 Hz, H-aromatic), 7.32 (d, 2H, J = 2.8 Hz, H_a, H_b), 7.4124 (t, 2H, J = 6.9 Hz, H-aromatic), 7.68 (d, 2H, J = 8.2 Hz, H-aromatic), 7.86 (d, 2H, J = 8.2 Hz, H-aromatic), 8.50 (t, 1H, J = 5.2 Hz, NH).

^{13}C NMR (DMSO-d_6), δ: 47.56 (CH_2, C-6'), 55.21 (CH_3, C-4', C-5'), 70.55 (CH, C-7'), 100.25, 104.69, 114.69, 126.20, 127.66, 127.91, 128.04, 130.17, 138.78 (CH, aromatic and alkene), 133.27 (C, C-1), 139.63 (C, C-1"), 139.91 (C, C-4), 160.67 (C, C-3", C-5"), 162.23 (C, C-1'), 165.99 (C, C-4''').

4.2.13. 2-{4-[(*E*)-2-(3,5-Dimethoxyphenyl)-1-ethenyl]phenyl-5-phenyl}-4,5-dihydro-1,3-oxazole (82).

(Mol. Formula: $C_{25}H_{23}NO_3$, M. W.: 385.46)

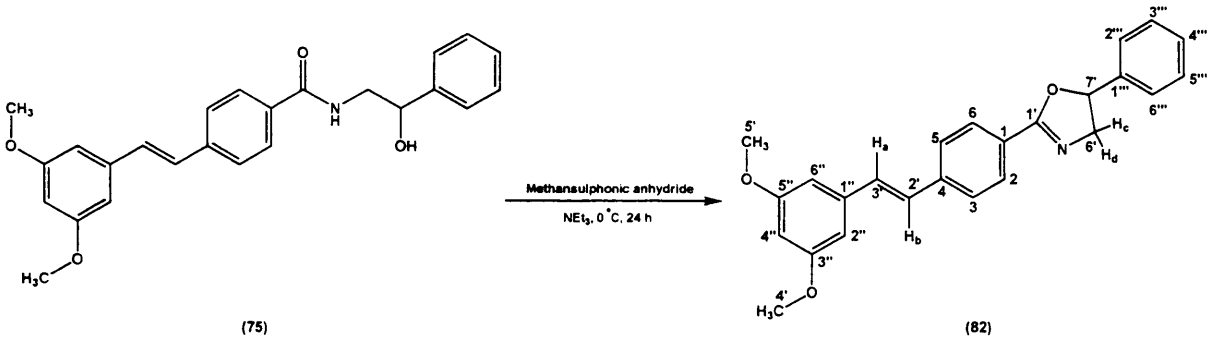

(75) (82)

To a suspension of *N*-(2-hydroxy-2-phenylethyl)-4-[(*E*)-2-(3,5-dimethoxy-phenyl)-1-ethenyl]benzamide (**75**) (0.8 g, 2 mmol) in anhydrous THF (15 mL) was added methanesulphonic anhydride (0.52 g, 3 mmol) dissolved in anhydrous THF (5 mL). The mixture was stirred at 0 °C for 15 min, then NEt_3 (0.84 mL, 6 mmol) was added dropwise to the mixture, which results in a homogenous solution. The homogenous solution was kept in the fridge at 0 °C for 24 h. The mixture was quenched by the addition of aqueous NH_3 solution (28%, 1 mL). After stirring at room temperature for 15 min, the mixture was concentrated *in vacuo* and finally distributed between EtOAc (150 mL) and aqueous $NaHCO_3$ solution (2 x 100 mL). The organic phase was dried ($MgSO_4$), concentrated under reduced pressure and the crude product purified by flash column chromatography (petroleum ether – EtOAc 100:0 v/v increasing to 70:30 v/v) to give pure 2-4-[(*E*)-2-(3,5-dimethoxyphenyl)-1-ethenyl]phenyl-5-phenyl-4,5-dihydro-1,3-oxazole (**82**) as a yellow oily product. Yield: 0.8 g (100%), t.l.c. system: petroleum ether – EtOAc 3:1 v/v, R_F: 0.31, vanillin stain positive.

HRMS (EI): Calculated mass: 386.1751 $[M+H]^+$, Measured mass: 386.1753 $[M+H]^+$.

^{1}H-NMR ($CDCl_3$), δ: 3.86 (s, 6H, 2 O-CH_3), 4.03 (dd, 1H, J = 8.0 Hz, 14.8 Hz, H_c), 4.51 (dd, 1H, J = 10.2 Hz, 14.8 Hz, H_d), 5.69 (t, 1H , J = 9.1 Hz, O-CH), 6.45 (s, 1H, H-aromatic), 6.72 (d, 2H, J = 2.0 Hz, H-aromatic), 7.14 (d, 2H, J = 3.9 Hz, H_a, H_b), 7.36-7.43 (m, 5H, H-aromatic), 7.59 (d, 2H, J = 8.3 Hz, H-aromatic), 8.03 (d, 2H, J = 8.2 Hz, H-aromatic).

^{13}C NMR ($CDCl_3$), δ: 55.40 (CH_3, C-4', C-5'), 63.16 (CH_2, C-6'), 81.11 (CH,

C-7'), 100.49, 104.81, 125.76, 126.35, 127.53, 128.33, 128.57, 128.73, 130.79 (CH, aromatic and alkene), 126.51 (C, C-1), 138.93 (C, C-1'''), 140.26 (C, C-4), 141.02 (C, C-1''), 161.05 (C, C-3'', C-5''), 163.88 (C, C-1').

4.2.14. 5-Phenyl-2-{4-[(*E*)-2-phenyl-1-ethenyl]phenyl}-4,5-dihydro-1,3-oxazole (83).

(Mol. Formula: $C_{23}H_{19}NO$, M. W.: 325.40)

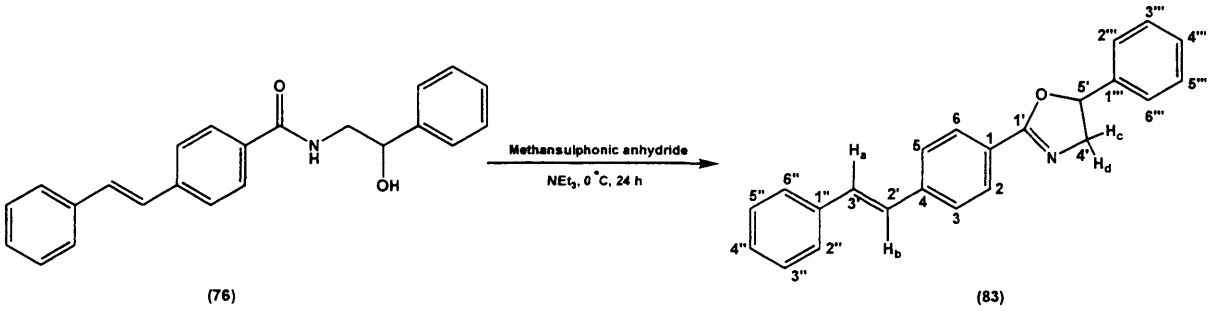

(76) (83)

To a suspension of *N*-(2-hydroxy-2-phenylethyl)-4-[(*E*)-2-phenyl-1-ethenyl]benzamide (**76**) (0.65 g, 1.9 mmol) in anhydrous THF (15 mL) was added methanesulphonic anhydride (0.5 g, 2.8 mmol) dissolved in anhydrous THF (5 mL). The mixture was stirred at 0 °C for 15 min, then NEt_3 (0.8 mL, 5.7 mmol) was added dropwise to the mixture, which results in a homogenous solution. The homogenous solution was kept in the fridge at 0 °C for 24 h. The mixture was quenched by the addition of aqueous NH_3 solution (28%, 1 mL). After stirring at room temperature for 15 min, the mixture was concentrated *in vacuo* and finally distributed between EtOAc (150 mL) and aqueous $NaHCO_3$ solution (2 x 100 mL). The organic phase was then dried ($MgSO_4$) and concentrated under reduced pressure. The crude product was then recrystallised from ethanol to give pure 5-phenyl-2-{4-[(*E*)-2-phenyl-1-ethenyl]phenyl}-4,5-dihydro-1,3-oxazole (**83**) as white crystals. Yield: 0.6 g (97%), t.l.c. system: petroleum ether – EtOAc 3:1 v/v, R_F: 0.57, vanillin stain positive.

Melting point: 126-127 °C.

Microanalysis: Calculated for $C_{23}H_{19}NO$ (325.40), Theoretical: %C= 84.89, %H= 5.88, %N= 4.30, Found: %C= 84.70, %H= 5.94, %N= 4.11.

^{1}H-NMR (DMSO-d_6), δ: 3.88 (dd, 1H, J = 7.5 Hz, 14.9 Hz, H_c), 4.48 (dd, 1H, J = 10.1 Hz, 14.9 Hz, H_d), 5.80 (dd, 1H , J = 7.7 Hz, 9.9 Hz, O-CH), 7.46-7.33 (m, 10H, H-aromatic and alkene), 7.67 (d, 2H, J = 7.5 Hz, H-aromatic), 7.76 (d, 2H, J = 8.3 Hz, H-aromatic), 7.97 (d, 2H, J = 8.3 Hz, H-aromatic).

^{13}C NMR (DMSO-d_6), δ: 62.60 (CH_2, C-4'), 80.10 (CH, C-5'), 125.60, 126.60, 126.70, 127.50, 128.05, 128.10, 128.20, 128.70, 130.40 (CH, aromatic and alkene), 126.20 (C, C-1), 136.70 (C, C-1''), 140.10 (C, C-1'''), 141.30 (C, C-4), 162.20 (C, C-1').

4.2.15. 2-{4-[(*E*)-2-(3,5-Dimethoxyphenyl)-1-ethenyl]phenyl}-5-(4-fluorophenyl)-4,5-dihydro-1,3-oxazole (84).

(Mol. Formula: $C_{25}H_{22}FNO_3$, M. W.: 403.45)

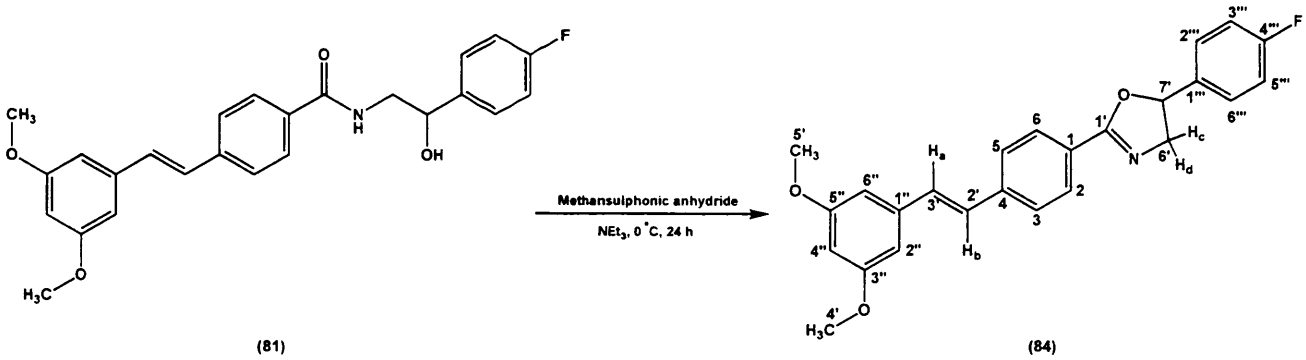

(81) (84)

To a suspension of *N*-(2-hydroxy-2-phenylethyl)-4-[(*E*)-2-(3,5-dimethoxyphenyl)-1-ethenyl]benzamide (**81**) (0.63 g, 1.5 mmol) in anhydrous THF (15 mL) was added methanesulphonic anhydride (0.39 g, 2.25 mmol) dissolved in anhydrous THF (5 mL). The mixture was stirred at 0 °C for 15 min, then NEt_3 (0.63 mL, 4.5 mmol) was added dropwise to the mixture, which results in a homogenous solution. The homogenous solution was kept in the fridge at 0 °C for 24 h. The mixture was quenched by the addition of aqueous NH_3 solution (28%, 1 mL). After stirring at room temperature for 15 min, the mixture was concentrated *in vacuo* and finally distributed between EtOAc (150 mL) and aqueous $NaHCO_3$ solution (2 x 100 mL). The organic phase was then dried ($MgSO_4$) and concentrated under reduced pressure. The crude product was then purified by flash column chromatography (petroleum ether – EtOAc 100:0 v/v increasing to 70:30 v/v) to give pure 2-4-[(*E*)-2-(3,5-dimethoxyphenyl)-1-ethenyl]phenyl-5-(4-fluorophenyl)-4,5-dihydro-1,3-oxazole (**84**) as a yellow oily product. Yield: 0.6 g (98%), t.l.c. system: petroleum ether – EtOAc 3:1 v/v, R_F: 0.25, vanillin stain positive.

HRMS (EI): Calculated mass: 404.1656 $[M+H]^+$, Measured mass: 404.1652 $[M+H]^+$.

^{1}H-NMR ($CDCl_3$), δ: 3.86 (s, 6H, 2 O-CH_3), 4.00 (dd, 1H, J = 7.9 Hz, 14.8 Hz,

H_c), 4.50 (dd, 1H, J = 10.1 Hz, 14.9 Hz, H_d), 5.66 (t, 1H , J = 9.0 Hz, O-C<u>H</u>), 6.45 (t, 1H, J = 2.2 Hz, H-aromatic), 6.71 (d, 2H, J = 2.2 Hz, H-aromatic), 7.08-7.11 (m, 2H, H-aromatic), 7.14 (d, 2H, J = 4.4 Hz, H_a, H_b), 7.34-7.7.37 (m, 2H, H-aromatic), 7.59 (d, 2H, J = 8.4 Hz, H-aromatic), 8.01 (d, 2H, J = 8.4 Hz, H-aromatic).

<u>^{13}C NMR ($CDCl_3$), δ</u>: 55.39 (CH_3, C-4', C-5'), 63.22 (CH_2, C-6'), 80.45 (CH, C-7'), 100.49, 104.82, 115.77, 126.51, 128.25, 128.69, 128.69, 130.58, 138.90 (CH, aromatic and alkene), 136.85 (C, C-1), 140.31 (C, C-4), 161.06 (C, C-3", C-5"), 161.68 (C, C-1"), 163.88 (C, C-1'), 163.73 (C, C-4'").

4.2.16. *N*-[2-(1*H*-1-Imidazolyl)-2-phenylethyl]-4-[(*E*)-2-(3,5-dimethoxy-phenyl)-1-ethenyl]benzamide (85).

(<u>Mol. Formula</u>: $C_{28}H_{27}N_3O_3$, <u>M. W.</u>: 453.53)

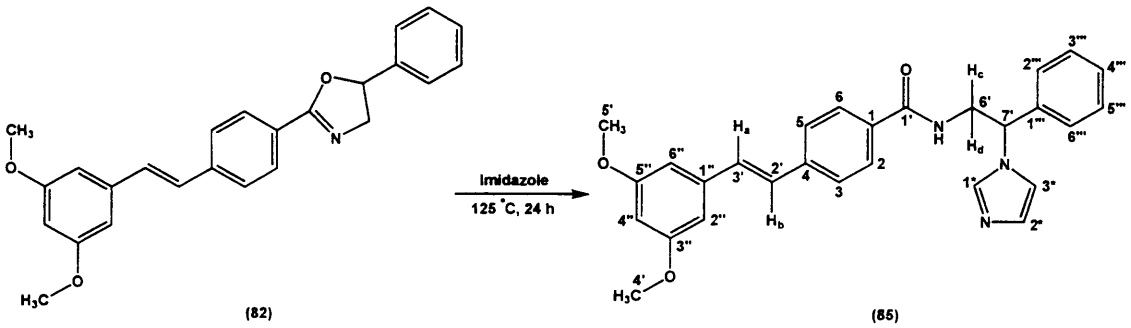

(82) (85)

A mixture of 2-4-[(*E*)-2-(3,5-dimethoxyphenyl)-1-ethenyl]phenyl-5-phenyl-4,5-dihydro-1,3-oxazole (**82**) (0.6 g, 1.56 mmol) and imidazole (4.2 g, 62.26 mmol) dissolved in isopropyl acetate (10 mL) was heated at 125 °C for 24 h. After completion of the reaction, the mixture was partitioned between H_2O (100 mL) and EtOAc (150 mL). The organic layer was washed with H_2O (3 x 100 mL), dried ($MgSO_4$) and concentrated under reduced pressure. The residue was recrystallised from aqueous EtOH to give yellow crystals of *N*-[2-(1*H*-1-imidazolyl)-2-phenylethyl]-4-[(*E*)-2-(3,5-dimethoxy- phenyl)-1-ethenyl]benzamide (**85**). Yield: 0.48 g (68%), t.l.c. system: CH_2Cl_2 – MeOH 90:10 v/v, R_F: 0.77, vanillin stain positive.

<u>Melting point:</u> 216-218 °C.

<u>HRMS (EI):</u> Calculated mass: 454.2125 $[M+H]^+$, Measured mass: 454.2120 $[M+H]^+$.

<u>^{1}H-NMR (DMSO-d_6), δ</u>: 3.79 (s, 6H, 2 O-C<u>H_3</u>), 3.97-4.02 (m, 1H, H_c), 4.07-4.17 (m, 1H, H_d), 5.68-5.70 (m, 1H, CH_2-C<u>H</u>-Ar), 6.45 (t, 1H, J = 2.2 Hz, H-aromatic), 6.82 (d, 2H, J = 2.2 Hz, H-aromatic), 6.91 (s, 1H, H-aromatic), 7.31 (d, 2H,

J = 3.4 Hz, H_a, H_b), 7.32-7.34 (m, 2H, H-aromatic), 7.38-7.40 (m, 4H, H-aromatic), 7.67 (d, 2H, J = 8.4 Hz, H-aromatic), 7.78 (d, 2H, J = 8.4 Hz, H-aromatic), 8.84 (s, 1H, H-aromatic), 8.74 (t, 1H, J = 5.5 Hz, NH).

^{13}C NMR (DMSO-d_6), δ: 43.46 (CH_2, C-6'), 55.21 (CH_3, C-4', C-5'), 59.43 (CH, C-7'), 100.31, 104.69, 118.34, 126.24, 126.81, 127.63, 127.97, 128.04, 128.49, 128.70, 130.32, 136.75 (CH, aromatic and alkene), 132.81 (C, C-1), 138.73 (C, C-1"), 139.31 (C, C-4), 139.88 (C, C-1'"), 160.66 (C, C-3", C-5"), 166.26 (C, C-1').

4.2.17. *N*-[2-(1*H*-1-Imidazolyl)-2-phenylethyl]-4-[(*E*)-2-phenyl-1-ethenyl] benzamide (86).

(Mol. Formula: $C_{26}H_{23}N_3O$, M. W.: 393.48)

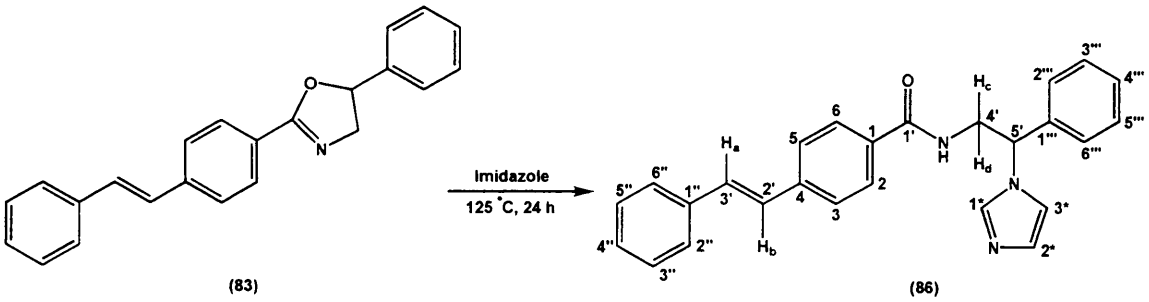

A mixture of 5-phenyl-2-{4-[(*E*)-2-phenyl-1-ethenyl]phenyl}-4,5-dihydro-1,3-oxazole (**83**) (0.34 g, 1.04 mmol) and imidazole (1.42 g, 20.90 mmol) dissolved in isopropyl acetate (10 mL) was heated at 125 °C for 24 h. After completion of the reaction, the mixture was partitioned between H_2O (100 mL) and EtOAc (150 mL). The organic layer was washed with H_2O (3 x 100 mL), dried ($MgSO_4$) and concentrated under reduced pressure. The residue was then purified by flash column chromatography (CH_2Cl_2 – MeOH 99:1 v/v increasing to 97:3 v/v) to give *N*-[2-(1*H*-1-imidazolyl)-2-phenylethyl]-4-[(*E*)-2-phenyl-1-ethenyl]benzamide (**86**). Yield: 0.2 g (47%), t.l.c. system: CH_2Cl_2 – MeOH 90:10 v/v, R_F: 0.77, vanillin stain positive.

Melting point: 190-192 °C.

Microanalysis: Calculated for $C_{26}H_{23}N_3O$ (393.48), Theoretical: %C= 79.36, %H= 5.89, %N= 10.67, Found: %C= 79.10, %H= 5.80, %N= 10.43.

^{1}H-NMR (DMSO-d_6), δ: 3.97-4.02 (m, 1H, H_c), 4.07-4.17 (m, 1H, H_d), 5.73 (dd, 1H, J = 5.8 Hz, 8.7 Hz, CH_2-CH-Ar), 6.96 (s, 1H, imidazole), 7.32-7.43 (m, 11H, H-aromatic and akene), 7.66 (d, 2H, J = 7.4 Hz, H-aromatic), 7.71 (d, 2H, J = 8.0 Hz, H-aromatic), 7.81 (d, 2H, J = 8.0 Hz, H-aromatic), 7.89 (s, 1H, imidazole), 8.77 (s,

1H, NH).

^{13}C NMR (DMSO-d_6), δ: 43.46 (CH_2, C-4'), 59.43 (CH, C-5'), 126.20, 126.70, 126.80, 127.40, 127.60, 128.00, 128.10, 128.50, 128.70, 128.73, 130.30 (CH, aromatic and alkene), 132.81 (C, C-1), 136.73 (C, C-1"), 139.31 (C, C-4), 140.00 (CH, C-1'"), 166.30 (C, C-1').

4.2.18. *N*-[2-(4-Fluorophenyl)-2-(1*H*-1-imidazolyl)ethyl]-4-[(*E*)-2-(3,5-dimethoxyphenyl)-1-ethenyl]benzamide (87).

(Mol. Formula: $C_{28}H_{26}FN_3O_3$, M. W.: 471.52)

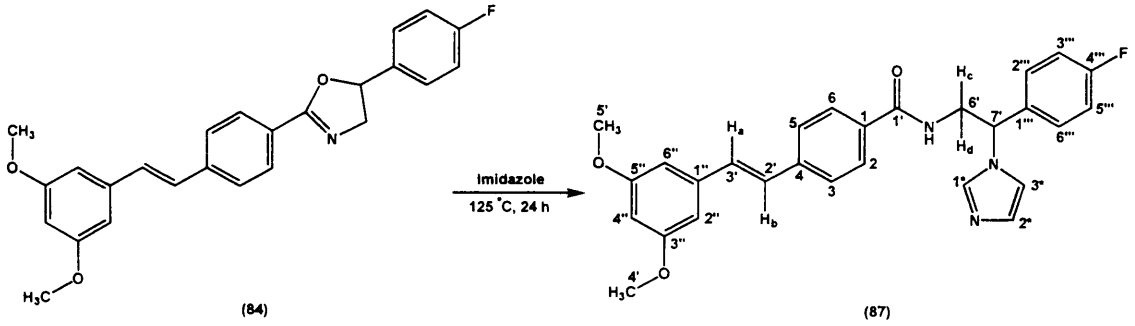

(84) (87)

A mixture of 2-4-[(*E*)-2-(3,5-dimethoxyphenyl)-1-ethenyl]phenyl-5-(4-fluorophenyl)-4,5-dihydro-1,3-oxazole (**84**) (0.6 g, 1.5 mmol) and imidazole (4 g, 59.4 mmol) dissolved in isopropyl acetate (10 mL) was heated at 125 °C for 24 h. After completion of the reaction, the mixture was partitioned between H_2O (100 mL) and EtOAc (150 mL). The organic layer was washed with H_2O (3 x 100 mL), dried ($MgSO_4$) and concentrated under reduced pressure. The residue was recrystallised from aqueous EtOH to give yellow crystals of *N*-[2-(4-fluorophenyl)-2-(1*H*-1-imidazolyl)ethyl]-4-[(*E*)-2-(3,5-dimethoxyphenyl)-1-ethenyl]benzamide (**87**). Yield: 0.25 g (35%), t.l.c. system: CH_2Cl_2 – MeOH 90:10 v/v, R_F: 0.77, vanillin stain positive.

Melting point: 193-196 °C.

HRMS (EI): Calculated mass: 472.2031 $[M+H]^+$, Measured mass: 472.2026 $[M+H]^+$.

^{1}H-NMR ($CDCl_3$), δ: 3.84 (s, 6H, 2 O-CH_3), 3.86-3.90 (m, 1H, H_c), 4.32-4.36 (m, 1H, H_d), 5.63-5.66 (m, 1H, CH_2-CH-Ar), 6.44 (t, 1H, J = 2.2 Hz, H-aromatic), 6.68 (d, 2H, J = 2.3 Hz, H-aromatic), 7.00 (s, 1H, H-aromatic), 7.07-7.12 (m, 5H, H_a, H_b, H-aromatic), 7.24-7.27 (m, 2H, H-aromatic), 7.29 (t, 1H, J = 5.5 Hz, NH), 7.50 (d,

2H, J = 8.4 Hz, H-aromatic), 7.54 (s, 1H, H-aromatic), 7.72 (d, 2H, J = 8.4 Hz, H-aromatic).

^{13}C NMR ($CDCl_3$), δ: 44.56 (CH_2, C-6'), 55.39 (CH_3, C-4', C-5'), 59.69 (CH, C-7'), 100.57, 104.85, 116.14, 118.32, 126.59, 127.56, 127.83, 128.45, 129.6, 130.99, 132.39 (CH, aromatic and alkene), 132.39 (C, C-1), 133.47 (C, C-1''), 138.70 (C, C-4), 140.75 (C, C-1'''), 161.06 (C, C-3'', C-5''), 163.66 (C, C-1'), 167.75 (C, C-4''').

4.2.19. 6-Methoxy-2-{1-[2-(trifluoromethyl)phenyl]methylidene}-1,2,3,4-tetrahydro-1-naphthalenone (90).

(Mol. Formula: $C_{19}H_{15}F_3O_2$, M. W.: 334.33)

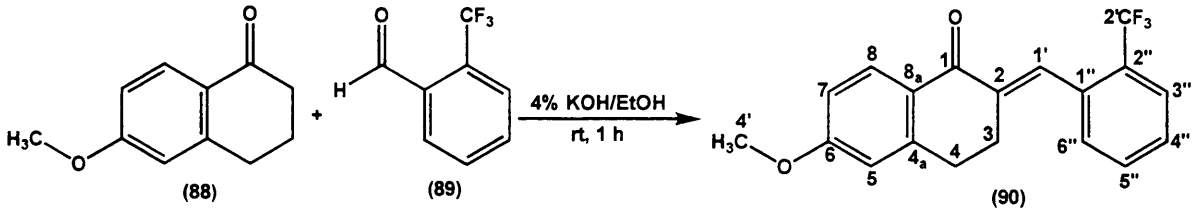

A mixture of the 6-methoxytetralone (**88**) (2.0 g, 11 mmol) and 2-(trifluoromethyl)benzaldehyde (**89**) (1.45 mL, 11 mmol) in 4 % ethanolic KOH (100 mL) was stirred at room temperature for 1 h. The resulting precipitate was collected, washed with water and finally recrystallised from EtOH to give 6-methoxy-2-{1-[2-(trifluoromethyl)phenyl]methylidene}-1,2,3,4-tetrahydro-1-naphthalenone (**90**) as a cream crystalline solid. Yield: 2.48 g (68 %), t.l.c. system: petroleum ether – EtOAc 3:1 v/v, R_F: 0.54, vanillin stain positive.

Melting point: 81-83 °C.

Microanalysis: Calculated for $C_{19}H_{15}F_3O_2$ (334.33): Theoretical: %C= 68.67, %H= 4.59, Found: %C= 68.24, %H= 4.55.

^{1}H-NMR ($CDCl_3$), δ: 2.83-2.87 (m, 2H, CH_2-C-CO), 2.90-2.93 (m, 2H, Ar-CH_2- CH_2), 3.89 (s, 3H, OCH_3), 6.72 (d, 1H, J = 2.4 Hz, H-aromatic), 6.91 (dd, 1H, J = 2.5 Hz, 8.8 Hz, H-aromatic), 7.34 (d, 1H, J = 7.6 Hz, H-aromatic), 7.47 (t, 1H, J = 7.7 Hz, H-aromatic), 7.58 (t, 1H, J = 7.6 Hz, H-aromatic), 7.75 (d, 1H, J = 7.9 Hz, H-aromatic), 7.96 (s, 1H, -C=CH-Ph), 8.17 (d, 1H, J = 8.8 Hz, H-aromatic).

^{13}C NMR ($CDCl_3$), δ: 27.4 (CH_2, C-3), 29.5 (CH_2, C-4), 55.5 (CH_3, C-4'), 112.4, 113.5, 126.1, 127.9, 130.4, 130.9, 131.5 (CH, aromatic), 122.9, 129.1, 129.34 (C, C-F), 125.0 (C, C-2''), 126.8 (C, C-8_a), 132.3 (CH, C-1'), 135.2 (C, C-1''), 138.2

(C, C-2), 146.0 (C, C-4_a), 163.8 (C, C-6), 189.2 (C, C-1).

4.2.20. 6-Methoxy-2-[2-(trifluoromethyl)benzyl]-1,2,3,4-tetrahydro-1-naphthalenone (91).

(Mol. Formula: $C_{19}H_{17}F_3O_2$, M. W.: 334.337)

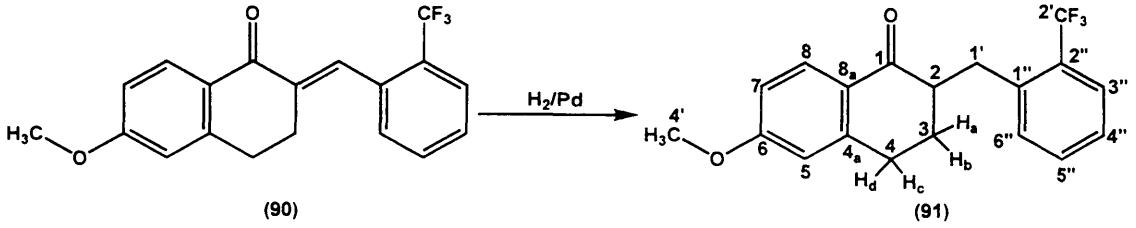

To a suspension of 5% Pd-C (10 mol %) in MeOH (100 mL) was added, under nitrogen, a solution of 6-methoxy-2-(*E*)-1-[2-(trifluoromethyl)phenyl]methylidene-1,2,3,4-tetrahydro-1-naphthalenone (**90**) (2.0 g, 6 mmol) in MeOH (20 mL). Then, the reaction atmosphere was changed to hydrogen and the reaction mixture stirred at room temperature. After a period of 1 h, the suspension was filtered over a pad of celite and the solvent removed under reduced pressure to give a yellow residue. The residue was purified by flash column chromatography (petroleum ether – EtOAc 100:0 increasing to 90:10 v/v) to give 6-methoxy-2-[2-(trifluoromethyl)benzyl]-1,2,3,4-tetrahydro-1-naphthalenone (**91**) as a cream crystalline solid. Yield: 1.03 g (53 %), t.l.c. system: petroleum ether – EtOAc 3:1 v/v, R_F: 0.60, vanillin stain positive.

Melting point: 82-84 °C.

Microanalysis: Calculated for $C_{19}H_{17}F_3O_2$ (334.33): Theoretical: %C= 68.26, %H= 5.12, Found: %C= 68.03, %H= 5.13.

^{1}H-NMR ($CDCl_3$), δ: 1.84-1.87 (m, 1H, H_a), 2.05-2.07 (m, 1H, H_b), 2.81-2.83 (m, 2H, CO-CH-CH_2-Ar), 2.91-2.95 (m, 2H, H_c, H_d), 3.80 (m, 1H, CO-CH-CH_2-Ar) 3.88 (s, 3H, O-CH_3), 6.69 (d, 1H, J = 2.4 Hz, H-aromatic), 6.87 (dd, 1H, J = 2.5 Hz, 8.8 Hz, H-aromatic), 7.34 (t, 1H, J = 7.6 Hz, H-aromatic), 7.42 (d, 1H, J = 7.7 Hz, H-aromatic), 7.51 (t, 1H, J = 7.6 Hz, H-aromatic), 7.68 (d, 1H, J = 7.9 Hz, H-aromatic), 8.08 (d, 1H, J = 8.8 Hz, H-aromatic).

^{13}C NMR ($CDCl_3$), δ: 28.2 (CH_2, C-4), 29.4 (CH_2, C-3), 32.3 (CH_2, C-1'), 49.0 (CH, C-2), 55.4 (CH_3, C-4'), 112.4, 113.2, 126.15, 126.2, 130.0, 131.6, 131.7 (CH, aromatic), 123.5, 125.7, 129.1, 129.3 (C, C-F), 126.1 (C, C-8_a), 136.1 (C, C-2''), 139.3 (C, C-1''), 146.4 (C, C-4_a), 163.5 (C, C-6), 197.6 (C, C-1).

4.2.21. 2-[1-(2-Ethylphenyl)methylidene]-6-methoxy-1,2,3,4-tetrahydro-1-naphthalenone (93).

(Mol. Formula: $C_{20}H_{20}O_2$, M. W.: 292.37)

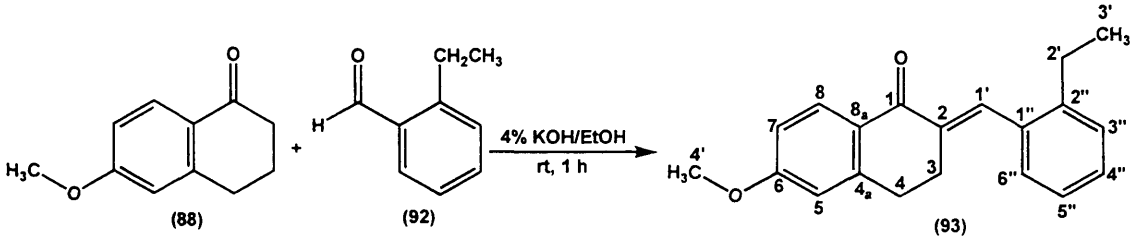

A mixture of the 6-methoxytetralone (**88**) (2.0 g, 11 mmol) and 2-ethyl benzaldehyde (**92**) (1.5 mL, 11 mmol) in 4 % ethanolic KOH (100 mL) was stirred at room temperature for 1 h. The resulting precipitate was collected, washed with water and finally recrystallised from EtOH to give 2-[1-(2-ethylphenyl)methylidene]-6-methoxy-1,2,3,4-tetrahydro-1-naphthalenone (**93**) as a light yellow crystals. Yield: 2.33 g (72 %), t.l.c. system: petroleum ether – EtOAc 3:1 v/v, R_F: 0.74, vanillin stain positive.

Melting point: 77-80 °C.

Microanalysis: Calculated for $C_{20}H_{20}O_2$ (292.37): Theoretical: %C= 82.16, %H= 6.89, Found: %C= 82.25, %H= 7.15.

^{1}H-NMR ($CDCl_3$), δ: 1.21 (t, 3H, J = 7.6 Hz, CH_2CH_3), 2.72 (q, 2H, J = 7.6 Hz, 21.4 Hz, CH_2CH_3), 2.89-2.91 (m, 2H, CH_2-C-CO), 2.95-2.98 (m, 2H, Ar-CH_2-CH_2), 3.90 (s, 3H, OCH_3), 6.73 (d, 1H, J = 2.4 Hz, H-aromatic), 6.91 (dd, 1H, J = 2.5 Hz, 8.8 Hz, H-aromatic), 7.28-7.34 (m, 4H, H-aromatic), 7.97 (s, 1H, -C=CH-Ph), 8.18 (d, 1H, J = 8.8 Hz, H-aromatic).

^{13}C NMR ($CDCl_3$), δ: 15.1 (CH_3, C-3'), 26.7 (CH_2, C-2'), 27.3 (CH_2, C-3), 29.7 (CH_2, C-4), 55.5 (CH_3, C-4'), 112.4, 113.4, 125.5, 127.1, 128.5, 129.1, 130.8 (CH, aromatic), 125.6 (C, C-8_a), 134.6 (C, C-2), 135.0 (CH, C-1'), 136.4 (C, C-2''), 143.8 (C, C-4_a), 146.0 (C, C-1''), 163.6 (C, C-6), 186.8 (C, C-1).

4.2.22. 2-(2-Ethylbenzyl)-6-methoxy-1,2,3,4-tetrahydro-1-naphthalenone (94).

(Mol. Formula: $C_{20}H_{22}O_2$, M. W.: 294.39)

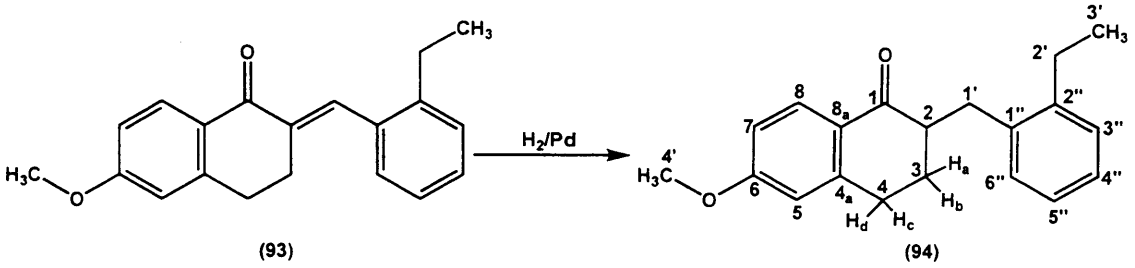

To a suspension of 5% Pd-C (10 mol %) in MeOH (100 mL) was added, under nitrogen, a solution of 2-[1-(2-ethylphenyl)methylidene]-6-methoxy-1,2,3,4-tetrahydro-1-naphthalenone (**93**) (2.0 g, 6.85 mmol) in MeOH (20 mL). Then, the reaction atmosphere was changed to hydrogen and the reaction mixture stirred at room temperature. After a period of 1 h, the suspension was filtered over a pad of celite and the solvent removed under reduced pressure to give a yellow residue. The residue was purified by flash column chromatography (petroleum ether – EtOAc 100:0 increasing to 90:10 v/v) to give 2-(2-ethylbenzyl)-6-methoxy-1,2,3,4-tetrahydro-1-naphthalenone (**94**) as a dark orange syrup. Yield: 1.49 g (64 %), t.l.c. system: petroleum ether – EtOAc 3:1 v/v, R_F: 0.71, vanillin stain positive.

HRMS (EI): Calculated mass: 295.1693 $[M+H]^+$, Measured mass: 295.1695 $[M+H]^+$.

^{1}H-NMR ($CDCl_3$), δ: 1.27 (t, 3H, J = 7.6 Hz, CH_2CH_3), 1.84-1.87 (m, 1H, H_a), 2.09-2.12 (m, 1H, H_b), 2.55 (dd, 1H, J = 10.5 Hz, 14.2 Hz, CO-CH-CH_2-Ar), 2.61-2.72 (m, 4H, CH_2CH_3, CO-CH-CH_2-Ar), 2.91-2.95 (m, 2H, H_c, H_d), 3.88 (s, 3H, O-CH_3), 6.70 (d, 1H, J = 2.4 Hz, H-aromatic), 6.87 (dd, 1H, J = 2.5 Hz, 8.8 Hz, H-aromatic), 7.29-7.12 (m, 4H, Ar), 8.09 (d, 1H, J = 8.8 Hz, H-aromatic).

^{13}C NMR ($CDCl_3$), δ: 15.4 (CH_3, C-3'), 25.5 (CH_2, C-2'), 28.0 (CH_2, C-4), 29.3 (CH_2, C-3), 33.7 (CH_2, C-1'), 48.7 (CH, C-2), 55.4 (CH_3, C-4'), 112.5, 113.2, 126.2, 126.4, 128.6, 130.0, 130.2 (CH, aromatic), 125.6 (C, C-8_a), 137.8 (C, C-2"), 142.5 (C, C-1"), 146.5 (C, C-4_a), 163.5 (C, C-6), 198.2 (C, C-1).

4.2.23. 2-[1-(2-Bromophenyl)methylidene]-6-methoxy-1,2,3,4-tetrahydro-1-naphthalenone (96) [224].

(Mol. Formula: $C_{18}H_{15}BrO_2$, M. W.: 343.21)

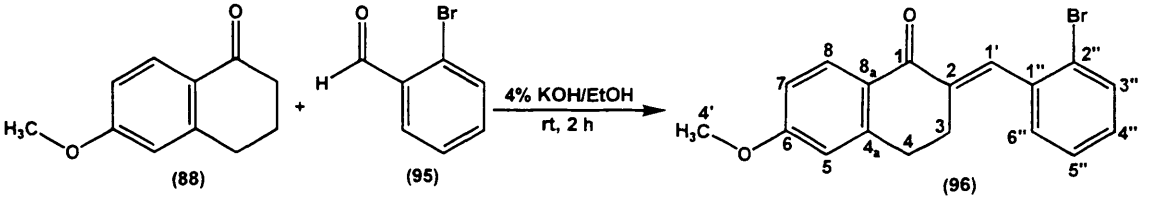

(88) (95) (96)

A mixture of the 6-methoxytetralone (**88**) (2.0 g, 11 mmol) and 2-bromo benzaldehyde (**95**) (1.3 mL, 11 mmol) in 4 % ethanolic KOH (100 mL) was stirred at room temperature for 2 h. The resulting precipitate was collected, washed with water and finally recrystallised from EtOH to give 2-[1-(2-bromophenyl)methylidene]-6-methoxy-1,2,3,4-tetrahydro-1-naphthalenone (**96**) as a light yellow crystals. Yield: 2.61 g (76 %), t.l.c. system: petroleum ether – EtOAc 3:1 v/v, R_F: 0.62, vanillin stain positive.

Melting point: 77-80 °C (lit. m.p. 78-80 °C) [224].

^{1}H-NMR ($CDCl_3$), δ: 2.89-2.91 (m, 2H, CH_2-C-CO), 2.95-2.98 (m, 2H, Ar-CH_2- CH_2), 3.92 (s, 3H, OCH_3), 6.75 (d, 1H, J = 2.4 Hz, H-aromatic), 6.93 (dd, 1H, J = 2.5 Hz, 8.8 Hz, H-aromatic), 7.26-7.28 (m, 1H, H-aromatic), 7.35-7.37 (m, 2H, H-aromatic), 7.69 (d, 1H, J = 7.9 Hz, H-aromatic), 7.85 (s, 1H, -C=CH-Ph), 8.19 (d, 1H, J = 8.8 Hz, H-aromatic).

^{13}C NMR ($CDCl_3$), δ: 27.8 (CH_2, C-4), 29.9 (CH_2, C-3), 55.9 (CH_3, C-4'), 112.8, 113.9, 127.4, 130.2, 130.9, 131.23, 133.3 (CH, aromatic), 125.3 (C, C-2''), 127.3 (C, C-8_a), 135.4 (CH, C-1'), 136.9 (C, C-1''), 137.5 (C, C-2), 146.0 (C, C-4_a), 164.2 (C, C-6), 186.9 (C, C-1).

4.2.24. 6-Methoxy-2-(1-{2-[(*E*)-2-phenyl-1-ethenyl]phenyl}methylidene)-1,2,3,4-tetrahydro-1-naphthalenone (98).

(Mol. Formula: $C_{26}H_{22}O_2$, M. W.: 366.45)

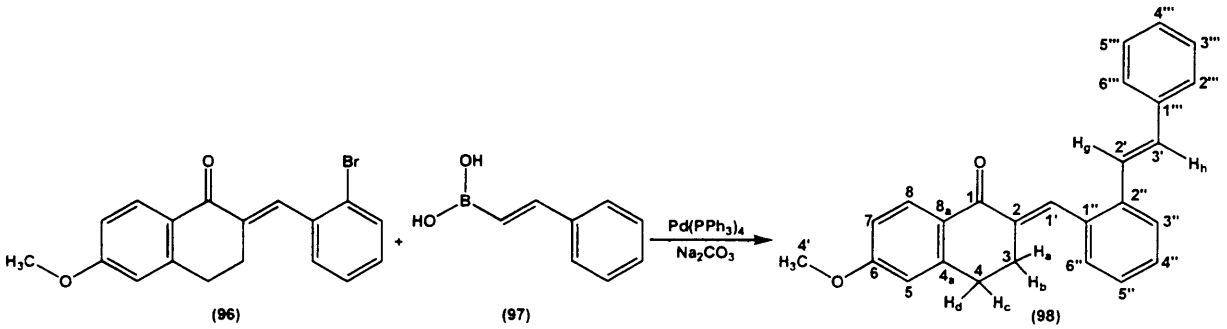

2M aqueous Na_2CO_3 (8.50 mL) was added to a solution of 2-[1-(2-bromophenyl)methylidene]-6-methoxy-1,2,3,4-tetrahydro-1-naphthalenone (**96**) (1.0 g, 2.42 mmol) in toluene (20 mL). To the mixture $Pd(PPh_3)_4$ (0.14 g, 0.12 mmol), and then *trans*-2-phenylvinylboronic acid (**97**) (0.72 g, 4.84 mmol) in ethanol (5 mL) were added. The reaction mixture was refluxed at 90 °C for 5 h. After the reaction was complete, the residual borane was oxidized by the addition of H_2O_2 (30 %, 2.5 mL) at room temperature for 1 h. The crude product was extracted with CH_2Cl_2 (100 mL) and H_2O (3 x 100 mL). The organic layer was dried with $MgSO_4$ and reduced *in vacuo* to give a light yellow oily residue which was purified by flash column chromatography (petroleum ether – EtOAc 100:0 v/v increasing to 90:10 v/v) to give 6-methoxy-2-(1-{2-[(*E*)-2-phenyl-1-ethenyl]phenyl}methylidene)-1,2,3,4-tetrahydro-1-naphthalenone (**98**) as a light brown solid which was recrystallised with EtOH. Yield: 0.45 g (51 %), t.l.c. system: petroleum ether – EtOAc 3:1 v/v, R_F: 0.68, vanillin stain positive.

Melting point: 120-122 °C.

Microanalysis: $C_{26}H_{22}O_2$. $0.2H_2O$ (370.062): Theoretical: %C= 84.39, %H= 6.10, Found: %C= 84.57, %H= 6.49, N.b. this compound is very hygroscopic, and this microanalysis is the best one obtained after five days drying in the oven.

^{1}H-NMR ($CDCl_3$), δ: 2.93-2.98 (m, 4H, H_a, H_b, H_c and H_d), 3.89 (s, 3H, O-CH_3), 6.72 (d, 1H, J = 2.5 Hz, H-aromatic), 6.92 (dd, 1H, J = 2.5 Hz, 8.7 Hz, H-aromatic), 7.08 (d, 1H, J = 16.1 Hz, H_g), 7.11 (d, 1H, J = 16.1 Hz, H_h), 7.26-7.41 (m, 8H, H-aromatic), 7.51 (d, 1H, J = 7.3 Hz, H-aromatic), 7.76 (d, 1H, J = 7.8 Hz, H-aromatic), 8.06 (s, 1H, -C=C*H*–Ph). 8.20 (d, 1H, J = 8.7 Hz, H-aromatic).

^{13}C NMR ($CDCl_3$), δ: 27. 51 (CH_2, C-3), 29.62 (CH_2, C-4), 55.54 (CH_3, C-4'),

112.40, 113.50, 125.7, 126.33, 126.76, 126.98, 127.92, 128.46, 128.73, 129.60, 130.81, 130.92, 134.72 (CH, aromatic and alkene), 127.12 (C, C-8_a), 134.80 (C, C-2), 136.88 (C, C-1'''), 137.22 (C, C-4_a), 137.25 (C, C-1''), 146.14 (C, C-2''), 163.70 (C, C-6), 186.75 (C, C-1).

4.2.25. 6-Methoxy-2-(2-phenethylbenzyl)-1,2,3,4-tetrahydro-1-naphthalenone (99).

(Mol. Formula: $C_{26}H_{26}O_2$, M. W.: 370.48)

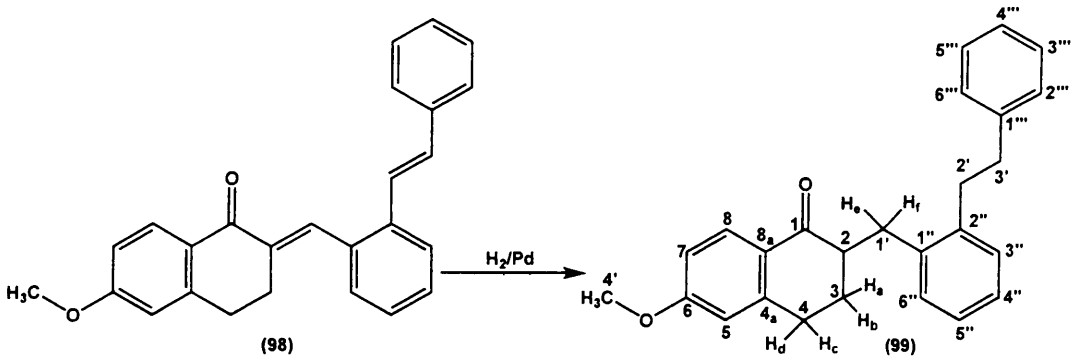

To a suspension of 5% Pd-C (10 mol %) in MeOH (100 mL) was added, under nitrogen, a solution of 6-methoxy-2-(1-{2-[(*E*)-2-phenyl-1-ethenyl]phenyl} methylidene)-1,2,3,4-tetrahydro-1-naphthalenone (**98**) (0.5 g, 1.36 mmol) in MeOH (20 mL). Then, the reaction atmosphere was changed to hydrogen and the reaction mixture stirred at room temperature. After a period of 1 h, the suspension was filtered over a pad of celite and the solvent removed under reduced pressure to give a yellow residue. The residue was purified by flash column chromatography (petroleum ether – EtOAc 100:0 increasing to 90:10 v/v) to give 6-methoxy-2-(2-phenethylbenzyl)-1,2,3,4-tetrahydro-1-naphthalenone (**99**) as a pale orange waxy solid. Yield: 0.32 g (72 %), t.l.c. system: petroleum ether – EtOAc 3:1 v/v, R_F: 0.69, vanillin stain positive.

HRMS (EI): Calculated mass: 371.2006 $[M+H]^+$, Measured mass: 371.2004 $[M+H]^+$.

^{1}H-NMR ($CDCl_3$), δ: 1.80-1.87 (m, 1H, H_a), 2.13-2.08 (m, 1H, H_b), 2.53-2.65 (m, 2H, Ph-CH_2-CH_2-Ph-CH_eH$_f$), 2.83-3.05 (m, 6H, CH_2-Ph-CH_eH$_f$, H_c, H_d), 3.69 (dd, 1H, J = 3.0 Hz, 13.6 Hz, CO-CH-CH_2-Ar), 3.88 (s, 3H, O-CH_3), 6.70 (d, 1H, J = 2.3 Hz, H-aromatic), 6.88 (dd, 1H, J = 2.3 Hz, 8.8 Hz, H-aromatic), 7.20-7.31 (m, 9H, H-aromatic), 8.20 (d, 1H, J = 8.8 Hz, H-aromatic).

^{13}C NMR ($CDCl_3$), δ: 28. 07 (CH_2, C-4), 29.26 (CH_2, C-3), 32.39 (CH_2, C-1'), 34.83 (CH_2, C-2'), 37.74 (CH_2, C-3'), 48.80 (CH, C-2), 55.41 (CH_3, C-4'), 112.46, 113.20, 126.16, 126.37, 127.11, 128.49, 129.28, 128.49, 129.54, 129.91, 130.03, 130.30 (CH, aromatic), 136.88 (C, C-8_a), 138.14 (C, C-1''), 140.15 (C, C-1'''), 141.15 (C, C-2''), 146.47 (C, C-4_a), 163.51 (C, C-6), 197.96 (C, C-1).

4.2.26. Ethyl 6-methoxy-1-oxo-1,2,3,4-tetrahydro-2-naphthalene-carboxylate (100) [238].

(Mol. Formula: $C_{14}H_{16}O_4$, M. W.: 248.27)

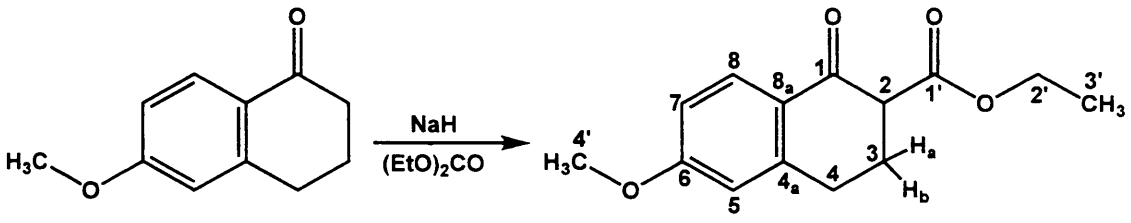

(88) (100)

A solution of 6-methoxy-1-tetralone (**88**) (2.6 g, 15 mmol) in anhydrous toluene (50 mL) was slowly added to a mixture of NaH (2.22 g of 60% dispersion in oil, 55.5 mmol) and diethyl carbonate (5.5 mL, 45 mmol) in anhydrous toluene (10 mL) under reflux. The mixture was stirred for 18 h under reflux, cooled to room temperature and treated with H_2O (50 mL) and glacial AcOH (5 mL) and subsequently extracted with Et_2O (3 x 100mL). The combined organic layers were washed with brine (50 mL), dried ($MgSO_4$) and concentrated under reduced pressure. The oily residue was then purified by flash column chromatography (petroleum ether – EtOAc 100:0 v/v increasing to 80:20 v/v) to give ethyl 6-methoxy-1-oxo-1,2,3,4-tetrahydro-2-naphthalenecarboxylate (**100**) as a colourless solid. Yield: 2.6 g (70%), t.l.c. system: petroleum ether – EtOAc 3:1 v/v, R_F: 0.69, vanillin stain positive.

Melting point: 49-52 °C (lit. m.p. 50-52 °C) [238].

^{1}H-NMR ($CDCl_3$), δ: 1.32 (t, 3H, J = 7.2 Hz, CH_2-CH_3), 2.33-2.37 (m, 1H, H_a), 2.46-2.51 (m, 1H, H_b), 2.94-3.07 (m, 2H, Ar-CH_2-CH_aH_b), 3.57 (dd, 1H, J = 4.7 Hz, 10.2 Hz, CO-CH-CO), 3.87 (s, 3H, O-CH_3), 4.23-4.28 (m, 2H, O-CH_2-CH_3), 6.71 (d, 1H, J = 2.4 Hz, H-aromatic), 6.85 (dd, 1H, J = 2.5 Hz, 8.8 Hz, H-aromatic), 8.04 (d, 1H, J = 8.8 Hz, H-aromatic).

^{13}C NMR ($CDCl_3$), δ: 14.36 (CH_3, C-3'), 26.46 (CH_2, C-3), 28.04 (CH_2, C-4), 54.33 (CH, C-2), 55.46 (CH_3, C-4'), 61.18 (CH_2, C-2'), 112.60, 113.44, 130.26 (CH,

aromatic), 125.40 (C, C-8_a), 146.15 (C, C-4_a), 163.93 (C, C-6), 170.42 (C, C-1'), 191.88 (C, C-1).

4.2.27. Ethyl 2-(2-bromobenzyl)-6-methoxy-1-oxo-1,2,3,4-tetrahydro-2-naphthalenecarboxylate (102).

(Mol. Formula: $C_{21}H_{21}BrO_4$, M. W.: 417.29)

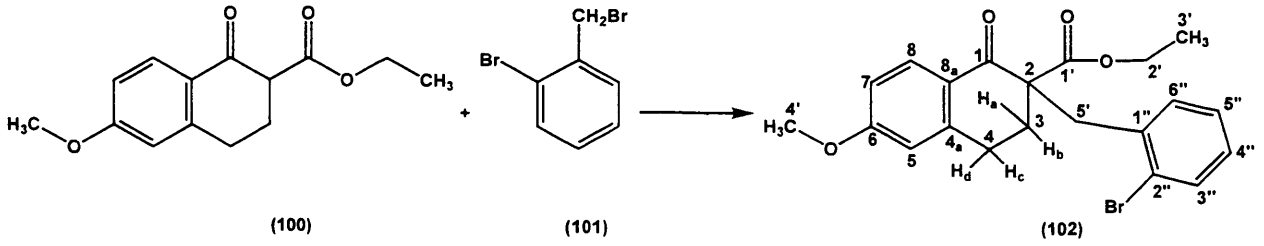

A mixture of NaH (0.415 g of 60% dispersion in oil, 10.37 mmol) and ethyl 6-methoxy-1-oxo-1,2,3,4-tetrahydro-2-naphthalenecarboxylate (**100**) (2.5 g, 10.07 mmol) in DMF (30 mL) was heated at 60 °C for 1 h. A solution of 2-bromobenzyl bromide (**101**) (2.67 g, 10.67 mmol) in DMF (10 mL) was added and the mixture was heated at 60 °C for 8 h. A few drops of H_2O were added and the suspension was extracted with Et_2O (3 x 50 mL). The combined organic layers were washed with brine (50 mL), dried ($MgSO_4$) and concentrated *in vacuo*. The oily residue was purified by flash column chromatography (petroleum ether – EtOAc 100:0 v/v increasing to 80:20 v/v) to give ethyl 2-(2-bromobenzyl)-6-methoxy-1-oxo-1,2,3,4-tetrahydro-2-naphthalenecarboxylate (**102**) as a thick yellow oil. Yield: 2.9 g (69%), t.l.c. system: petroleum ether – EtOAc 3:1 v/v, R_F: 0.69, vanillin stain positive.

HRMS (EI): Calculated mass: 417.0696 (^{79}Br) $[M+H]^+$, Measured mass: 417.0694 $[M+H]^+$.

^{1}H-NMR ($CDCl_3$), δ: 1.17 (t, 3H, J = 7.1 Hz, CH_2-CH_3), 2.01-208 (m, 1H, H_a), 2.59-2.63 (m, 1H, H_b), 2.76-2.81 (m, 1H, H_c), 3.03-3.09 (m, 1H, H_d), 3.69 (dd, 2H, J = 14.2 Hz, 24.4 Hz, C-CH_2-Ar), 3.85 (s, 3H, O-CH_3), 4.14-4.18 (m, 2H, O-CH_2-CH_3), 6.62 (d, 1H, J = 2.5 Hz, H-aromatic), 6.85 (dd, 1H, J = 2.5 Hz, 8.8 Hz, H-aromatic), 7.06 (m, 1H, H-aromatic), 7.19 (td, 1H, H-aromatic), 7.30 (dd, 1H, J = 1.7 Hz, 7.8 Hz, H-aromatic), 7.55 (dd, 1H, J = 1.3 Hz, 8.0 Hz, H-aromatic), 8.09 (d, 1H, J = 8.8 Hz, H-aromatic).

^{13}C NMR ($CDCl_3$), δ: 13.98 (CH_3, C-3'), 26.45 (CH_2, C-3), 30.07 (CH_2, C-4), 38.41 (CH_2, C-5'), 55.41 (CH_3, C-4'), 58.67 (C, C-2), 61.56 (CH_2, C-2'), 112.26,

113.46 (CH, aromatic), 125.94 (C, C-2"), 125.40 (C, C-8_a), 127.26, 128.25, 130.66, 132.17, 132.89 (CH, aromatic), 136.89 (C, C-1"), 145.75 (C, C-4_a), 163.67 (C, C-6), 171.28 (C, C-1'), 193.21 (C, C-1).

4.2.28. 2-(2-Bromobenzyl)-6-methoxy-1,2,3,4-tetrahydro-1-naphthalenone (103) and 2-(2-bromobenzyl)-6-hydroxy-1,2,3,4-tetrahydro-1-naphthalenone (104).

(Compound (**103**): Mol. Formula: $C_{18}H_{17}BrO_2$, M. W.: 345.23)

(Compound (**104**): Mol. Formula: $C_{17}H_{15}BrO_2$, M. W.: 331.20)

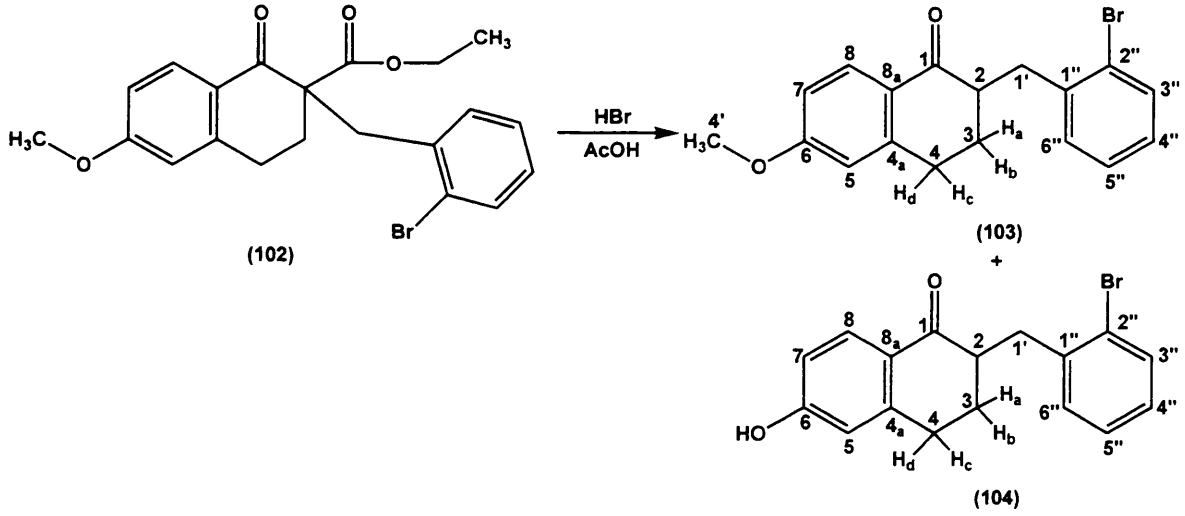

A suspension of ethyl 2-(2-bromobenzyl)-6-methoxy-1-oxo-1,2,3,4-tetrahydro-2-naphthalenecarboxylate (**102**) (2.6 g, 6.23 mmol), 48% HBr (13.76 mL) and 96% AcOH (11.5 mL) was stirred at 120 °C for 1.5 h. The mixture was cooled and diluted with water (5 mL). The reaction mixture was extracted with Et_2O (3 x 50 mL) and the combined organic extracts were dried ($MgSO_4$) and concentrated *in vacuo*. The solid was purified by flash column chromatography (petroleum ether – EtOAc 100:0 v/v increasing to 80:20 v/v) to give 2-(2-bromobenzyl)-6-methoxy-1,2,3,4-tetrahydro-1-naphthalenone (**103**) as a yellow oily product. Yield: 0.55 g (26%), t.l.c. system: petroleum ether – EtOAc 3:1 v/v, R_F: 0.82, vanillin stain positive. Also 2-(2-bromobenzyl)-6-hydroxy-1,2,3,4-tetrahydro-1-naphthalenone (**104**) was produced as a major product in the form of a white solid Yield: 0.8 g (39%), t.l.c. system: petroleum ether – EtOAc 3:1 v/v, R_F: 0.61, vanillin stain positive.

- 2-(2-Bromobenzyl)-6-methoxy-1,2,3,4-tetrahydro-1-naphthalenone (**103**):

HRMS (EI): Calculated mass: 345.0485 (^{79}Br) $[M+H]^+$, Measured mass: 345.0484 $[M+H]^+$.

^{1}H-NMR ($CDCl_3$), δ: 1.86-1.90 (m, 1H, H_a), 2.07-2.11 (m, 1H, H_b), 2.73-2.78 (m, 1H, H_c), 2.85-2.95 (m, 3H, H_d, CO-CH-CH_2-Ar), 3.72 (dd, 1H, J = 4.4 Hz, 13.9 Hz, CO-CH-CH_2-Ar), 3.87 (s, 3H, O-CH_3), 6.69 (d, 1H, J = 2.5 Hz, H-aromatic), 6.85 (dd, 1H, J = 2.5 Hz, 8.8 Hz, H-aromatic), 7.11 (m, 1H, H-aromatic), 7.27-7.31 (m, 2H, H-aromatic), 7.58 (dd, 1H, J = 1.0 Hz, 7.9 Hz, H-aromatic), 8.07 (d, 1H, J = 8.8 Hz, H-aromatic).

^{13}C NMR ($CDCl_3$), δ: 28.11 (CH_2, C-4), 29.34 (CH_2, C-3), 36.08 (CH_2, C-1'), 47.67 (CH, C-2), 55.41 (CH_3, C-4'), 112.45 (CH, C-7), 113.19 (CH, C-5), 124.91 (C, C-2"), 126.15 (C, C-8_a), 127.30 (CH, C-4"), 127.86 (CH, C-5"), 129.97 (CH, C-3"), 131.70 (CH, C-8), 132.96 (CH, C-6"), 139.85 (C, C-1"), 146.45 (C, C-4_a), 163.50 (C, C-6), 197.77 (C, C-1).

• 2-(2-Bromobenzyl)-6-hydroxy-1,2,3,4-tetrahydro-1-naphthalenone (**104**):

Melting point: 171-174 °C.

Microanalysis: Calculated for $C_{17}H_{15}BrO_2$ (331.2), Theoretical: %C= 61.65, %H= 4.56, Found: %C= 61.59, %H= 4.58.

^{1}H-NMR (DMSO-d_6), δ: 1.70-1.77 (m, 1H, H_a), 1.86-1.99 (m, 1H, H_b), 2.61-2.66 (m, 1H, H_c), 2.75-2.86 (m, 3H, H_d, CO-CH-CH_2-Ar), 3.35 (s, 3H, O-CH_3), 3.52 (dd, 1H, J = 4.4 Hz, 13.8 Hz, CO-CH-CH_2-Ar), 6.63 (d, 1H, J = 2.3 Hz, H-aromatic), 6.74 (dd, 1H, J = 2.4 Hz, 8.6 Hz, H-aromatic), 7.17 (m, 1H, H-aromatic), 7.31-7.37 (m, 2H, H-aromatic), 7.60 (dd, 1H, J = 1.0 Hz, 8.0 Hz, H-aromatic), 7.80 (d, 1H, J = 8.6 Hz, H-aromatic), 10.32 (s, 1H, OH).

^{13}C NMR (DMSO-d_6), δ: 27.47 (CH_2, C-4), 28.15 (CH_2, C-3), 35.40 (CH_2, C-1'), 46.57 (CH, C-2), 114.10, 114.40 (CH, aromatic), 124.09 (C, C-2"), 124.16 (C, C-8_a), 127.60, 128.23, 129.40, 131.78, 132.59 (CH, aromatic), 139.28 (C, C-1"), 146.72 (C, C-4_a), 162.05 (C, C-6), 196.47 (C, C-1).

4.2.29. 2-(2-Bromobenzyl)-6-methoxy-1,2,3,4-tetrahydro-1-naphthalenone (103).

(Mol. Formula: $C_{18}H_{17}BrO_2$, M. W.: 345.23)

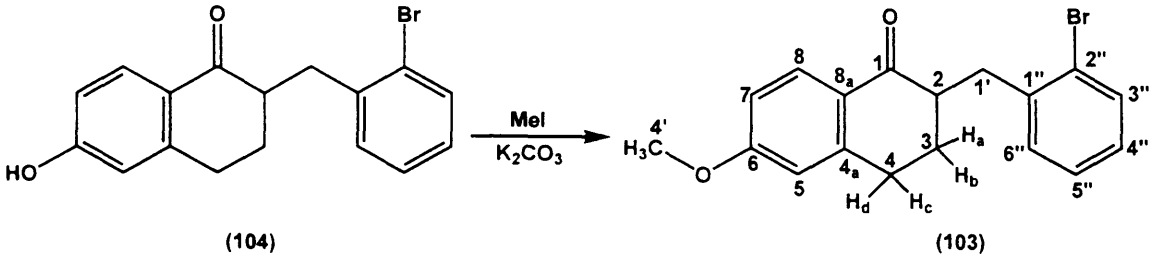

(104) (103)

A solution of 2-(2-bromobenzyl)-6-hydroxy-1,2,3,4-tetrahydro-1-naphthalenone (**104**) (0.7 g, 2.11 mmol) and K_2CO_3 (0.583 g, 4.22 mmol) in anhydrous acetone (30 mL) was refluxed for 2 h, MeI (0.2 mL, 2.47 mmol) was added and the resulting mixture stirred at reflux for a further 3 h. After cooling to room temperature, inorganic salts were filtered off, the filtrate was concentrated under reduced pressure to give 2-(2-bromobenzyl)-6-methoxy-1,2,3,4-tetrahydro-1-naphthalenone (**103**) as a colourless oil. Yield: 0.7 g (96%), t.l.c. system: petroleum ether – EtOAc 3:1 v/v, R_F: 0.82, vanillin stain positive.

^{1}H-NMR and ^{13}C NMR as previously described (see page 183).

4.2.30. 6-Methoxy-2-[2-[(*E*)-2-phenyl-1-ethenyl]benzyl]-1,2,3,4-tetrahydro-1-naphthalenone (105).

(Mol. Formula: $C_{26}H_{24}O_2$, M. W.: 368.47)

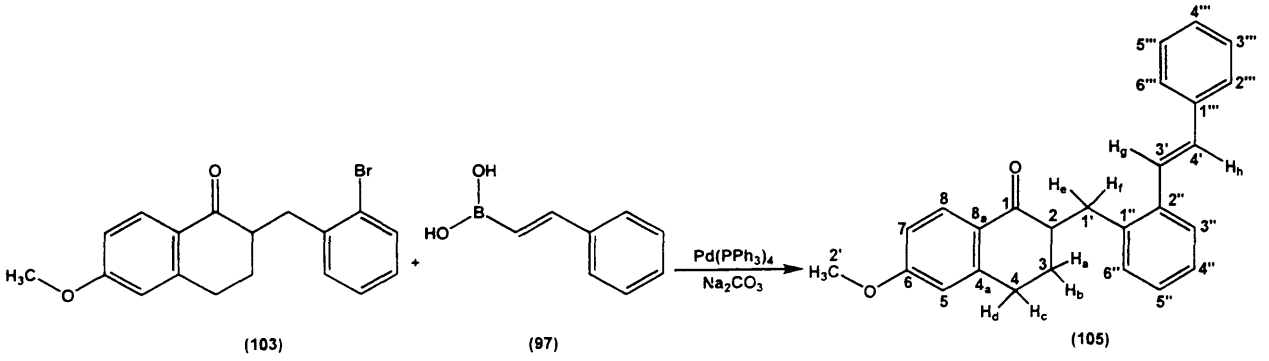

(103) (97) (105)

2M aqueous Na_2CO_3 (5 mL) was added to a solution of 2-(2-bromobenzyl)-6-methoxy-1,2,3,4-tetrahydro-1-naphthalenone (**103**) (0.35 g, 1 mmol) in toluene (15 mL). To the mixture $Pd(PPh_3)_4$ (0.057 g, 0.05 mmol), and then *trans*-2-phenylvinylboronic acid (**97**) (0.296 g, 2 mmol) in ethanol (5 mL) were added. The reaction mixture was refluxed at 90 °C for 5 h. After the reaction was complete, the

residual borane was oxidized by the addition of H_2O_2 (30 %, 2.5 mL) at room temperature for 1 h. The crude product was extracted with CH_2Cl_2 (50 mL) and H_2O (3 x 50 mL). The organic layer was dried over $MgSO_4$ and reduced *in vacuo* to give an oily residue which was purified by flash column chromatography (petroleum ether – EtOAc 100:0 v/v increasing to 70:30 v/v) to give 6-methoxy-2-[2-[(*E*)-2-phenyl-1-ethenyl]benzyl]-1,2,3,4-tetrahydro-1-naphthalenone (**105**) as a thick colourless oil. Yield: 0.35 g (95%), t.l.c. system: petroleum ether – EtOAc 3:1 v/v, R_F: 0.82, vanillin stain positive.

HRMS (EI): Calculated mass: 369.1849 $[M+H]^+$, Measured mass: 369.1843 $[M+H]^+$.

^{1}H-NMR ($CDCl_3$), δ: 1.80-1.87 (m, 1H, H_a), 2.07-2.12 (m, 1H, H_b), 2.65-2.75 (m, 2H, H_c, H_e), 2.85-2.94 (m, 2H, H_d, H_f), 3.87 (s, 3H, O-CH_3), 3.93 (dd, 1H, J = 3.2 Hz, 13.6 Hz, CO-CH-CH_2-Ar), 6.69 (d, 1H, J = 2.5 Hz, H-aromatic), 6.87 (dd, 1H, J = 2.6 Hz, 8.8 Hz, H-aromatic), 7.07 (d, 1H, J = 16.1 Hz, H_h), 7.24-7.32 (m, 5H, H-aromatic, H-g), 7.39 (t, 2H, J = 7.5 Hz, H-aromatic), 7.55 (t, 2H, J = 7.3 Hz, H-aromatic), 7.73 (d, 1H, J = 7.4 Hz, H-aromatic), 8.11 (d, 1H, J = 8.8 Hz, H-aromatic).

^{13}C NMR ($CDCl_3$), δ: 27.95 (CH_2, C-4), 29.17 (CH_2, C-3), 33.45 (CH_2, C-1'), 48.77 (CH, C-2), 55.42 (CH_3, C-2'), 112.46, 113.25, 125.91, 126.33, 126.76, 126.98, 127.69, 128.41, 129.30, 130.05, 130.46, 130.92 (CH, aromatic and alkene), 125.98 (C, C-8_a), 136.40 (C, C-1'''), 137.51 (C, C-1''), 138.26 (C, C-2''), 146.57 (C, C-4_a), 163.54 (C, C-6), 197.91 (C, C-1).

4.2.31. 2-{2-[(*E*)-2-(3,5-Dimethoxyphenyl)-1-ethenyl]benzyl}-6-methoxy-1,2,3,4-tetrahydro-1-naphthalenone (106).

(Mol. Formula: $C_{28}H_{28}O_4$, M. W.: 428.52)

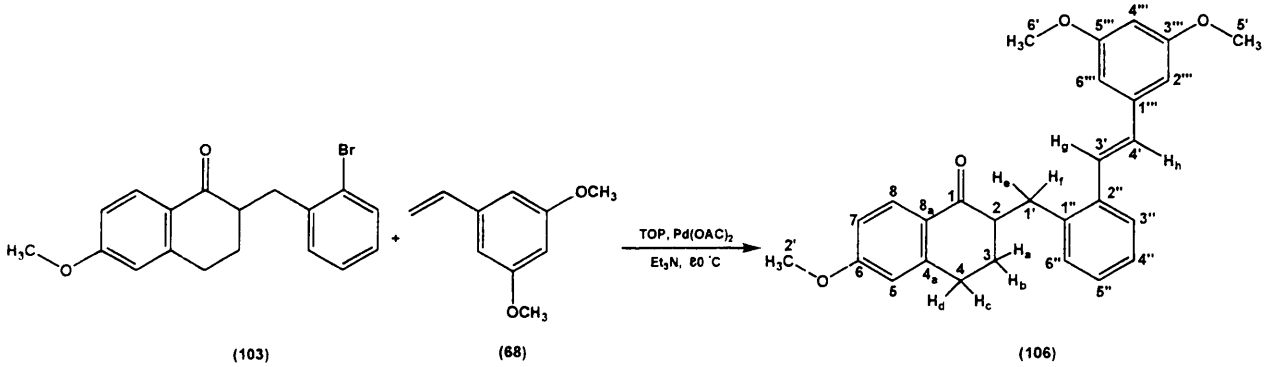

(103) (68) (106)

A solution of 1,3-dimethoxy-5-vinylbenzene (**68**) (0.269 g, 1.64 mmol), $Pd(OAc)_2$ (0.015 g, 0.066 mmol), tri(o-tolyl)phosphine (ToP, 0.03 g, 0.098 mmol) and 2-(2-bromobenzyl)-6-methoxy-1,2,3,4-tetrahydro-1-naphthalenone (**103**) (0.51 g, 1.48 mmol) in dry Et_3N (25 mL) was stirred for 2 h at 60 °C under nitrogen. Then the mixture was stirred for 3 day at 80 °C. After the reaction was complete, the solvent was evaporated. The crude product was dissolved in CH_2Cl_2 (50 mL) and washed with H_2O (50 mL), dried ($MgSO_4$) and the solvent evaporated. The crude product was purified by flash column chromatography (petroleum ether – EtOAc 100:0 v/v increasing to 70:30 v/v) to give 2-{2-[(*E*)-2-(3,5-dimethoxyphenyl)-1-ethenyl]benzyl}-6-methoxy -1,2,3,4-tetrahydro-1-naphthalenone (**106**) as a colourless oil. Yield: 0.45 g (64%), t.l.c. system: petroleum ether – EtOAc 3:1 v/v, R_F: 0.57, vanillin stain positive.

HRMS (EI): Calculated mass: 429.2060 $[M+H]^+$, Measured mass: 429.2067 $[M+H]^+$.

^{1}H-NMR ($CDCl_3$), δ: 1.81-1.85 (m, 1H, H_a), 2.08-2.12 (m, 1H, H_b), 2.65-2.75 (m, 2H, H_c, H_e), 2.66-2.71 (m, 2H, H_d, H_f), 3.86 (s, 3H, O-CH_3), 3.93 (dd, 1H, J = 3.2 Hz, 13.6 Hz, CO-C<u>H</u>-CH_2-Ar), 6.67 (d, 1H, J = 2.5 Hz, H-aromatic), 6.72 (d, 2H, J = 2.3 Hz, H-aromatic), 6.84 (dd, 1H, J = 6.4 Hz, 15.2 Hz, H-aromatic), 6.98 (d, 1H, J = 16.1 Hz, H_h), 7.23-7.33 (m, 4H, H-aromatic, H_g), 7.51 (d, 1H, J = 16.1 Hz, H-aromatic), 7.69 (d, 2H, J = 8.6 Hz, H-aromatic), 8.07 (d, 1H, J = 8.8 Hz, H-aromatic).

^{13}C NMR ($CDCl_3$), δ: 27.99 (CH_2, C-4), 29.17 (CH_2, C-3), 33.49 (CH_2, C-1'), 48.94 (CH, C-2), 55.31 (CH_3, C-2'), 55.42 (CH_3, C-5', C-6'), 100.23, 104.57, 112.43, 113.25, 125.87, 126.54, 126.76, 127.65, 129.97, 130.29, 130.85 (CH, C-aromatic and alkene), 125.87 (C, C-8_a), 136.10 (C, C-1''), 138.49 (C, C-1'''), 139.55 (C, C-2''), 146.57 (C, C-4_a), 161.00 (C, C-3''', C-5'''), 163.50 (C, C-6), 197.77 (C, C-1).

4.3.CYP26A1 Biological Evaluation

4.3.1. Cell Based Assay:

These assays were performed using all-*trans* retinoic acid (ATRA) as substrate and using methods previously developed by our group.

4.3.1.1. Materials and equipment

Material/Chemical	**Source**
ATRA	Sigma Chemicals (Dorset, UK)
[^{3}H-11,12] ATRA (9.25 MBq, 250 μCi)	Perkin Elmer Life Science Ltd. (Massachussets, USA)
HPLC grade solvents (CH_3CN, MeOH)	Fisher Scientific (Leicestershire, UK)
Buffer (see preparation below)	Aldrich Chemicals, UK
EtOAc, EtOH, CH_3Cl, ammonium acetate	Sigma Chemicals, UK
OptiFlow Safe 1 liquid scintillation cocktail	Fisions Chemicals, UK
Borosilicate tubes (12 × 75 mm and 13 × 100 mm)	Corning (New York, USA)
Equipment	**Source**
Centrifuge	MSE Harrier 18/80, Santo, Japan
Pump	Milton-Roy
H_2O bath with shaker	Grant, UK
Rotating evaporator	Christ Alpha RVC (Germany)
10 μm C_{18} μBondapak® 309 × 300 mm column	Waters, UK
Beta-RAM online scintillation detector	LKB Wallace 1217 Rackbeta
Computer	Compaq ™
Laura data acquisition and analysis software	Lablogic Ltd.

- *Preparation of [^{3}H] ATRA stock solution*

  100 μL of 1.2 mM ATRA in EtOH was diluted with 900 μL of of ^{i}PrOH:EtOH 1:1 v/v. To this was added 10 μL of [^{3}H] ATRA (9.25 MBq, 250 μCi).

- 1 mL of the above stock solution contains 10/250 x 9.25 MBq = 0.37 MBq.
- 10 μL of the stock solution contains 0.01 μCi x 0.37 MBq/0.037 MBq = 0.10 μCi.

- *Preparation of phosphate buffer (PBS) (50 mM, pH 7.4)*

  To prepare 1000 mL of phosphate buffer (50 mM, pH 7.4), 6.68 g of disodium hydrogen orthophosphate dodecahydrate was dissolved in 750 mL of H_2O and 1.95 g of monosodium dihydrogen orthophosphate dihydrate was dissolved in 250 mL of H_2O.

- *Preparation of mobile phase:*

  To prepare 1000 mL of the mobile phase, 2.5 g NH_4OAc was dissolved in 250 mL filtered distilled H_2O and 1 mL formic acid was added, followed by completing the solution to 1000 mL using CH_3CN.

- *Preparation of extraction phase:*

  To prepare 500 mL, 0.25g of butylated hydroxyanisole was dissolved in 500 mL EtOAc.

4.3.1.2. Cell-line used

Retinoids have been known to have anti-proliferative effects on the growth of breast carcinoma cells (MCF-7, ZR-75.1) [239-240]. The cell line used in this assay is the oestrogen responsive MCF-7 human mammary-carcinoma cell line which is oestrogen receptor-positive. This cell line is also known as the wild-type MCF-7 cell line. This cell was routinely grown in RPMI medium, supplemented with 5 % (v/v) foetal calf serum (FCS), antibiotics (streptomycin and penicillin) and fungizone at the same concentration of 10 iU/mL. This is the basal medium for MCF-7. This cell line was chosen because it is available at the Welsh School of Pharmacy from the Tenovus group.

4.3.1.3. General method for the MCF-7 wild type ATRA assay

The method described below was based on a modification of the method of Jarno [160] and Farhan *et al* [241].

1. The wild-type MCF-7 cell lines supplied by Tenovus were seeded at 3 x 10^6 cells per plate (12 wells) and left to settle for 24 h.

2. After 24 h, the experimental medium of the wild-type MCF-7 cells were removed and then 1 mL of PBS was added to each well then removed and replaced by fresh experimental medium plus various treatments.
3. These treatments were prepared as follows: each treatment was performed in duplicate (one tube for 2 wells) therefore, 6 well dried and sterile glass tubes were prepared. To the first one was added 200 μL of EtOH as control and to the other five tubes was added separately 200 μL of five different concentrations of the inhibitor ranging from 50-1 μmol one concentration for each tube. 2 mL of the experimental media supplied by Tenovus was added to each tube (1 mL per well). 20 μL of [^{3}H] ATRA was then added quickly to avoid exposure to air to each of the six tube (10 μL per well). The tubes were placed in the H_2O bath and were shaken gently for 10-15 minutes.
4. The corresponding experimental media containing the substrate and inhibitor or control is transferred by the aid of micropipettes to the corresponding well (each glass tube into 2 wells).
5. Tissue culture plates were then wrapped in aluminium foil and incubated for 9 hours.
6. The incubation with the respective substrate was stopped by the addition of 2 % v/v AcOH (100 μL/well).
7. The medium and AcOH from each well was then removed and transferred to borosilicate glass tubes (13 x 100 mm) which contained 2 mL solution of EtOAc with 0.05 % (w/v) butylated-hydroxyanisole.
8. 0.5 mL of distilled H_2O was subsequently added to each well plate and the cells were scrapped off using the rubber end of a 1 mL syringe.
9. The cell suspension from each tube was transferred to the respective glass tubes.
10. Finally, each well was rinsed with 0.5 mL of distilled H_2O and then transferred to the respective glass tubes.
11. The glass tubes were centrifuged (6000 rpm for 15 min at room temperature).
12. The top organic layer containing the substrate and metabolites was transferred into respective borosilicate glass tubes (12 x 75 mm).
13. The tubes were placed in a rotating evaporator for 35 min.
14. The residues in each tube were redissolved in MeOH, then analysed using an on-line radioactive detector connected to a HPLC.

The HPLC system was equipped with a high pressure pump (Milton-Roy pump), injector with a 50 µL loop connected to a beta-RAM radioactivity detector, connected to a Compaq™ computer running Laura® data acquisition and analysis software. This enabled on-line detection and quantification of radioactive peaks. A 10 µm C_{18} µBondapak® 3.9 x 300 mm column (for ATRA assay) operating at ambient temperature was used to separate the metabolites which were eluted with mobile phase at a flow rate of 1.9 mL/min.

The experimental medium used was as follows: RPMI phenol red-free, supplemented with 5 % (v/v) stripped foetal calf serum (S-FCS), antibiotics (streptomycin and penicillin) and fungizone at the same concentration of 10 iU/mL and 2 % v/v L-glutamine (200 mM).

4.3.1.4. Experimental results

The HPLC and the Laura software were used to measure the IC_{50} of our final compounds.

4.3.2. Biochemical Assay:

The inhibitory activity using microsomal preparations from MCF7 cells of the most promising compounds (**14, 15, 19 and 20**) versus CYP26A1 was performed by Dr Caroline Bridgens, Northern Institute for Cancer Research, Newcastle University, Newcastle, United Kingdom. Microsomes were prepared by differential centrifugation of homogenised cells.

4.4.CYP24A1 Biological Evaluation

4.4.1. V79-CYP24 Assay:

The inhibitory activity of the novel compounds versus CYP24A1 was performed by Anna Robotham and Bart Makowski in the labs of Professor Glen Jones, Queen's University Kingston, Ontario, Canada. This involved an *in vitro* assay using recombinant cell lines expressing human CYP24 enzyme (V79-CYP24) [109, 117, 242]. Chinese hamster lung fibroblasts (V79-4) stably expressing either CYP24A1 (WT, L148F, M252L, V391L, or M416T) or CYP27A1 (WT) were maintained and grown using Dulbecco's Modified Eagle Medium (DMEM) purchased from Invitrogen Life Technologies. The growth medium was supplemented with foetal calf serum (FCS) as well as antibiotics (1% v/v) and hygromycin (0.2% v/v) and glucose (1g/500mL). Cells were plated on standard 100mm cell culture dishes and were maintained in a humidified atmosphere of 5% CO_2 in air.

Inhibitor Preparations

Milligram quantities were dissolved in 100% ethanol, while ketoconazole was dissolved in 0.05 M HCl. A 1 mg/mL stock solution was made up for each inhibitor to be tested. Serial 1/10 dilutions were then made to give stock solutions suitable for the low concentration incubations.

Incubations

Prior to incubation, cells were grown on P-150 plates until reaching ~100% confluence. The cells were then subcultured onto 6-well plates in the FCS-supplemented DMEM for 24 hours. The incubation medium for the experiments was bovine serum albumin (BSA) supplemented (1% w/v) DMEM containing the appropriate substrate; 10^5 CPM per well of [1β-^{3}H]1α,25-$(OH)_2D_3$ for the CYP24A1-containing cells and 10 μM of 1α-OH-D_3 for the CYP27A1-containing cells. Each well also contained 1 μL of N,N-diphenyl-p-phenylene diamine (DPPD) (100 μM) to act as an anti-oxidant.

Each assay was conducted with a 'no inhibitor', 'dead cell' and 'no cell' control. The 'dead cell' control was prepared by microwaving the plate of cells for 30 seconds prior to incubation. Each well contained 1mL of incubation medium and each data point was performed in triplicate. Each inhibitor was tested at 4 different concentrations; $1x10^{-4}$ M, $1x10^{-5}$ M, $1x10^{-6}$ M, and $1x10^{-7}$ M. The CYP24A1 assays were carried out at an optimised 6 hour time interval, while the CYP27A1 assay was carried out at a 24 h interval which had been previously optimised. The incubations

were arrested by the addition of 2.5 mL of methanol to each well.

Extraction

The incubation medium was extracted using a modified Bligh and Dyer extraction [243]. For samples destined for HPLC analysis (mainly samples taken from CYP27A1 assays), 2μg of 25-OH-D_3 was added to each sample as an internal recovery standard for subsequent normalisation of metabolite quantification.

Analysis

The samples from the CYP24A1 assays were analysed using scintillation counting of 0.5mL of the aqueous phase (from the Bligh and Dyer extraction). Beckman Coulter Ready Safe™ Liquid Scintillation Cocktail for Aqueous Samples (5mL) was added to the 0.5mL samples, and scintillation counting was performed using a Beckman Coulter L6500 Multipurpose Scintillation Counter.

To determine the amount of metabolite formed in the CYP27A1 incubations, HPLC paired with a photodiode array detector (Waters 996 PDA) or a RadioFlow Detector (LB509; EG&G Berthold, Bad Wilbad, Germany) was used.

4.4.2. VitD3 CLL Study:

The activity of the novel compounds versus these cells was performed by Dr Chris Pepper, University of Wales College of Medicine, Cardiff, United Kingdom.

The assay has been done using the following procedure: freshly isolated peripheral blood lymphocytes ($1x10^6$/mL) were cultured in Eagle medium (Invitrogen, Paisley, United Kingdom) supplemented with penicillin, streptomycin, and 10% foetal calf serum (FCS). The cultures were incubated at 37°C in a humidified 5% carbon dioxide atmosphere in the presence of tested compounds (10^{-12} to 10^{-5} M). In addition, control cultures were carried out to which no drug was added to cultured B-CLL cells. Cells were subsequently harvested by centrifugation and were analysed by flow cytometry. Experiments were performed in duplicate.

5. Conclusion

5. Conclusion:

The main aim for this project was to develop agents which are capable of inhibiting the metabolism of two essential vitamins, A and D3 and their analogues. These vitamins are reported [43, 109] to have the ability to restore the normal function of different types of cancer cells through cellular differentiation. The use of these vitamins and their analogues as anticancer drugs has been restricted due to the development of resistance to their action, and hence the need to increase their doses to reach the optimal plasma concentration and the subsequent development of the side effects. One of the main reasons for this development of resistance is due to the upregulation of the catabolic pathways of these vitamins through the endogenous CYPs. Blocking the effect of these CYPs; i.e. CYP26 inhibition in case of vitamin A and CYP24 inhibition in case of vitamin D3, could result in keeping the optimal plasma concentration level of these vitamins without the need for increasing the dose, and so they can proceed to perform their function in cellular differentiation of the cancer cells.

This project was divided into two main parts; development of potential inhibitors firstly for CYP26 and secondly for CYP24 that could be used in conjunction with vitamin A and vitamin D3 respectively or their analogues in differentiation therapy for different types of cancer, like prostate and breast cancer.

5.1. CYP26A1 inhibitors:

As for CYP26, the project involved first the construction of a pharmacophore model for CYP26A1 inhibitors that was used together with the homology model of CYP26A1 which was developed previously within our group [163] in the rational design of potential inhibitors. This was followed by chemical synthesis and biological evaluation of some of the promising compounds.

The pharmacophore model of CYP26A1 inhibitors was constructed using MOE software. A database of 71 CYP26A1 inhibitors with different conformations has been built and arranged according to activity. This resulted in a pharmacophore with 8 features, as shown in **Figure 5.1.1**.

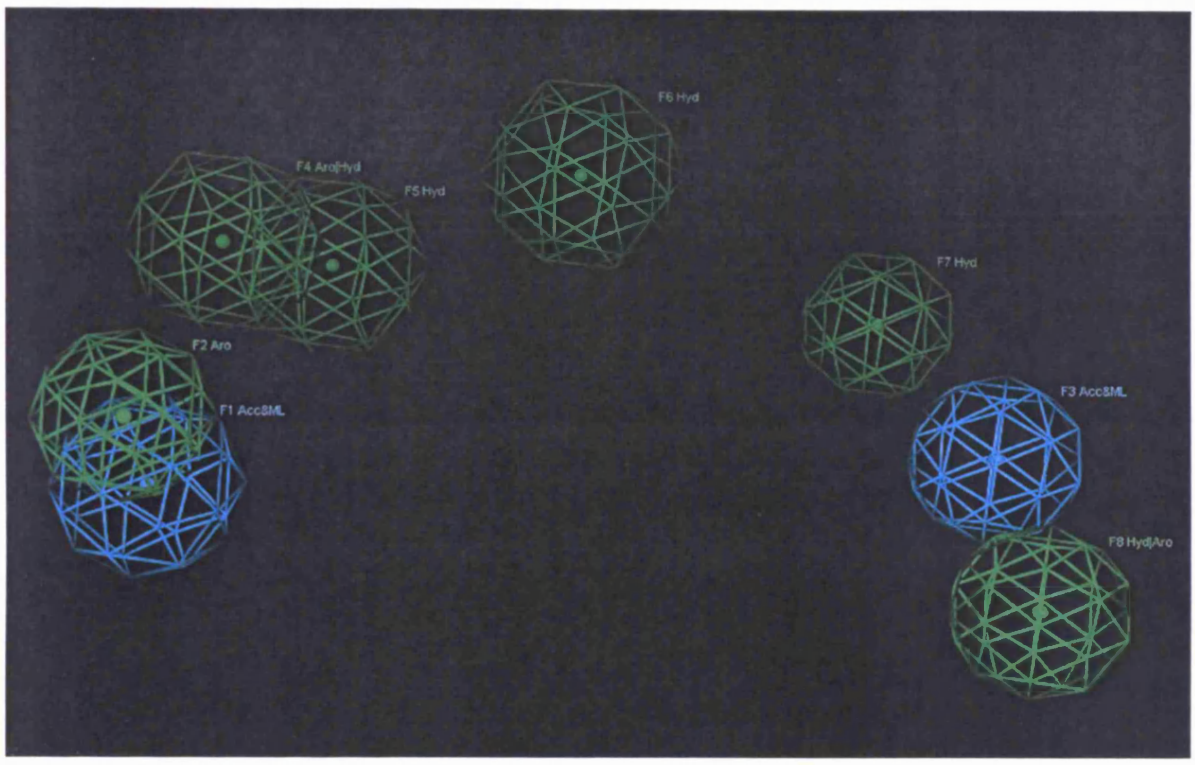

Figure 5.1.1. The suggested pharmacophore from the consensus.

After refining the query, CYP26A1 inhibitors pharmacophore has been found to have 8 features, of which only 5 features should be fulfilled to have an active inhibitor Those five features are F1, F2, F4, F5, F6.Therefore, a partial match could be allowed, so long as these 5 features are fulfilled from the 8 features identified.

The designed model was used first to investigate the ability of our lead compound to tolerate the changes in its structure, and also the model was used to build new inhibitors, which could have reasonable activity.

Investigation of the match of the lead compound with the CYP26A1 inhibitors pharmacophore shows that the lead compound has a very good hit with the essential pharmacophoric features, i.e. F1, F2, F4, F5, F6. As for the changes in the lead compound structure, some changes seems to be tolerated within the pharmacophore, such as replacement of the dimethyl groups with mono methyl or replacement of the naphthyl moiety with a phenyl one. Whereas, other changes in the lead compound, such as removing of the imidazole ring or replacing the imidazole moiety with imidazolyl carbonyloxy one do not seem to be tolerated within the pharmacophore as shown from decreased number of the pharmacophoric hits to the essential pharmacophoric features.

As for the search for new molecules which could have activity as inhibitors of

CYP26A1, the newly designed compounds which resulted from the search through the NCI database, showed very good alignment to the essential pharmacophoric features, i.e. F1, F2, F4, F5, F6.

Regarding the synthesis of new compounds, two series were synthesised for CYP26A1 inhibition. The first series was designed to investigate the effect of changing the structure of the lead compound on the inhibitory activity against CYP26A1 and was depending mainly on presence of imidazole moiety, and the second series was a result of the pharmacophore search and was mainly oxadiazole derivatives. These two series were biologically evaluated using a MCF-7 breast cancer cell assay previously described by our group and also some of the compounds were tested in the biochemical assay.

From the biological data; it seems that the dimethyl substitution (IC_{50} = 2.8 nM) at the α-carbon is much more preferable than the mono-methyl substitution (IC_{50} = 26 nM) as can be seen from the huge decrease in inhibitory activity by about 10 fold. As the free acid seems not to be the active form of our compounds, it may be the presence of the dimethyl group has a steric effect that restrains the attack of the esterase enzyme. Of course, this steric effect decreases with the introduction of the mono-methyl group resulting in more rapid removal of the esters to give the free acid, this may explain the loss in inhibitory activity. Also it appears that the difference in the diastereoisomerism does not affect the inhibitory activity.

The presence of the imidazole is essential for the inhibitory activity, removal of the imidazole or replacement with the 1,3,4-oxadiazole ring, or introducing of a link between the imidazole and the β-carbon, dramatically decreases the activity. Introduction of a link between the imidazole and the β-carbon may make the compound too big to enter the active site cavity of the enzyme. As for the replacement of the imidazole with the 1,3,4-oxadiazole part, although these compounds showed good match to the CYP26A1 pharmacophore model and dock very well in the CYP26A1 homology model, the decrease in the flexibility of the molecules may explain the decrease in the activity. The non-conformity between the biological results and the modelling suggest a limitation of the CYP26A1 pharmacophore and homology models.

The CYP26A1 biochemical assay of the most promising compounds showed that some compounds are good CYP26A1 inhibitors being about 70-100 times more

active than the well-known CYP26A1 inhibitor liarazole (IC_{50}= 6 μM). However, they were still less active than R115866. Also, these compounds are much less active than our lead compound which showed an IC_{50} of 2.8 nM.

5.2. CYP24A1 inhibitors:

As for CYP24A1 inhibition, two series; the azoles and the tetralones, were synthesised. Most of these compounds has been tested against CYP24A1 and CYP27A1.

The results showed that the inclusion of a double bond at the position of attachment between the tetralone and benzyl ring appeared to reduce the inhibitory effect of the inhibitors. The double bond will conjugate with the adjacent phenyl group resulting in decreased conformational flexibility of the structure. This loss of flexibility could inhibit the entrance of the inhibitor through the access channel of CYP24A1 thus decreasing its access to the enzyme cavity where it would exert its inhibitory effect. Alternatively, the loss of conformational flexibility could prevent a favourable conformation that stabilises the inhibitor inside the enzyme cavity.

The strong inhibitory capacity of 6-methoxy-2-[2-(trifluoromethyl)benzyl]-1,2,3,4-tetrahydro-1-naphthalenone could reflect a trend observed in inhibitor design; the addition of fluorine groups increases the inhibitory capacity of a compound. It has been suggested that this increase is not caused by a stronger enzyme-inhibitor complex, but by increasing the cell-membrane penetrating capacity and thus increasing the bio-availability. However, many of the compounds appear to be hydrophobic and should have little problem penetrating cell membranes. As such, the fluorination may have a stabilising effect on the inhibitor inside the enzyme resulting in more effective inhibition.

As for the azoles, from the results, it seems that the azoles would be much more active than the tetralone derivatives with *N*-[2-(1*H*-1-Imidazolyl)-2-phenylethyl]-4-[(*E*)-2-phenyl-1-ethenyl]benzamide (IC_{50} = 0.3 μM) displaying greater inhibitory activity than the standard ketoconazole (IC_{50} = 0.52 μM). This activity may also be attributed to the resemblance between the structure of these azoles and calcitriol.

Also the activity of some of the novel compounds versus B-cell chronic lymphocytic leukemia (B-CLL) cells was performed. The results showed that the azole compounds have very good antiproliferative activity against B-CLL. Introduction of the dimethoxy groups did not greatly affect the activity, with only a fold increase in the activity which was the same case for the introduction of the fluorine group, as both compounds with or without the fluorine group showed comparable activity. Also, from the results, the tetralones seem to be much less active than the azoles, which suggest the low antiproliferative activity of these tetralones, this may reflect the difference in CYP24 inhibitory activity. These results encourages for further development and investigation of this type of azoles as CYP24A1 inhibitors.

6. References

1) Goodsell, D. S. The molecular perspective: Cytochrome P450. *Stem Cells* **2001,** *19,* 263-264.

2) Schenkman, J. B.; Greim, H. "*Cytochrome P450*", 1st ed.; Springer-Verlag: Berlin **1993**, Chapter 1, pp 3-13.

3) Williams, R. T. "*Detoxication mechanisms: The metabolism and detoxication of drugs, toxic substances, and other organic compound*", 2nd ed., Wiley: San Francisco, **1959**.

4) Brodie B. B.; Axelrod, J.; Cooper J. R.; Gaudette, L. E.; La Du, B. N.; Mitowa, C.; Udenfriend, S. Detoxication of drugs and other foreign compounds by liver microsomes. *Science* **1955**, *121*, 603-604.

5) Müller, G. C.; Miller, J. A. The metabolism of methylated aminoazo dyes II. oxidative demethylation by rat liver homogenates. *J. Biol. Chem.* **1953**, *202*, 579-587.

6) Guengerich F. P. Cytochromes P450, drugs, and diseases. *Mol. Interventions* **2003**, *3*, 194-204.

7) Anandatheerthavarada, H. K.; Vijayasarathy, C.; Bhagwat, S. V.; Miswas, G.; Mullick, J.; Avadhani, N. G. Physiological role of the N-terminal processed P4501A1 targeted to mitochondria in erythromycin metabolism and reversal of erythromycin-mediated inhibition of mitochondrial protein synthesis. *J. Biol. Chem.* **1999**, *274*, 6617–6625.

8) Nelson, D.R. Comparison of P450s from human and fugu: 420 million years of vertebrate P450 evolution. *Arch. Biochem. Biophys.* **2003**,*409*, 18–24.

9) Guengerich, F.P. "*Human cytochrome P450 enzymes In Cytochrome P450*", 3rd ed. **2003.**

10) Brodie, A.M.H. Aromatase inhibition and its pharmacologic implications. *Biochem. Pharmacol.* **1985**, *34*, 3213–3219.

11) Vane, J.R. "*Advances in prostaglandin and thromboxane research*", Raven Press: New York, **1978**, 27–44.

12) Fu, G.K.; Lin, D.; Zhang, M.Y.H.; Bikle, D.D.; Schackleton, C.H.L.; Miller, W.L.; Portale, A.A. *Mol. Endocrinol.* **1997**, *11*, 1961–1970.

13) Adamson, P. C. All-Trans-Retinoic Acid Pharmacology and Its Impact on the Treatment of Acute Promyelocytic Leukemia. *Oncologist* **1996**, *1*, 305-314.

14) Nakagawa, T.; Shimizu, M.; Shirakami, Y.; Tatebe, H.; Yasuda, I.; Tsurumi, H.; Moriwaki, H. Synergistic effects of acyclic retinoid and gemcitabine on growth inhibition in pancreatic cancer cells. *Cancer lett.* **2009**, *273*, 250-256.

15) Gudas, L. J. Retinoids and vertebrate development. *J Biol. Chem.* **1994,** *269,* 15399-15402.

16) Tate, B. F.; Levin, A. A.; Grippo, J. F. The discovery of 9-*cis* retinoic acid: a hormone that binds the retinoid-X receptor. *Trends Endocrinol. Metab.* **1994**, *5*, 189-194.

17) Lavau, C.; Dejean, A. The t(15;17) translocation in acute promyelocytic leukemia. *Leukemia* **1994**, *8*, 1615-1621.

18) Fontana, J. A.; Rishi A. K. Classical and novel retinoids: their targets in cancer therapy. *Leukemia* **2002**, *16*, 463–472.

19) Petkovich, M.; Brand, N. J.; Krust, A.; Chambon, P. A human retinoic acid receptor which belongs to the family of nuclear receptors. *Nature* **1987,** *330*, 444-450.

20) Giguere, V.; Ong, E. S.; Segui, P; Evans, R. M. Identification of a receptor for the morphogen retinoic acid. *Nature* **1987,** *330*, 624-629.

21) Mangelsdorf, D. J.; Ong, E. S.; Dyck, J. A.; Evans, R. M. Nuclear receptor that identifies a novel retinoic acid response pathway. *Nature* **1990**, *345*, 224-229.

22) Mangelsdorf, D. J.; Umesono, K.; Kliewer, S. A.; Borgmeyer, U.; Ong, E. S.; Evans, R. M. A direct repeat in the cellular retinol-binding protein type II gene confers differential regulation by RXR and RAR. *Cell* **1991**, *66*, 555-561.

23) Mangelsdorf, D. J.; Borgmeyer, U.; Heyman, R. A.; Zhou, J. Y.; Ong, E. S.; Oro, A. E.; Kakizuka, A.; Evans, R. M. Characterization of three RXR genes that mediate the action of 9-*cis* retinoic acid. *Genes Dev.* **1992**, *6*, 329-344.

24) Heyman, R. A; Mangelsdorf, D. J.; Dyck, J. A.; Stein, R. B.; Eichele, G.; Evans, R. M.; Thaller, C. 9-*cis* retinoic acid is a high affinity ligand for the retinoid X receptor. *Cell* **1992**, *68*, 397-406.

25) Napoli, J. L; Posch, K. P.; Fiorella, P. D.; Boerman, M. Physiological occurrence, biosynthesis and metabolism of retinoic acid: evidence for roles of cellular retinol-binding protein (CRBP) and cellular retinoic acid-binding protein (CRABP) in the pathway of retinoic acid homeostasis. *Biomed. Pharmacother.* **1991**, *45*, 131-143.

26) Ross, A. C. Cellular metabolism and activation of retinoids: roles of cellular retinoid-binding proteins. *FASEB J.* **1993**, *7*, 317-327.

27) Donovan, M.; Olofsson, B.; Gustafson, A. L.; Dencker, L.; Eriksson, U. The cellular retinoic acid binding proteins. *J. Steroid Biochem. Mol. Biol.* **1995**, *53*, 459-465.

28) Boylan, J. F.; Gudas, L. J. The level of CRABP-I expression influences the amounts and types of all-*trans*-retinoic acid metabolites in F9 teratocarcinoma stem cells. *J. Biol. Chem.* **1992**, *267*, 21486-21491.

29) Napoli, J. L.; Boerman, M.; Chai, X.; Zhai, Y.; Fiorella, P. D. Enzymes and binding proteins affecting retinoic acid concentrations. *J. Steroid Biochem. Mol. Biol.* **1995**. 53, 497-502.

30) Njar, V. C. O.; Gediya, L.; Purushottamachar, P.; Chopra, P.; Vasaitis, T. S.; Khandelwal, A.; Mehta, J.; Huynh, C.; Belosay, A.; Patel, J. Retinoic acid metabolism blocking agents (RAMBAs) for treatment of cancer and dermatological diseases. *Bioorg. Med. Chem.* **2006**, *14*, 4323–4340.

31) Soprano, K. J.; Soprano, D. R. Retinoic acid receptors and cancer. *J. Nutr.* **2002**, *132*, S3809– S3813.

32) De Luca, L. M. Retinoids and their receptors in differentiation, embryogenesis, and neoplasia. *FASEB J.* **1991,** *5*, 2924–2933.

33) Gudas, L.; Sporn, M. B.; Roberts, A. B. *"The Retinoids: biology, chemistry and medicine"*, 2nd ed., Raven Press, New York, **1993**, pp. 443–520.

34) Sun, S.; Yue, P.; Mao, L.; Dawson, M. I.; Shroot, B.; Lamph, W. W.; Heyman, R. A.; Chandraratna, R. A. S.; Shudo, K.; Hong, W. K.; Lotan, R. Identification of receptor-selective retinoids that are potent iInhibitors of the growth of human head and neck squamous cell carcinoma cells. *Clin. Cancer Res.* **2000**, *6*, 1563–1573.

35) Lippman, S. M.; Parkinson, D. R.; Itri, L. M.; Weber, R. S.; Schantz, S. P.; Ota, D. M.; Schusterman, M. A.; Krakoff, I. H.; Gutterman, J. U.; Hong, W. K. 13-*cis*-Retinoic Acid and interferon α-2a: effective combination therapy for advanced squamous cell carcinoma of the skin. *J. Natl. Cancer Inst.* **1992**, *84*, 235-241.

36) Edward, M.; Mackie, R. M. Retinoic acid-induced inhibition of lung colonization and changes in the synthesis and properties of glycosaminoglycans of metastatic B16 melanoma cells. *J. Cell Sci.* **1989**, *94*, 537-543.

37) Zheng, Y.; Kramer, P. M.; Lubet, R. A.; Steele, V. E.; Kelloff, G. J.; Pereira, M. A. Effect of retinoids on AOM-induced colon cancer in rats: modulation of cell proliferation, apoptosis and aberrant crypt foci. *Carcinogenesis* **1999**, *20*, 255–260.

38) Grubbs, C. J.; Lubet, R. A.; Atigadda, V. R.; Christov, K.; Deshpande, A. M.; Tirmal, V.; Xia, G.; Bland, K. I.; Eto, I.; Brouillette, W. J.; Muccio, D. D. Efficacy of new retinoids in the prevention of mammary cancers and correlations with short-term biomarkers. *Carcinogenesis* **2006**, *27*, 1232–1239.

39) Blutt, S. E.; Allegretto, E. A.; Pike, J. W.; Weigel, N. L. 1,25-Dihydroxyvitamin D3 and 9-*cis*-retinoic acid act synergistically to inhibit the growth of LNCaP prostate cells and cause accumulation of cells in G1. *Endocrinology* **1997**, *138*. 1491-1497.

40) Guo, W.; Gill, P. S.; Antak, T. Inhibition of AIDS-Kaposi's sarcoma cell proliferation following retinoic acid receptor activation. *Cancer Res.* **1995**, *55*, 823-829.

41) Nagpal, S.; Cai, J.; Zheng, T.; Al Patel, S.; Masood, R.; Lin, G. Y.; Friant, S.; Johnson, A.; Smith, D. L.; Chandraratna, R. A. S.; Gill, P. S. Retinoid antagonism of NF-IL6: insight into the mechanism of antiproliferative effects of retinoids in kaposi's sarcoma. *Mol. Cell. Biol.* **1997**, *17*, 4159–4168.

42) Flynn, P. J.; Miller, W. J.; Weisdorf, D. J.; Arthur, D. C.; Brunning, R.; ; Branda, R. F. Retinoic acid treatment of acute promyelocytic leukemia: in vitro and in vivo observations. *Blood* **1983**, *62*, 1211-1217.

43) Breitman, T. R.; Selonick, S. E.; Collins, S. J. Induction of differentiation of the human promyelocytic leukemia cell line (HL-60) by retinoic acid. *Proc. Natl. Acad. Sci. U.S.A.* **1980**, *77*, 2936–2940.

44) Kelloff, G. J.; Boone, C. W.; Crowell, J. A.; Steele, V. E.; Lubet, R. A.; Doody, L. A.; Malone, W. F.; Hawk, E. T.; Sigman, C. C. New agents for cancer chemoprevention. *J. Cell. Biochem.* **1996**, *26*, S1–S28.

45) Lotan, R. Retinoids in chemoprevention. *FASEB J.* **1996**, *10*, 1031–1039.

46) Anadolu, R. Y.; Sen, T.; Tarimci, N.; Birol, A.; Erdem, C. *J. Eur. Acad. Dermatol.* **2004**, *18*, 416–421.

47) Saurat, J. Retinoids and psoriasis: Novel issues in retinoid pharmacology and implications for psoriasis treatment. *J. Am. Acad. Dermatol.* **1999**, *41*, S2-S6.

48) Chung, J. C.; Law, M. Y.; Elliott, S. T.; Elias, P. M. Diazacholesterol-induced ichthyosis in the hairless mouse. Assay for comparative potency of topical retinoids. *Arch Dermatol.* **1984**, *120*, 342-347.

49) Brecher, A. R.; Orlow, S. J. Oral retinoid therapy for dermatologic conditions in children and adolescents. *J. Am. Acad. Dermatol.* **2003**, *49*, 171-182.

50) Dillehay, D.L.; Walia, A. S.; Lamon, E.W. Effects of Retinoids on Macrophage Function and IL-1 Activity. *J. Leukocyte Biol.* **1988**, *44*, 353-360.

51) Murtaugh, M.P.; Dennison, O.; Stein, J. P.; Davies, P. J. A.; Retinoic acid-induced gene expression in normal and leukemic myeloid cells. *J. Exp. Med.* **1986**, *163*, 1325-1330.

52) Goldman, R. Effect of retinoic acid on the proliferation and phagocytic capability of murine macrophage-like cell lines. *J. Cell. Physiol.* **1984**, *120*, 91-102.

53) Blalock, J. E.; Gifford, G. E. Retinoic acid (vitamin A acid) induced transcriptional control of interferon production. *Proc. Natl. Acad. Sci. U.S.A.* **1977**, *74*, 5382-5386.

54) Day, R. M.; Lee, Y. H.; Park, A.; Suzuki, Y. J. Retinoic acid inhibits airway smooth muscle cell migration. *Am. J. Resp. Cell Mol.* **2006**, *34*, 695-703.

55) Paiva, S. A. R.; Matsubara, L. S., Matsubara, B. B.; Minicucci, M. F.; Azevedo, P. S.; Campana, A. O.; Zornoff, L. A. M. Retinoic Acid Supplementation Attenuates Ventricular Remodeling after Myocardial Infarction in Rats. *J. Nutr.* **2005**, *135*, 2326–2328.

56) Paquette, D.; Badiavas, E.; Falanga, V. Short-contact topical tretinoin therapy to stimulate granulation tissue in chronic wounds. *J. Am. Acad. Dermatol.* **2001**, *45*, 382-386.

57) Luu, L.; Ramshaw, H.; Tahayato, A.; Stuart, A.; Jones, G.; White, J.; Petkovich, M. Regulation of retinoic acid metabolism. *Advan. Enzyme Regul.* **2001**, *41*, 159–175.

58) Pautus, S.; Yee, S. W.; Jayne, M.; Coogan, M. P.; Simons, C. Synthesis and CYP26A1 inhibitory activity of 1-[benzofuran-2-yl-(4-alkyl/aryl-phenyl)-methyl]-1*H*-triazoles. *Bioorg. Med. Chem.* **2006**, *14*, 3643–3653.

59) White, J.; Guo, Y.; Baetz, K.; Beckett-Jones, B.; Bonasoro, J.; Hsu, K.; Dilworth, J.; Jones, G.; Petkovich, M. Identification of the retinoic acid-inducible all-*trans*-retinoic acid 4-hydroxylase. *J. Biol. Chem.* **1996**, *271*, 29922–29927.

60) Nelson, D. R. A second CYP26 P450 in humans and zebrafish: CYP26B1. *Arch. Biochem. Biophys.* **1999**, *371*, 345–347.

61) Sonneveld, E.; Van der Saag, P. T. Metabolism of retinoic acid: implications for development and cancer. *Int. J. Vitam. Nutr. Res.* **1998**, *68*, 404–410.

62) Trofimova-Griffin, M. E.; Brzezinski, M. R.; Juchau, M. R. Patterns of CYP26 expression in human prenatal cephalic and hepatic tissues indicate an important role during early brain development. *Dev. Brain Res.* **2000**, *120*, 7–16.

63) Makin, G.; Lohnes, D.; Byford, V.; Ray, R.; Jones, G. Target cell metabolism of 1,25-dihydroxyvitamin D3 to calcitroic acid. Evidence for a pathway in kidney and bone involving 24-oxidation. *Biochem. J.* **1989**, *262*, 173–180.

64) Pijnappel, W. M. M.; Hendriks, H. F. J.; Folkers, G. E.; van den Brink, C. E.; Dekker, E. J.; Edelenbosch, C.; van der Saag, P. T.; Durston, A. J. The retinoid ligand 4-oxo-retinoic acid is a highly active modulator of positional specification. *Nature* **1993**, *366*, 340–344.

65) de Roos, K.; Sonneveld, E.; Compaan, B.; ten Berge, D.; Dunston, A. J.; van der Saag, P. T. Expression of retinoic acid 4-hydroxylase (CYP26) during mouse and *Xenopus laevis* embryogenesis. *Mech. Dev.* **1999**, *82*, 205–211.

66) Smith, M. A.; Adamson, P. C.; Bails, F. M.; Feusner, J.; Aronson, L.; Murphy, R. F.; Horowitz, M. E.; Reaman, G.; Hammond, G. D.; Hittelman, W. N.; Poplack, D. G. Phase I and pharmacokinetic evaluation of all-trans-retinoic acid in pediatric patients with cancer. *J. Clin. Oncol.* **1992**, *10*, 1666–1673.

67) Warrell, R. P., Jr. Retinoid resistance in acute promyelocytic leukemia: new mechanisms, strategies, and implications. *Blood* **1993**, *82*, 1949–1953.

68) Warrell, R. P., Jr.; de The, H.; Wang, Z. Y.; Degos, L. Acute promyelocytic leukemia. *N. Engl. J. Med.* **1993**, *329*, 177–189.

69) Kizaki, M.; Ueno, H.; Yamazeo, Y.; Shimada, M.; Takayama, N.; Muto, A.; Matsushita, H.; Nakajima, H.; Marikawa, M.; Koeffler, H. P.; Ikeda, Y. Mechanisms of retinoid resistance in leukemic cells: possible role of cytochrome P450 and P-glycoprotein. *Blood* **1996**, *87*, 725–733.

70) Reichman, M. E.; Hayes, R. B.; Ziegler, R. G.; Schatzkin, A.; Taylor, P. R.; Kahel, L. L.; Fraumein, J. F., Jr. Serum vitamin A and subsequent development of prostate cancer in the first national health and nutrition examination survey epidemiologic follow-up study. *Cancer Res.* **1990**, *50*, 2311–2315.

71) Peehl, D. M.; Wong, S. T.; Stamey, T. A. Vitamin A regulates proliferation and differentiation of human prostatic epithelial cells. *Prostate* **1993**, *23*, 69–78.

72) Pasquali, D.; Rossi, V.; Prezioso, D.; Gentile, V.; Colantuani, V.; Lotti, T.; Bellastella, A.; Sinisi, A. A. Changes in tissue transglutaminase activity and

expression during retinoic acid-induced growth arrest and apoptosis in primary cultures of human epithelial prostate cells. *J. Clin. Endocrinol. Metab.* **1999**, *84*, 1463–1469.

73) Orfanos, C. E.; Zouboulis, C. C.; Almond-Roestler, B.; Geilen, C. C. Current use and future potential role of retinoids in dermatology. *Drugs* **1997**, *53*, 358–388.

74) White, J. A.; Beckett, B.; Scherer, S. W.; Herbrick, J.; Petkovich, M. P450RAI (CYP26A1) maps to human chromosome 10q23–q24 and mouse chromosome 19C2-3. *Genomics* **1998**, *48*, 270–272.

75) Gray, I. C.; Phillips, S. M.; Lee, S. J.; Neoptolemos, J. P.; Weissenbach, J.; Spurr, N. K. Loss of the chromosomal region 10q23–25 in prostate cancer. *Cancer Res.* **1995**, *55*, 4800–4803.

76) Gurrieri, F.; Prinos, P.; Tackels, D.; Kilpatrick, M. W.; Allanson, J.; Genuardi, M.; Vuckov, A.; Nanni, L.; Sangiorgi, E.; Gorofola, G.; Nunes, M. E.; Neri, G.; Schwartz, C.; Tsipouras, P. A split hand-split foot (SHFM3) gene is located at 10Q24→25. *Am. J. Med. Genet.* **1996**, *62*, 427–436.

77) White, J. A.; Ramshaw, H.; Taimi, M.; Stangle, W.; Zhang, A.; Evaeringham, S.; Creighton, S.; Tam, S.-P.; Jone, G.; Petkovich, M. Identification of the human cytochrome P450, P450RAI-2, which is predominantly expressed in the adult cerebellum and is responsible for all-trans-retinoic acid metabolism. *Proc. Natl. Acad. Sci. U.S.A.* **2000**, *97*, 6403–6408.

78) Taimi, M.; Helvig, C.; Wisniewski, J.; Ramshaw, H.; White, J.; Amad, M.; Korczak, B.; Petkovich, M. A novel human cytochrome P450, CYP26C1, involved in metabolism of 9-cis and all-trans isomers of retinoic acid. *J. Biol. Chem.* **2004**, *279*, 77–85.

79) Williams, J. B.; Napoli, J. L. Inhibition of retinoic acid metabolism by imidazole antimycotics in F9 embryonal carcinoma cells. *Biochem. Pharmacol.* **1987**, *36*, 1386-1388.

80) Wauwe, J. P. V. ; Coene, M-C.; Goossens, J.; Van Nijen, G.; Cools, W.; Lauwers, W. Ketoconazole inhibits the in vitro and in vivo metabolism of all-trans-retinoic acid. *J. Pharm. Exper. Ther.* **1988**, *245*, 718-722.

81) Wauwe, J. V.; Nyen, G. V.; Coene, M-C.; Stoppie, P.; Cools, W.; Goossens, J.; Borghgraef, P.; Janssen, P. A. J. Liarozole, an inhibitor of retinoic acid metabolism, exerts retinoid- mimetic effects in vivo. *J. Pharm. Exper. Ther.* **1992**, *261*, 773-779.

82) Goss, P. E.; Strasser, K.; Marques, R.; Clemons, M.; Oza, A.; Goel, R.; Blackstein, M.; Kaizer, L.; Sterns, E. E.; Nabholtz, J-M.; De Coster, R.; Crump, M.; Abdolell, M.; Qi, S. Liarozole fumarate (R85246): In the treatment of ER negative, Tamoxifen refractory or chemotherapy resistant postmenopausal metastatic breast cancer. *Breast Cancer Res. Treat.* **2000**, *64*, 177–188.

83) Lorię, E. P.; Li, H.; Vahlquist, A.; Törmä, H. The involvement of cytochrome p450 (CYP) 26 in the retinoic acid metabolism of human epidermal keratinocytes. *Biochim. Biophys. Acta* **2009**, *1791*, 220-228.

84) Stoppie, P.; Borgers, M.; Borghgraef, P.; Dillen, L.; Goossens, J.; Sanz, G.; Szel, H.; Hove, C. V.; Nyen, G. V.; Nobels, G.; Bossche, H. V.; Venet, M.; Willemsens, G.; Wauwe, J. V. R115866 inhibits all-trans-retinoic acid metabolism and exerts retinoidal effects in rodents. *J. Pharm. Exper. Ther.* **2000**, *293*, 304-312.

85) Heusden, J. V.; Ginckel, R. V.; Bruwierel, H.; Moelans, P.; Janssen, B.; Floren, W.; der Leede, B. J. V.; Dun, J. V.; Sanz, G.; Venet, M.; Dillen, L.; Hove, C. V.; Willemsens, G.; Janicot, M.; Wouters, W. Inhibition of all-trans-retinoic acid metabolism by R116010 induces antitumour activity. *British J. Cancer* **2002**, *86*, 605 – 611.

86) Njar, V. C. O.; Nnaneb, I. P.; Brodie, A. M. H. Potent inhibition of retinoic acid metabolism enzyme(s) by novel azolyl retinoids. *Bioorg. Med. Chem. Lett.* **2000**, *10*, 1905-1908.

87) Patel, J. B.; Huynh, C. K.; Handratta, V. D.; Gediya, L. K.; Brodie, A. M. H.; Goloubeva, O. G.; Clement, O. O.; Nanne, I. P.; Soprano, D. R.; Njar, V. C. O. Novel retinoic acid metabolism blocking agents endowed with multiple biological activities are efficient growth inhibitors of human breast and prostate cancer cells in vitro and a human breast tumor xenograft in nude mice. *J. Med. Chem.* **2004,** *47,* 6716-6729.

88) Huynh, C. K.; Brodie, A. M. H.; Njar, V. C. O. Inhibitory effects of retinoic acid metabolism blocking agents (RAMBAs) on the growth of human prostate cancer cells and LNCaP prostate tumour xenografts in SCID mice. *British J. Cancer* **2006**, *94*, 513 – 523.

89) Kirby, A. J.; Le Lain, R.; Maharlouie, F.; Mason, P.; Nicholls, P. J.; Smith, H. J.; Simons C. Inhibition of retinoic acid metabolising enzymes by 2-(4-aminophenylmethyl)-6-hydroxy-3,4-dihydronaphthalen-1(2H)-one and related compounds. *J. Enzym. Inhib. Med. Chem.* **2003**, *18*, 27–33.

90) Mulvihill, M. J.; Kan, J. L. C.; Beck, P.; Bittner, M.; Cesario, C.; Cooke, A.; Keane, D. M.; Nigro, A. I.; Nillson, C.; Smith, V.; Srebernak, M.; Sun, F-L.; Vrkljan, M.; Winski, S. L.; Castelhano, A. L.; Emersonb, D.; Gibsona, N. Potent and selective [2-imidazol-1-yl-2-(6-alkoxy-naphthalen-2-yl)-1-methyl-ethyl]-dimethyl-amines as retinoic acid metabolic blocking agents (RAMBAs). *Bioorg. Med. Chem. Lett.* **2005**, *15*, 1669–1673.

91) Mulvihill, M. J.; Kan, J. L. C.; Cooke, A.; Bhagwat, S.; Beck, P.; Bittner, M.; Cesario, C.; Keane, D.; Lazarescu, V.; Nigro, A.; Nillson, C.; Panicker, B.; Smith, V.; Srebernak, M.; Sun, F-L.; O'Connor, M.; Russo, S.; Fischetti, G.; Vrkljan, M.; Winski, S. L.; Castelhano, A. L.; Emersonb, D.; Gibsona, N. W. 3-[6-(2-Dimethylamino-1-imidazol-1-yl-butyl)-naphthalen-2-yloxy]-2,2-dimethyl-propionic acid as a highly potent and selective retinoic acid metabolic blocking agent. *Bioorg. Med. Chem. Lett.* **2006**, *16*, 2729–2733.

92) Vasudevan, J.; Johnson, A. T.; Wang, L.; Huang, D.; Chandraratna, R. A. Compounds having activity as inhibitors of cytochrome P450RAI. *US Patent* 6252090, **2001**.

93) Kirby, A. J.; Le Lain, R.; Maharlouie, F.; Mason, P.; Nicholls, P. J.; Smith, H. J.; Simons C. Some 3-(4-Aminophenyl)pyrrolidine-2,5-diones as All-trans-retinoic acid metabolising enzyme inhibitors (RAMBAs). *J. Enz. Inhib. Med. Chem.* **2002**, *17*, 321–327.

94) Le Borgne, M.; Marchand, P.; Le Baut, G.; Ahmadib, M.; Smith H. J.; Nicholls, P. J. Retinoic acid metabolism iInhibition by 3-azolylmethyl-1*H*-indoles and 2, 3 or 5-(α-azolylbenzyl)-1H-indoles. *J. Enz. Inhib. Med. Chem.* **2003**, *18*, 155–158.

95) Greer, V. P.; Mason, P.; Kirby, A. J.; Smith, H. J.; P.J. Nicholls, P. J.; Simons C. Some 1,2-diphenylethane derivatives as inhibitors of retinoic acid-metabolising enzymes. *J. Enz. Inhib. Med. Chem.* **2003**, *18*, 431–443.

96) Yee, S. W.; Jarno, L.; Gomaa, M. S.; Elford, C.; Ooi, L-L.; Coogan, M. P.; McClelland, R.; Nicholson, R. I.; Evans, B. A. J.; Brancale, A.; Simons, C. Novel tetralone-derived retinoic acid metabolism blocking agents: synthesis and in vitro evaluation with liver microsomal and MCF-7 CYP26A1 cell assays. *J. Med. Chem.* **2005,** *48,* 7123-7131.

97) Mehta, R. G.; Mehta, R. R. Vitamin D and cancer. *J. Nutr. Biochem.* **2002**, *13*, 252-264

98) Chen, K.S.; Prahl, J.M; DeLuca, H.F. Isolation and expression of human 1,25-dihydroxyvitamin D_3 24-hydroxylase cDNA. *Proc. Nat. Acad. Sci. U.S.A.* **1993**, *90*, 4543-4547.

99) Guo, Y.; Strugnell, S.A.; Back, D.W.; Jones, G.W. Transfected human liver cytochrome P-450 hydroxylates vitamin D analogs at different side-chain positions. *Proc. Nat. Acad. Sci. U.S.A.* **1993**, *90*, 8668-8672.

100) Monkawa, T.; Yoshida, T.; Wakino, S.; Shinki, T.; Anazawa, H.; DeLuca, H.F.; Suda, T.; Hayashi, M.; Saruta, T. Molecular cloning of cDNA and genomic DNA for human 25-hydroxyvitamin D_3 1alpha-hydroxylase. *Biochem. Biophys. Res. Commun.* **1997**, *239*, 527-533.

101) Ghazarian, J.G.; Jefcoate, C.R.; Knutson, J.C.; Orme-Johnson, W.H.; DeLuca, H.F. Mitochondrial cytochrome P450. A component of chick kidney 25-hydrocholecalciferol-1alpha-hydroxylase. *J. Biol. Chem.* **1994**, *249*, 3026-3033.

102) Friedman, P. A.; Brunton, L. L.; Lazo, J. S.; Parker, K. L. "*Goodman & Gilman's the pharmacological basis of therapeutics*", 11th ed., chapter *61*, McGraw-Hill medical publishing division, New York, **2006**.

103) Nagpal, S.; Na, S.; Rathnachalam, R. Noncalcemic actions of vitamin D receptor ligands. *Endocr. Rev.* **2005**, *26*, 662-687.

104) Jones, G.W.; Strugnell, S.A.; DeLuca, H.F. Current understanding of the molecular actions of vitamin D. *Physiol. Rev.* **1998**, *78*, 1193-1231.

105) Kliewer, S.A.; Umesono, K.; Mangelsdorf, D.J.; Evans, R.M. Retinoid X receptor interacts with nuclear receptors in retinoic acid, thyroid hormone and vitamin D_3 signaling. *Nature* **1992**, *355*, 446-449.

106) Mullin, G. E.; Dobs, A. Vitamin D and its role in cancer and immunity: A prescription for sunlight. *Nutr. Clin. Pract.* **2007**; *22*; 305-322.

107) Liu, M; Lee, M. H.; Cohen, M; Bommakanti, M; Freedman, L. P. Transcriptional activation of the Cdk inhibitor p21 by vitamin D3 leads to the induced differentiation of the myelo-monocytic cell line U937. *Genes Dev.* **1996**, *10*, 142–153.

108) Jones, G; Strugnell, S. A.; DeLuca, H. F. Current understanding of the molecular actions of vitamin D. *Physiol. Rev.* **1998**, *78*, 1193–1231.

109) Masuda, S.; Jones, G. Promise of vitamin D analogues in the treatment of hyperproliferative conditions. *Mol. Cancer Ther.* **2006**, *5*, 797-808.

110) Omdahl, J.A.; Morris, H.A.; May, B.K. Hydroxylase enzymes of the vitamin D pathway: Expression, function and regulation. *Annu. Rev. Nutr.* **2002**, *22*, 139-166.

111) Bouillon, R.; Okamura, W.H.; Norman, A.W. Structure-function-relationships in the vitamin-D endocrine system. *Endocr. Rev.* **1995**, *16*, 200-257.

112) Ettinger, R.A.; DeLuca, H.F. The Vitamin D endocrine system and its therapeutic potential. *Advances in Drug Research* **1996**, *28*, 269-312.

113) Akiyoshi-Shibata, M.; Sakaki, T.; Ohyama, Y.; Noshiro, M.; Okuda, K.; Yabusaki, Y. Further oxidation of hydrocalcidiol by calcidiol-24-hydroxylase: A study with the mature enzyme expressed in Escherichia Coli. *Eur. J. Biochem.* **1994**, *224*, 335-343.

114) Ohyama, Y.; Okuda, K. Isolation and characterization of a cytochrome P-450 from rat kidney mitochondria that catalyzes the 24-hydroxylation of 25-hydroxyvitamin D_3. *J. Biol. Chem.* **1991**, *266*, 8690-8695.

115) Schuster, I.; Egger, H.; Nussbaumer, P.; Kroemer, R.T. Inhibitors of vitamin D hydroxylases: structure-activity relationships. *J. Cell. Biochem.* **2003**, *88*, 372-380.

116) Schuster, I.; Egger, H.; Astecker, N.; Herzig, G.; Schussler, M.; Vorisek, G. Selective inhibitors of CYP24: mechanistic tools to explore vitamin D metabolism in human keratinocytes. *Steroids* **2001**, *66*, 451-462.

117) Posner, G. H.; Crawford, K. R.; Yang, H. W.; Kahraman, M.; Jeon, H. B.; Li, H.; Lee, J. K.; Suh, B. C.; Hatcher, M. A.; Labonte, T.; Usera, A.; Dolan, P. M.; Kensler, T. W.; Peleg, S.; Jones, G.; Zhang, A.; Korczak, B.; Saha, U.; Chuang, S. S. Potent low calcemic selective inhibitors of CYP24 hydroxylase: 24-sulfone analogs of the hormone 1α,25-dihydroxyvitamin D_3. *J. Steroid Biochem. Mol. Biol.* **2004**, *89-90*, 5-12.

118) Kahraman, M.; Sinishtag, S.; Dolan, P. M.; Kensler, T. W.; Peleg, S.; Saha, U.; Chuang, S. S.; Bernstein, G.; Korczak, B.; Posner, G. H. Potent selective and low calcemic inhibitors of CYP24 hydroxylase: 24-sulfoximine analogues of the hormone 1α,25-dihydroxyvitamin D_3. *J. Med. Chem.* **2004**, *47*, 6854-6863.

119) Farhan, H.; Wahala, K.; Cross, H. S. Genistein inhibits vitamin D hydroxylase CYP24 and CYP27B1 expression in prostate cells. *J. Steroid Biochem. Mol. Biol.* **2003**, *84*, 423-429.

120) Ly, L. H.; Zhao, X. Y.; Holloway, L.; Feldman, D. Liarozole acts synergistically with 1 alpha,25-dihydroxyvitamin D-3 to inhibit growth of DU 145

human prostate cancer cells by blocking 24-hydroxylase activity. *Endocrinology* **1999**, *140*, 2071-2076.

121) Seidmon, E. J.; Trump, D. L.; Kreis, W.; Hall, S. W.; Kurman, M. R.; Ouyang, P.; Wu, J. M.; Kremer, A. B. Pharse I/II dose escalation study of liarozole in patients with stage D, hormone refractory carcinoma of the prostate. *Ann. Surg. Oncol.* **1995**, *2*, 550-556.

122) Peehl, D. M.; Seto, E.; Feldman, D. Rationale for combination ketoconazole/vitamin D treatment of prostate cancer. *Urology* **2001**, *58*, 123-126.

123) Peehl, D. M.; Seto, E.; Hsu, J. Y.; Feldman, D. Preclinical activity of ketoconazole in combination with calcitriol or the vitamin D analogue EB 1089 in prostate cancer cells. *J. Urology* **2002**, *168*, 1583-1588.

124) Reinhardt, T. A.; Horst, R. L. Ketoconazole inhibits self-induced metabolism of 1,25-dihydroxyvitamin D_3 and amplifies 1,25-dihydroxyvitamin D_3 receptor up-regulation in rat osteosarcoma cells. *Arch. Biochem. Biophys.* **1989**, *272*, 459-465.

125) Zhao, J.; Tan, B. K.; Marcelis, S.; Verstuyf, A.; Bouillon, R. Enhancement of antiproliferative activity of 1 alpha,25- dihydroxyvitamin D-3 (analogs) by cytochrome P450 enzyme inhibitors is compound- and cell-type specific. *J. Steroid Biochem. Mol. Biol.* **1996**, *57*, 197-202.

126) Yee, S. W.; Campbell, M. J., Simons, C. Inhibition of vitamin D_3 metabolism enhances VDR signaling in androgen-independent prostate cancer cells. *J. Steroid Biochem. Mol. Biol.* **2006**, *98*, 228-235.

127) Vaishampayan, U.; Hussain, M.; Seren, S.; Sakar, F. H.; Forman, J. D.; powell, I.; Pontes, J. E.; Kucuk, O. Lycopene and soy isoflavones in the treatment of prostate cancer. *Nutr. Cancer* **2007**, *59*, 1-7.

128) Zhao, X. Y.; Feldman, D. The role of vitamin D in prostate cancer. *Steroids* **2001**, *66*, 293-300.

129) Gomaa, M. S. M. " Design and synthesis of some CYP26 and CYP24 inhibitors as indirect differentiating agents for prostate and breast cancer " PhD thesis, **2008**.

130) Wermuth, C. G.; Ganellin, C. R.; Lindberg, P.; Mitscher, L. A. Glossary of terms used in medicinal chemistry (IUPAC Recommendations 1997). *Annu. Rep. Med. Chem.* **1998**, *33*, 385–395.

131) Evans, B. E.; Rittle, K. E.; Bock, M.G.; Di-Pardo, R. M.; Freidinger, R. M.; Whitter, W. L.; Lundell, G.F.; Veber, D. F.; Anderson, P. S.; Chang, R. S.; Lotti, V. J.; Cerno, D.J.; Chen, T. B.; Kling, P. J.; Kunkel, K. A.; Springer, J. P.; Hirshfield, J. Methods for drug discovery: development of potent, selective, orally effective cholecystokinin antagonists. *J. Med. Chem.* **1988**, *31*, 2235–2246.

132) Langer, T.; Hoffmann, R. D. "Methods and Principles in Medicinal Chemistry: Pharmacophores and Pharmacophore Searches". WILEY-VCH Verlag GmbH & Co. KGaA, Weinheim, Germany **2006**, *vol. 32*.

133) Snyder, J. P.; Rao, S. N.; Koehler, K. F.; Vedani, A.; Pellicciari, R. APOLLO Pharmacophores and the Pseudoreceptor Concept, in "*Trends in QSAR and Molecular Modeling*", C.G.Wermuth, Y. Rival (eds.). **1993**, Elsevier: Amsterdam. p. 367–403.

134) Van Drie, J. H.; Weininger, D.; Martin, Y. C. ALADDIN: An integrated tool for computer-assisted molecular design and pharmacophore recognition from geometric, steric, and substructure searching of three-dimensional molecular structures. *J. Comput.-Aided Mol. Des.*, **1989**, *3*, 225–251.

135) Van Drie, J. H. An inequality for 3D database searching and its use in evaluating the treatment of conformational flexibility. *J. Comput.-Aided Mol.Des.*, **1996**, *10*, 623-630.

136) Van Drie, J. H. Strategies for the determination of pharmacophoric 3D database queries. *J. Comput.-Aided Mol.Des.*, **1997**, *11*, 39–52.

137) Van Drie, J. H. "Shrink-Wrap" Surfaces: A New Method for Incorporating Shape into Pharmacophoric 3D Database Searching. *J. Chem. Inf. Comput. Sci.*, **1997**, *37*, 38–42.

138) Van Drie, J. H., Nugent, R. A. Addressing the Challenges Posed by Combinatorial Chemistry: 3D Databases, Pharmacophore Recognition and Beyond. *SAR QSAR Environ. Res.*, **1998**, *9*, 1–21.

139) Finn, P.W.; Karraki, L. E.; Latombe, J.-C.; Motwani, R.; Shelton, C.; Venkatasubramanian, S.; Yao, A. RAPID: randomized pharmacophore identification for drug design, in "*Proc. of the 3rd annual symposium on computational geometry*", Nice, France, ACM Press, p. 324–333.

140) *SCREEN*. http://www.jchem.com/index. html/content=doc/user/Screen.html.

141) Mason, J. S.; Good, A. C.; Martin, E. J. 3-D Pharmacophores in Drug Discovery. *Curr. Pharm. Des.* **2001**, *7*, 567–597.

142) Langer, T.; Wolber, G. Pharmacophore definition and 3D searches. Drug Discov. Today: Technologies. **2004**, *1*(3), 203-207.

143) *Cerius*^{2}. Accelrys Software, San Diego,CA; http://www.accelrys.com/.

144) *Unity*. Tripos, St. Louis, MO; http://www.tripos.com/.

145) *Molecular Operating Environment*. Chemical Computing Group, Montreal, QC; http://www.chemcomp.com/.

146) *Catalyst*. Accelrys Software, San Diego, CA; http://www.accelrys.com.

147) *Discotech*. Tripos, St. Louis, MO; http://www.tripos.com/.

148) *Gasp*. Tripos, St. Louis, MO; http://www.tripos.com/.

149) CCG: Methodology Development and Deployment; http://www.chemcomp.com/software-mdd.htm., SVL Exchange; http://svl.chemcomp.com/.

150) Wauwe, J. P. V., Coene, M.-C., Goossens, J., Nijen, G. V., Cools, W., Lauwers, W. Ketoconazole Inhibits the in Vitro and in Vivo Metabolism of All-*trans*-Retinoic acid. *J. Pharmacol. Exp. Ther.* **1988**, *245*(2), 718-722.

151) Wauwe, J. V.; Nyen, G. V.; Coene, M-C.; Stoppie, P.; Cools, W.; Goossens, J.; Borghgraef, P.; Janssen, P. A. J. Liarozole, an Inhibitor of Retinoic Acid Metabolism, Exerts Retinoid-Mimetic Effects *in Vivo*. *J. Pharmacol. Exp. Ther.* **1992**, *261*(2), 773-779.

152) De Coster, R.; Wouters, W.; Ginckel, R. V.; End, D.; Krekels, M.; COEne, M.-C.; Bowden, C. Experimental studies with Liarozole (R75 251): an antitumoral agent which inhibits retinoic acid breakdown. *J. Steroid Biochem. Molec. Biol.* **1992**, *43*, 197-201.

153) Joseph, N. P.; John, S. H.; Masoud, A.; Hassanzadeh, M. F. Benzyl and benzylidene tetralins and derivatives. *WO Patent* 9935115, **1999**.

154) Njar, V. C. O.; Nnane, I. P.; Brodie, A. M. H. Potent Inhibition of Retinoic Acid Metabolism Enzyme(s) by Novel Azolyl Retinoids. *Bioorg. Med. Chem. Lett.* **2000**, *10*, 1905–1908.

155) Stoppie, P.; Borgers, M.; Borghgraef, P.; Dillen, L.; Goossens, J.; Sanz, G.; Szel, H.; Hove, C. V.; Nyen, G. V.; Nobels, G.; Bossche, H. V.; Venet, M.; Willemsens, G.; Wauwe, J. V. R115866 Inhibits All-*trans*-Retinoic Acid Metabolism and Exerts Retinoidal Effects in Rodents. *J. Pharmacol. Exp. Ther.* **2000**, *293*(1), 304–312.

156) Kirby, A. J.; Le Lain, R.; Mason, P.; Maharlouie, F.; Nicholls, P. J.; Smith, H. J.: Simons, C. Some 3-(4-Aminophenyl)pyrrolidine-2,5-diones as All-trans-retinoic Acid Metabolising Enzyme Inhibitors (RAMBAs). *J. Enzym. Inhib. Med. Chem.* **2002**, *17*(5), 321–327.

157) Kirby, A. J.; Le Lain, R.; Maharlouie, F.; Mason, P.; Nicholls, P. J.; Smith, H. J.; Simons, C. Inhibition of Retinoic Acid Metabolising Enzymes by 2-(4-aminophenylmethyl)-6-hydroxy-3,4-dihydronaphthalen-1(2H)-one and Related Compounds. *J. Enzym. Inhib. Med. Chem.* **2003**, *18*(1), 27–33.

158) Greer, V.P.; Mason, P.; Kirby, A. J.; Smith, H. J.; Nicholls, P. J.; Simons, C. Some 1,2-Diphenylethane Derivatives as Inhibitors of Retinoic Acid—Metabolising Enzymes. *J. Enzym. Inhib. Med. Chem.* **2003**, *18*(5), 431-443.

159) Patel, J. B.; Huynh, C. K.; Handratta, V. D.; Gediya, L. K.; Brodie, A. M. H.; Goloubeva, O. G.; Clement, O. O.; Nanne, I. P.; Soprano, D. R.; Njar, V. C. O. Novel Retinoic Acid Metabolism Blocking Agents Endowed with Multiple Biological Activities Are Efficient Growth Inhibitors of Human Breast and Prostate Cancer Cells in Vitro and a Human Breast Tumor Xenograft in Nude Mice. *J. Med. Chem.* **2004**, *47*, 6716-6729.

160) Yee, S. W.; Jarno, L.; Gomaa, M. S.; Elford, C.; Ooi, L-L.; Coogan, M. P.; McClelland, R.; Nicholson, R. I.; Evans, B. A. J.; Brancale, A.; Simons, C. Novel Tetralone-Derived Retinoic Acid Metabolism Blocking Agents: Synthesis and in Vitro Evaluation with Liver Microsomal and MCF-7 CYP26A1 Cell Assays. *J. Med. Chem.* **2005**, *48*, 7123-7131.

161) Mulvihill, M. J.; Kan, J. L. C.; Beck, P.; Bittner, M.; Cesario, C.; Cooke, A.; Keane, D. M.; Nigro, A. I.; Nillson. C.; Smith, V.; Srebernak, M.; Sun, F.-L.;

Vrkljan, M.; Winski, S. L.; Castelhano, A. L.; Emerson, D.; Gibson, N. Potent and selective [2-imidazol-1-yl-2-(6-alkoxynaphthalen-2-yl)-1-methyl-ethyl]-dimethyl-amines as retinoic acid metabolic blocking agents (RAMBAs). *Bioorg. Med. Chem. Lett.* **2005**, *15*, 1669–1673.

162) Mulvihill, M. J.; Kan, J. L. C.; Cooke, A.; Bhagwat, S.; Beck, P.; Bittner, M.; Cesario, C.; Keane, D.; Lazarescu, V.; Nigro, A.; Nillson, C.; Panicker, B.; Smith, V.; Srebernak, M.; Sun, F.-L.; O'Connor, M.; Russo, S.; Fischetti, G.; Vrkljan, M.; Winski, S.; Castelhano, A. L.; Emerson, D.; Gibson, N. 3-[6-(2-Dimethylamino-1-imidazol-1-yl-butyl)-naphthalen-2-yloxy]-2,2- dimethyl-propionic acid as a highly potent and selective retinoic acid metabolic blocking agent. *Bioorg. Med. Chem. Lett.* **2006**, *16*, 2729–2933.

163) Gomaa, M. S.; Yee, S. W.; Milbourne, C. E.; Barbera, M. C.; Simons, C.; Brancale, A. Homology model of human retinoic acid metabolising enzyme cytochrome P450 26A1 (CYP26A1): active site architecture and ligand binding. *J. Enzyme Inhib. Med. Chem.* **2006**, *21*, 361–369.

164) Morris, G. M.; Goodsell, D. S.; Huey, R.; Olson, A. J. Distributed automated docking of flexible ligands to proteins: parallel application of AutoDock 2.4. *J. Comput. Aid. Mol. Des.* **1996**, *10*, 293-304.

165) Jones, G.; Willett, P.; Glen, R.C.; Leach, A.R.; Taylor, R. Development and validation of genetic algorithm for flexible docking. *J. Mol. Biol.* **1997,** *267*, 727-748.

166) Kharkar, P. S.; Kulkarni, V. M. A proposed model of mycobacterium avium complex dihydrofolate reductase and its utility in drug design. *Org. Biomol. Chem.* **2003**, *1*, 1315-1322.

167) Ewing, T.; Kuntz, I. D. Critical evaluation of search algorithms for automated molecular docking and database screening. *J. Comput. Chem.* **1997**, *18*, 1175-1189.

168) Rarey, M.; Wefing, S.; Lengauer, T. Placement of medium-sized molecular fragments into active sites of proteins. *J. Comput. Aid. Mol.* Des. **1996**, *10*, 41-54.

169) Rarey, M.; Kramer, B.; Lengauer, T.; Klebe, G. A fast flexible docking method using an incremental construction algorithm. *J. Mol. Biol.* **1996**, *261*, 470-489.

170) Bohm, H. J. The computer program LUDI: a new method for the *de novo* design of enzyme inhibitors. *J. Comput. Aid. Mol. Des.* **1992**, *6*, 61-78.

171) Welch, W.; Ruppert, J.; Jain, A. N. Hammer-Head: fast, fully automated docking of flexible ligand to protein binding sites. *Chem. Biol.* **1996**, *3*, 449-462.

172) Bohacek, R. S.; Mcmartin, C. Modern computational chemistry and drug discovery: structure generating programs. *Curr. Opin. Chem. Biol.* **1997**, *1*, 157-161.

173) Eisen, M. D.; Wiley, D. C.; Karplus, M.; Hubbard, D. E. Hook-A program for finding novel molecular architectures that satisfy the chemical and steric requirements of a molecular binding site. *Proteins.* **1994**, *19*, 199-221.

174) Wang, J.; Kollman, P. A.; Kuntz, I. D. Flexible ligand docking: A multistep strategy approach. *Proteins.* **1999**, *36*, 1-19.

175) Lyne, P. D. Structure-based virtual screening: An overview. *Drug Discov. Today.* **2002**, *7*, 1047-1055.

176) Maechajewski, T. D.; Wong, C. H. The catalytic asymmetric aldol reaction. *Angew. Chem. Int. Ed.* **2000**, *39*, 1352-1374.

177) Mukaiyama, T. Explorations into new reaction chemistry. *Angew. Chem. Int. Ed.* **2004**, *43*, 5590-5614.

178) Hagiwara, H.; Inoguchi, H.; Fukushima, M.; Hoshi T.; Suzuki, T. Aldol reaction of trimethylsilyl enolate with aldehyde catalyzed by pyridine-*N*-oxide as a Lewis base catalyst. *synlett* **2005**, *15*, 2388-2390.

179) Corey E. J.; Gross, A. W. Highly selective, kinetically controlled enolate formation using lithium dialkylamides in the presence of trimethylchlorosilane. *Tetrahedron Lett.* **1984**, *25*, 495-498.

180) Baylis, A. B.; Hillman, M. E. D. *German Patent*, 2155113 (1972); *Chem. Abstr.* **1972**, *77*, 34174.

181) Basavaiah, D.; Rao, P. O.; Hyma, R. S. The Baylis-Hillman reaction: A novel carbon-carbon bond forming reaction. *Tetrahedron* **1996**, *52*, 8001-8062.

182) Kohn, L. K.; Pavam, C.H.; Veronese, D.; Coelho, F.; De Carvalho, J. E.; Almeida, W. P. Antiproliferative effect of Baylis–Hillman adducts and a new phthalide derivative on human tumor cell lines. *Eur. J. Med. Chem.* **2006**, *41*, 738-744.

183) Krishna, P. R.; Manjuvani, A.; Kannan V.; Sharma, G. V. M. Sulpholane—A new solvent for the Baylis–Hillman reaction. *Tetrahedron Lett.* **2004**, *45*, 1183–1185.

184) Chandrasekhar, S.; Narsihmulu, C.; Saritha, B.; Sultana, S. S. Poly(ethyleneglycol) (PEG): a rapid and recyclable reaction medium for the

DABCO-catalyzed Baylis–Hillman reaction. *Tetrahedron Lett.* **2004**, *45*, 5865–5867.

185) Krishna, P. R.; Manjuvani, A.; Sekhar, E. R. Novel aprotic polar solvents for facile Baylis-Hillman reaction. *ARKIVOC* **2005**, *III*, 99-109.

186) Krishna, P.nR.; Sekhar, E. R.; Kannan, V. N-Methylmorpholine and urotropine as useful base catalysts in Baylis-Hillman reaction. *Synthesis* **2004**, *6*, 857-860.

187) Oishi, T.; Oguri, H.; Hirama, M. Asymmetric Baylis-Hillman reactions using chiral 2,3-disubstituted 1,4-diazabicyclo[2.2.2]octanes catalysts under high pressure conditions. *Tetrahedron: Asymmetry* **1995**, *6*, 1241-1244.

188) Hayashi, Y.; Okado, K.; Ashimine, I.; Shoji, M. The Baylis–Hillman reaction under high pressure induced by water-freezing. *Tetrahedron Lett.* **2002**, *43*, 8683-8686.

189) Cai, J.; Zhou, Z.; Zhao, G.; Tang, C. Dramatic rate acceleration of the Baylis-Hillman reaction in homogeneous medium in the presence of water. *Org. Lett.* **2002**, *4*, 4723-4725.

190) Aggarwal, V. K.; Mereu, A. Superior amine catalysts for the Baylis–Hillman reaction: the use of DBU and its implications. *Chem. Commun.* **1999**, 2311–2312.

191) Mateus, C. R.; Almeida, W. P.; Coelho, F. Diastereoselective heterogeneous catalytic hydrogenation of Baylis–Hillman adducts. *Tetrahedron Lett.* **2000**, *41*, 2533–2536.

192) Lindley, J. Copper assisted nucleophilic substitution of aryl halogen. *Tetrahedron* **1984**, *40*, 1433-1456.

193) Wolf, J. P.; Buchwald, S. L. Room temperature catalytic amination of Aryl iodides. *J. Org. Chem.* **1997**, *62*, 6066-6068.

194) Yamamoto, T.; Nishityama, M.; Koie, Y. Palladium-catalyzed synthesis of triarylamines from aryl halides and diarylamines. *Tetrahedron Lett.* **1998**, *39*, 2367-2370.

195) Chan, D. M. T.; Monaco, K. L.; Wang, R.; Winters, M. P. New N- and O-arylations with phenyl boronic acids and cupric acetate. *Tetrahedron Lett.* **1998**, *39*, 2933-2936.

196) Evans, D. A.; Katz, J. L.; West, T. R. Synthesis of diaryl ethers through the copper-promoted arylation of phenols with arylboronic acids. An expedient synthesis of thyroxine. *Tetrahedron Lett.* **1998**, *39*, 2937-2940.

197) Antilla, J. C.; Buchwald, S. L. Copper-catalyzed coupling of arylboronic acids and amines. *Org. Lett.* **2001**, *3*, 2077-2079.

198) Barton, D. H. R.; Finet, J. P.; Khamsi, J. Copper-salts catalysis of *N*-phenylation of amines by trivalent organobismuth compounds. *Tetrahedron Lett.* **1987**, *28*, 887-890.

199) Lubineau, A.; Auge', J.; Queneau, Y. Water-Promoted Organic Reactions. *Synthesis* **1994**, 741–760.

200) Lubineau, A. Water-promoted organic reactions: aldol reaction under neutral conditions. *J. Org. Chem.* **1986**, *51*, 2142–2144.

201) Lubineau, A.; Meyer, E. Water-promoted organic reactions. aldol reaction of silyl enol ethers with carbonyl compounds under atmospheric pressure and neutral conditions. *Tetrahedron* **1988**, *44*, 6065–6070.

202) Loh, T-P.; Feng, L-C.; Wei, L-L. Water-Accelerated aldol reaction of ketene silyl acetals with carbonyl compounds. *Tetrahedron* **2000**, *56*, 7309–7312.

203) Nascimento, M. G.; Zanotto, S. P.; Melegari, S. P.; Fernandes, L.; Mandolesi Sa, M. Resolution of α-methylene-β-hydroxy esters catalyzed by free and immobilized *Pseudomonas* sp. Lipase. *Tetrahedron: Asymmetry* **2003**, *14*, 3111-3115.

204) Varma, R. S. Synthesis of substituted 2-anilino-benzoxazole. *Curr. Sci India* **1976**, *45*, 53-54.

205) Billeau, S.; Chatel, F.; Robin, M.; Faure, R.; Galy, J.-P. ^{1}H and ^{13}C chemical shifts for 2-aryl and 2-*N*-arylamino benzothiazole derivatives. *Magn. Reson. Chem.* **2006**, *44*, 102–105.

206) Parikh, J. P.; Doering, W.E. Sulfur trioxide in the oxidation of alcohols by dimethyl sulfoxide. *J. Am. Chem. Soc.*, **1967**, *89*, 5505-5507.

207) Torasell, K. Mechanisms of dimethylsulfoxide oxidations. *Tetrahedron Lett.* **1966**, *7*, 4445-4451.

208) Wamhoff, H.; Richardt, G. and Stölben, S. *Adv. Heterocycl. Chem.*, Academic Press, New York. **1995**, *64*, 159-249.

209) Sherman, W. R. 5-(5-nitro-2-furyl)-1,3,4-oxadiazoline-2-one or thione and process. *US Patent* 2918473, **1959**.

210) Sherman, W. R. 5-Nitro-2-furyl-substituted 1,3,4-oxadiazoles, 1,3,4-thiadiazoles, and 1,3,5-triazines. *J. Org. Chem.* **1961**, *26*, 88-95.

211) Mulvihill, J. M.; Nguyen, V. D.; Mac-Dougall, S. B. Process for 2,4-disubstituted-1,3,4-oxadiazoline-5-thione and 5-one compounds. *WO Patent* 02079176, **2002.**

212) Boschelli, D. H.; Connor, D. T.; Kostlan, C. R.; Kramer, J. B.; Mullican, M. D.; Sircar, J. C. 3,5-ditertiarybutyl-4-hydroxyphenyl, 1,3,4-thiadiazoles and oxadiazoles linked by carbon, oxygen, and sulfur residues. *Eur. Patent* 0449211, **1991.**

213) Hoggarth, E. 2-Benzoyldithiocarbazinic acid and related compounds. *J. Chem. Soc.* **1952**, 4811-4817.

214) Young, R. W.; Wood, K. H. The cyclization of 3-acyldithiocarbazate esters. *J. Am. Chem. Soc.* **1955**, *77*, 400-403.

215) Steynberg, J. P.; Ferreira, D.; Roux, D. G. Synthesis of condensed tannins. part 18. stilbenes as potent nucleophiles in regio- and stereo-specific condensations: novel guibourtinidol-stilbenes from *Guibourtia co feosperma*. *J. Chem. Soc. Perkin Trans. 1* **1987**, 1705-1712.

216) Allinga, C.; Riegera, A. L.; Tanner, D. D. Positive halogen compounds. VIII. structure and reactivity in *N*-bromosuccinimide brominations. *J. Am. Chem. Soc.* **1963**, *85*, 3129-3134.

217) Gehringer, L.; Bourgogne, C.; Guillon, D.; Donnio, B. Liquid-crystalline octopus dendrimers: block molecules with unusual mesophase morphologies. *J. Am. Chem. Soc.* **2004**, *126*, 3856-3867.

218) Smith, M. B.; March, J. *"March's advanced organic chemistry Reactions, mechanisms and structure"*, 6th ed. John Wiley & Sons, Inc., New Jersey, **2007**, 1369-1980.

219) Ozawa, F.; Kubo, A.; Hayashi, T. Generation of tertiary phosphine-coordinated Pd(0) species from $Pd(OAc)_2$ in the catalytic Heck reaction. *Chem. Lett.* **1992**, *21*, 2177-2180.

220) Patel, B. A.; Ziegler, C. B.; Cortese, N. A.; Plevyak, J. E.; Zebovitz, T. C.; Terpko, M.Heck, R. F. Palladium-Catalyzed Vinylic Substitution Reactions with Carboxylic Acid Derivatives. *J. Org. Chem.* 1977, *42*, 3903-3907.

221) Gant, T. G.; Meyers, A. I. The chemistry of 2-oxazolines (1985-present). *Tetrahedron.* **1994**, 2297-2360.

222) Sund, C.; Ylikoski, J.; Kwiathowski, M. A new simple and mild synthesis of 2-substituted 2-oxazolines. *Synthesis-stuttgart* **1987**, 853-854.

223) Wehrmeister, H. L. Reactions of aromatic thiols with oxazolines. *J. Org. Chem.* **1963**, *28*, 2587-2588.

224) Yee, S. W.; Simons, C. Synthesis and CYP24 inhibitory activity of 2-substituted-3,4-dihydro-2H-naphthalen-1-one (tetralone) derivatives. *Bioorg. Med. Chem. Lett.* **2004**, *14*, 5651–5654.

225) Rapson, W. S.; Shuttleworth, R. G. J. The production of polycyclic aromatic types through the cyclodehydration of unsaturated ketones. *J. Chem. Soc.* **1940**, 636-641.

226) Morrison, R. T.; Boyd, R. N. "Organic chemistry", 5th ed., Englewood Cliffs, New Jersy, **1987**, pp 905-929.

227) Yee, W. Y. " Synthesis and evaluation of inhibitors against vitamin D3 and all-trans retinoic acid metabolising enzymes as potential therapy for androgen-independent prostate cancer" PhD thesis, **2005**.

228) Miyaura, N.; Yanagi, T.; Suzuki, A. The palladium-catalyzed cross-coupling reaction of phenylboronic acid with haloarenes in the presence of bases. *Synthetic Commun.* **1981**, *11*, 513-519.

229) Rosenwald, A.; Alizadeh, A. A.; Widhopf, G. Relation of gene expression phenotype to immunoglobulin mutation genotype in B cell chronic lymphocytic leukemia. *J. Exp. Med.* **2001**, *194*, 1639-1647.

230) Ayi, A.I.; Condom, R.; Wade, T.N.; Guedj, R. Monofluoration quantitative par le phenyltetrafluorophosphorane influence de la temperature. *J. Fluorine Chem.* **1979**, *14*, 437-454.

231) Nisson, Y. G.; L. Gorrichon. Spontaneous aldol and Michael additions of simple enoxytrimethylsilanes in DMSO. *Tetrahedron Lett.* **2000**, *41*, 4881-4884.

232) Chankeshwara, S. V.; Chakraborti, A. K. Copper(II) tetrafluoroborate as a novel and highly efficient catalyst for N-tert-butoxycarbonylation of amines under

solvent-free conditions at room temperature. *Tetrahedron Lett.* **2006**, *47*(7), 1087-1091.

233) Chaistos, D. A.; Vagenas, G. V.; Tzavellas, L. C.; Tsoleridis, C. A.; Rodios, N. A. Synthesis and a UV and IR spectral study of some 2-Aryl-Δ^2-1,3,4-oxadiazoline-5-thiones. *J. Hetercycl. Chem.* **1994**, *31*, 1593-1598.

234) Durantini, E. N. Synthesis of *meso*-nitrophenylporphyrins covalently linked to a polyphenylene chain bearing methoxy groups. *J. Porphyrins Phthalocyanines* **2000**, *4*, 233–242.

235) Nishimura, D.; Oshikiri, T.; Takashima, Y.; Hashidzume, A.; Yamaguchi, H.; Harada, A. Relative rotational motion between r-cyclodextrin derivatives and a stiff axle molecule. *J. Org. Chem.* **2008**, *73*, 2496-2502.

236) Watanabe, M.; Murata, K; Ikariya, T. Practical synthesis of optically active amino alcohols via asymmetric transfer hydrogenation of functionalized aromatic ketones. *J. Org. Chem.* **2002**, *67*, 1712-1715.

237) Cho, B. T.; Kang, S. K.; Shin, S. H. Application of optically active 1,2-diol monotosylates for synthesis of β-azido and β-amino alcohols with very high enantiomeric purity. Synthesis of enantiopure (*R*)-octopamine, (*R*)-tembamide and (*R*)-aegeline. *Tetrahedron: Asymmetry.* **2002**, *13*, 1209-1217.

238) Baston, E.; Salem, O. I. A.; Hartmann, R. W. 6-Substituted 3,4-dihydro-naphthalene-2-carboxylic Acids: synthesis and structure–activity studies in a novel class of human 5a reductase inhibitors. *J. Enzyme Inhib. Med. Chem.* **2002**, *17*, 303–320.

239) Van Heusden, J.; Wouters, W.; Ramakaers, F.C.S.; Krekels, M.D.W.G.; Dillen, L.; Borgers, M.; Smets, G., The anti-proliferative activity of ATRA catabolites and isomers is differentially modulated by liarozole-fumarate in MCF-7 human breast cancer cells. *Br. J. Cancer* **1998**, *77*, 1229-1235.

240) Toma, S.; Isnardi, L.; Raffo, P.; Dastoli, G.; Francisci, E.D.; Riccardi, L.; Palumbo, R.; Bollag, W., Effects of all-*trans*-retinoic acid and 13-cis retinoic acid on breast cancer cell lines: growth inhibition and apoptosis induction. *Int. J. Cancer* **1997**, *70*, 619-627.

241) Farhan, H.; Wahala, K.; Adlercreutz, H.; Cross, H.S. Isoflavonoids inhibit catabolism of vitamin D in prostate cancer cells. *J. Chromatogr. B* **2002**, *777*, 261-268.

242) Prosser, D.E.; Kaufmann, M.; O'Leary, B.; Byford, V.; Jones, G. Single A326G mutation converts human CYP24A1 from 25-OH-D3-24-hydroxylase into -23-hydroxylase, generating 1α,25-(OH)2D3-26,23-lactone. *PNAS* **2007**, *104*, 12673-12678.

243) Bligh, E. G.; Dyer, W. J. A rapid method of total lipid extraction and purification. *Can. J. Biochem. Physiol.* **1959**, *37*, 911-917.

244) Aboraia, A. S.; Brancale, A.; Gomaa, M. S.; Simons, C. Novel CYP26 inhibitors. *GB Patent* 0811091.8, filed **2008**.

Appendix I

CYP26A1 Pharmacophore search resulting fragments

F1&F2	F3	F4& F8	F5, F6& F7
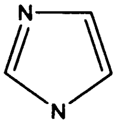	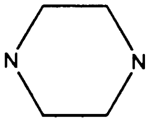	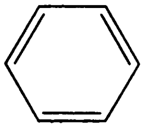	F
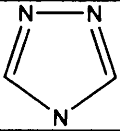	-N-	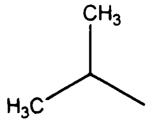	Cl
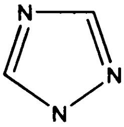	-O-	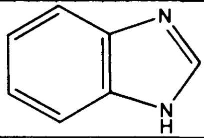	Br
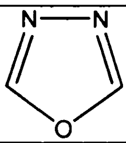	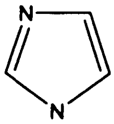	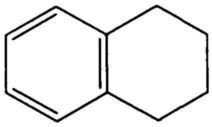	I
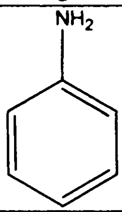	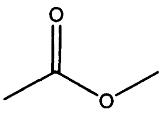	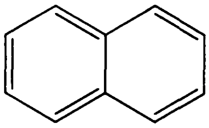	CH_3
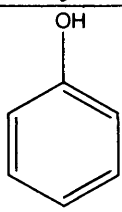	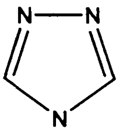	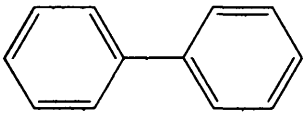	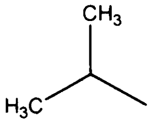
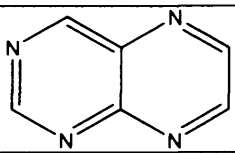	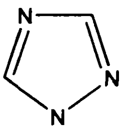	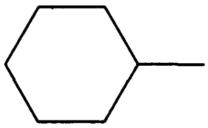	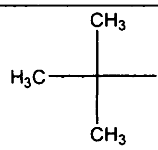
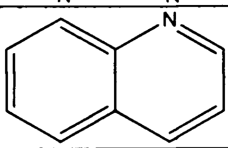	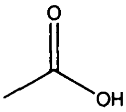	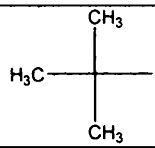	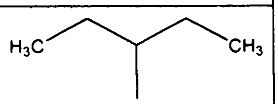
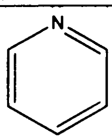	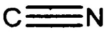	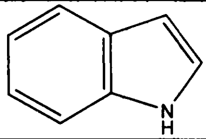	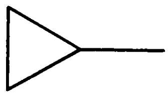
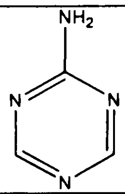	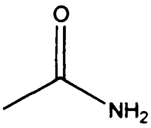	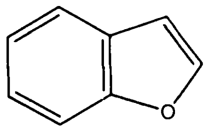	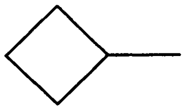
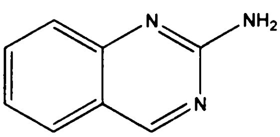	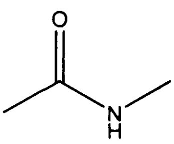	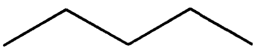	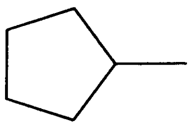

F1&F2	F3	F4& F8	F5, F6& F7
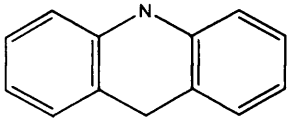	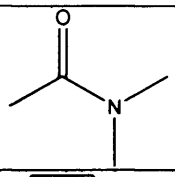	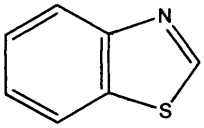	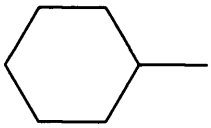
	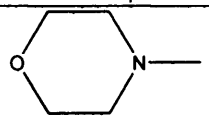		
	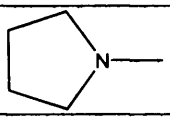		
	-S-